

David C. Wyld
Natarajan Meghanathan (Eds)

Computer Science & Information Technology

9th International Conference on Information Technology Convergence
and Services (ITCSE 2020)
May 30~31, 2020, Vancouver, Canada



AIRCC Publishing Corporation

Volume Editors

David C. Wyld,
Southeastern Louisiana University, USA
E-mail: David.Wyld@selu.edu

Natarajan Meghanathan,
Jackson State University, USA
E-mail: nmeghanathan@jsums.edu

ISSN: 2231 - 5403

ISBN: 978-1-925953-19-0

DOI: 10.5121/csit.2020.100501- 10.5121/csit.2020.100525

This work is subject to copyright. All rights are reserved, whether whole or part of the material is concerned, specifically the rights of translation, reprinting, re-use of illustrations, recitation, broadcasting, reproduction on microfilms or in any other way, and storage in data banks. Duplication of this publication or parts thereof is permitted only under the provisions of the International Copyright Law and permission for use must always be obtained from Academy & Industry Research Collaboration Center. Violations are liable to prosecution under the International Copyright Law.

Typesetting: Camera-ready by author, data conversion by NnN Net Solutions Private Ltd., Chennai, India

Preface

The 9th International Conference on Information Technology Convergence and Services (ITCSE 2020) May 30~31, 2020, Vancouver, Canada, International conference on Natural Language Computing Advances (NLCA 2020), 9th International Conference on Advanced Computer Science and Information Technology (ICAIT 2020), International Conference on Artificial Intelligence and Machine Learning (CAIML 2020), 9th International Conference on Digital Image Processing and Vision (ICDIPV 2020), 9th International Conference on Cryptography and Information Security (CRYPIS 2020) and 12th International Conference on Wireless & Mobile Network (WiMo 2020) was collocated with 9th International Conference on Information Technology Convergence and Services (ITCSE 2020). The conferences attracted many local and international delegates, presenting a balanced mixture of intellect from the East and from the West.

The goal of this conference series is to bring together researchers and practitioners from academia and industry to focus on understanding computer science and information technology and to establish new collaborations in these areas. Authors are invited to contribute to the conference by submitting articles that illustrate research results, projects, survey work and industrial experiences describing significant advances in all areas of computer science and information technology.

The ITCSE 2020, NLCA 2020, ICAIT 2020, CAIML 2020, ICDIPV 2020, CRYPIS 2020 and WiMo 2020 Committees rigorously invited submissions for many months from researchers, scientists, engineers, students and practitioners related to the relevant themes and tracks of the workshop. This effort guaranteed submissions from an unparalleled number of internationally recognized top-level researchers. All the submissions underwent a strenuous peer review process which comprised expert reviewers. These reviewers were selected from a talented pool of Technical Committee members and external reviewers on the basis of their expertise. The papers were then reviewed based on their contributions, technical content, originality and clarity. The entire process, which includes the submission, review and acceptance processes, was done electronically.

In closing, ITCSE 2020, NLCA 2020, ICAIT 2020, CAIML 2020, ICDIPV 2020, CRYPIS 2020 and WiMo 2020 brought together researchers, scientists, engineers, students and practitioners to exchange and share their experiences, new ideas and research results in all aspects of the main workshop themes and tracks, and to discuss the practical challenges encountered and the solutions adopted. The book is organized as a collection of papers from the ITCSE 2020, NLCA 2020, ICAIT 2020, CAIML 2020, ICDIPV 2020, CRYPIS 2020 and WiMo 2020.

We would like to thank the General and Program Chairs, organization staff, the members of the Technical Program Committees and external reviewers for their excellent and tireless work. We sincerely wish that all attendees benefited scientifically from the conference and wish them every success in their research. It is the humble wish of the conference organizers that the professional dialogue among the researchers, scientists, engineers, students and educators continues beyond the event and that the friendships and collaborations forged will linger and prosper for many years to come.

David C. Wyld
Natarajan Meghanathan(Eds)

General Chair

David C. Wyld,
Natarajan Meghanathan(Eds),

Organization

Southeastern Louisiana University, USA
Jackson State University, USA

Program Committee Members

Abdel-Badeeh M. Salem,	Ain Shams University, Egypt
Abdelhadi Assir,	Hassan 1st University, Morocco
Abhay Kumar Agarwal,	Kamla Nehru Institute of Technology, India
Abhishek Shukla,	A P J Abdul Kalam Technical University, India
Ahmed Farouk AbdelGawad,	Zagazig University, Egypt
Ajit Singh,	Patna Women's College, India
Akhil Gupta,	Lovely Professional University, India
Ana Paula Ferreira Fernandes Lopes,	Polytechnic of Porto, Portugal
Anand Nayyar,	Duy Tan University, Vietnam
Antonios Andreatos,	Hellenic Air Force Academy, Greece
Ayman EL-SAYED,	Menoufia University, Egypt
Azeddine Wahbi,	Hassan II University, Morocco
B.K. Verma, Ph.D.,	Chandigarh Engineering College, India
Bahadorreza OFOGHI,	Deakin University, Australia
Bela Genge,	Petru Maior University, Romania
Benali Abdelkamel,	University of El Oued, Algeria
Chiranjiv Chingangbam,	Manipur Technical University, India
Claudiu Mereuta,	Dunarea de Jos University of Galati, Romania
Daniel Hunyadi,	Lucian Blaga University of Sibiu, Romania
Daniela Litan,	Hyperion University, Romania
Desmond Bala,	Cranfield University, United Kingdom
Dharani Punithan,	Seoul National University, South Korea
Durmus Harman,	Fraunhofer Institute for Production Technology, Germany
Emilio Jimenez Macias,	University of La Rioja, Spain
Enrique Herrera-Viedma,	University of Granada, Spain
Eyad M. Hassan ALazam,	Yarmouk University, Jordan
Felix J. Garcia Clemente,	University of Murcia, Spain
Fernando Tello Gamarra,	Federal University of Santa Maria, Brazil
Fernando Zacarias Flores,	Universidad Autonoma de Puebla, Mexico
Francisco Martínez-Alvarez,	Pablo de Olavide University, Spain
G. Rajkumar,	N.M.S.S.Vellaichamy Nadar College, India
G.Padmavathi,	HCU Campus, India
Giuseppe Carbone,	University of Calabria, Italy
Guilong Liu,	Beijing Language and Culture University, China
Hafed Elfeki,	University of Sfax, Tunisia

Hamed Taherdoost,	Hamta Business Solution Sdn Bhd, Malaysia
Hamid Ali Abed Al-asadi,	Iraq University College, Iraq
Hashem H.M.Ramadan,	Tesseract Learning Pvt Lmt, India
Hassan Ali,	University of Newcastle, Australia
Hongzhi,	Harbin Institute of Technology, China
Ihab Zaqout,	Al-Azhar University - Gaza, Palestine
Jae Kwang Lee,	Hannam University, South Korea
Jamal El Abbadi,	Mohammadia V University Rabat, Morocco
Janusz Starczewski,	Czestochowa University of Technology, Poland
Jitendra Maan,	Tata Consulting Services Ltd, India
JueuSam Chou,	Nanhua University, Taiwan
Kawahata Yasuko,	Kyushu University, Japan
Khalid M.O. Nahar,	Yarmouk University, Jordan
Klenilmar Lopes Dias,	Federal University of Minas Gerais, Brazil
Liyakath Unisa,	Prince Sultan University, Saudi Arabia
Lorenzo Carnevale,	Humanizing Technologies GmbH, Austria
Luca Romeo,	Universita di Macerata, Italy
M V Ramana Murthy,	Osmania university, India
M.Prabukumar,	VIT University, India
Majid EzatiMosleh,	Power Research Institute, Iran
Mehmet Yavuz,	University of Exeter, UK
Mehregan Mahdavi,	University of Guilan, Iran
Milena Stefanova,	University of Veliko Tarnovo, Bulgaria
Mingming Zhou,	University Of Macau, Macau
Mohamed Fakir,	university Sultan Moulay Slimane, Morocco
Mohamed Hamlich,	ENSAM, UH2C, Morocco
Mohamed Najeh Lakhoua,	University of Carthage, Tunisia
Mohamed Quafafou,	Aix-Marseille University, France
Mohammad Al-Maghasbeh,	University of Malaysia, Jordan
Mohammad Aqel,	Al-Azhar University-Gaza, Palestine
Muhammad Jaju Abubakar,	Ahmadu Bello University, Nigeria
Nicolas Durand,	Aix-Marseille University, France
Niloofar rastin,	Shiraz University, Iran
Nour El-Houda Golea,	Batna 2 university, Algeria
Omar Nofal,	Researcher, Jordan
Osama Rababah,	The University of Jordan, Jordan
Osamah Ibrahim Khalaf,	Al-Nahrain University, Iraq
Pereira Guimaraes,	Federal University of Alagoas, Brazil
Picky Butani,	Shubh Solutions LLC, USA
Pierre BORNE,	Ecole Centrale de Lille Cité Scientifique, France
Pierre Bricage,	Universite de Pau, France
Poo Kuan Hoong,	Multimedia University, Malaysia
Pranita Mahajan,	Mumbai University, India
Samir Ghouali,	Mustapha Stambouli University, Algeria
Sarachandran Nair,	Muscat College, Oman
Satish Gajawada,	Indian Institute of Technology, India
Saud S Alotaibi,	Umm Al-Qura Univesity, Saudi Arabia
Serena Doria,	Univeristy G.d'Annunzio, Italy

Shahram Babaie,
Shashirekha,
ShengLi Yan,
Shirish Patil,
Sikandar Ali,
Smain Femman,
Solale Tabarestani,
Stanislaw Deniziak,
Sukhdeep Singh,
T.P.Anithaashri,
Tatiana Tambouratzis,
Ted J. Shin,
Titas De,
Vahideh Hayyolalam,
Wei Cai,
Xiaofeng Liao,
Yina Li,
Yousfi Abdellah,
Youssef TAHER ,
Yuriy Syerov,
Zakia Hammouch,
Zoran Bojkovic,

Islamic Azad University, Iran
Mangalore University, India
Tencent, China
Lead Enterprise Data Architect, Sitek Inc. , USA
China University of Petroleum- Beijing, China
UHA University France, France
Florida International University, USA
Kielce University of Technology, Poland
Punjabi University, Patiala
Saveetha School of Engineering, India
University of Piraeus, Greece
Metropolitan State University of Denver, USA
Microsoft, India
Islamic azad university of Tabriz, Iran
Qualcomm Tech, USA
Chongking University, China
South China University of Technology, China
University Mohamed , Morocco
Mohammed V University , Maroc
Lviv Polytechnic National University, Ukraine
Université Moulay Ismail, Morocco
University of Belgrade, Serbia

Technically Sponsored by

Computer Science & Information Technology Community (CSITC)



Artificial Intelligence Community (AIC)



Soft Computing Community (SCC)



Digital Signal & Image Processing Community (DSIPC)



Organized By



Academy & Industry Research Collaboration Center (AIRCC)

TABLE OF CONTENTS

9th International Conference on Information Technology Convergence and Services (ITCSE 2020)

Identification of Technology-Relevant Entities Based on Trend Curves.....01 - 13
*Sukhwan Jung, Rachana Reddy Kandadi, Rituparna Datta,
Ryan Benton and Aviv Segev*

**Contextual Factors Influencing the Design and Management of Health
Information Systems' Interoperability.....** 15 - 27
Grace Kobusinge

Transcript Level Analysis Improves the Understanding of Bladder Cancer..... 29 - 40
Xiang Ao and Shuaicheng Li

Leading DevOps Practice and Principle Adoption 41 - 56
Krikor Maroukian and Stephen R. Gulliver

Communication between Coroutines on Sunway Many-core Platform..... 57 - 67
Shaodi Li, Junmin Wu, Yi Zhang and Yawei Zhou

**An Automatic Detection of Fundamental Postures in Vietnamese
Traditional Dances.....** 263 - 277
Ngan-Khanh Chau and Truong-Thanh Ma

International conference on Natural Language Computing Advances (NLCA 2020)

Linking Social Media Posts to News with Siamese Transformers.....69 - 79
Jacob Danovitch

Hate Speech Detection of Arabic Shorttext..... 81 - 94
Abdullah Aref, Rana Husni Al Mahmoud, Khaled Taha and Mahmoud Al-Sharif

**Topic Detection from Conversational Dialogue Corpus with Parallel Latent
Dirichlet Allocation Model and Elbow Method.....** 95 - 102
Haider Khalid and Vincent Wade

**Quantum Criticism: a Tagged news Corpus Analysed for Sentiment
and Named Entities.....** 103 - 120
*Ashwini Badgajar, Sheng Cheng, Andrew Wang, Kai Yu, Paul Intrevado
and David Guy Brizan*

**VSMbM: A New Metric for Automatically Generated Text
Summaries Evaluation.....** 121 - 128
Alaidine Ben Ayed, Ismail Biskri and Jean-Guy Meunier

**Free-text and Structured Clinical Time Series for Patient
Outcome Predictions.....** 129 - 136
Emilia Apostolova, Joe Morales, Ioannis Koutroulis and Tom Velez

9th International Conference on Advanced Computer Science and Information Technology (ICAIT 2020)

A Novel Bit Allocation Algorithm in Multi-view Video..... 137 - 144
Tao Yan, In-Ho Ra, Deyang Liu, Jiajun Hong, Jingyu Feng and Shaojie Hou

**A Semi-supervised Learning Approach to Forecast CPU Usages under
Peak Load in an Enterprise Environment.....** 145 - 154
Nitin Khosla and Dharmendra Sharma

Advanced Rate Control Technologies for MVC..... 155 - 161
Tao Yan, In-Ho Ra, Na Song, Yu Youhao, Zhicheng Wu and Zhongyu Shi

**Multi-task Knowledge Distillation with Rhythm Features for
Speaker Verification** 249 - 262
Ruyun Li, Peng Ouyang, Dandan Song and Shaojun Wei

International Conference on Artificial Intelligence and Machine Learning (CAIML 2020)

**Oversampling Log Messages using A Sequence Generative Adversarial
Network for Anomaly Detection and Classification** 163 - 175
Amir Farzad and T. Aaron Gulliver

**Industrial Duct Fan Maintenance Predictive Approach Based on
Random Forest** 177 – 184
*Mashaël Maashi, Nujood Alwhibi, Fatima Alamr, Rehab Alzahrani,
Alanoud Alhamid and Nourah Altawallah*

**Classification of Computer Hardware and Performance Prediction using
Statistical Learning and Neural Networks** 185 - 195
Courtney Foots, Palash Pal, Rituparna Datta and Aviv Segev

**9th International Conference on Digital Image
Processing and Vision (ICDIPV 2020)**

Safety Helmet Detection in Industrial Environment using Deep Learning..... 197 - 208
Ankit Kamboj and Nilesh Powar

Rate Control Based on Similarity Analysis in Multi-view Video Coding..... 209 - 215
Tao Yan, In-Ho Ra, Deyang Liu, Deli Chen, Yu Youhao and Shaojie Hou

**9th International Conference on Cryptography and
Information Security (CRYPIS 2020)**

TPM Based Design for Enhanced Trust in SaaS Services..... 217 - 226
Mustapha Hedabou, Ali Azougaghe, Ahmed Bentajer

**Design and Hardware Implementation of A Separable Image Steganographic
Scheme using Public-key Cryptosystem.....** 227 - 240
Salah Harb, M. Omair Ahmad and M.N.S Swamy

**12th International Conference on Wireless & Mobile
Network (WiMo 2020)**

**Use of an IoT Technology to Analyse the Inertial Measurement of Smart
Ping-pong Paddle.....** 241 - 248
Rajeev Kanth, Tuomas Korpi and Jukka Heikkonen

**Performance Analysis of AODV, DSDV and ZRP Routing Protocols for
Wireless Sensor Networks using NS2 Tool.....** 279 – 297
Faïza Tabbana

IDENTIFICATION OF TECHNOLOGY-RELEVANT ENTITIES BASED ON TREND CURVES

Sukhwan Jung, Rachana Reddy Kandadi, Rituparna Datta,
Ryan Benton and Aviv Segev

Department of Computer Science, University of South Alabama,
Mobile, Alabama, USA

ABSTRACT

Technological developments are not isolated and are influenced not only by similar technologies but also by many entities, which are sometimes unforeseen by the experts in the field. The authors propose a method for identifying technology-relevant entities with trend curve analysis. The method first utilizes the tangential connection between terms in the encyclopedic dataset to extract technology-related entities with varying relation distances. Changes in their term frequencies within 389 million academic articles and 60 billion web pages are then analyzed to identify technology-relevant entities, incorporating the degrees and changes in both academic interests and public recognitions. The analysis is performed to find entities both significant and relevant to the technology of interest, resulting in the discovery of 40 and 39 technology-relevant entities, respectively, for unmanned aerial vehicle and hyperspectral imaging with 0.875 and 0.5385 accuracies. The case study showed the proposed method can capture hidden relationships between semantically distant entities.

KEYWORDS

Technology Forecasting, Trend Curve, Big Data, Academic Articles, Web Pages

1. INTRODUCTION

Identification of relevant terms for a specific technology plays a crucial role in technology funds and government research grants, allowing them to better direct their investments to encourage technological developments beneficial to the target technology. It is also one of the main research fields for stock market prediction as technology development directions affect the stock markets. The current work proposes an approach for identifying any type of entities relevant to the given technology, based on the trend curves of related entities found from recursive encyclopedic connections to the technology. This perspective offers a novel approach of technology trend analysis, granting a possibility of detecting seemingly unrelated entities that cannot be found with conventional means.

The proposed method offers a means of identifying significant entities relevant to a given technology based on term frequency and degree of usage growth. It analyzes technology-relevant entities from Wikipedia in the whole domain of academic articles (academia) and web pages (web) with the help of Google search engine, incorporating both the academic interests and public recognitions of the given entities, each representing the earliest and the latest predictive time windows. Wikipedia, an online encyclopedia with built-in page links between related

articles, allows the extraction of not only the related technologies but also any related entities, providing generalizability to the proposed method if desired. The authors previously showed technology trends in different datasets contain distinct patterns while sharing an overall shape on different time windows [1]. The comparison of the proposed method on two datasets analyzes the differences in the list of entities deemed relevant to them. In addition, the analysis of entities common in both datasets and their respective trend curves presents an integrated view of the technology-relevant entities over multiple dimensions.

The main contributions of this work are as follows:

- On an algorithmic level, the authors provide an implementation of the proposed method based on the academia and web.
- On a conceptual level, the authors propose a multi-domain approach for identifying any entities relevant to a specific technology based on term frequency and moving gradient, which can be semantically and syntactically unrelated to the technology.
- On a practical level, the authors identify a list of relevant, possibly hidden, entities for the target technology and how different datasets contribute to the result.

Section 2 reviews the related work on technology forecasting with regard to the necessity of normative approaches based on technological curves and their limitations. Section 3 explains the proposed method and experiment in detail. The experiment results in Section 4 show that the proposed method can identify entities related to the given technology with hidden relationships, and Section 5 states the concluding remarks and future work.

2. RELATED WORK

The traditional approach for technology forecasting is a manual approach, including scenario building [2], forecast by analogy [3], and the Delphi method [4]. Scenario building lets analysts generate a series of plausible scenarios with both optimistic and pessimistic developments; these developments aim to be compatible, with substantial effects, with unlikely events that are often disregarded in other methods. Forecast by analogy employs analogical comparison between the known phenomena and the technology trends with the assumption they behave similarly. The Delphi method is a more structured technique, first developed as a systematic and interactive method of forecasting. It relies on a consensus among a panel of experts, which is reached by repeated rounds of questionnaires to the participating experts. The belief is that the variance of the answers will decrease with each iteration and the group will converge towards an answer that can be regarded as correct. The process ends once it either reaches a certain number of rounds or achieves a steady consensus; the answers from the final round determine the result. These manual methods often require a large amount of contribution from numerous field-related experts and hence are expensive to utilize, but still have been used in recent years [5] for its high domain adaptability.

Normative methods such as morphological models [6] and mission flow diagrams [7] are complementary to such processes that attempt to automatically project future behaviors from past data. Based on systems analysis, normative methods view future needs in the field as the scheduled progress of the field and predict future behaviors based on them [7]. Extrapolations on past data are used to analyze changes in the popularity or intensity of a given topic, which can be matched into estimation lines such as linear, polynomial, exponential, and parabolic lines [8]. Extrapolation on a pre-defined technological curve is widely used as well, matching the past data to estimation lines such as Gartner's hype cycle or other technological growth curves such as S-curve [9]. The future technological stages are then predicted upon the estimation line. The limitations of normative methods suggested in more recent years include incongruencies found

from the Gartner dataset and its hype cycle [10] and less generalizability for different technology fields. This indicates that both the manual and extrapolation methods lack the ability to be implemented in related technological fields [11].

Other fields of research tried to address related fields to generate better technology forecasts. The content transition from one topic to another during topic evolution is identified in the form of complementary trend curve patterns, connecting multiple technologies in transitional states [12], [13]. The topics are extracted statistically from a document collection, and the popularity trend curve of each topic is generated by connecting their popularities in discretely divided document subsets per timeslots. The content transition between topics is identified when one topic experiences a significant drop in popularity when the other topic experiences a significant increase, which is translated as the former topic being transferred to the latter one. Technology diffusion can be used for a more specific case of technology transfer where the one is replaced by another, such as LED is replaced by OLED for the TV screen market [14]. The inconsistency problem remains, however; the technology trend curves can vary for different forecast methods and datasets on which they are used. Combining different forecasts of the same technology allows remediation of the disadvantages from individual forecasts at the potential expense of individual advantages [8]. The authors' previous work utilized a combination of forecasts from various datasets to show that the predictive power of different forecasts varies based on the nature of the dataset used. Changes in technology term frequencies in public datasets such as news, books, and web pages are preceded by more academic datasets such as academic articles and patents, resulting in a longer predictive time window for technology growth prediction [1].

The traditional manual approach for technology forecasting requires an extensive amount of time and resources, and cheaper alternatives are highly sought after. Normative methods extrapolate on predefined technological growth curves were successful in forecasting technological development within a given technology field. They showed limited performance in forecasting related technologies. Different technologies do not necessarily follow the same growth curve. However, our work proposes a more generic forecasting model for automatic technology forecasting.

3. METHOD

The proposed method is based on analyzing the frequency trends of technology-relevant entities on academia and web each representing two different dataset orientations – academic and public. Documents in both datasets are timestamped by their publication date and can be sequentially discretized. The method consists of 1) extraction of technology-related entities having recursive encyclopaedic connections to the technology in question, and 2) identification of technology-relevant entities through the entity filtering with their timeline trend curves over two different datasets, incorporating both academic and public interests. The analysis was performed for two selected technologies, Unmanned Aerial Vehicle (UAV) and Hyperspectral Imaging (HSI), identifying relevant entities from Wikipedia articles using the entirety of academia and web. In addition, the entities were evaluated manually to showcase the necessity of multi-datasets and the possible applications of the proposed method.

3.1. Extracting Technology-Related Entities

The technology-related entities were extracted based on the Wikipedia articles. The semi-structured nature of the articles allow multiple extraction approaches; advanced natural language processing such as context recognition can be used to extract terms from the unstructured texts from the articles [15], structured data such as infobox tables or links can be utilized to extract

pre-defined terms, and the articles can be read to manually identify the related entities. The see-also section of the Wikipedia article is a list of internal pagelinks manually written by participants and moderators. The see-also section was used in this experiment as its semi-structured nature allows the extracted terms to be not limited to specific contents, domains, or types while providing human-verified semantic, syntactic, or conceptual connections between the original and linked articles.

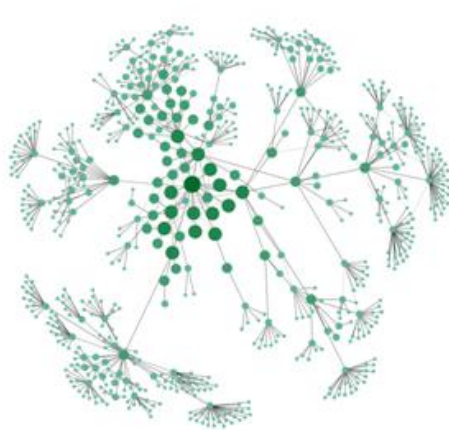


Figure 1(a). Related to *UAV*.

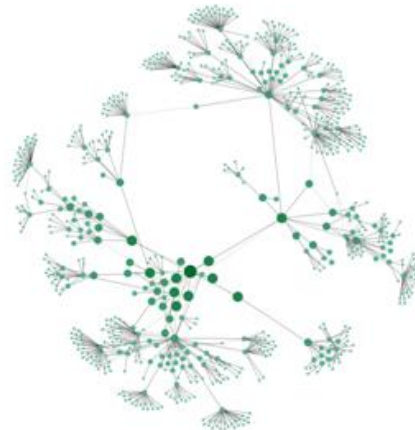


Figure 1(b). Related to *HSI*.

Figure 1. Visualizations of technology-related entities connected by see-also relationships with diminishing node size and color for entities more distant from the given technology.

Given a specified technology, such as UAV, its related entities are extracted by recursively parsing the Wikipedia articles starting from its article. The dedicated library for reading Wikipedia¹ is not ideal when multiple articles are considered, and a different approach is utilized instead. The Wikipedia article is retrieved via the webserver using a specified URL which is then processed with a Python library BeautifulSoup² to extract HTML snippet for the see-also section and the pagelinks contained within it. The articles from the collected pagelinks become the first set of technology-related entities with a distance of 1 from the seed article. The algorithm is then run recursively on the extracted articles for breadth-first entity extraction; the see-also sections for articles with distance = n are extracted to get entities with distance = $n+1$. The recursive search result in exponential growth is the number of entities found.

```

articles = technology_of_interest
output_size = 500

while articles.exists and output.length <= output_size
  for link in see_also_sections in articles
    if link is not in used
      add link to output, articles_for_next_loop
    articles = articles_for_next_loop
  return top output_size of output

```

Figure 2. Pseudocode for Extracting Technology-Related Entities.

¹<https://pypi.org/project/wikipedia/>

²<https://code.launchpad.net/beautifulsoup/>

Examples of entities with distance ≤ 4 are displayed in Figure 1(a) and Figure 1(b) based on two technologies, with articles as nodes and see-also connection as links. The node size and color intensity reflect the distance from the root node, and the graph shows mostly tree structures with only a fraction of the links between branches; such a link indicates that the articles were inversely connected. They show the majority of entities, 71.39% for UAV and 76.49% for HSI, are the furthest from the technology with distance = 4. The exhaustive search can be done for

longer distances for more than a quarter of million entities but is impractical; the authors used the first 500 results as the technology-related entities which can be satisfied with distance ≤ 4 . The pseudocode for extracting technology-related entities is shown in Figure 2, where articles are recursively searched until the given number of related articles, 500 in the experiment, are collected. Breadth-first search is done for each of the links in the articles' see-also section. The possibility of cycling is removed by only accessing newly-met articles in the process.

3.2. Extracting Technology-Related Entity Trends

The next step is the extraction of trend curves of the list of the entities found from the previous step. This is achieved by extracting their term frequencies in the large document collections at discrete timeslots, which, in this study, was yearly intervals. The whole domains of academia and web were chosen as the document collections in the experiments. The sheer volume of research publications of the WWW hinders effective searching, and the Google search engine is utilized which searches the documents indexed by Google, respectively exceeding 389 million articles [16] and 60 billion pages [17]. This allowed utilization of Google search engine APIs during the trend curve extraction process, where each data point is the number of search results in a given year. The search result for academia is the number of academic articles containing the term in their titles and abstracts, or full texts when the Google API can access them. For web, the total number of webpages containing the term is used instead. The trend curves are generated by connecting the discrete data points into a series of line graphs. The trend curves are not normalized as in the previous research [18] since the process searches not only for curves with a specific growth pattern but also curves with overall elevated values. All entities are deemed related to the technology in question and are treated equally regardless of their distances from it, or the number of see-also sections between them.

```

tag_primary, tag_secondary = "#mBMHK", "#result-stats"

for entity in entities
  for response_year in year = [2000, 2020)
    stats_year =
      if tag_primary in response_year
        then response_year.tag_primary
      else response_year.tag_secondary
    frequency = stats.result.numeric
    add (entity, year, frequency) to output
  return output

```

Figure 3. Pseudocode for Extracting Technology-Related Entity Trends.

Figure 3 shows the pseudocode for the entity trends extraction process. For each entity obtained in the previous section, the Google search result in HTML format is retrieved for every year from 2000 to 2019. The statistical metadata of the response is stored within a HTML div tag

identifiable by two possible ids, result-stats and mBMHK, which is extracted as a snippet. The search result count within the snippet is then extracted and stored as the frequency for the year. The only difference between academia and web is the structure of the URL the Google search engine requires; therefore the same implementation is used for both. The number of calls to the Google search engine is limited to 100 per day, and queries were required to be made every 100 seconds.

Results of entity trends extraction are shown in Figure 4 with four graphs. Entities related to both the UAV and HSI share similar patterns, diminishing towards the year 2019 after plateauing at around 2010 in academia in Figure 4(a) and Figure 4(c) while showing exponential growth in web in Figure 4(b) and Figure 4(d). This suggests the entities related to both technologies are experiencing initial hype with the public while the researchers have already passed this stage and show diminished interests in the same entities. Such differences are validated by the authors' previous research on the different time windows for technology growth curves in different datasets, where the technology's development starts with the academic domain and the public inherits the changes afterward [1], [18].

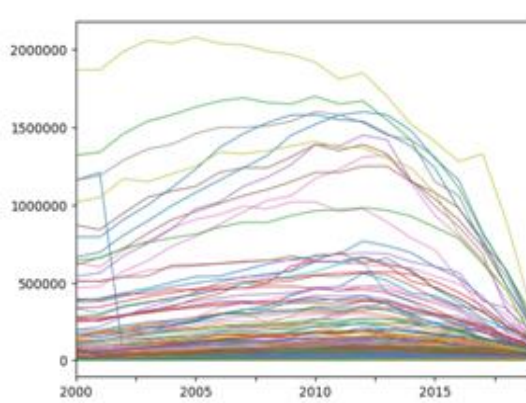


Figure 4(a). For UAV in academia.

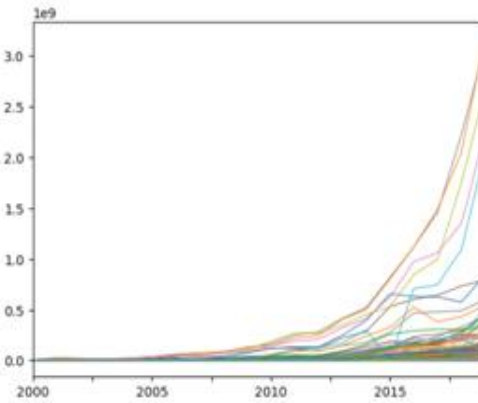


Figure 4(b). For UAV in web.

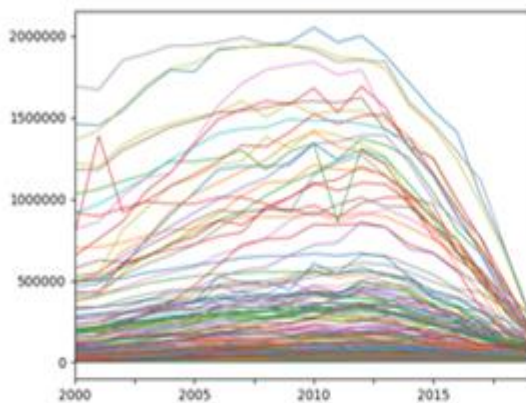


Figure 4(c). For HSI in academia.

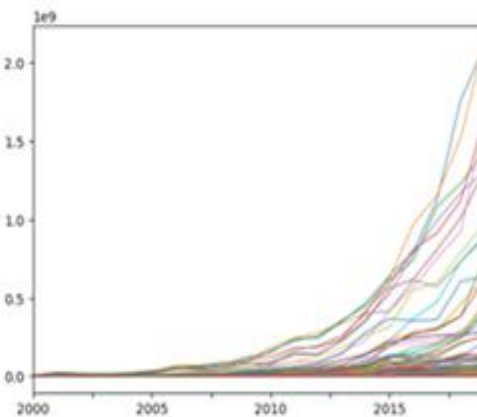


Figure 4(d). For HSI in web

Figure 4. Trend curves for technology-related entities for two technologies of interest in two different document collections.

3.3. Identifying Technology-Relevant Entities

The final process is the identification of technology-relevant entities using the trend curves extracted from the previous section. The candidates are filtered by the combined value of two features: *total_sum* representing the highest trend curves for *academia* and *moving_gradient* representing the highest growth rate at a given interval for *web*. *Total_sum* is calculated as the normalized sum of the frequencies used in the trend curve. *Moving_gradient* is calculated as the maximum normalized average gradient, where the average gradient is calculated for each timeslot using the set time window, which is set to five in this experiment; time windows over 2000 ~ 2019 are reduced to the limit of the extracted data to deal with over/underflow problems. The frequency values vary greatly from 0 to more than $2.0e^9$; therefore logscale values are used to reduce the differences between them. The algorithm uses the weighted sum of both *total_sum* and *moving_gradient* to identify top $n = 100$ entities from both *academia* and *web*. Datasets show distinctive differences in their patterns as shown in Figure 4; *academia* shows plateaued curves while *web* shows exponentially growing curves. More weight is given to the feature for the dataset it's more relevant to; *total_sum* = 0.75 and *moving_gradient* = 0.25 for *academia* and the reverse for *web* as shown in Figure 5.

```

window = 5
top_n = 100

def get_entities(data, w1, w2)
    v1 = data.log.sum.normalized * w1
    v2 = max(data.log.gradient_average_within(window).normalized) * w2
    return v1 + v2

top_entity1 = get_entities(data['academia'], 0.75, 0.25).top(top_n)
top_entity2 = get_entities(data['web'], 0.25, 0.75).top(top_n)
return common_set(top_entity1, top_entity2)

```

Figure 5. Pseudocode for identifying technology-relevant entities.

Technology-relevant entities are identified from the common denominator between the two resulting sets to allow remediation of disadvantages from individual forecasts at the expense of individual advantages [8]. Incorporating both *academia* and *web*, each representing the earliest and the latest predictive time windows, results in a set of relevant entities related to the technology of interest of both the academic interests and public recognitions. Only the entities in the final ranked list from two datasets are selected as the technology-relevant entities, allowing a different number of entities to be found for each technology.

40 for *UAV* and 39 for *HIS* appeared in both the datasets and were deemed as the technology-relevant entities as shown in Table 1 and Table 2. The score used in this stage is not used for evaluation, hence the entities are not ranked and listed in alphabetical order. They include a range of entities, from high-level domain entities such as *physics* and *data mining* to technology-specific topics such as *ultrasound* and *privacy*, to even seemingly unrelated terms such as *History of the Internet* and *CITES*. The found entities are manually inspected to discern the false positives to calculate the precision of the proposed method at identifying the relevant technologies.

Table 1. List of 40 Technology-Relevant Entities for UAV

3D modeling	Core concern	Open architecture	Ranging
Acoustic location	Data mining	Open source	Real time location system
Actuator	Digital identity	Open source hardware	Structured Analysis
Architecture description language	Environment minister	Paper plane	Surveillance
CITES	Integration platform	Privacy	System design
Configuration design	Library (computing)	Privacy by design	System in package
Conservation law	Model aircraft	Privacy laws of the United States	System of record
Continuous integration	Model engine	Privacy policy	System on a chip
Control line	Model ship	Process philosophy	Targeted advertising
Conversation (<i>disambiguation</i>)	Modular design	Radio navigation	Vocational education

Table 2. List of 39 Technology-Relevant Entities for HSI

Acoustics	Digital divide	Page table
Base address	Digital electronics	Physical symbol system
Black box	Digital recording	Physics
Candidate key	Digital video	Remote sensing
Channel (communications)	Grid computing	Search data structure
Comparison of network diagram software	History of the Internet	Shift register
Computer architecture	Information Age	Simulator
CPU design	Information system	Software diversity
Data (computing)	Internet forum	State machine
Data hierarchy	Machine vision	Ultrasound
Data mining	Memory address register	Value (computer science)
Data processing	Memory model (programming)	Web service
Digital control	Memory protection	Wireless sensor network

4. RESULTS AND DISCUSSIONS

The manual analysis showed that 35 out of the 40 entities found for UAV are relevant, resulting in a precision value of 0.875. Most of the entities fall under six major categories: 1) eight physical components such as actuator, 2) eight vehicle designs methods such as 3D modeling, 3) four navigational features such as radio navigation, 4) four surveying functions such as CITES, 5) six privacy concerns such as digital identity, 6) three other unmanned vehicles, and three uncategorized entities.

The uncategorized technology-relevant entities show hidden connections. Targeted advertising is a marketing strategy optimizing ads to the specific audiences and is mostly employed in the cyberspace, while UAV provides a physical advertising medium in the air capable of following the movement of target audiences over a long period; UAV also allows an easier generation of target-specific contents as well as cheaper aerial accessibility. Data mining is a combination of

computer science and statistics seemingly unrelated to UAV, but the increasing number of large-scale datasets such as GIS generated by drones leads to an increased need for data mining to process the raw data.

Figure 6 visualizes Wikipedia articles in a directed graph, where entities are linked by their see-also relationships with diminishing node size with longer distances from the seed. The non-relevant entities acting as a pathway are not colored to distinguish them, while the technology of interest, is colored red to signify the root node in the graph. The tree graph is divided by branches from quadcopter for UAV design and modeling, from human bycatch for navigation and privacy, and micro air vehicle for model and surveillance. The branches do not represent the human categorization; privacy and surveillance branches are far from each other even though the former is the result of the capability of the latter. This suggests that the entities are not necessarily grouped by their graphical structure, nor by their conceptual similarities. CITES, which stands for the Convention on International Trade in Endangered Species of Wild Fauna and Flora, is not related to the surveillance branch, supporting this claim. The graph also explains the existence of seemingly unrelated entities, Conversation (disambiguation) and conservation law; both are connected to the conservation node suggesting that while the former is included as a precaution for mistaking it for conversation, while the latter represents its use in the physics domain.



Figure 6. Visualization of paths to the technology-relative entities for UAV.

The manual analysis for HSI resulted in a much lower accuracy of 0.5385, showing only 21 out of the 39 entities as relevant. The majority of the entities are about the actual process of HSI, with eleven related to the data acquisition and preprocessing such as digital video and simulators and eight related to the technical and computational methods used during the process such as digital divide and shift register. Two of the remaining entities are acoustics and ultrasound related to the sound.

The differences in the accuracy can be explained by the skewness of their propagation patterns. Figure 6 for UAV shows a more balanced entity propagation – design perspective, conservation/privacy perspective, and use of micro-size vehicles. On the other hand, the tree graph in Figure 7 for HSI is more skewed towards data (computing) which has a high connection with other entities having less relationship with HSI; 17 out of the 18 unrelated entities were identified from its branch. This shows the danger of utilizing entities with too broad spectrums, where the innate connection to the technology of interest is lost, leading to highly unrelated entities such as history of the internet or physics.

Data mining is more closely related to HSI not only in the graph but also in context, as it is the data analysis technique. More layers are used compared to the related multispectral imaging, increasing the necessity of data mining techniques. Two sound-related entities connected to the root node through sonoluminescence seem unrelated, but acoustics and ultrasound are connected to HSI as they are the non-invasive remote sensing approaches sharing the same goal of collecting information without making physical contact. None of the entities directly connected to the root node in Figure 6 and Figure 7 were identified as technology-relevant entities, which, although not necessarily by design, nonetheless validates the ability of the method to identify remotely-connected entities.

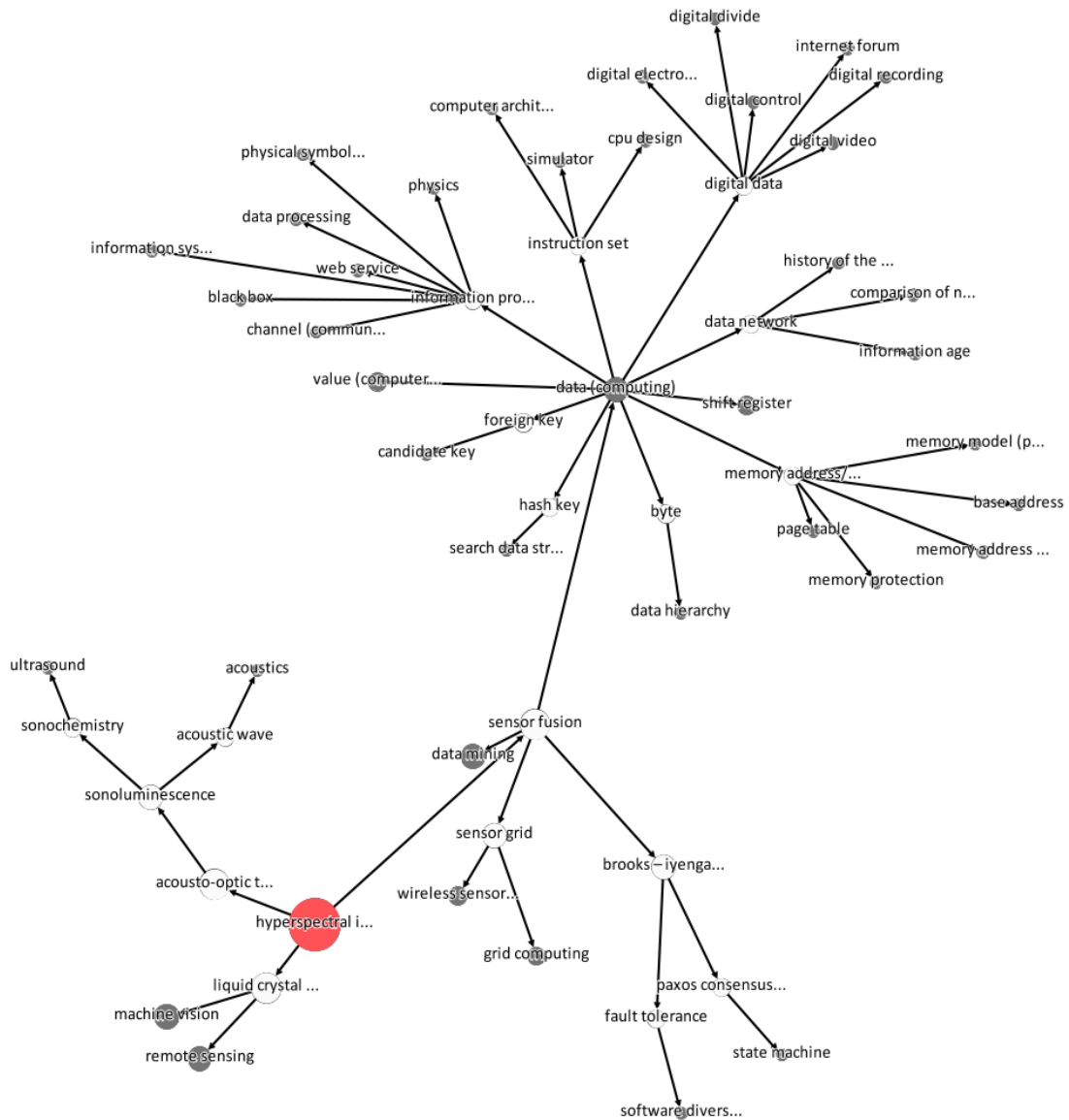


Figure 7. Visualization of paths to the technology-related entities for HSI.

5. CONCLUSION

The authors propose a method of identifying any type of entities related to a given technology based on their trend curves. The results showed that the entities with recursive relationships in Wikipedia have connections to the target technology not directly observed by either of their encyclopedic descriptions. Case studies revealed that the proposed method can identify entities related to the given technology with hidden relationships. This discovery suggests that the tacit relationships between semantically and syntactically distant technologies can be captured automatically from existing dataset. This opens a path of technology forecasting utilizing the growth of other relevant technologies.

One of the issues for the proposed method is the computational delay when generating the trend curves. The computational complexity is low for trend extraction with $O(nt)$ where n is the number of trends and t is the number of years analyzed. The computation time suffers mostly

from the Google search engine API restrictions; the number of query requests is limited to one per 100 seconds. With 20 years to analyze in two different datasets, trend curves for technology-relevant entities can be extracted in over 55.5 hours on a standard computer. Another issue that has an influence on the result is that the relatedness between technology and entities is defined as a binary, treating all related entities equally. Graphical and semantic similarities between them are omitted in the proposed method, rendering it hard to distinguish how related an entity is to the target technology, thus resulting in poor precision for *HSI* due to the entities related to *data (computing)* polluting the entity pool. Future work includes the combination of trend curves with graphical and semantic similarities. Incorporating graphical similarities would allow the method to selectively filter for specific degree of similarities, while implementation of entity filtering with textual similarities would reduce the number of times necessary to generate trend curves, speeding up the method while providing semantic similarity measures between the terms. The future works would also include experimenting on a known case of technology impacted by seemingly unrelated entities to evaluate whether the proposed method can detect such entities beforehand.

ACKNOWLEDGMENTS

This work was supported by the Deep Neural Networks for Forensic and Industry Classifications funded by the Industry Advisory Board (IAB) of an NSF Industry–University Cooperative Research Center (IUCRC) under Grant No. DFII-1903-USA.

REFERENCES

- [1] A. Segev, S. Jung, and S. Choi, “Analysis of Technology Trends Based on Diverse Data Sources,” *IEEE Trans. Serv. Comput.*, vol. 2015 Vol.8, no. 06, pp. 903–915, Dec. 2015, doi: 10.1109/TSC.2014.2338855.
- [2] P. Durance and M. Godet, “Scenario building: Uses and abuses,” *Technol. Forecast. Soc. Change*, vol. 77, no. 9, pp. 1488–1492, Nov. 2010, doi: 10.1016/j.techfore.2010.06.007.
- [3] K. C. Green and J. S. Armstrong, “Structured analogies for forecasting,” *Int. J. Forecast.*, vol. 23, no. 3, pp. 365–376, Jul. 2007, doi: 10.1016/j.ijforecast.2007.05.005.
- [4] N. Dalkey and O. Helmer, “An Experimental Application of the DELPHI Method to the Use of Experts,” *Manag. Sci.*, vol. 9, no. 3, pp. 458–467, Apr. 1963, doi: 10.1287/mnsc.9.3.458.
- [5] S. Li, E. Garces, and T. Daim, “Technology forecasting by analogy-based on social network analysis: The case of autonomous vehicles,” *Technol. Forecast. Soc. Change*, vol. 148, p. 119731, Nov. 2019, doi: 10.1016/j.techfore.2019.119731.
- [6] F. Zwicky, “The Morphological Approach to Discovery, Invention, Research and Construction,” in *New Methods of Thought and Procedure*, Berlin, Heidelberg, 1967, pp. 273–297, doi: 10.1007/978-3-642-87617-2_14.
- [7] J. P. Martino, *Technological forecasting for decision making*, 3rd ed. New York: McGraw-Hill, 1993.
- [8] J. S. Armstrong, “Forecasting by Extrapolation: Conclusions from 25 Years of Research,” *Inf. J. Appl. Anal.*, vol. 14, no. 6, pp. 52–66, Dec. 1984, doi: 10.1287/inte.14.6.52.
- [9] D. Henton and K. Held, “The dynamics of Silicon Valley: Creative destruction and the evolution of the innovation habitat,” *Soc. Sci. Inf.*, vol. 52, no. 4, pp. 539–557, Dec. 2013, doi: 10.1177/0539018413497542.
- [10] O. Dedehayir and M. Steinert, “The hype cycle model: A review and future directions,” *Technol. Forecast. Soc. Change*, vol. 108, pp. 28–41, Jul. 2016, doi: 10.1016/j.techfore.2016.04.005.
- [11] J. S. Armstrong and F. Collopy, “Error measures for generalizing about forecasting methods: Empirical comparisons,” *Int. J. Forecast.*, vol. 8, no. 1, pp. 69–80, Jun. 1992, doi: 10.1016/0169-2070(92)90008-W.
- [12] D. M. Blei and J. D. Lafferty, “Dynamic Topic Models,” in *Proceedings of the 23rd International Conference on Machine Learning*, New York, NY, USA, 2006, pp. 113–120, doi: 10.1145/1143844.1143859.

- [13] N. Takeda, Y. Seki, M. Morishita, and Y. Inagaki, "Evolution of Information Needs based on Life Event Experiences with Topic Transition," in Proceedings of the 40th International ACM SIGIR Conference on Research and Development in Information Retrieval, Shinjuku, Tokyo, Japan, Aug. 2017, pp. 1009–1012, doi: 10.1145/3077136.3080703.
- [14] Y. Cho and T. Daim, "OLED TV technology forecasting using technology mining and the Fisher-Pry diffusion model," *Foresight*, vol. 18, no. 2, pp. 117–137, Jan. 2016, doi: 10.1108/FS-08-2015-0043.
- [15] A. Segev, "Circular context-based semantic matching to identify web service composition," in Proceedings of the 2008 international workshop on Context enabled source and service selection, integration and adaptation organized with the 17th International World Wide Web Conference (WWW 2008) - CASSIA '08, Beijing, China, 2008, pp. 1–5, doi: 10.1145/1361482.1361489.
- [16] M. Gusenbauer, "Google Scholar to overshadow them all? Comparing the sizes of 12 academic search engines and bibliographic databases," *Scientometrics*, vol. 118, no. 1, pp. 177–214, Jan. 2019, doi: 10.1007/s11192-018-2958-5.
- [17] M. de Kunder, "The size of the World Wide Web (The Internet)," Mar. 07, 2020. <https://www.worldwidewebsite.com/>.
- [18] A. Segev, C. Jung, and S. Jung, "Analysis of Technology Trends Based on Big Data," in 2013 IEEE International Congress on Big Data (BigData Congress), Jun. 2013, pp. 419–420, doi: 10.1109/BigData.Congress.2013.65.

AUTHORS

Sukhwan Jung is a Postdoc in the Department of Computer Science, University of South Alabama. He earned his Ph.D. in Knowledge Service Engineering at KAIST in 2020



Rachana Reddy Kandadi is a Master's degree student in the Department of Computer Science, University of South Alabama. She earned her undergraduate degree from JNTUH in Computer Science and Engineering.



Rituparna Datta is a Computer Research Associate-II in the Department of Computer Science, University of South Alabama. Prior to that, he was an Operations Research Scientist in Boeing Research & Technology (BR&T), BOEING, Bangalore



Ryan Benton is an Assistant Professor in the Department of Computer Science at the University of South Alabama. His research interests lie in the fields of data mining and machine learning, with a current focus upon advanced pattern mining methods, novel graph mining algorithms, and applied applications



Segev Aviv is an Associate Professor in the Department of Computer Science at the University of South Alabama. His research interest is looking for the DNA of knowledge, an underlying structure common to all knowledge, through analysis of knowledge models in natural sciences, knowledge processing in natural and artificial neural networks, and knowledge mapping between different knowledge domains.



CONTEXTUAL FACTORS INFLUENCING THE DESIGN AND MANAGEMENT OF HEALTH INFORMATION SYSTEMS' INTEROPERABILITY

Grace Kobusinge^{1,2}

¹Gothenburg University, Gothenburg, Sweden

²Makerere University, P.O. Box 7062 Kampala, Uganda

ABSTRACT

Due to their renowned great information processing and dissemination power, Health information systems (HIS) can readily avail past patient medical information across the continuum of care in order to facilitate ongoing treatment. However, a number of existing HIS are designed as vertical silos with no interoperability onuses and therefore, cannot exchange patient information. At the same time, there is limited knowledge about the intricacies and factors that surround HIS' interoperability implementations. This study therefore, employs an institutional lens perspective to investigate contextual factors influencing HIS' interoperability designing. Through this perspective, seven contextual factors were arrived at institutional autonomism, intended system goals, existing health-information-systems, national HIS implementation guidelines, interoperability standards, policy and resources in terms of money and labour. A further study implication is the use of institutional lens in making sense of the institutions' context of integration in order to discover salient factors that might influence health-information-systems' interoperability designing.

KEYWORDS

Health Information Systems' Interoperability, Design and Management, Contextual Factors.

1. INTRODUCTION

Health information system (HIS) implementation has of recent been top on agenda of most federal governments and healthcare institutions [1]. This is because HIS have proved to be useful in managing health information [2, 3] and still promise among others improved patient care and coordination as they become more interoperable [4-6]. HIS are interoperable if they can work together to effectively deliver healthcare within and across organizational boundaries [7]. Currently, a number of HIS are non-interoperable, given that they are designed as vertical silos [8-10]. Consequently, in efforts to aid ongoing treatment, several healthcare centers experience patient information exchange challenges [11, 12]. Nonetheless, to overcome such challenges, [8] among other authors call for the design and implementation of horizontally integrated health information systems.

However, there exists considerable research about interoperability and HIS integrated systems [8], but there is limited knowledge on the intricacies of their implementation processes [1, 13-15]. Yet according to [16] a system is as good as its implementation process. Therefore, to further understanding of the HIS implementation process intricacies, [17-22] emphasize the examination of salient contextual factors that influence the implementation process. Contextual factors are key

features within the environment that influence the intervention [23]. They can either enable or hinder successful implementation of information communication systems [23, 24]. According to [25-27] successful information system interoperability implementations depend on the context of integration. They [25] and [27] state that the choice of an

interoperability principle greatly depends on the context of integration. An interoperability principle is a communication link between information systems that enables them to exchange information [27]. Therefore, a thorough analysis of the context of integration [25, 27] and the discovery of salient contextual factors might increase HIS interoperability implementations [28]. To better understand salient organizational and institutional factors [29] recommend the use of institutional theory in such studies. They assert that institutional theory helps researchers to analyze both internal and external factors influencing the implementation process. At the same time [30] calls for proper management of the entire context analysis process, and [31] argues for both management and designing of organizational interoperability. Indeed several authors argue for interoperability designing during system implementation [6, 32], and [15] argues for tactful management of the implementation process. Therefore, in order to improve understanding of the intricacies surrounding the design and management of HIS interoperability process, this study draws on institutional theory to examine contextual factors that influence such processes.

The structure of this paper is as follows: In the theoretical framing section, institutional theory is explored as a framework within which to analyze internal and external contextual factors that influence HIS interoperability implementations. The research approach section describes the study as an interpretative case study, and explains the data collection and analysis methods applied. Study findings are presented in the fourth section as contextual factors. This is followed by a discussion of identified contextual factors according to their degree of controllability and their influence on HIS interoperability implementations. The final section concludes the paper and proposes future works regarding contextual HIS interoperability management and designing.

2. THEORETICAL FRAMING: INSTITUTIONAL THEORY

Healthcare systems usually consist of a number of institutions [33], and according to [34] institutions are social structures that have attained higher degrees of resilience, and legitimacy. Institutions are composed of cultural-cognitive, normative, and regulative elements that together with other factors provide stability [34, 35]. Therefore according to institutional theory, organizations are influenced by both internal and external pressures within the environment in which they operate [36]. Accordingly, institutional theory helps in understanding inherent relationships among institutional mechanisms and other organizational factors [37]. Usually, prevailing coercive, mimetic and normative isomorphic forces largely shape the institution [38]. Whereby coercive forces are formal and informal political influences that institutionalize certain practices, mimetic forces are pressures to mimic other similar institutions, and normative forces are those associated with professionalization of organizational actors [38]. A number of researchers have used institutional theory, but this study has been inspired by [29] who used institutional theory to understand barriers to e-government interoperability, and [39] who used it to study enterprise architectures and interoperability in governments. Thus, this study employs institutional theory to analyse internal and external contextual factors that influence health institutions' legitimate behaviours [38] during the design and management of HIS interoperability.

3. RESEARCH APPROACH

The study employed a case study perspective [40] where participants' responses were conceptualized to construct meaning according to the study objectives [41]. A case study perspective was chosen in order to explore and illustrate the HIS implementation phenomena in action [40, 42]. Through qualitative research methods that included; semi-structured interviews, document reviews and focused group meetings [40, 43] data was collected and analysed through the general inductive analysis method [44]. The inductive analysis method consisted of several phases, right from interview transcription to refinement of categories in relation to the study objectives [44].

3.1. Case Study Setting and Description

The case study investigated health information systems used across health facilities in Uganda. Uganda is a developing country in Africa that is highly embracing HIS use at most of its health facilities [45]. Health facilities in Uganda are either public or privately owned, and are at different regulatory levels; national/regional referrals, district hospitals and health-center IV-I respectively [45]. However, each health institution operates independently and can implement its own HIS, thus the numerous HIS in use within the country [46]. Particularly, for this study, participating HIS were identified through a field exploration of the implemented HIS within the country that was carried out from July 2017 to July 2018. Through this field exploration it was discovered that many systems were donor funded and would not go beyond the piloting stage whenever the funded project ended [47]. Therefore, stable health information systems that were sustainable and widely used across health facilities were singled out. Consequently, with insights from the ministry of health officials, five outstanding health information systems were considered for the study. They included Uganda-EMR, District Health Information System - DHIS2, HeleCare2x, Clinic master and Nganisha health information system as per their description in Table 1. Consequently, the study participants consisted of five ministry of health officials, fifteen systems developers, and seven projects managers for the identified HIS.

Table 1. Description of studied HIS.

Health information system	Description
Uganda-EMR	Uganda-EMR. This is customized 'Open-MRS' electronic medical records system for Uganda. The ministry of health has recommended it to be the nation's patient records' system. Pilot testing on the HIV-AIDS module are ongoing in selected districts within the country. http://emrportal.mets.or.ug/
DHIS2	District Health Information System -DHIS2 is a health management system that provides a logical platform for data entry, processing, and data presentation to national planners" [33]
HeleCare2x	HeleCare2x: Customized for Uganda from Care2x, it is an Integrated Hospital Information System that includes: Admission, Surgery, Outpatient, Nursing, Wards, Pharmacy, Labs and Security among others [48]. It provides one complete single patient record at the health facility. (http://care2x.org/).
Clinic master	Clinic master: this integrated health information management and medical billing system automates patients' transactions at the clinic on a visit basis. It is mostly used by private health institutions. https://clinicmaster.net/about-us/
Nganisha	Nganisha health information system is an all-inclusive health management information system that provides real time and complete patient health data at a health facility. Current pilots are in government health facilities (western and eastern Uganda) by health net chattered Uganda. https://twitter.com/ugandahealthnet .

3.2. Data Collection

Data collection involved interviews, focus group discussions, and document reviews [43]. Semi-structured interviews were used to generate deep and rich interactions during the interviews, whereby the researcher made sense of the interviews by constructing meaning. Interviews for project managers and system developers focused on extracting responses regarding external and internal salient factors onto which they based HIS implementation decisions. Whereas ministry of health officials' interviews focused on the kind of HIS in use, interoperability structures or policies in place and national HIS implementation guidelines in place. All interviews were recorded with permission and each session lasted approximately 70 minutes. System developers were interviewed more than once in order to get rich data and insights of what transpired during the HIS implementation process. In order to confirm what was reported in the interviews [41], key documents including Uganda e-health policy, HIS developers' websites and the national sector development plan were reviewed. In addition, this study adhered to ethical issues of confidentiality, integrity and anonymity [49].

3.3. Data Analysis

The data analysis stage consisted of several phases, with verbatim transcription [50] in the early phases. This was followed by reading the interview transcripts several times in order to make sense of the study objectives [44]. This analysis phase enabled the identification and construction of contextual factors that influence the design and management of HIS interoperability. Inspired by institutional theory the researcher identified respondent phrases that pointed to either an external or an internal need/pressure that influenced their HIS implementation decisions concerning interoperability. The last phase was to revisit the data in order to re-examine the identified working categories and refine them into final categories. Particularly, ten working categories were refined into seven final categories of contextual factors.

4. RESULTS

This section presents seven contextual factors that influence the design and management of HIS interoperability as described below. These factors were determined from external and internal pressures that influenced the HIS implementation process according to institutional theory.

4.1. Intended System Goals

In order to fulfil their core values, institutions often implement information systems for smooth operations. However, in any system development process, the first phase is always focused on eliciting the requirements of the system [51]. For successful requirement elicitation [51] recommends a goal driven approach. Therefore, in consultation with the system users, designers look out for system requirements vs intended system goals. They ask questions like; why is the system being designed, and what is it going to serve. Within this phase the intended system users present their requests of what the system should offer, and to the designers these form system requirements. Ultimately, these system requirements mirror the intended goal of the system. The system is then designed according to the requirements presented by its intended users. For example, if the users' requirement were that the system should share data with other HIS, then it would be designed as interoperable else it would be designed with no focus on interoperability. This is evident in the following participants' verbatim quotes.

“Implementation decisions are made based on client needs”, “Yes so it is more of demand driven, we build on demand” and “but if we have a requirement (need/goal) that it must talk to

some other system, then we ensure we produce the right data either as input or output for any system.”

Therefore, if interoperability is among system requirements, then it can inherently/purposively be designed [6] else it will be designed in future as need arises. Therefore, initial goals of the system/system requirements can greatly influence system design and implementation. They determine whether interoperability capabilities should be designed along or not [52].

4.2. National HIS Implementation Guidelines

Systems cannot interoperate unless interoperability capabilities are designed consciously into them, either inherently or at the time of need [52, 53]. This implies that in order to have HIS that are interoperable, there ought to be standard HIS implementation guidelines for all participating systems [54, 55]. ISO-2004 standard asserts that any systems planning to integrate should do so according to prescribed methods [56] and according [57] organizations have to mutually agree to interact, though this tends to be hard in practice [58]. In Uganda, HIS developers are required to follow the current HMIS tools during system implementation as a minimum ministry of health directive. HMIS tools are local paper forms that are standardised specifically for data collection about key health indicators at health facilities. Therefore, authorities in a given country ought to enforce uniform HIS interoperability implementation guidelines, else every single HIS will be developed independently following institution specific guidelines. Below is a respondent verbatim quote about HIS implementation guidelines in Uganda.

“We had no regulatory framework, no policy, no standards, no interoperability framework, people just implement haphazardly without following any guidelines from the ministry.”

However, all hope for Uganda is not lost as the design for an interoperability architecture is underway. Once the interoperability architecture is institutionalized and operationalized, all HIS developed in the country will be required to adhere to it, which could advance HIS interoperability implementations in the country. Here we clearly see coercive forces at play, when standard HIS implementation guidelines become a rule of thumb.

4.3. Interoperability Standards

Interoperability standards “facilitate seamless sharing of information between health information systems” [54, 59]. They could be messaging standards, terminology standards and general interoperability standards [54, 59] specifically, for healthcare they could include standard disease classifications and standardized electronic health records among others [54]. Enforcement of such uniform interoperability standards at national or institutional level might lead to implementation of interoperable HIS. The importance of interoperability standards is actually identified in the following respondent verbatim quotes:

“Mainly, we look at software development standards that allow interoperability, we use mainly REST.” “As long as that system is compatible to some standard there can be a possibility of sharing data with the other systems.” “... On top of what the users have requested, there are some standards.”

In contrast, lack of uniform interoperability standards leads to the design of health information systems that are not interoperable [11], since they are designed following institution specific standards. This is reflected in the following respondent verbatim quote. “That is one of the main problems of systems we have been having, most of them have their own standards.” Nevertheless, it is important to know the kind of data that needs to be shared, else each system

will define its own, and there will not be a standard patient record to share. The importance of defining a standard patient record can be seen in the following participants' verbatim quotes.

"We are restricted in what to move." "We have tried to look for any document that defines that but in vain. All of them stop on the point of integration and interoperability but they don't narrow down on what should be shared."

4.4. Institutional Autonomism

According to [60] institutional autonomism can greatly influence the system integration process. In Uganda health institutions are either publically owned or privately owned [45]. The public owned are entirely under government leadership and the private ones are under institutional governance. Whereas public health institutions entirely implement government directives and recommended health systems, private institutions tend to be hesitant. A case in point is the Uganda Ministry of health directive to use DHIS2 system at all health facilities, whereas public health institutions use DHIS, private institutions rarely use it, as reflected in the following respondent verbatim quote.

"...all these health facilities are obliged to report ...whether private or public, but again the private clinics they do not report."

In most cases, autonomous institutions implement their own HIS and follow their own institution-specific implementation guidelines. Due to institutional logics, [39] argues that organizations can implement their own systems, and can even mimic other systems. Such practises can increase system fragmentation and duplication, and can affect a countries' HIS interoperability plans. Consequently, the nation ends up having numerous silos HIS that are non-interoperable and cannot share/exchange health data. For example three of the studied Uganda systems (Nganisha, Clinic master and HeleCare 2x) are all focused on providing one complete single patient record at the health facility.

On the other hand collaboration among health institutions is a key ingredient to interoperability designing however, there is little coordination amongst healthcare units and little communication between different health information systems [61]. In effect, most institutions tend to own their health data and are not open to external discussions [6]. They usually consider their data as an institutional asset or are prohibited by donor specific regulation as evident in the following participants' verbatim quotes.

"There is no will to share in private hospitals, though the government wants to integrate health systems." "... ownership of the data is a big issue, each entity believe that they own there data and remember each entity is autonomous so there is a lot of negotiation that is involved."

"... We have asked how come they are not interoperable... this is given by the donor and they are not willing to integrate."

4.5. Policy

Due to coercive isomorphism, institutions are subjected to certain important laws or rules that govern them [62]. These laws could be in form of policies since a policy is a rule of law according to [63]. Regarding HIS implementations, policies could concern system development, system integration, data sharing and information exchange, security and privacy of sensitive health data among others. Such policies once institutionalized [55, 64] could help direct HIS

interoperability implementations within a country. For example, Uganda has an operational e-health policy within which all HIS in the country must be interoperable, and must integrate with DHIS2. DHIS2 is the countries' national aggregation system for key health indicators. For example, data sharing policies ought to take into consideration the sensitivity of health data, when it comes to cross boundaries exchanges. For example, due to the sensitivity of health data, HIS in Uganda are restricted from exchanging or even clouding patient medical information. In effect, policy regulations influence the way HIS are implemented, either as interoperable or as non-interoperable. The following are respondent verbatim quotes concerning the influence of policy to HIS interoperability implementations.

"...policy is one of those challenges." "...but the challenge comes in with policy, policy of Uganda especially health does not allow clouding patient information." what is restricting is not the technology but is policy and maybe human resource but technology-wise we are already there."

4.6. Existing Health Information Systems

Health information systems' interoperability is achieved when all participating systems are able to share and exchange health data amongst themselves [65]. However, interoperability is a capability [31, 53] which can be present or missing in a given system. It is therefore, important to scrutinize all existing HIS of their interoperability capabilities [66] in order to plan their compatibility with other systems [67]. According to [58] existing systems highly influence interoperability designing, they determine if a standard-approach can be taken or not. For instance, the Ministry of health of Uganda in 2018 carried out an e-health readiness assessment to examine existing HIS in order to determine those to scale out and those to eliminate.

"...in the interim period we wanted to look at the criteria.... For example EMRs what should they look at, before I approve an EMR to be used in the country ... to have a benchmark, to see how can we assess and agree whether we should adopt this or we feel this EMR has worked in five districts why can't we scale it up instead of having another one"

In addition, observed benefits from existing systems can lead to implementation of similar interoperable systems due to institutional mimetic forces. A case in point is the district health information system – DHIS2, which is taken as the countries' model system, and thus the proposal to integrate all other systems to DHIS2. Therefore, existing systems have a great influence on the design and management of health information systems' interoperability, as expressed in the following respondent verbatim quotes:

"Yeah we looked at other systems." "...of course there were systems that were running like open MRS but they were specific to programs. They were not general, that is when we opted to design our own health management system."

4.7. Resources

To have successful interventions and system sustainability, stable resources are required. These resources could include money, labour and time among others. For HIS interoperability implementation projects having skilled system developers and experienced top managers would be rewarding [68]. Managers and systems developers would work collaboratively for the success of the HIS interoperability implementation project. [68] refers to a successful HIS interoperability intervention where managers worked closely with system designers and vendors. For example in Uganda at the national level, the authorities have planned for interoperability, but at the implementation level these authorities are missing and have not managed the design of

interoperability. As a result a number of silos HIS have been developed independently [46] with no or limited reference to the national interoperability architecture that is under construction. It is therefore, not enough for the authorities to issue a directive on interoperable systems, but rather they should supervise and enforce strict adherence to the recommended HIS interoperability implementation guidelines. In addition, the available staff should be skilled and should be able to carry out their roles effectively, though this is still a challenge in Uganda. The following respondent verbatim quotes point human resources as an important factor for the design and management of HIS interoperability.

“...there is a lot of things that need to be thought thru ...policies and other players say human resource and all that to deal with interoperability.” “Human recourse in Uganda is still lacking a lot when it comes to technology empowerment.”

On the other hand, another important resource is having enough money to finance all project activities [17, 68] as need arises. For example, a number of HIS implementations in Uganda are donor funded and are not sustainable once the project ends. Most of these donor-funded projects are disease specific e.g HIV-AIDS, so they focus on a narrow problem and lead to a pool of fragmented HIS all over the country, as reflected in the following respondent quote.

“..However, that RX-solution doesn't have an API, doesn't talk to macs & sage....we have asked how come they are not interoperable,....this is given by the donor and they are not willing to integrate.”

It implies that having enough money to implement and sustain inclusive interoperable HIS, might eliminate standalone disease specific systems. Yet, implementing inclusive interoperable HIS is very costly, and the health institutions are not ready to bear that high cost as seen in the following respondent verbatim quotes.

“...because you see the cost of integration is going to be borne by the facilities..... I do not think they have been able to quantify the exact benefit. “It would not actually be hard...I think it is an issue of resources not being allocated to that.”

In other words, HIS interoperability implementations within a country could increase once a country's digital healthcare system is centrally driven and financed by the government. As seen in the five countries investigated by [69] that have employed a centralised mechanism of coordination, legislation and management of all their healthcare services. Therefore, cost and human resources highly influence HIS interoperability implementations.

5. DISCUSSION

This study presents a number of contextual factors that can influence HIS interoperability implementations, and further discusses their levels of controllability, as emphasised by [70]. Particularly, in this study some of the identified factors were controlled to some degree yet others could not be controlled at the implementation level -they were a 'must' follow [70]. The degree of controllability could be attributed to isomorphism forces, which according to [38] include coercive, normative and memetic institutional forces. With such forces at play sometimes, organizations live in what [71] refer to as an iron cage. For instance, in this case-study internal factors that were determined locally at the institutional level or by the implementation team could be controlled, but external factors were not feasibly controllable. External factors were primarily influenced by coercive forces and internal factors were primarily influenced by normative and memetic forces.

Coercive forces could include national, international, or institutional policies, norms, values [38], standard operating procedures as well as national system implementation guidelines, which health institutions have to adhere to. In this study, coercive external factors included policy, interoperability standards, HIS implementation guidelines and existing health information systems. These were followed as is with exception of 'existing health information systems' that could be manipulated by the implementers, through human agency [72] and enactment [73]. Whereas internal factors included intended system goals, existing health information systems, resources and institutional autonomism, which were greatly manipulated by the HIS implementers. It is therefore important to understand beforehand the kind of contextual factors that might affect the HIS implementation process in order to mitigate them accordingly. As it is likely that the implementers will have limited or no control on external factors but can fully control the internal factors, for optimal management and design of health information systems' interoperability. However, depending on the prevailing conditions and the degree of controllability a given contextual factor can either hinder or enable intervention success [23, 24]. For example, when the initial system goals, policies, standards, and HIS interoperability implementation guidelines are in support of HIS interoperability, the developed systems are often interoperable else they are non-interoperable. At the same time when there are enough recourses in terms of money and skilled labour the HIS interoperability intervention would be successful else it would be negatively affected [68]. Yet again when existing HIS have attained a certain degree of interoperability maturity, then HIS interoperability implementations could be feasibly negotiated and enhanced.

Consequently, this study highlights the importance of context awareness and readiness, since awareness of the likely influence of certain contextual factors and their degree of controllability beforehand would prepare the system implementers [55, 70] on how to design and manage HIS interoperability. For instance, in situations where organisations live in what [71] calls a 'cage', organizations can be empowered and prepared to overcome the prevailing institutional logics, and pressures.

6. CONCLUSION AND FUTURE WORKS

This study intended to investigate contextual factors that influence the design and management of HIS interoperability. Expediently, a number of contextual factors including institutional autonomism, intended system goals, existing health information systems, national HIS implementation guidelines, interoperability standards, policy and resources were arrived at. However, due to institutional isomorphism, external contextual factors are not feasibly controllable at the project implementation level, but internal factors could be controlled. The study holds that contextual factors could either enable or hinder HIS interoperability implementations. Therefore, awareness of the likely contextual factors beforehand would greatly improve HIS' interoperability design and management. In conclusion, the study proposes the following as future works: (a) a focus on contextual factors in HIS interoperability design and management. (b) A focus on institutionalising laws, frameworks, guidelines, standards and policies that support HIS integration [64]. (c) Investigation of the potential of institutional lens in making sense of the institutions' context of integration, in order to discover salient factors that might affect HIS' interoperability designing.

REFERENCES

- [1] Heavin, C., Health Information Systems—Opportunities and Challenges in a Global Health Ecosystem. *Journal of the Midwest Association for Information Systems* | Vol, 2017. 2017(2): p. 1.
- [2] Demirci, U., S. Wang, and F. Inci, Editorial for Advanced Health Care Technologies. *Advanced Health Care Technologies*, 2015. 1: p. 1-2.
- [3] Demiris, G., et al., Patient-centered applications: use of information technology to promote disease management and wellness. A white paper by the AMIA knowledge in motion working group. *J Am Med Inform Assoc*, 2008. 15(1): p. 8-13.
- [4] Bodenheimer, T., Coordinating care—a perilous journey through the health care system. 2008, Mass Medical Soc.
- [5] Coleman, E.A., Falling through the cracks: challenges and opportunities for improving transitional care for persons with continuous complex care needs. *Journal of the American Geriatrics Society*, 2003. 51(4): p. 549-555.
- [6] Kobusinge, G., et al. The (Missing?) Role of Health Information Systems (HIS) in Patient Care Coordination and Continuity (PCCC): The Case of Uganda. in *International Conference on e-Infrastructure and e-Services for Developing Countries*. 2018. Springer.
- [7] HIMSS, *Dictionary of Healthcare Information Technology Terms, Acronyms and Organizations*, p. 75. 3rd ed. 2013.
- [8] Adenuga, O.A., R.M. Kekwaletswe, and A. Coleman, eHealth integration and interoperability issues: towards a solution through enterprise architecture. *Health information science and systems*, 2015. 3(1): p. 1-8.
- [9] Bygstad, B., O. Hanseth, and D.T. Le. From IT Silos to Integrated Solutions. A Study in E-Health Complexity. in *ECIS*. 2015.
- [10] Weber-Jahnke, J., L. Peyton, and T. Topaloglou, eHealth system interoperability. *Information Systems Frontiers*, 2012. 14(1): p. 1-3.
- [11] Adebessin, F., et al., A review of interoperability standards in e-Health and imperatives for their adoption in Africa. *South African Computer Journal*, 2013. 50(1): p. 55-72.
- [12] Kuziemsky, C.E. and J.H. Weber-Jahnke, An ebusiness-based framework for ehealth interoperability. *Journal of Emerging Technologies in Web Intelligence*, 2009. 1(2): p. 129-136.
- [13] Abbott, P.A., et al., Complexity and the science of implementation in health IT—knowledge gaps and future visions. *International journal of medical informatics*, 2014. 83(7): p. e12-e22.
- [14] Barbarito, F., et al., Implementing standards for the interoperability among healthcare providers in the public regionalized Healthcare Information System of the Lombardy Region. *Journal of biomedical informatics*, 2012. 45(4): p. 736-745.
- [15] Kobusinge, G., et al. An Implementation Process of Interoperability: A Case-Study of Health Information Systems (HIS). in *Designing Digitalization, ISD*. 2018. Lund, Sweden.
- [16] Ludwick, D.A. and J. Doucette, Adopting electronic medical records in primary care: lessons learned from health information systems implementation experience in seven countries. *International journal of medical informatics*, 2009. 78(1): p. 22-31.
- [17] Axelsson, K. and U. Melin. Contextual Factors Influencing Health Information Systems Implementation in Public Sector—Investigating the Explanatory Power of Critical Success Factors. in *International Conference on Electronic Government*. 2014. Springer.
- [18] Brown, N. and I. Brown. Contextual factors influencing strategic information systems plan implementation. in *Proceedings of the South African Institute of Computer Scientists and Information Technologists Conference on Knowledge, Innovation and Leadership in a Diverse, Multidisciplinary Environment*. 2011. ACM.
- [19] Carvalho, J.V., Á. Rocha, and A. Abreu, Maturity models of healthcare information systems and technologies: a literature review. *Journal of medical systems*, 2016. 40(6): p. 131.
- [20] Coles, E., et al., The influence of contextual factors on healthcare quality improvement initiatives: what works, for whom and in what setting? Protocol for a realist review. *Systematic reviews*, 2017. 6(1): p. 168.
- [21] Cucciniello, M., et al., Understanding key factors affecting electronic medical record implementation: a sociotechnical approach. *BMC health services research*, 2015. 15(1): p. 268.

- [22] Dopson, S., L. Fitzgerald, and E. Ferlie, Understanding change and innovation in healthcare settings: reconceptualizing the active role of context. *Journal of change management*, 2008. 8(3-4): p. 213-231.
- [23] Ogrinc, G., et al., SQUIRE 2.0 (Standards for Quality Improvement Reporting Excellence): revised publication guidelines from a detailed consensus process. *The Journal of Continuing Education in Nursing*, 2015. 46(11): p. 501-507.
- [24] Gichoya, D., Factors affecting the successful implementation of ICT projects in Government. 2005.
- [25] Hugoson, M.-Å., T. Magoulas, and K. Pessi, Interoperability strategies for business agility, in *Advances in enterprise engineering I. 2008*, Springer. p. 108-121.
- [26] Novakouski, M. and G.A. Lewis, Interoperability in the e-Government Context. 2012, CARNEGIE-MELLON UNIV PITTSBURGH PA SOFTWARE ENGINEERING INST.
- [27] Solotruk, M. and M. Krištofič, Increasing the degree of information system integration and developing an integrated information system. *Information & Management*, 1980. 3(5): p. 207-212.
- [28] Ullah, F., et al., Semantic interoperability for big-data in heterogeneous IoT infrastructure for healthcare. *Sustainable Cities and Society*, 2017. 34: p. 90-96.
- [29] Manda, M.I. and J. Backhouse. An analysis of the barriers to e-government integration, interoperability and information sharing in developing countries: A systematic review of literature. in *Proceedings of the African Conference in Information Systems and Technology*, Accra, Ghana. 2016.
- [30] Pettigrew, A.M., Context and action in the transformation of the firm: A reprise. *Journal of Management studies*, 2012. 49(7): p. 1304-1328.
- [31] Rauffet, P., C. Da Cunha, and A. Bernard. Designing and managing Organizational Interoperability with organizational capabilities and roadmaps. in *Interoperability for Enterprise Software and Applications China, 2009. IESA'09. International Conference on. 2009. IEEE.*
- [32] Harvey, F., Designing for interoperability: Overcoming semantic differences, in *Interoperating Geographic Information Systems. 1999*, Springer. p. 85-97.
- [33] Braa, J., et al., Developing health information systems in developing countries: the flexible standards strategy. *Mis Quarterly*, 2007: p. 381-402.
- [34] Scott, W.R., *Institutions and Organizations. 2nd ed ed. Vol. 2nd ed. 2001: Thousand Oaks, CA: Sage, 2nd ed.*
- [35] Scott, W.R., Institutional theory: Contributing to a theoretical research program. *Great minds in management: The process of theory development*, 2005. 37(2005): p. 460-484.
- [36] Bjorck, F. Institutional theory: A new perspective for research into IS/IT security in organisations. in *37th Annual Hawaii International Conference on System Sciences, 2004. Proceedings of the. 2004. IEEE.*
- [37] Luna-Reyes, L.F., J.R. Gil-Garcia, and C.B. Cruz, Collaborative digital government in Mexico: Some lessons from federal Web-based interorganizational information integration initiatives. *Government Information Quarterly*, 2007. 24(4): p. 808-826.
- [38] DiMaggio, P.J. and W.W. Powell, The iron cage revisited: Institutional isomorphism and collective rationality in organizational fields. *American sociological review*, 1983: p. 147-160.
- [39] Hjort-Madsen, K. Enterprise architecture implementation and management: A case study on interoperability. in *System Sciences, 2006. HICSS'06. Proceedings of the 39th Annual Hawaii International Conference on. 2006. IEEE.*
- [40] Creswell, J.W., *Research Design: Qualitative, Quantitative and Mixed Method Approaches 3rd ed. 2009, Los Angeles: SAGE Publications.*
- [41] Rowlands, B., Employing interpretive research to build theory of information systems practice. *Australasian Journal of Information Systems*, 2003. 10(2).
- [42] Thomas, G., A typology for the case study in social science following a review of definition, discourse, and structure. *Qualitative inquiry*, 2011. 17(6): p. 511-521.
- [43] Cibangu, S.K., Qualitative research: The toolkit of theories in the social sciences, in *Theoretical and methodological approaches to social sciences and knowledge management. 2012, InTech.*
- [44] Thomas, D.R., A general inductive approach for analyzing qualitative evaluation data. *American journal of evaluation*, 2006. 27(2): p. 237-246.
- [45] Mukasa, N., Uganda Healthcare system profile: background, organization, polices and challenges. *J Sustain Reg Health Syst*, 2012. 1: p. 2-10.
- [46] Kiberu, V.M., M. Mars, and R.E. Scott, Barriers and opportunities to implementation of sustainable e-Health programmes in Uganda: A literature review. *African Journal of Primary Health Care and Family Medicine*, 2017. 9(1): p. 1-10.

- [47] Omaswa, C. UGANDA NATIONAL EHEALTH STRATEGIC PLAN 2012/2013 – 2014/2015 2012 [cited 2018 20/06]; Available from: http://www.ubts.go.ug/assets/publications/Uganda%20National%20eHealth%20Strategic%20Plan_April%202013.pdf.
- [48] Kanagwa, B., J. Ntacyo, and S. Orach, Towards Paperless Hospitals: Lessons Learned From 15 Health Facilities In Uganda, in *New Advances in Information Systems and Technologies*. 2016, Springer. p. 23-32.
- [49] Walsham, G., Doing interpretive research. *European journal of information systems*, 2006. 15(3): p. 320-330.
- [50] Hennink, M., I. Hutter, and A. Bailey, “Data preparation and developing code”, Chapter 9 in “Qualitative Research Methods”, SAGE Publications, pp. 203-232. . 2010: Sage.
- [51] Van Lamsweerde, A. Goal-oriented requirements engineering: A guided tour. in *Proceedings fifth iee international symposium on requirements engineering*. 2001. IEEE.
- [52] Rothenberg, J., Interoperability as a semantic cross-cutting concern. *Interoperabiliteit: Eerlijk zullen we alles delen.*, 2008.
- [53] Salas, P.E., et al. Interoperability by design using the StdTrip tool: an a priori approach. in *Proceedings of the 6th International Conference on Semantic Systems*. 2010. ACM.
- [54] Adebesin, F., et al., Barriers & challenges to the adoption of E-Health standards in Africa. 2013.
- [55] Luna, D., et al., Health informatics in developing countries: going beyond pilot practices to sustainable implementations: a review of the current challenges. *Healthcare informatics research*, 2014. 20(1): p. 3-10.
- [56] ISO, Interoperability of telehealth systems and networks- - Part 1: Introduction and definitions, in *ISO/TR 16056-1:2004 Health informatics -- 2004*.
- [57] Commission, E., *New European interoperability framework. Promoting seamless services and data flows for European public administrations*. 2017, Publications Office of the European Union Luxembourg.
- [58] Mu-Hsing Kuo, A. Kushniruk, and B. Elizabeth, A Comparison of National Health Data Interoperability Approaches in Taiwan, Denmark and Canada. *ElectronicHealthcare*, 2011. 10(2): p. e14-e25.
- [59] HIQA, *Overview of Healthcare Interoperability Standards*, Health Information and Quality Authority 2013.
- [60] Berre, A.J., et al., The ATHENA interoperability framework. In *Enterprise interoperability II* (pp. 569-580). Springer London. 2007.
- [61] Svensson, A., Challenges in Using IT Systems for Collaboration in Healthcare Services. *International journal of environmental research and public health*, 2019. 16(10): p. 1773.
- [62] Meyer, J.W. and B. Rowan, Institutionalized organizations: Formal structure as myth and ceremony. *American journal of sociology*, 1977. 83(2): p. 340-363.
- [63] Lowi, T.J., Four systems of policy, politics, and choice. *Public administration review*, 1972. 32(4): p. 298-310.
- [64] Juzwishin, D.W. Political, policy and social barriers to health system interoperability: emerging opportunities of Web 2.0 and 3.0. in *Healthcare management forum*. 2009. SAGE Publications Sage CA: Los Angeles, CA.
- [65] IEEE, (Institute of Electrical and Electronics Engineers).: *Standard computer dictionary a compilation of IEEE standard computer glossaries*. 1990.
- [66] Chen, D., G. Doumeings, and F. Vernadat, Architectures for enterprise integration and interoperability: Past, present and future. *Computers in industry*, 2008. 59(7): p. 647-659.
- [67] Mosweu, O., K.J. Bwalya, and A. Mutshewa, A probe into the factors for adoption and usage of electronic document and records management systems in the Botswana context. *Information development*, 2017. 33(1): p. 97-110.
- [68] Kobusinge, G. “Putting Interoperability on Health-information-systems’ Implementation Agenda.” in *In Proceedings of the 53rd Hawaii International Conference on System Sciences*. 2020.
- [69] Carnicero, J. and D. Rojas, *Application of information and communication technologies for health systems in Belgium, Denmark, Spain, the United Kingdom and Sweden*. 2010: ECLAC.
- [70] Olbrich, S., J. Poppelbuß, and B. Niehaves. Critical contextual success factors for business intelligence: A Delphi study on their relevance, variability, and controllability. in *2012 45th Hawaii International Conference on System Sciences*. 2012. IEEE.

- [71] Jensen, T.B., A. Kjærgaard, and P. Svejvig, Using institutional theory with sensemaking theory: a case study of information system implementation in healthcare. *Journal of Information Technology*, 2009. 24(4): p. 343-353.
- [72] Orlikowski, W.J., The duality of technology: Rethinking the concept of technology in organizations. *Organization science*, 1992. 3(3): p. 398-427.
- [73] Weick, K., *Sensemaking in organizations* Sage Publications. Thousand Oaks, CA, 1995.

AUTHOR

Grace Kobusinge, Health Informatics PhD Candidate, Faculty of Applied IT, Informatics Department, University of Gothenburg-Sweden, Assistant Lecturer, Department of Information Systems, College of Computing and Information Science, School of Computing and IT, Makerere University Uganda. Research areas of interest: ICT4D, Health informatics, Health information systems' interoperability, knowledge management and human computer interaction.



© 2020 By AIRCC Publishing Corporation. This article is published under the Creative Commons Attribution (CC BY) license.

TRANSCRIPT LEVEL ANALYSIS IMPROVES THE UNDERSTANDING OF BLADDER CANCER

Xiang Ao and Shuaicheng Li

Department of Computer Science, City University of Hong Kong, Hong Kong

ABSTRACT

Bladder cancer (BC) is one of the most globally prevalent diseases, attracting various studies on BC relevant topics. High-throughput sequencing renders it convenient to extensively explore genetic changes, like the variation in gene expression, in the development of BC. In this study, we did differential analysis on gene and transcript expression (DGE and DTE) and differential transcript usage (DTU) analysis in an RNA-seq dataset of 42 bladder cancer patients. DGE analysis reported 8543 significantly differentially expressed (DE) genes. In contrast, DTE analysis detected 14350 significantly DE transcripts from 8371 genes, and DTU analysis detected 27914 significantly differentially used (DU) transcripts from 8072 genes. Analysis of the top 5 DE genes demonstrated that DTE and DTU analysis provided the source of changes in gene expression at the transcript level. The transcript-level analysis also identified some DE and DU transcripts from previously reported mutated genes that related to BC, like ERBB2, ESPL1, and STAG2, suggesting an intrinsic connection between gene mutation and alternative splicing. Hence, the transcript-level analysis may help disclose the underlying pathological mechanism of BC and further guide the design of personal treatment.

KEYWORDS

Bladder Cancer, Differential Gene Expression, Differential Transcript Expression, Differential Transcript Usage

1. INTRODUCTION

Bladder cancer (BC) is the 10th most common malignant carcinoma worldwide, with about an estimate of 549,000 new cases and 200,000 deaths in 2018 [1]. Depending on the invasion state of tumor cells in the muscle layer, bladder cancer is clinically sorted out into two distinct subtypes. One is non-muscle invasive bladder cancer (NMIBC), and the other is muscle-invasive bladder cancer (MIBC). NMIBCs are rarely muscle-invasive and incline recurrence, reporting a rate as high as 70%. Its five-year survival rate is about 90% [2]. MIBCs are, in contrast, frequently metastasize, with a five-year survival rate of less than 50%. Currently, the main treatments for NMIBCs are transurethral resection and postoperative intravesical chemotherapy. In comparison, the treatments of MIBCs involve radical cystectomy or radiotherapy [3-6]. A systemic therapy, such as agents targeting dysfunctional or mutational genes or agents acting at the molecular level for BC treatment, is not available for BC patients at present and is in an urgent need [7-9].

The advance of the treatment of BC requires a comprehensive understanding of its pathogenesis. So far, researchers have paid substantial effort in investigating the potential mechanisms of BC [8, 10-14]. For example, elaborate differential gene expression (DGE) analyses of BC expression data advance our understanding of BC and are expected to improve its current treatments and therapies [15,16]. However, differential expression analysis at the gene level unable to reveal the

details and changes in the composition of gene expression when gene generates more than one transcripts. Changes in the population and proportion of the entire transcripts from the same gene are vague from the result of DGE analysis. Therefore, transcript-level analysis is requisite and necessary to discover variant transcripts that lead to changes in gene expression and contribute to abnormality or phenotype of interest [17].

Consequently, differential transcript expression (DTE) analysis and differential transcript usage (DTU) analysis rose to respond to the needs. They are aiming at detecting the transcript that presents variance in its expression level or abundance. Here, we combine gene-level analysis (DGE analysis) and transcript-level analysis (DTE analysis and DTU analysis) to reveal the potential critical biomarkers contributing to the development of BC.

2. MATERIALS AND METHODS

2.1. Data Preparation

Guo G et al. presented an RNA-seq dataset of 42 bladder cancer patients to study the genetic basis of transitional cell carcinoma in [18]. We utilized such a dataset throughout this manuscript. The cohort contains 42 patients of bladder tumor, 16 of which contained paired morphological normal bladder tissue. Among the 42 patients, 6 were females, and 36 were males. The range of age of the cohort was 25 to 87 years old at the time when recruited the patients. The overall mean and median age was 62.3 and 64.5 years, respectively. Besides, 25 of 42 samples were MIBC, while 17 were NMIBC. Table 1 manifests the details about the clinical characteristics of the cohort.

We collected the data (accession code SRA063495) from the Sequence Read Archive (SRA). The mRNA libraries were generated from the TruSeq RNA Sample Preparation kit (Illumina), and the sequencing platform was the HiSeq 2000. We refer to [18] for the procedures of reads sequencing. We downloaded all the raw “.sra” files from SRA and used the fastq-dump program from the SRA toolkit (version 2.9.6) to obtain clean fastq files by decompressing such “.sra” files. We then treated those fastq files as the input to our analysis pipeline.

2.2. Expression Quantification

Our analysis pipeline contains three main steps, including expression quantification, differential analysis, and gene enrichment analysis. Figure 1 shows the flowchart of our pipeline. In expression quantification, we quantified the genome-wide expression level of genomic features, i.e., the expression level of genes and transcripts. In the differential analysis, we did differential expression analysis on genes and transcripts and differential usage analysis on transcripts. Finally, we did gene enrichment analysis on the results from the differential analysis.

In the quantification step, the expression level of each genomic feature (either gene or transcript) was represented by the number of reads originated from the feature. We adopted two distinct programs to quantify expression levels. More precisely, we used featureCounts from the Subread package (version 1.6.4) [19] to measure gene-level expression while applied Salmon (version 0.13.1) [20] to estimate transcript-level expression. For gene-level expression quantification, we first applied STAR (version 2.5.3a) [21] to align reads to human genome reference GRCh38.p2, and then adopted featureCounts for each gene to calculate the number of reads mapped to the gene (genes that shared overlapping regions were merged into one unique gene). For transcript-level expression quantification, we incorporated the Salmon to estimate the counts of reads for each transcript. The reference human gene annotation utilized in this step was from Ensembl

release 79, which consisted of 65217 records of genes and 213622 records of transcripts. After quantification, we obtained counts of reads for all the genes as well as the transcripts. We then used them in the differential expression analysis.

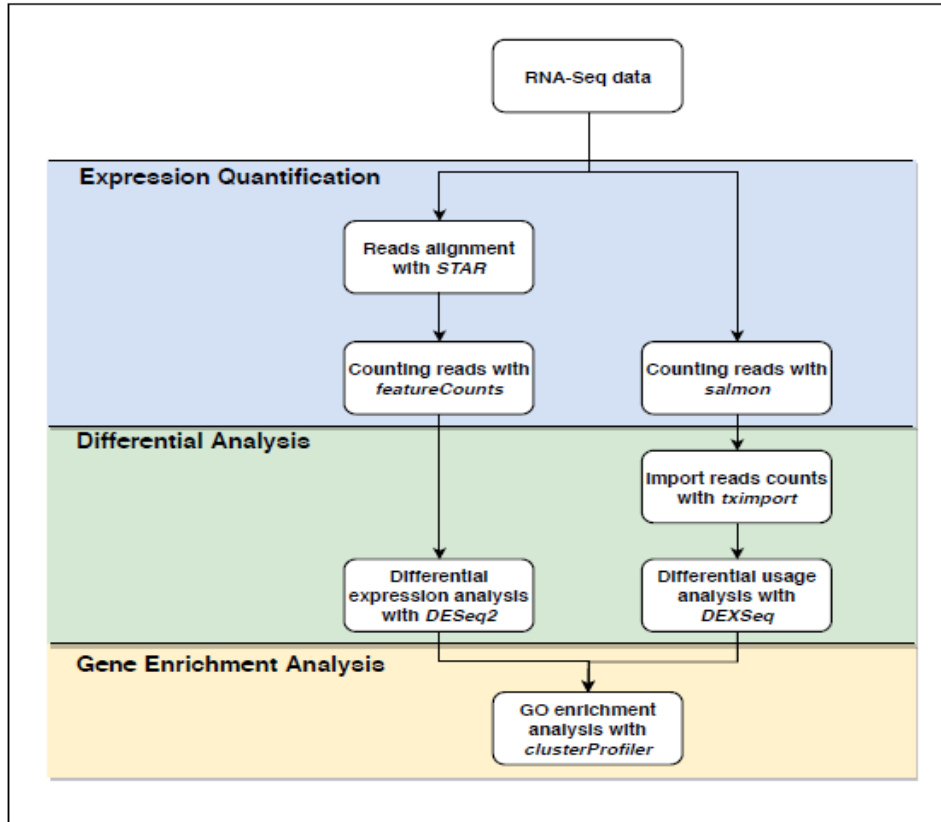


Figure 1. Flowcharts of the analysis pipeline. Our analysis pipeline contains three main parts: expression quantification, differential analysis, and gene enrichment analysis.

2.3. Differential Analysis

In step 2, we did differential expression analysis at both gene-level and transcript-level to compute the variance of expression between tumor and normal samples. Because of alternative splicing, major human genes generate more than one transcript. Consequently, we can present transcripts' expression levels in both absolute values (reads counts) and relative values (transcript usage, defined as (number of a transcript) / (amount number of transcripts from the same gene)). Transcripts from a single gene (i.e., isoforms) may hold comparable usages between conditions but increase dramatically in absolute expression, and reverse cases exist as well. Differential transcript usage analysis thus complements differential gene/transcript expression analysis. We did DGE, DTE, and DTU analysis on a BC cohort, to extensively explore the differences between BC and normal tissue and further discover the potential mechanisms behind the development of BC.

We made use of an R package DESeq2 (version: 1.24.0) [22] to do differential expression (DE) analysis. For each genomic feature and the counts of reads aligned to it, DESeq2 adopts a generalized linear model to fit the counts to a negative binomial distribution to detect differentially expressed features. Depending on the distinct read-counting programs for genes and transcripts, we took diverse data importing methods. For DGE analysis, we directly import reads

counts data from the featureCounts. As to DTE analysis, we used an R package tximport (version: 1.12.3) [17] to import counts data from the Salmon by setting the argument countsFromAbundance to “scaledTPM”. Non-expressed genes/transcripts in all samples (defined as genes/transcripts with a sum of counts across all samples less than 10) were filtered out to reduce computational burdens. Samples’ sex, age, bladder cancer subtype (muscle / non-muscle invasive), cancer grade, cancer recurrence status, and condition (cancer/normal) served as independent variables. We did differential comparison between cancer and normal samples. We selected significantly DE feature according to its \log_2 fold change ($\log_2(\text{FC})$) and false discovery rate (FDR). The threshold was $|\log_2(\text{FC})| \geq 1$ and $\text{FDR} < 0.05$.

As a complementary analysis method, we did DTU analysis by taking advantage of an R package DEXSeq (version: 1.30.0) [23, 24]. Anders, et al., incipiently designed it for the exon-level differential usage analysis. To infer changes in exon usage, it compared the number of reads mapping to a certain exon to the number mapping to any other exons generated from the same gene. We used it for the transcript-level differential usage analysis. We applied the same method (i.e., tximport) to import reads counts for each transcript and also excluded non-expressed transcripts from analysis. The same independent variables used in DE analysis were adopted in DTU analysis as well. Besides, the same criteria were applied to choose significant DU transcripts.

2.4. Gene Ontology Enrichment Analysis

We used the R package clusterProfiler (version: 3.12.0) [25] to do gene ontology (GO) enrichment analysis. Significant genes were employed as input and converted to ENTREZ identifiers. A threshold was set to p-value < 0.05 to select significantly enriched GO terms.

3. RESULTS

From differential gene expression analysis, we found 8543 significantly differentially expressed genes between bladder cancer samples and normal bladder samples from 65065 tested genes. Of all the significant DE genes, 5293 genes were down-regulated with a mean $\log_2(\text{Fold Change})$ equals to -2.52 while 3250 were up-regulated with a mean $\log_2(\text{Fold Change})$ equals to 1.76. Principle component analysis (PCA) with the gene expression data shows that a normal sample B77_Normal was more likely to be a cancer sample (Figure 2). However, including this sample in DE analysis did not affect its result as DESeq2 sets aside outliers from the analysis. Figure 3 shows the volcano plot of DE genes, with the gene names of the top 5 over-expressed and suppressed genes labeled (names of merged genes contain a plus symbol). We used the expression level of the top 500 significant DE genes to do hierarchical clustering (Figure 4). In Figure 4, most cancer samples and normal samples were grouped correctly except the sample B77_Normal, which was more likely a cancer sample and illustrated by PCA. Among the 37 significantly mutated genes reported in [18], 10 of them (27%) were found differentially expressed (Table 1).

Gene ontology (GO) enrichment analysis was done for DE genes to identify the GO terms that were activated by DE genes. GO enrichment analysis demonstrated that extracellular matrix (GO:0031012), collagen-containing extracellular matrix (GO:0062023), muscle system process (GO:0003012), muscle contraction (GO:0006936), extracellular matrix organization (GO:0030198), extracellular structure organization (GO:0043062), extracellular matrix structural constituent (GO:0005201), muscle organ development (GO:0007517), regulation of leukocyte activation (GO:0002694), external side of plasma membrane (GO:0009897) were the top 10 significantly enriched terms (Table 2).

Table 1. The 37 significantly mutated genes and the distribution in DGE, DTE and DTU.

Gene set	Genes
Significantly Mutated genes	ANK2, ANK3, ARID1A, ATM, CHD6, CREBBP, CSMD3, ELF3, EP300, ERBB2, ERBB3, ERCC2, ESPL1, FAT4, FGFR3, HRAS, KALRN, KRAS, LAMA4, LRP2, MLL, MLL3, NCOR1, NF1, NFE2L3, PDZD2, PIK3CA, PIK3R4, RB1, STAG2, SYNE1, SYNE2, TP53, TRAK1, TRRAP, TSC1, UTX
DE genes	ANK2, CSMD3, ERBB2, ESPL1, FAT4, FGFR3, HRAS, LAMA4, SYNE1, TRAK1
DTE genes	ANK2, ARID1A, ATM, CREBBP, ELF3, ERBB2, ERBB3, ESPL1, FAT4, FGFR3, HRAS, KRAS, LAMA4, NF1, NFE2L3, STAG2, SYNE1, TP53, TRAK1
DTU genes	ANK2, ANK3, ARID1A, ATM, CREBBP, CSMD3, ELF3, ERBB2, ERBB3, ERCC2, ESPL1, FGFR3, HRAS, KALRN, LAMA4, NCOR1, NF1, PDZD2, PIK3R4, RB1, STAG2, SYNE2, TP53, TRAK1, TRRAP

Differential transcript expression (DTE) analysis and differential transcript usage (DTU) analysis provide details of the change in gene expression. From 213622 transcripts that were generated by all 65065 genes, DTE analysis identified 14350 significant DE transcripts, in which 6053 were up-regulated and 8297 were down-regulated. Table 3 lists the top 10 differentially expressed transcripts. In contrast, DTU analysis detected 27914 significant DU transcripts where contained 15012 over-expressed transcripts and 12902 down-regulated transcripts. Table 4 presents the top 10 differentially used transcripts. To discover the contrast of the results from DTE analysis and DTU analysis, we separated both results in positive (over-expressed) and negative (down-regulated) subgroups and showed their intersections in Figure 5a. The figure shows that 5502 transcripts changed their absolute expression level as well as their proportions in gene expression simultaneously. Among such 5502 transcripts, most of them showed the same direction of changes. That is, 2623 (46.7%) transcripts' absolute expression level and relative usage level obtained increase in BC samples, and 2742 (49.8%) transcripts got both types of levels decreased. However, some transcripts displayed opposite directions of changes. For example, there were 9 (0.2%) transcripts whose absolute expression level got promoted while usage level reduced in BC samples. Besides, there were 128 (2.3%) transcripts had pure expression level decreased while relative usage increased.

Table 2. The top 10 enriched GO terms of differentially expressed genes.

Ontology	ID	Functional Term	Gene Count	Adjusted p-value
CC	GO:0031012	extracellular matrix	218	8.59E-38
CC	GO:0062023	collagen-containing extracellular matrix	194	5.26E-37
BP	GO:0003012	muscle system process	192	1.19E-25
BP	GO:0006936	muscle contraction	159	1.21E-25
BP	GO:0030198	extracellular matrix organization	147	5.62E-21
BP	GO:0043062	extracellular structure organization	163	5.62E-21
MF	GO:0005201	extracellular matrix structural constituent	85	1.16E-18
BP	GO:0007517	muscle organ development	157	3.25E-16
BP	GO:0002694	regulation of leukocyte activation	181	6.04E-16
CC	GO:0009897	external side of plasma membrane	93	8.64E-16

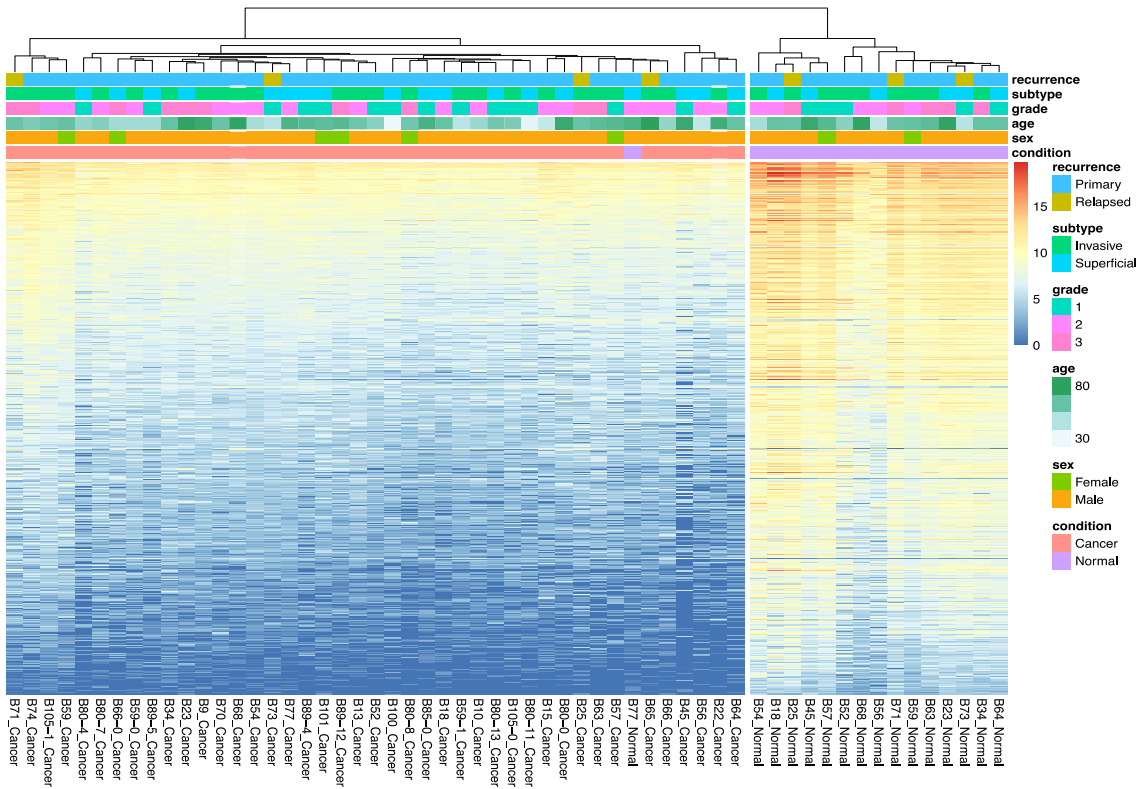


Figure 4. The hierarchical clustering result of the top 500 DE genes. Columns stood for samples while rows indicated genes. The vertical white band separated samples into two subgroups. The degree of gene expression corresponded to the transition from blue to red. Independent variables were shown as well.

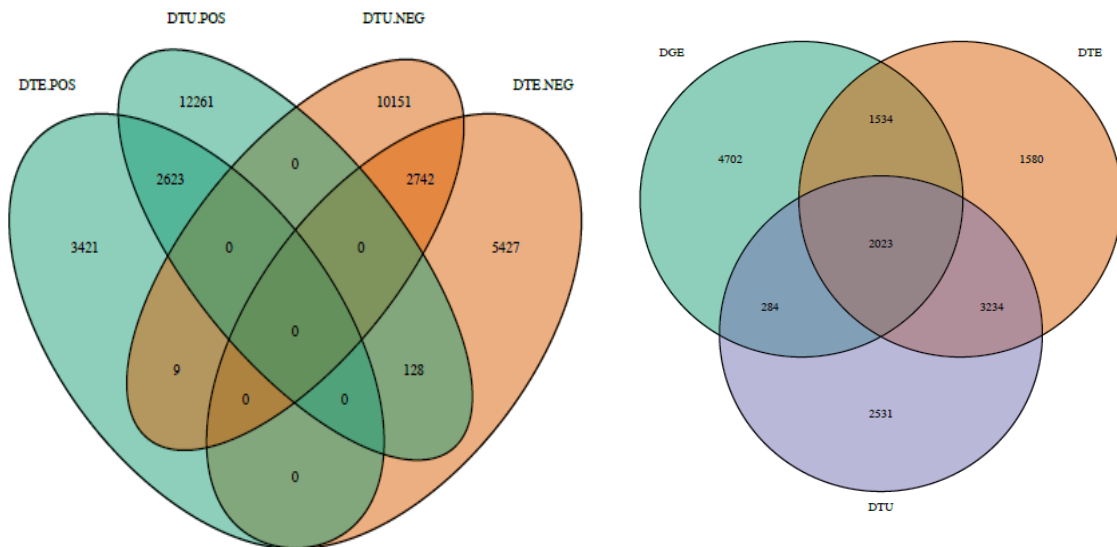


Figure 5. (a) the left Venn diagram exhibits the transcript overlaps among DTE.POS, DTE.NEG, DTU.POS and DTU.NEG and (b) the right diagram exposes gene intersections from DGE, DTE, and DTU analysis. POS and NEG stand for over-expressed and down-expressed features, respectively.

Table 3. The top 10 differentially expressed transcripts.

Transcript	Gene	Mean Expression	log2FoldChange	Adjusted p-value
ENST00000588553	AC005786.3	11.53	27.66	2.37E-14
ENST00000618836	UBE2D3	13.20	16.16	1.64E-05
ENST00000557860	ACTC1	550.95	-12.24	9.05E-19
ENST00000492726	DES	466.95	-11.39	1.21E-13
ENST00000290378	ACTC1	831.71	-11.13	7.32E-27
ENST00000611814	PI16	614.92	-10.87	1.55E-70
ENST00000373960	DES	11908.26	-10.85	4.78E-48
ENST00000560765	FGF7	287.42	-10.78	1.37E-15
ENST00000461273	RP11-274B21.5	11.39	10.54	1.63E-02
ENST00000347557	SMTN	159.59	-10.47	2.57E-19

Table 4. The top 10 differentially used transcripts

Transcript	Gene	Mean Expression	log2FoldChange	Adjusted p-value
ENST00000543780	IGJ	3632.15	-60.74	1.25E-22
ENST00000305046	ADH1B	28.92	-49.90	0.00E+00
ENST00000355722	TRPM8	10.63	-48.37	1.66E-06
ENST00000577017	MAPT	11.82	-47.00	3.37E-06
ENST00000510545	CLDND1	54.47	44.93	2.80E-13
ENST00000466266	PRUNE2	30.03	-39.34	6.97E-20
ENST00000355426	EFEMP1	426.46	-36.24	2.52E-119
ENST00000472859	SGK1	32.38	-35.94	1.15E-02
ENST00000457773	PLCD4	36.87	-33.52	0.00E+00
ENST00000618157	HLA-DRB4	13.78	-27.55	1.26E-07

Table 5. The top 10 enriched GO terms of genes that produced differentially expressed transcripts

Ontology	ID	Functional Term	Gene Count	Adjusted p-value
CC	GO:0062023	collagen-containing extracellular matrix	244	1.91E-22
CC	GO:0005925	focal adhesion	241	8.23E-22
CC	GO:0005924	cell-substrate adherens junction	241	1.25E-21
CC	GO:0030055	cell-substrate junction	243	1.25E-21
CC	GO:0031012	extracellular matrix	273	1.25E-21
CC	GO:0005912	adherens junction	286	1.25E-21
BP	GO:0030198	extracellular matrix organization	209	2.06E-19
BP	GO:0043062	extracellular structure organization	228	7.88E-17
CC	GO:0015629	actin cytoskeleton	238	1.30E-14
MF	GO:0005201	extracellular matrix structural constituent	112	2.68E-14

Table 6. The top 10 enriched GO terms of genes that produced differentially used transcripts

Ontology	ID	Functional Term	Gene Count	Adjusted p-value
CC	GO:0005925	focal adhesion	306	2.19E-33
CC	GO:0005924	cell-substrate adherens junction	306	4.56E-33
CC	GO:0030055	cell-substrate junction	309	4.56E-33
CC	GO:0005912	adherens junction	364	1.31E-32
CC	GO:0005813	centrosome	320	7.28E-19
CC	GO:0031252	cell leading edge	268	1.29E-18
BP	GO:0000226	microtubule cytoskeleton organization	314	3.02E-17
BP	GO:0043087	regulation of GTPase activity	285	3.02E-17
CC	GO:0005819	spindle	229	2.09E-16
BP	GO:0006914	autophagy	315	1.51E-15

We then look at genes that generated significant DE and DU transcripts. In total, 8371 genes produced all the significant DE transcripts compared to 8072 genes that generated such DU transcripts. A Venn diagram in Figure 5b exhibits the overlaps among genes from distinct analysis methods (i.e., DGE, DTE, and DTU). From Figure 5b, 3841 (45%) DE genes generated either significant DE transcripts or significant DU transcripts or both. We also explored the transcript-level changes in the 37 significantly mutated genes. We found that 19 of 37 (51.4%) genes produced DE transcripts, and 25 of such genes (67.6%) had DU transcripts (Table 1).

We also did GO enrichment analysis for the genes that generated DE transcripts and DU transcripts. GO enrichment analysis on DTE genes found that collagen-containing extracellular matrix (GO:0062023), focal adhesion (GO:0005925), cell-substrate adherens junction (GO:0005924), cell-substrate junction (GO:0030055), extracellular matrix (GO:0031012), adherens junction (GO:0005912), extracellular matrix organization (GO:0030198), extracellular structure organization (GO:0043062), actin cytoskeleton (GO:0015629), extracellular matrix structural constituent (GO:0005201) were the top 10 significantly enriched terms (Table 5). In contrast, the top 10 terms found from DTU genes were focal adhesion (GO:0005925), cell-substrate adherens junction (GO:0005924), cell-substrate junction (GO:0030055), adherens junction (GO:0005912), centrosome (GO:0005813), cell leading edge (GO:0031252), microtubule cytoskeleton organization (GO:0000226), regulation of GTPase activity (GO:0043087), spindle (GO:0005819), autophagy (GO:0006914) (Table 6).

4. DISCUSSION

This study of RNA-seq of human bladder reveals some crucial genes and transcripts as well as functional characteristics related to bladder cancer development. From the differential analysis of expression of gene and transcript and usage of the transcript, we identified potential biomarkers that may help in bladder cancer diagnosis, treatment, and prognoses.

Human bladder cancer is a type of disease that full of complex genetic causes. DGE analysis discovered 8543 differentially expressed genes that enriched in plenty of GO terms in distinct biological processes and molecular functions, while DTE analysis discovered 14350 transcripts originated from 8371 genes, and DTU analysis revealed 27914 transcripts from 8072 genes, all of which may contribute to the development of BC.

Although DGE analysis discovered a large range of genes related to BC, DTE analysis and DTU analysis provided a new dimension to explore cancer RNA-seq data. There were 4814 and 5765 novel genes found by DTE analysis and DTU analysis, respectively. Furthermore, changes in the expression of some DE genes were attributable to its transcripts. We identified ACTC1 as the

most down-regulated gene in bladder cancer, which was previously recognized as a commonly down-regulated gene in BC [26]. Gene ACTC1 had expressed three transcripts, i.e., ENST00000290378, ENST00000557860, and ENST00000560563, in the dataset. DTE analysis found that such three transcripts were significantly decreased ($\log_2FC < -8.2$, adjusted p-value $< 7E-8$). DTU analysis revealed that only transcript ENST00000560563 displayed a significant change in relative usage ($\log_2FC = 1.3$, adjusted p-value $< 1E-2$). A similar situation happened on two of the most suppressed genes, DES and PII6, where their transcripts' expression decreased in tumor and each had only one significant DU transcript. Another two genes, ASB5 and PCP4, however, showed a more complicated pattern. Although expression degrees at the gene level and the transcript level both inhibited in BC, some of their isoforms' usage presented an opposite direction of change. For example, isoform ENST00000510578 from gene ASB5 gained an increase in its relative usage level.

Differential analysis verified that some significantly mutated BC-related genes also experienced variations in expression (Table 1). DGE analysis found that 10 of 37 significantly mutated genes were differentially expressed. Moreover, extra genes were detected to contain either DE transcripts or DU transcripts (19 genes and 25 genes, respectively). It suggests that there may be an underlying link from gene mutation to gene expression and transcriptional composition that contributed to the development of bladder cancer.

This work was based on the analysis of RNA-seq data and revealed potential biomarkers associated with bladder cancer. Further expansion of the study may be an experimental validation to fortify and narrow the findings so that promising therapies can be derived.

5. CONCLUSION

In conclusion, we conducted both gene-level and transcript-level differential analyses on 42 bladder cancer samples, including differential expression analysis and differential usage analysis. Transcript level analysis results revealed details contributing to the significant changes in gene expression level. Furthermore, we discovered additional genes that didn't detect by gene-level analysis and may relate to the development of bladder cancer. We also did GO enrichment analysis based on the differential analysis results and disclosed candidate pathways that potentially associated with bladder cancer. Despite the analytical study we completed, experimental validation is expected to fortify our findings.

REFERENCE

- [1] Bray, Freddie, et al. "Global cancer statistics 2018: GLOBOCAN estimates of incidence and mortality worldwide for 36 cancers in 185 countries." *CA: a cancer journal for clinicians* 68.6 (2018): 394-424.
- [2] Kaufman, Donald S., William U. Shipley, and Adam S. Feldman. "Bladder cancer." *The Lancet* 374.9685 (2009): 239-249.
- [3] Sylvester, Richard J., Willem Oosterlinck, and ADRIAN PM van der MEIJDEN. "A single immediate postoperative instillation of chemotherapy decreases the risk of recurrence in patients with stage Ta T1 bladder cancer: a meta-analysis of published results of randomized clinical trials." *The Journal of urology* 171.6 Part 1 (2004): 2186-2190.
- [4] Mant, Jonathan, et al. "Systematic review and individual patient data meta-analysis of diagnosis of heart failure, with modelling of implications of different diagnostic strategies in primary care." *NIHR Health Technology Assessment programme: Executive Summaries*. NIHR Journals Library, 2009.

- [5] Shariat, Shahrokh F., et al. "Outcomes of radical cystectomy for transitional cell carcinoma of the bladder: a contemporary series from the Bladder Cancer Research Consortium." *The Journal of urology* 176.6 (2006): 2414-2422.
- [6] McAlpine, Kristen, et al. "Radiotherapy with radical cystectomy for bladder cancer: A systematic review and meta-analysis." *Canadian Urological Association Journal* 12.10 (2018): 351.
- [7] Kim, Jaegil, et al. "Invasive bladder cancer: genomic insights and therapeutic promise." *Clinical Cancer Research* 21.20 (2015): 4514-4524.
- [8] Inamura, Kentaro. "Bladder cancer: new insights into its molecular pathology." *Cancers* 10.4 (2018): 100.
- [9] Abbosh, Philip H., and Elizabeth R. Plimack. "Molecular and clinical insights into the role and significance of mutated DNA repair genes in bladder cancer." *Bladder Cancer* 4.1 (2018): 9-18.
- [10] Jung, Ichabod, and Edward Messing. "Molecular mechanisms and pathways in bladder cancer development and progression." *Cancer control* 7.4 (2000): 325-334.
- [11] Pelucchi, Claudio, et al. "Mechanisms of disease: the epidemiology of bladder cancer." *Nature Reviews Urology* 3.6 (2006): 327.
- [12] McConkey, David J., et al. "Molecular genetics of bladder cancer: Emerging mechanisms of tumor initiation and progression." *Urologic Oncology: Seminars and Original Investigations*. Vol. 28. No. 4. Elsevier, 2010.
- [13] Ahmad, Imran, Owen J. Sansom, and Hing Y. Leung. "Exploring molecular genetics of bladder cancer: lessons learned from mouse models." *Disease models & mechanisms* 5.3 (2012): 323-332.
- [14] Fantini, Damiano, et al. "A Carcinogen-induced mouse model recapitulates the molecular alterations of human muscle invasive bladder cancer." *Oncogene* 37.14 (2018): 1911.
- [15] Hussain, Syed A., et al. "Gene expression profiling in bladder cancer identifies potential therapeutic targets." *International journal of oncology* 50.4 (2017): 1147-1159.
- [16] Sanchez-Carbayo, Marta, Paola Capodieci, and Carlos Cordon-Cardo. "Tumor suppressor role of KiSS-1 in bladder cancer: loss of KiSS-1 expression is associated with bladder cancer progression and clinical outcome." *The American journal of pathology* 162.2 (2003): 609-617.
- [17] Sonesson, Charlotte, Michael I. Love, and Mark D. Robinson. "Differential analyses for RNA-seq: transcript-level estimates improve gene-level inferences." *F1000Research* 4 (2015).
- [18] Guo, Guangwu, et al. "Whole-genome and whole-exome sequencing of bladder cancer identifies frequent alterations in genes involved in sister chromatid cohesion and segregation." *Nature genetics* 45.12 (2013): 1459.
- [19] Liao, Yang, Gordon K. Smyth, and Wei Shi. "The Subread aligner: fast, accurate and scalable read mapping by seed-and-vote." *Nucleic acids research* 41.10 (2013): e108-e108.
- [20] Patro, Rob, et al. "Salmon provides fast and bias-aware quantification of transcript expression." *Nature methods* 14.4 (2017): 417.
- [21] Dobin, Alexander, et al. "STAR: ultrafast universal RNA-seq aligner." *Bioinformatics* 29.1 (2013): 15-21.
- [22] Love, Michael I., Wolfgang Huber, and Simon Anders. "Moderated estimation of fold change and dispersion for RNA-seq data with DESeq2." *Genome biology* 15.12 (2014): 550.

- [23] Anders, Simon, Alejandro Reyes, and Wolfgang Huber. "Detecting differential usage of exons from RNA-seq data." *Genome research* 22.10 (2012): 2008-2017.
- [24] Reyes, Alejandro, et al. "Drift and conservation of differential exon usage across tissues in primate species." *Proceedings of the National Academy of Sciences* 110.38 (2013): 15377-15382.
- [25] Yu, Guangchuang, et al. "clusterProfiler: an R package for comparing biological themes among gene clusters." *Omics: a journal of integrative biology* 16.5 (2012): 284-287.
- [26] Zaravinos, Apostolos, et al. "Identification of common differentially expressed genes in urinary bladder cancer." *PloS one* 6.4 (2011): e18135.

© 2020 By AIRCC Publishing Corporation. This article is published under the Creative Commons Attribution (CC BY) license.

LEADING DEVOPS PRACTICE AND PRINCIPLE ADOPTION

Krikor Maroukian¹ and Stephen R. Gulliver²

¹Microsoft, Kifissias Ave., Athens, Greece

²University of Reading, Henley Business School, Business Informatics Systems and Accounting, Reading, UK

ABSTRACT

This research, undertaken in highly structured software-intensive organizations, outlines challenges associated to agile, lean and DevOps practices and principles adoption. The approach collected data via a series of thirty (30) interviews, with practitioners from the EMEA region (Czech Republic, Estonia, Italy, Georgia, Greece, The Netherlands, Saudi Arabia, South Africa, UAE, UK), working in nine (9) different industry domains and ten (10) different countries. A set of agile, lean and DevOps practices and principles, which organizations choose to include in their DevOps adoption journeys were identified. The most frequently adopted structured service management practices, contributing to DevOps practice adoption success, indicate that those with software development and operation roles in DevOps-oriented organizations benefit from existence of highly structured service management approaches such as ITIL®.

KEYWORDS

Agile, Lean, Practices and Principles, DevOps Leadership, IT service management

1. INTRODUCTION

The software product development industry is increasingly focused in the pursuit to unlock the full potential of its workforce. There is a requirement to deliver value adding software faster, more reliably and in a secure way. There is immense pressure to support the existing software product portfolio and develop new versions of it with richer features and fewer defects. Therefore, the adaptability of the IT organization to rapidly changing business demand is becoming, in its turn, increasingly important in delivering value to customer experiences. Business demand is translated to frequent releases, powered by automated build, testing and deployment processes whereby automation reduces required effort to setup new product releases. To that extent business demand should be translated to more daily commits of code with improved quality assurance, enhanced collaboration and communication means, improved visibility of implemented features to the customer, including testing with customers.

In a world where every Company is a software company [1] and software is eating the world [2], adaptability has become the new competitive advantage shifting focus from position, scale, and “first order” capabilities in producing or delivering an offering, to “second order” organizational capabilities that foster rapid adaptation [3].

Traditional structured approaches in software product development and project management in software intensive industries have had to IT project failure [4] [5] [6] [7] [8] and software project failure [9] [10] with a number of examples from the public sector [11] [12] [13]. In addition, traditional software security has also witnessed research by academia on this topic [53].

David C. Wyld et al. (Eds): ITCSE, NLCA, ICAIT, CAIML, ICDIPV, CRYPIS, WiMo - 2020

pp. 41-56, 2020. CS & IT - CSCP 2020

DOI: 10.5121/csit.2020.100504

Considering this, organizations have focused on fostering agility in their software development and operations team structures. These organizational changes entail transitioning software development practices, transition team practices, transitioning management approach, transitioning reflective practices and transitional culture [15].

1.1. Structured, Agile, Lean and DevOps Challenges

Structured IT service management (ITSM) frameworks such as ITIL® [16], and project management frameworks such as PRINCE2® [17] and PMBOK® [18] have been introducing numerous decision making roles and gates in IT organizations and thus have allowed more delays in the product development lifecycle. In addition, accountability in structured approaches supports increased culpability in process ownership, which although leads to accountability reduces flexibility, since all changes require the approval of multiple stakeholders. Furthermore, structured approaches to change, release, and deployment management of new products and services within the IT industry, has led to the innate proclivity to be blameful within post implementation reviews, or within post-project delivery lessons-learned meetings.

Agile, lean and DevOps principles and practices aim to identify value and non-value adding activities within ITSM processes. Specifically, the identification regards the end-to-end ownership of associated roles, processes and technology [19] to the software product development lifecycle [20] [21] [22]. IT organization willing to adopt agility find that the more defined processes leads to restricting agility [23]. Therefore, there is clearly a need to extend, and or shift, from structured service management practices towards agility and leanness. The transition, i.e. from a framework or process-led organizational environment to the adoption of groups of best practices, entails a significant shift in individual and organizational mindset. There needs to be a clear organization-specific roadmap on the types of practices and principles that need to be adopted, including i) team structures that needs to be applies, and ii) leadership styles that can help guide others towards agility/leanness adoption.

This research firstly aims is to identify the practices and principles that Agile, lean and DevOps communities have developed, in regard to product development and its overlap with ITSM processes. Secondly, to realize the effect that Agile, Lean and DevOps practice and principle adoption has on structured service management processes. Finally, as a consequence, it is important to realize whether Agile, Lean and DevOps practice and principle adoption requires any sort of leadership and/or determine whether that these leadership needs already form part of an individual leader role or team structure. This aim is reflected in the defined research questions: **RQ1)** Which agile, lean and DevOps practices / principles can improve productivity in a business environment that has adopted a structured service management approach? **RQ2)** Can DevOps-oriented environments benefit from structured service management practices? **RQ3)** Can Leadership affect DevOps adoption within an organization and to which extent?

2. DEFINING AGILE, LEAN AND DEVOPS PRACTICES AND PRINCIPLES

The Fourth Industrial Revolution, characterized by the growing utilization of disruptive digital technologies, is transforming the world of work; e.g. both the jobs and the skills that are needed in business to compete. Moreover, research by McKinsey [24] suggests that globally about half of the jobs performed today by humans will be disrupted in some ways by automation, and the World Economic Forum [25] stated that 42% of the core job skills required today are set to substantially change by 2022. In addition, leading cultural change will be key to digital business transformation [26]. Within this dynamically changing business world, use of software management is playing a much larger and more strategic role in shaping how companies

compete, with large ‘traditional’ organizations finding themselves limited in their ability to respond at market and customer needs.

2.1. Agile Software Development

During the 1990s, individuals with a desire to think and act outside the structured approaches imposed in project and product management began forming the agile community; a term formally coined in 2001 Agile Manifesto [27]. The manifesto set out to establish principles to improve the existing software development approaches. Agility aimed at solving a lot of the issues that were created in information intensive organizations by structured approaches. In addition, Agile Software Development (ASD), which emerged in 2001 as an evolutionary practice to existing structured approaches, advocated for iterative short-cycled development increments and continuous integration - as opposed to structured engineering stage-gate models [28]. SCRUM [29], i.e. “a framework within which people can address complex adaptive problems, while productively and creatively delivering products of the highest possible value.” [30], is commonly used as an agile product development approach in software-intensive organizations.

2.2. Lean Mindset

The roots of Lean Enterprise stretch as far back as 1908 – i.e. to a time when Henry Ford’s Ford Motor Company was designing and producing Ford Model T automotive cars. The grandiose Model T mass production plan was successful because it provided inexpensive transportation, which symbolised both innovation and modernization for the rising middle classes in the US. The set of practices and principles employed by Henry Ford’s automotive production factories developed to what is known Ford Production System (FPS). Moreover, FPS became the baseline synthesis of lean manufacturing [31]. Henry Ford extended organizational considerations to human psychology which aimed at an inclusive work environment where each and every one factory employee partnered with the organization to achieve its goals. Following World War II, FPS was transformed by Toyota into two pillars known as i) Just In Time (JIT) and ii) Jidoka aka autonomation [32] [33] – making kanban boards, kaizen (continuous improvement), and poka-yoke (error-proofing) a key part of the Toyota Production System (TPS) [32] [33].

In the early 20th century Japan was already adopting a lot of the FPS techniques and adapting them to the proven methods for automotive mass production purposes aiming for cost efficiencies and increased quality. Developing a Lean Enterprise is all about eliminating friction and introduced waste in the value stream [59] [60] and reducing the time taken to deliver a product or service to market consumers. The term “Lean” was coined in 1988 by John Krafcik [34] and popularized in 1990 by James P. Womack [35], with the aim to remove the following waste: 1) partially completed work, 2) unneeded product features, 3) relearning/skilling of staff, 4) poor handoff, 5) task switching, 6) delays, 7) product defects [36], and a later addendum 8) underutilized staff. Lean IT’s providers aim to transpose the same approaches to waste to software development, i.e. to eliminate or reduce their impact on product development lead times to market delivery. In comparison to ASD, it is notable that Lean Software Development (LSD) was an incremental improvement on top of it [37].

2.3. DevOps and its Adoption

DevOps offers an unprecedented opportunity for organizations to transform their Software Development lifecycle to increase efficiency and meet end-users’ changing expectations. DevOps attempts to redefine the foundations of software development and management recasting

the approach concerning development of every element [38] even in cloud services provisioning [14]. The reformation that DevOps brings, with its set of developed practices, also extends to the customer experience.

There are a number of terms and variety of practices and definitions that software practitioners use when defining DevOps [39] [40] [41] [42] [43] [44]. In practice the use of different DevOps definitions leads to unnecessary confusion when it comes to IT organizations adopting a ‘DevOps-oriented mindset’. Moreover, the numerous associated acronyms that accompany DevOps has a significant role to play in the result of indecisiveness or definition diversity. DevSecOps [45] or SecDevOps (Development-Security-Operations), BizDevOps (Business-Development-Operations) [46] and DevNetOps [21], are all part of the DevOps definition held within organizations. The majority of the descriptions specify DevOps as a term that is used to emphasize the collaboration between software development and operations. Additionally, there is a growing requirement from the research industrial communities to define DevOps [43]. There is also published research work that downplays the fact of not having consensus over a DevOps definition [21].

However, DevOps is more than just a mindset but rather patterns of DevOps practices [41]. In Agile software development there is a distinction between practices and influences [47] which can be extended by a lean principles background that form a prerequisite for successful DevOps adoption [44]. Furthermore, there is research that categorizes advisory skills, testing skills, analysis skills, functional skills, social skills, decision making skills and full stack development skills as the skillset that can result to successful DevOps cross-functional teams [48]. This can be further complemented by a set of practices (common among development and operations teams, development-specific, operations-specific) and a set of principles (social aspects, automation, quality assurance, leanness, sharing measurement) [40]. This is closely linked to CAMS (Culture-Automation-Measurement-Sharing) model originally coined by John Willis and Damon Edwards [19] and later refined to CALMS (Culture-Automation-Lean-Measurement-Sharing) by Jez Humble. CALMS shares similarities with another model that involves a specific set of categories namely: agility, automation, collaborative culture; also called DevOps Culture [49], continuous measurement, quality assurance, resilience, sharing and transparency [50]. This can be further extended to include collaboration in terms of empathy [44], respect, trust, responsibility and incentive alignment and open communication [51]. There are recurring studies to suggest that the lack of a ‘collaborative culture’ is detrimental to the success of DevOps teams and DevOps practice and principle adoption in an organisation [14] [40] [44] [48] [49] [51].

2.4. Leadership styles relevant to DevOps

There are various leadership styles that should be considered when considering DevOps – especially if a highly structured organization is attempting to adopt agile, lean and DevOps practices and principles. A non-exhaustive list of those leadership styles is provided:

- Transactional Leadership [52]
- Transformational Leadership [53]
- Authentic Leadership [54]
- Servant Leadership [55]
- Ad Hoc Leadership [56]

The State of DevOps Report in 2017 discovered a correlation between transformational leadership and organizational performance [57]. Transformational leadership comprises of four dimensions: idealized influence, inspirational motivation, intellectual stimulation, and

individualized consideration [52] and was first posited by James McGregor Burns in 1978 [53]. The State of DevOps Report 2017 report conveys that DevOps leaders with a servant leadership mentality inspired better team performance [57]. In fact, Servant Leadership Theory is a mixture of transformational and transactional styles of leadership. In essence, the leader is serving rather than being served and therefore, creates an environment of trust, collaboration and reciprocal service which ultimately leads higher performance [52]. On the other hand, ad hoc leadership is constituted of three poles (the team, the customer, the management) as opposed to two poles that formulate other leadership styles and its lifecycle is characterized by a leadership style fading and another one becoming prevalent in a software development team setting [56].

3. METHOD AND APPROACH

Having distinguished between agile, lean and DevOps practices and principles described in literature, it is now essential to determine whether these views align with industry domain practitioners.

3.1. Research Design and Interview Structure

To capture contextually relevant data, semi-structured interviews were conducted with thirty (30) practitioners in companies working within a wide range of countries (Czech Republic, Estonia, Italy, Georgia, Greece, The Netherlands, Saudi Arabia, South Africa, UAE, UK). All interviewees contributed to DevOps adoption processes in their respective companies. Participants were recruited using two approaches: 1) through direct contact at an ITSM / DevOps event in Europe, and 2) via a general call for participation posted on professional social media networks; including LinkedIn and IT societies such as IT Service Management Forum (itSMF) and British Computer Society (BCS) – The Chartered Institute for IT. To achieve a heterogeneous perspective, and to increase the wealth of information, practitioners from a variety of organisations were invited and consulted. Although face-to-face interviews were preferred, a number of web interviews were conducted using a range of online tools (Skype for Business and Zoom). Table 2 presents the characteristics of the participants. To maintain anonymity, in conformance with the human ethics guidelines, we refer to the participants as P1–P30 (see Table 3). At the beginning of each interview the interviewee consented to: i) an audio recording being taken, and ii) the transcript being used only in the context of the research. Instructions were clear to state that no names or organisation titles would be disclosed as part of this research.

Table 1. Interview participant profile. PX means professional experience in years, CN means country of work and CS means company size (Micro - MC < 5, Small < 50, Medium - M < 250, Large > 251) [58].

P#	Job Title	PX	CN	Domain	CS
P1	PMO Director	14	Saudi Arabia	Aviation	L
P2	Principal Consultant, IT Service Management	13	Italy	IT Consulting Services	L
P3	CIO	26	Greece	Insurance	L
P4	Principal Consultant, IT Service Management	11	UK	IT Consulting Services	MC
P5	Managing Director, IT Service Management	32	UK	IT Consulting Services	S
P6	Smart Systems Manager	23	Greece	IT Consulting Services	L
P7	Senior Digital Transformation Technologist & Solution Practice Lead	30	UAE	IT Consulting Services	L

P8	Principal Consultant, IT Service Management	34	UK	IT Consulting Services	L
P9	Founding Consultant, IT Service Management	19	UK	IT Consulting Services	S
P10	Managing Director	29	UK	IT Consulting Services	S
P11	Head of Remote Transactions	16	Greece	Banking	L
P12	Consultant	34	Netherlands	IT Consulting Services	M
P13	Deputy CIO	22	Greece	Construction Management	L
P14	Head of Applications	18	Greece	Lottery	L
P15	Principal Consultant, IT Service Management	21	South Africa	IT Consulting Services	MC
P16	Founding Consultant, IT Service Management	34	UK	IT Consulting Services	MC
P17	Managing Director, IT Service Management	19	UK	IT Consulting Services	MC
P18	Managing Director and Lead Consultant	14	UK	IT Consulting Services	MC
P19	IT Operations Manager	13	Greece	Lottery	L
P20	IT Operations Manager	15	UK	Government	M
P21	Founding Consultant, IT Service Management	34	UK	IT Consulting Services	MC
P22	Assistant General Manager, IT Operations	28	Greece	Banking	L
P23	CDO	13	Estonia	Government	L
P24	CIO	20	Greece	Insurance	L
P25	CIO	27	Greece	Aviation	L
P26	Development Team Lead	11	Greece	Lottery	L
P27	IT Operations Lead	12	Georgia	Government	M
P28	Business Development Director	18	Greece	IT Consulting Services	L
P29	Operations and Innovation Lead, IT Services	11	Czech Republic	Courier Services	L
P30	CIO	28	Greece	Automotive	M

Interviews were conducted between September 2018 and January 2019. The interviews lasted a minimum of 34 min, a maximum of 67 min, and an average of 50 min. Data collection and analysis was aggregated in order to answer the research questions posed at the end of section 2, and were mapped to interview questions (see Table 2). The whole set of interview questions is available at the following URL: <https://tinyurl.com/ybxrcujq>

Table 2. Research to interview questions mapping.

Research Question	Interview Question
Data collection for segmentation purposes	1, 2 & 3
R1) Which agile, lean and DevOps practices and principles can improve productivity in a business environment that has adopted a structured service management approach?	4, 5, 6, 7, 8, 9, 10, 11, 12, 15, 16
R2) Can DevOps-oriented environments benefit from structured service management practices.	13, 14, 15, 20
R3) How does Leadership affect DevOps adoption within an organisation?	17, 18, 19, 20

4. EVALUATION AND RESULTS DISCUSSION

The semi-structured interview, see Table 3, consisted of twenty (20) interview questions (Q1-Q20). The first three questions aimed to collect data on interviewee demographics i.e. job role, industry domain, and working country (see Tables 4-6 for demographic breakdown). The country of employment for interview participants included Greece (11), UK (10), Saudi Arabia (2), Czech Republic (1), Estonia (1), Georgia (1), Italy (1), Netherlands (1), South Africa (1), UAE (1), see also Tables 3-4 for demographic breakdown.

Table 3. Job role of interview participants (interviewee count: 30).

Job Title	No. of Participants
Principal Consultant	9
Managing Director	4
CIO	4
Deputy CIO/Assistant General Manager/CDO	3
IT Operations Manager	3
PMO Director	1
Head of Remote Transactions	1
Smart Systems Manager	1
Head of Applications	1
Development Team Lead	1
Business Development Director	1
Operations and Innovation Lead	1

Table 4. Job role of interview participants (interviewee count: 30).

Industry Segmentation	No. of Participants
Consulting Services	14
Aviation	3
Government	3
Lottery	2
Insurance	2
Finance	2
Manufacturing	1
Logistics	1
ISV	1
Automotive	1

Fifteen (15) participants were IT consultants and fifteen (15) were employed at customer organisations - characterised as “service providers” according to ITIL® [16], see Fig. 1.

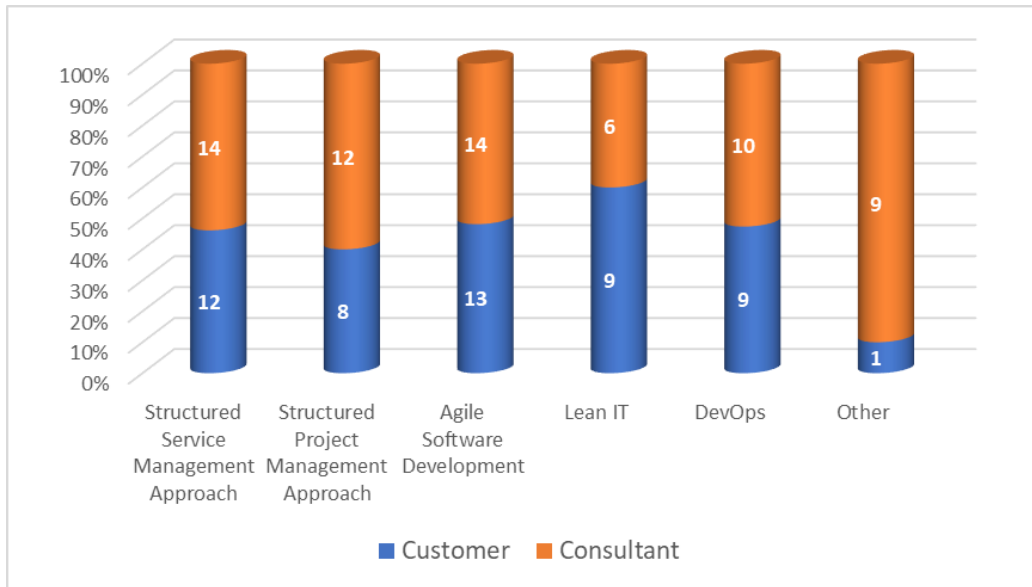


Figure 1. Agile and Lean Practices (Top 3 highlighted) [Interviewee count: 30].

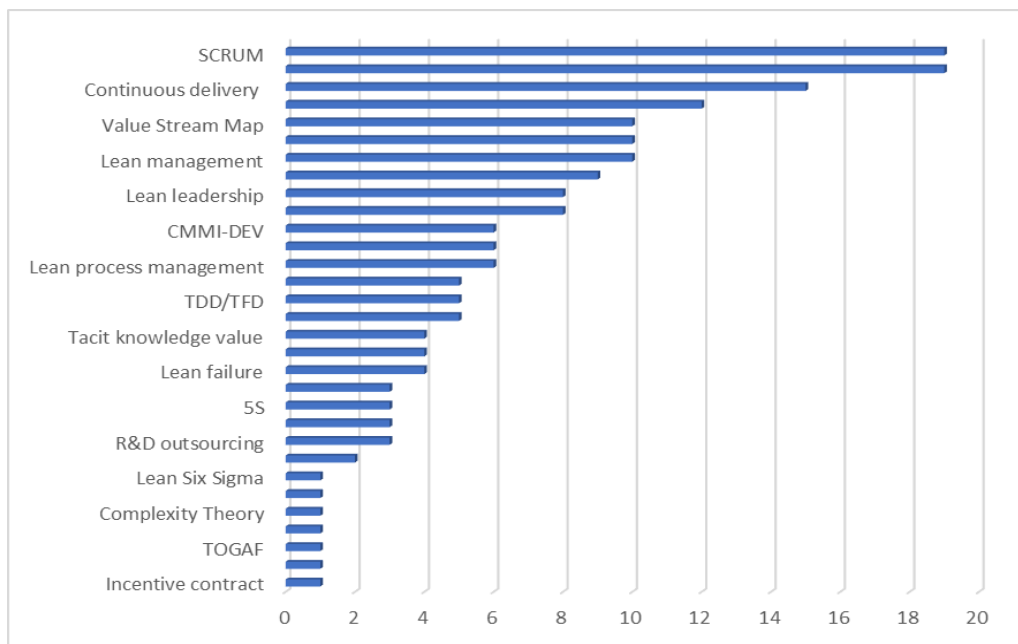


Figure 2. Agile and Lean Practices [Interviewee count: 30].

Interview participants indicated their most preferred structured, agile, and lean practices (see Fig.2) and principles (see Fig.3).

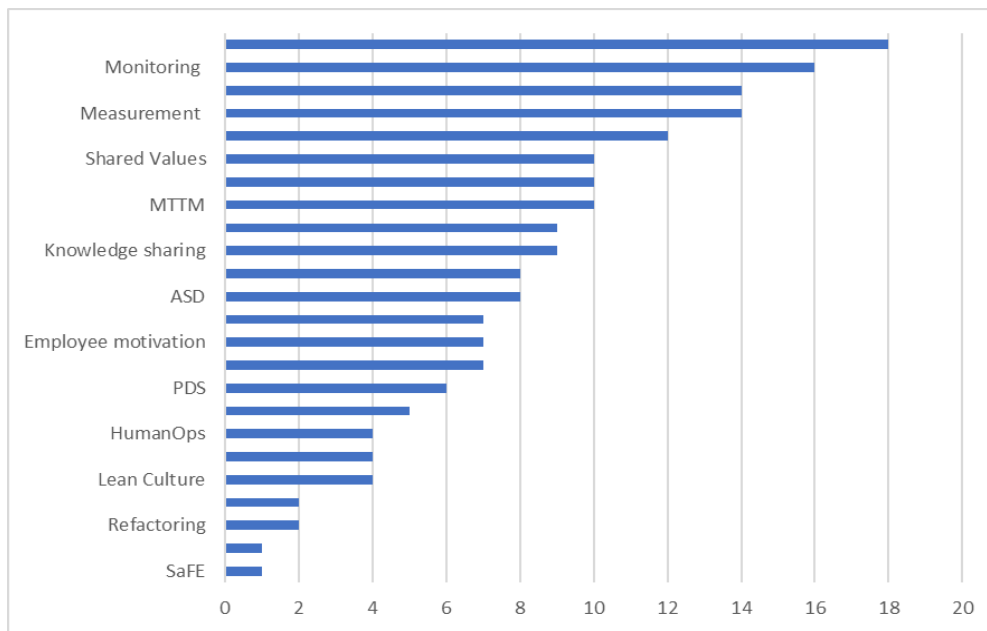


Figure 3. Agile and Lean Principles [Interviewee count: 30].

When considering structured IT service management (ITSM) processes, the interview participants identified a set of practices that contribute to value delivered to software development. Change Management was the most preferred process compared to the rest of the ITSM processes, see Table 5. Additionally, Release and Deployment, Incident and Problem and Service Level Management conclude the top four ITSM processes, which affect value delivery in software development. The prominence of change management was repeated many times throughout the course of interviews with P27 (Georgia, IT Operations Lead) stating that:

Any change can bring resistance and hinder adoption practices. Moving away from any already established approach generates resistance.

Moreover, P24 (Greece, CIO) adds to that:

Resistance happens because all the teams are getting out of their comfort zone. We are talking about different methodology, different structure, different KPIs, different roles, different rewarding scheme, different working location since the team is now collocated - everything is different.

Whereas P20 (UK, IT Operations Manager) states that:

Change management is not generally well understood within organisations

On the contrary P18 (UK, Managing Director and Lead Consultant) argued that:

Rather than adopting every new framework, methodology, set of practices, organizations should look into identifying the current bottlenecks and improvement areas.

Table 5. ITSM process significance to value delivery of software development [Interviewee count: 30].

IT Service Management Process	Adds Value to Software Development (%)
Change Management	24
Release and Deployment Management	15
Incident and Problem Management	10
Service Level Management	9
Availability Management	7

In addition, 66.67% of interviewees agree that agile and lean principle and practice adoption is an extension of established structured ITSM approaches - such as ITIL[®]. Only 20% stated that a complete replacement of those is required. However, concerns on ITIL adoption were mentioned by P6 (Greece, Smart Systems Manager):

ITIL is only used for IT operations and too many roles and responsibilities are defined within ITIL, which means that a poor adoption leads to increased confusion of the workforce adopting it.

In fact, the extension of principles and practices signals the transition an organisation has to pursue in order to achieve the desired adoption level. However, the top three challenges identified concerning DevOps practice and principle adoption journey were: 1) Poor communication and information flow; 2) Deep-seated company culture; 3) Operations not participating in the requirements specifications. Additionally a number of interviewees registered that blameful culture and time consuming bureaucratic processes do not promote a sense of change in behavior to adopt new practices and principles but maintained a collective cultural complacency among IT teams. P7 (UAE, Senior Digital Transformation Technologist & Solution Practice Lead) mentioned that:

Blame 'game' exists between IT teams which breeds increased blameful culture, especially between Dev and Ops teams. By bringing these two teams together to code, test, deploy - the blame game stops. So now a blame-free culture starts to be promoted and gradually become evident as change emerges in behavioral patterns.

P11 (Greece, Head of Remote Transactions) adds that:

Bureaucratic approach leads to informal ways of complete disregard of approval points. Senior management is keen to use this kind of approach to get things done quicker.

DevOps is highly regarded as a group of practices and principles that characterise collaborative culture [50] and these top three challenges indicate the requirement to address them from an organisational culture perspective. According to answers from Question 4, 66% of participants are aware of DevOps and its associated practices and principles. Therefore, naturally the participants were asked to define DevOps. The four most popular phrases used were "a shift of mindset", "enhanced collaboration and communication", "continuous deployment" and "automated testing process". The shift of mindset was pointing to established organizational cultural behaviors such as the one P3 (Greece, CIO) referred to:

There is a mindset to "never outshine the master".

P11 (Greece, Head of Remote Transactions) mentioned that:

The 'email culture' on which business units heavily rely is detrimental to DevOps adoption aspirations.

To that extent P18 (UK, Managing Director and Lead Consultant) mentioned that:

Culture is a very wide term. So if the incentives are in conflict with team expectations than there is going to be a situation of complaining about tool usage. Enterprise-wide incentives alignment is strongly required under such circumstances.

Moreover, 53% believe that the DevOps leader role should be an individual professional, whereas 33% would trust the role to a team. People suggested that it was best to have an individual lead DevOps adoption, and organisational transformation efforts initially, but that and then transition to a team effort was also deducted at 13%. Note that the adoption efforts should be continuous in nature, and not be conducted in a project-based manner as temporary endeavor. In this context P18 (UK, Managing Director and Lead Consultant) stated that:

DevOps adoption practices and principles should not be viewed as a project under the context of a transformation with a beginning and an end rather a continuous aspiration for improvement of the current state of adopted practices and principles.

In addition, P8 (UK, Principal Consultant, IT Service Management) added that a common pitfall is that:

Overestimation of DevOps practice adoption is common.

P10 (UK, Managing Director) mentioned one area that requires particular attention:

Uneven experience of people gives birth to assumptions. For instance, if not everyone in the same team has the same level of knowledge and understanding on ITIL then different people would assume different definition for IT service management. HR plays a big role in recruiting people with uneven skills. This is an unrecognised cost to the IT organization.

Furthermore, P21 (UK, Founding Consultant, IT Service Management) stated that:

The transformation of Waterfall-to-Agile-to-DevOps in an IT organization has to be an enterprise-wide endeavor. The missing link is HR not being on the same page with the efforts to change towards agility.

P1 (Saudi Arabia, PMO Director) added that:

The human resources department is an enabler leading the change.

Whereas P14 (Greece, Head of Applications) commented that:

Lack of continuous commitment to DevOps adoption by organization-internal IT customers inhibits the adoption itself.

The leadership skills that were mentioned by 50% of interview participants included: 1) technical background; 2) negotiation skills; 3) communication and collaboration skills; 4) previous experience on transformation. Holistic systems thinking was mentioned by 27% of interviewees. Business background by 17%. Strategic thinking by 13%. Furthermore, there was a lot of iteration around the influential skills, holistic systems thinking, a multi-cultural mindset and increased awareness around dealing with suboptimal productivity.

When considering DevOps leadership objectives, a remarkable 87% of interview participants agreed that DevOps practice adoption should be extended in an enterprise-wide fashion and should include external service providers in its scope. To overcome DevOps adoption inhibitors P19 (Greece, IT Operations Manager) stated that:

Leadership skillset is the most important thing to adoption barrier breakdown.

In addition, P23 (Estonia, CDO) added that:

A cross-functional leadership role with end-to-end ownership of DevOps adoption is imperative.

Lastly, the organizational teams should be part of a DevOps practice adoption journey are IT Development (97%), IT Operations (97%), Quality Assurance (93%), Information Security (80%) and Board of Directors (73%).

5. THREATS TO VALIDITY

Concerning construct validity, there is heavy reliance on each of the interviewed practitioners' subjective perception. However, currently there is no objective approach to measure whether or not a DevOps transition journey, in the context, of practice and principle adoption within organizations can be associated to successful outcomes. The semi-structured interview series approach undertaken offers rigorous procedures for data analysis but with a certain degree of research bias. It is probable, that other researchers might deduce different findings and outcomes looking at the same set of data but the author believes the main perceptions would be preserved. This is a typical threat related to similar studies, which do not claim to generate definitive findings.

The author welcomes extensions to the research or potential discovery of new dimensions for future study. Future work can focus on the identification of DevOps adoption leadership styles or leader characteristics that could "make" or "break" a transition journey towards a DevOps-oriented organization. Furthermore, concerning external validity, although the viewpoint of the interviewed practitioners is considered with different backgrounds, working in organizations from nine (9) different industry domains and ten (10) different countries the author does not claim that research results from this contribution are valid to other scenarios. However, saturation was achieved after the 20th interview.

6. FUTURE RESEARCH

This study can be further enhanced in the future by assessing and determining the usefulness of the outcomes under the prism of a survey which reiterates the questions posed to a wider participation such as a survey. The extension of the findings can be further evaluated under the lens of a case study.

7. CONCLUSIONS

The data collected from a series of interviews and participating practitioners, indicate a clear list of specific agile, lean and DevOps practices and principles that regarded an extension to structured service management approaches and are relevant to DevOps adoption theory. The main findings associated to the research questions are that:

1. Specific agile, lean and DevOps practices such as 1) organizational culture, 2) monitoring/measurement, 3) automation are crucial in the software development lifecycle (RQ1)
2. Specific agile, lean and DevOps principles such as 1) SCRUM 2), Kanban 3) Continuous Delivery are crucial in the software development lifecycle (RQ1)
3. The set of service management processes that continue to form a strong part of DevOps-oriented structures are Change Management, Service Portfolio Management (including Service Catalog Management), Release and Deployment Management and Service Level Management. (RQ2)
4. There is overwhelming consensus that a DevOps leadership role should exist (86%) and that the role should carry a continuous effect not a project based. (RQ3)
5. DevOps practices and principles adoption are challenged due to poor communication and information flow, deep-seated company culture and operations not being involved in the requirements specifications. (RQ3)
6. DevOps practice adoption should be extended in an enterprise-wide fashion (87%), with team structure based on existing Development (97%), Operations (97%), Quality Assurance (93%) and Information Security (80%) teams. (RQ3)

The outcomes of this paper can be used by practitioners in software-intensive organisations willing to introduce a DevOps orientation in terms of practices and principles adoption. The research can further be extended in the future to explore more of the facets of leadership style(s), capabilities, skills and competencies required in the context of continuous DevOps adoption.

ACKNOWLEDGEMENTS

The authors would like to thank the interview participants for all the committed time and efforts to contribute to research results and outcomes.

REFERENCES

- [1] Computer Weekly Digital Edition, <https://www.computerweekly.com/news/2240242478/Satya-Nadella-Every-business-will-be-a-software-business>. Accessed April 18, 2020
- [2] The Wall Street Journal, <https://www.wsj.com/articles/SB10001424053111903480904576512250915629460>. Accessed April 18, 2020
- [3] Reeves, M. Deimler, (2011) "Adaptability: The New Competitive Advantage. In: Harvard Business Review", *Harvard Business Review Press Books*, pp1-9.
- [4] Lauesen, S. (2020) "IT Project Failures, Causes and Cures," in *IEEE Access*, Vol.8, pp72059-72067, 2020.

- [5] Diaz Piraquive, F. N., Gonzalez Crespo, R., Medina Garcia, V. H. (2015) "Failure cases in IT project Management," in *IEEE Latin America Transactions*, Vol.13-7, pp2366-2371.
- [6] Gupta, S., Mishra, A., Chawla, M. (2016) "Analysis and recommendation of common fault and failure in software development systems," *2016 International Conference on Signal Processing, Communication, Power and Embedded System (SCOPES)*, pp1730-1734.
- [7] Liu, S., Wu, B., Meng, Q. (2012) "Critical affecting factors of IT project management," *2012 International Conference on Information Management, Innovation Management and Industrial Engineering*, pp494-497.
- [8] Altahtooth, U. A., Emsley, M. W. (2014) "Is a Challenged Project One of the Final Outcomes for an IT Project?," *47th Hawaii International Conference on System Sciences*, pp4296-4304.
- [9] Verner, J., Sampson, J., Cerpa, N. (2008) "What factors lead to software project failure?," *2nd International Conference on Research Challenges in Information Science*, pp71-80.
- [10] Sardjono, W., Retnowardhani, A. (2019) "Analysis of Failure Factors in Information Systems Project for Software Implementation at The organization," *International Conference on Information Management and Technology (ICIMTech)*, Jakarta/Bali, pp141-145.
- [11] Ashraf, J., Khattak, N.S., Zaidi, A.M. (2010) "Why do public sector IT projects fail," *7th International Conference on Informatics and Systems (INFOS)*, pp1-6.
- [12] Abbas, A., Faiz, A., Fatima, A., Avdic, A. (2017) "Reasons for the failure of government IT projects in Pakistan: A contemporary study," *International Conference on Service Systems and Service Management*, pp1-6.
- [13] Mohagheghi, P., Jørgensen, M. (2017) "What Contributes to the Success of IT Projects? Success Factors, Challenges and Lessons Learned from an Empirical Study of Software Projects in the Norwegian Public Sector," *IEEE/ACM 39th International Conference on Software Engineering Companion (ICSE-C)*, pp371-373.
- [14] Rajkumar, M., Pole, A.K., Adige, V.S., Mahanta, P. (2016) "DevOps culture and its impact on cloud delivery and software development," *International Conference on Advances in Computing, Communication, & Automation (ICACCA)*, pp1-6.
- [15] Hoda, R., Noble, J. (2017) "Becoming Agile: A Grounded Theory of Agile Transitions in Practice," *IEEE/ACM 39th International Conference on Software Engineering (ICSE)*, pp141-151.
- [16] Office of Government Commerce (OGC) (2011) "ITILv3 Core Publications", *TSO (The Stationery Office)*, UK.
- [17] Office of Government Commerce (OGC) (2017) "Managing Successful Projects with PRINCE2", *TSO (The Stationery Office)*, UK.
- [18] Project Management Institute (PMI) (2017) "A guide to the project management body of knowledge (PMBOK® Guide), 6th ed.", *Project Management Institute, Inc*, Pennsylvania, USA.
- [19] Willis, J., 2010. What DevOps means to me, <https://blog.chef.io/what-devops-means-to-me/>, Accessed April 25, 2020
- [20] Bass, L., Weber, IO., Zhu, L. (2015) "DevOps: A Software Architect's Perspective", *Addison Wesley*, US.
- [21] Dyck A., Penners R., Lichter H. (2015) "Towards Definitions for Release Engineering and DevOps", *IEEE/ACM 3rd International Workshop on Release Engineering*.
- [22] Kersten, M. (2018) "What Flows through a Software Value Stream?," in *IEEE Software*, Vol.35-4, pp8-11.
- [23] Horlach, B., Drews, P., Schirmer, I., and Boehmann, T. (2017) "Increasing the Agility of IT Delivery: Five Types of Bimodal IT Organization," *Hawaii International Conference on System Sciences*, USA.
- [24] The Countries Most (and Least) Likely to be Affected by Automation, <https://hbr.org/2017/04/the-countries-most-and-least-likely-to-be-affected-by-automation>, Accessed April 18, 2020
- [25] World Economic Forum - Strategies for the New Economy Skills as the Currency of the Labour Market, http://www3.weforum.org/docs/WEF_2019_Strategies_for_the_New_Economy_Skills.pdf, Accessed April 18, 2020\
- [26] Larjovuori, R.L., Bordi, L., Heikkilä-Tammi, K. (2018) Leadership in the digital business transformation" *Proceedings of the 22nd International Academic Mindtrek Conference (Mindtrek)*, Association for Computing Machinery, USA
- [27] Beck K. (2001) "Principles behind the Agile Manifesto", *Agile Alliance*.
- [28] Poppendieck, M. and Poppendieck, T. (2003) "Lean Software Development: An Agile Toolkit", *Addison-Wesley Professional*, Boston.

- [29] Takeuchi, H. and Nonaka, I. (1986) "The New New Product Development Game", *Harvard Business Review*, Vol. 64, pp137-146.
- [30] Sutherland, J., Schwaber, K. (2017) "The Definitive Guide to Scrum: The Rules of the Game", USA.
- [31] Levinson, W.A. (2002) "Henry Ford's Lean Vision: Enduring Principles from the First Ford Motor Plant", *Productivity Press*, New York.
- [32] Shingo, S., Dillon, A.P. (1988) "A study of the Toyota production system", *Productivity Press*, New York.
- [33] Ohno, T. (1988) "Toyota Production System: Beyond Large- Scale Production", *Productivity Press*, New York.
- [34] Krafcik, J. F. (1988) "Triumph of the Lean Production System", *Sloan Management Review*, Vol. 30 (1), pp41–52.
- [35] Womack, J.P. and Jones, D.T. (1990) "The Machine That Changed the World", *Rawson Associates*, New York.
- [36] Poppendieck, M. and Poppendieck, T. (2007) "Implementing Lean Software Development – From Concept to Cash", *Pearson Education*, Boston.
- [37] Rodríguez, P., Partanen, J., Kuvaja, P., Oivo, M. (2014) "Combining Lean Thinking and Agile Methods for Software Development A Case Study of a Finnish Provider of Wireless Embedded Systems", *Proceedings of the Annual Hawaii International Conference on System Sciences*, pp4770-4779.
- [38] Ravichandran, A., Taylor, K., Waterhouse, P. (2017) "DevOps for Digital Leaders, Reignite Business with a Modern DevOps-Enabled Software Factory", Winchester.
- [39] Jabbari R., Ali N.B., Petersen K., Tanveer B. (2016) "What is DevOps? A Systematic Mapping Study on Definitions and Practices", *Proceedings of the Scientific Workshop Proceedings of XP2016*, Edinburgh.
- [40] De França, B.B.N., Jeronimo, H., Travassos, G.H. (2016) "Characterizing DevOps by Hearing Multiple Voices", *Proceedings of the 30th Brazilian Symposium on Software Engineering (SBES)*, Association for Computing Machinery, New York, pp53–62.
- [41] Lwakatare, Lucy Ellen & Kuvaja, Pasi & Oivo, Markku. (2016) "An Exploratory Study of DevOps: Extending the Dimensions of DevOps with Practices", *The Eleventh International Conference on Software Engineering Advances (ICSEA)*, Rome.
- [42] Smeds, J., Nybom, K., Porres, I. (2015) "DevOps: A Definition and Perceived Adoption Impediments", *16th International Conference on Agile Software Development (XP)*, Springer International Publishing, pp. 166–177.
- [43] Dingsøyr T., Lassenius C. (2016) "Emerging themes in agile software development: Introduction to the special section on continuous value delivery", *Information and Software Technology*, pp. 56-60.
- [44] Lwakatare L.E., Kuvaja P., Oivo M. (2016) "Relationship of DevOps to Agile, Lean and Continuous Deployment", *PROFES*, pp. 399-415.
- [45] Myrbakken H., Colomo-Palacios R. (2017) "DevSecOps: A Multivocal Literature Review", *Software Process Improvement and Capability Determination, SPICE*, Communications in Computer and Information Science, Vol.770, Springer, Cham.
- [46] Drews, P., Schirmer, I., Horlach, B., Tekaat, C. (2017) "Bimodal Enterprise Architecture Management: The Emergence of a New EAM Function for a BizDevOps-Based Fast IT", *IEEE 21st International Enterprise Distributed Object Computing Workshop (EDOCW)*, pp57-64.
- [47] Kropp, M., Meier, A., Anslow, C., Biddle, R. (2018) "Satisfaction, Practices, and Influences in Agile Software Development", *Proceedings of the 22nd International Conference on Evaluation and Assessment in Software Engineering (EASE)*, Association for Computing Machinery, USA, pp112–121.
- [48] Wiedemann, A., Wiesche, M. (2018) "Are You Ready for DevOps? Required Skill Set for DevOps Teams", *Proceedings of the European Conference on Information Systems (ECIS)*, Portsmouth.
- [49] Sánchez-Gordón, M., Colomo-Palacios, R. (2018) "Characterizing DevOps Culture: A Systematic Literature Review", *Software Process Improvement and Capability Determination (SPICE)*, Communications in Computer and Information Science, Vol.918, Springer.
- [50] Luz, P.W., Pinto, G., Bonifácio, R. (2019) "Adopting DevOps in the real world: A theory, a model, and a case study", *Journal of Systems and Software*, pp157.

- [51] Masombuka, T., Mnkandla, E. (2018) “A DevOps collaboration culture acceptance model”, *Proceedings of the Annual Conference of the South African Institute of Computer Scientists and Information Technologists (SAICSIT)*, Association for Computing Machinery, USA, pp279–285.
- [52] The 4 Roles of DevOps Leadership, <https://devopscon.io/blog/the-4-roles-of-devops-leadership>, Accessed 26/04/2020
- [53] Sahu, S., Pathardikar, A., Kumar, A. (2018) “Transformational leadership and turnover: Mediating effects of employee engagement, employer branding, and psychological attachment”, *Leadership & Organization Development Journal*, Vol. 39, pp82-99.
- [54] Avolio, B.J., Gardner W.L. (2005) “Authentic leadership development: Getting to the root of positive forms of leadership”, *The Leadership Quarterly*, Vol.16-3.
- [55] Rudder, C.: 8 habits of successful DevOps team leaders, <https://enterpriseproject.com/article/2019/11/devops-habits-successful-leaders>, Accessed 26/04/2020
- [56] Dubinsky, Y., Hazzan, O (2010) “Ad-hoc leadership in agile software development environments” *Proceedings of the ICSE Workshop on Cooperative and Human Aspects of Software Engineering (CHASE)*, Association for Computing Machinery, USA.
- [57] Puppet, DORA, State of DevOps Report 2017, <https://puppet.com/resources/report/2017-state-devops-report>, Accessed 26/04/2020
- [58] Commission Recommendation of 6 May 2003 concerning the definition of micro, small and medium-sized enterprises, <https://eur-lex.europa.eu/eli/reco/2003/361/oj>, Accessed April 18, 2020
- [59] Martin, K., Osterling, M. (2014) “Value Stream Mapping: How to Visualize Work and Align Leadership for Organizational Transformation”, *McGraw-Hill Education*, UK.
- [60] Mujtaba, S., Feldt, R., Petersen, K. (2010) “Waste and Lead Time Reduction in a Software Product Customization Process with Value Stream Maps”, *21st Australian Software Engineering Conference*, pp139-148.

AUTHORS

Krikor Maroukian gained a BSc. (Hons) degree in Computer Science and a MSc. in Applied Informatics. Currently, he works as a Sr Modern Service Management consultant at Microsoft for Central Eastern Europe. He is also the International Representative of itSMF Hellas and BoD member of the British Computer Society (BCS), The Chartered Institute for IT, Hellenic Section. In the past, he has held Project Management and Security Management positions. Krikor is a PhD student at Henley Business School, University of Reading, UK. Krikor’s interest lie in the areas of service management, agile software development, lean product development, DevOps adoption. Krikor is author of Axelos ITIL4® – Managing Professional High Velocity IT. Krikor was awarded the Highly Commended Paper in the 2017 Emerald Literati Network Awards for Excellence.



Stephen R. Gulliver received a BEng. (Hons) degree in Microelectronics, an MSc. degree (Distributed Information Systems) and a PhD in 1999, 2001, and 2004 respectively. Stephen worked within the Human Factors Integration Defence Technology Centre (HFI DTC), before getting a job as a lecturer at Brunel University (2005-2008). Dr Gulliver joined Henley Business School (University of Reading) in 2008 as a lecturer and in 2014 was promoted to the role of Associate Professor. Since 2005 Dr Gulliver’s teaching and research (in the UK and abroad) has linked to the area of pervasive Informatics, and he has interests including: multimedia and information assimilation, e-learning and education systems, usability and human factors, technology acceptance, persuasion systems, health systems, and systems conflict and failure.



COMMUNICATION BETWEEN COROUTINES ON SUNWAY MANY-CORE PLATFORM

Shaodi Li¹, Junmin Wu², Yi Zhang² and Yawei Zhou²

¹School of Software Engineering, University of Science and Technology of China, Suzhou, China

²School of Computer Science and Technology, University of Science and Technology of China, Hefei, China

ABSTRACT

Communication between parallel programs is an indispensable part of parallel computing. SW26010 is a heterogeneous many-core processor used to build the Sunway TaihuLight supercomputer, which is well suited for parallel computing. Our team is designing and implementing a coroutine scheduling system on SW26010 processor to improve its concurrency, it is very important and necessary to achieve communication between coroutines for the coroutine scheduling system in advance. Therefore, this paper proposes a communication system for data and information exchange between coroutines on SW26010 processor, which contains the following parts. First, we design and implement a producer-consumer mode channel communication based on ring buffer, and designs synchronization mechanism for condition of multi-producer and multi-consumer based on the different atomic operation on the MPE (management processing element) and the CPE (computing processing element) of SW26010. Next, we design a wake-up mechanism between the producer and the consumer, which reduces the waiting of the program for communication. At last, we test and analyse the performance of channel in different numbers of producers and consumers, draw the conclusion that when the number of producers and consumers increases, the channel performance will decrease.

KEYWORDS

Coroutine, SW26010, Many-core, Parallel Communication, Synchronization

1. INTRODUCTION

The SW26010 is a heterogeneous many-core processor, which is a china-made high-performance processor developed by Wuxi Jiangnan Institute of Computing Technology. It belongs to the Sunway series. It has good performance in super computer and high performance computing area. And it is the main building-block of the current world's third fastest supercomputer: Sunway Taihu Light[1]. This processor has been used in many fields of high performance computing, such as computational mechanics[2], bioinformatics[3], deep learning[4] and so on. But for a long time, application development on this processor has several difficulties such as high learning costs, highly associated with hardware, hard to migrate and so on. A SW26010 processor consists of 4 management processing elements (MPE, also called master core) and 256 computing processing elements (CPE, also called slave core). However, one CPE of SW26010 processor can only run one thread and it doesn't support blocking and switching, which limits its parallel ability. Therefore, our team uses the idea of coroutine, and designs a coroutine running framework on SW26010 processor to replace the direct use of threads on the CPE, which breaks

through the parallel restriction of Sunway many-core processor, and makes the upper applications be run more efficiently.

As an indispensable part of the coroutine running framework, the communication between coroutines need to be discussed. Since the communication between threads on Sunway many-core processor is mainly based on batch data transfer, and there is no fine-grained communication method suitable for ordinary programs, this paper designs a channel communication method which can exchange messages between coroutines on either MPE or CPE of Sunway processor, and provides a guarantee for cooperation of parallel coroutines.

This paper includes the following parts: First, the channel communication in producer-consumer mode is implemented based on ring buffer, and then, to ensure that no errors occur on the condition of multi-producer or multi-consumer competing with each other, the mechanism of synchronization is designed based on the different atomic operations on the MPE and CPE, which ensures the correctness of data transmission. Next, we design a wake-up mechanism of producer and consumer, which reduces the waiting of the program for communication. At last, this paper tests the performance of channel in different numbers of producers and consumers.

2. BACKGROUND AND RELATED WORK

2.1. SW26010 Many-Core Processor

The SW26010 is a heterogeneous many-core processor independently developed and designed by Wuxi Jiangnan Institute of Computing Technology of China. The heterogeneous many-core architecture combining on-chip computing array cluster and distributed shared storage. Sunway many-core processor is commonly used for the execution of high-performance computing programs, its hardware architecture is shown in Figure 1.

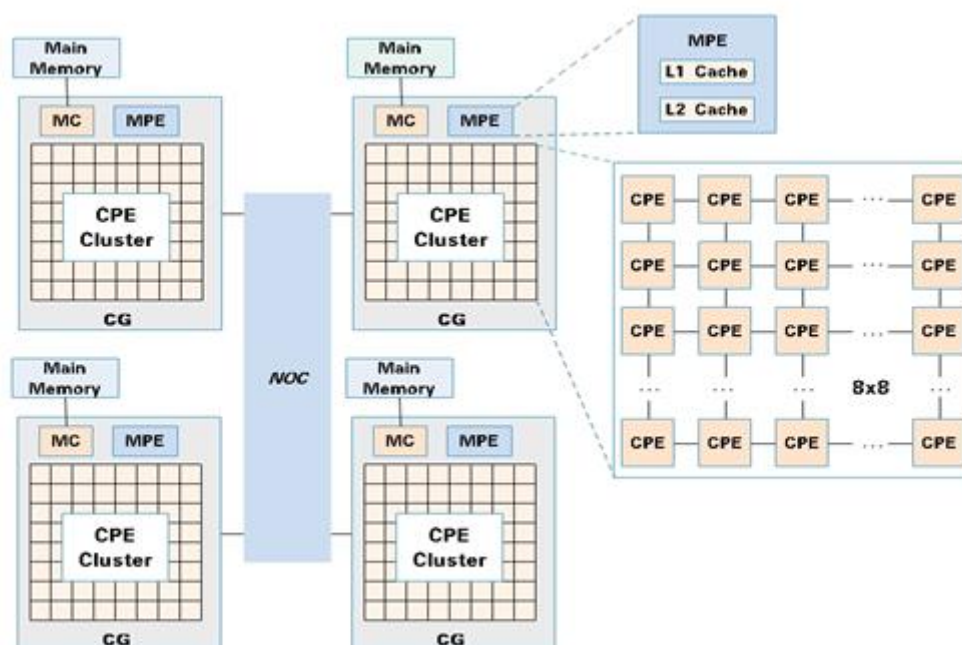


Figure 1. SW26010 processor.

Each SW26010 chip contains 260 cores, which are divided into four core groups (CGs). Each core group contains a management processing element (MPE, or master core), and subordinate 64 computing processing elements (CPE, or slave core). The frequency of the MPE and CPE is 1.45GHz. 64 CPEs are combined into a CPE cluster organized as an 8×8 mesh. Each core group is connected with an 8GB memory by a memory controller (MC), and the four core groups are connected by the network on-chip (Noc). SW26010 processor is designed based on the alpha instruction set, in which the MPE support complete alpha instruction set, while the CPE support simplified alpha instruction set. The whole chip can provide computing peak performance over 3TFlops. As for the storage structure, the MPE and the CPE both can access the main memory, Each MPE has 32KB L1 data cache and 256 KB L2 instruction/data cache to ensure the high efficiency of read and write to the main memory, while the CPE has no cache for memory read and write, resulting in inefficient access to main memory. But each CPE contains a 64KB local device memory (LDM), which can store the data needed for program running on the core. Each CPE can read and write its own LDM quickly, but cannot access LDM of other CPEs. A CPE can copy data from main memory to its LDM or write data back to main memory in batches by Direct Memory Access (DMA), which is the main data transmission method in high performance computing programs.

The operating system of SW26010 is a customized Linux flavour running on the first MPE, C/C++ and FORTRAN programs are supported on the MPE and C, FORTRAN programs are supported on the CPE. The MPE and CPE of Sunway many-core processor have different running environments, so the programs on the MPE and CPE need to be compiled separately, and then packaged in a single executable file by mixed compilation, finally submitted to work queue for execution. It can be seen from the calculation structure of SW26010 processor that the computing power of CPEs accounts for more than 98% of the computing power of the whole chip, so the development of application on SW26010 processor needs to give full play to the computing power of CPEs. In general, application development on SW26010 is based on the parallel execution of the MPE and CPE. Computing tasks are divided into small blocks and assigned to CPEs to execute, and the MPE executes communications or other parts that the CPE cannot run. This way, the core computing part of the program will be executed by the CPE, and the MPE only responsible for management part.

2.2. Implementation of Coroutine on SW26010 Processor

Coroutine is a user-controlled way of switching programs and achieving concurrency without operating system scheduling. The concept of coroutine is not complex. The basic principle is that when a program is running, it can actively give up its own control of running so that the thread can switch to other programs. Therefore, there are some simple coroutines implementations[5]. However, a good implementation of coroutine requires more detailed design in terms of scheduling and communication[6]. Owing to less system resource costs than threads, coroutine is often used in high-concurrency scenarios such as web crawlers, distributed system[7], simulation mechanism[8] and so on. In SW26010 processor, there are only one thread runs on a CPE. This scheme doesn't support blocking and switching, and limits its parallel ability. The use of coroutine can break through the concurrency restriction of the CPE, and can achieve multiple concurrency on a CPE only with one single thread. So our team decided to develop a framework of coroutine on SW26010 processor. Based on the master-slave parallel structure of SW26010 processor, we design and implement a coroutine library which combines dispatch, execution, communication and other modules. The coroutine framework based on the athread interface provided by SW26010, using thread on the CPE as coroutines instead of using it directly. In this way, upper applications can achieve higher concurrency and gain more efficiency. Coroutines on SW26010 processor is shown in Figure 2.

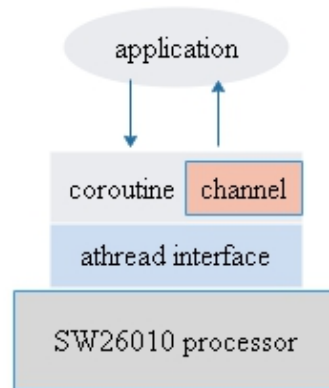


Figure 2. Coroutines on SW26010 processor

The implementation of coroutine on SW26010 Processor consists of the following parts:

1. Scheduler: The scheduler is running on the MPE, which creates a coroutine, initializes the coroutine, and assigns the coroutine to an execution queue of an executor on a CPE, waiting for the executor to execute.
2. Executor: Executor run on the CPE, and a CPE can only run one executor so each core group contains 64 executors, executors can execute specific programs. Each executor contains two queues, one is a runnable queue, the other is a wait queue, runnable queue contains coroutines that can be executes, wait queue contains coroutines blocked because of communication or other reason.
3. Communication module: If coroutines needs to cooperate with each other, they need to communicate and exchange data. The communication module of coroutine is called channel, a coroutine can send messages to others by using channel. This paper is mainly introduce the communication module.

3. DESIGN OF COMMUNICATION BETWEEN COROUTINES

3.1. Data Structure of Channel

Channel's data structure is based on ring buffer. Ring buffer[9] is a first-in-first-out data structure that reduces duplicate address operations and increases stability relative to queues[10]. Ring buffer is widely used in various fields[11]. It is easy to separate data writing from reading by using ring buffer, avoids competition between reading threads and writing threads, and reduces using of locks. We use ring buffer as channel's infrastructure. The working principle of ring buffer is shown in the Figure 3:

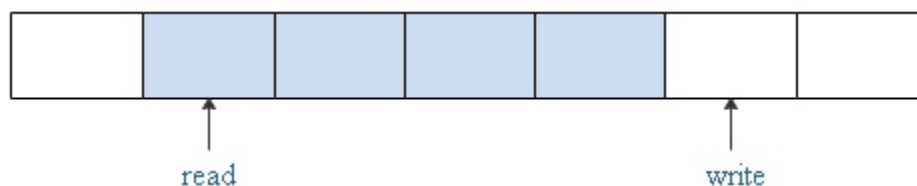


Figure 3. Ring buffer structure

As shown in the Figure 3, in a fixed size buffer, there are two pointers: read and write. When some data is written to buffer, write increases. When some data is read from buffer, read increases. Using ring buffer, we can simply realize producer-consumer mode. Because the producer only affects the write pointer and the consumer only affects the read pointer, when there is only one producer and one consumer, we do not need to lock the buffer, which increases the efficiency of communication. The channel structure including ring buffer is as follows:

```

1.  typedef struct {
2.      char *buffer;
3.      int capacity;
4.      int elem_size;
5.      int read;
6.      int write;
7.      int to_read;
8.      int to_write;
9.      list read_queue;
10.     list write_queue;
11. }channel;

```

Figure 4. Data structure of channel

In the channel structure, buffer refers to the buffer where data is stored, elem_size refers to the size of a message, capacity refers to the maximum number of messages stored in the buffer, write refers to the location where the message will be written, read refers to the next message can be read, to_read and to_write are used to ensure parallel synchronization when multiple producers or consumers are involved, which will be described in the next section in detail. The two lists are used to store coroutines waiting on the channel when send or receive fails, which will be described in Section 3.3. The data structure of channel is stored in main memory, so that both the MPE and the CPE can access.

3.2. Design of Parallel Synchronization Mechanism

With ring buffer, messages can be delivered safely without synchronization mechanism in the case of single producer and single consumer. But when there are multiple producers or consumers, the contention of multiple threads for the same data may result in data coverage. Therefore, we need to take certain measures to ensure that the data in the channel is correct[12]. In x86 instruction computers, CAS (compare and swap) atomic operation is often used to deal with multithreading competition[13]. In SW26010 processor, the MPE and CPE have different degrees of instruction support. CAS operation is supported on the MPE, but not on the CPE. We first use CAS operation to deal with multithreading competition on the MPE.

3.2.1. Parallel Synchronization Mechanism on the MPE

CAS (compare and swap) can compare and exchange data in one instruction, which is commonly used in the unlocked algorithm. Its common form is as follows:

CAS (dest, oldval, newval)

Where *dest* is the data address, *oldval* is the current value, and *newval* is the new value. When the value pointed to by *dest* is equal to *oldval*, the value will be updated to *newval* and *true* will be returned, otherwise it will not be updated and *false* will be returned. When two threads use CAS instruction at the same time, only one thread can succeed, and other threads will fail, thus we ensures that only one thread can complete CAS operation and process data. Using CAS operation to build the parallel synchronization mechanism of message sending is as follows:

```

1.    do {
2.        if (full(chan)){
3.            co_swap_out();
4.        }
5.        temp = chan->write;
6.        next = temp + 1;
7.        ok = CAS(&chan->write, temp, next);
8.    } while (!ok);
9.    //copy data here

```

Figure 5. Message send with parallel synchronization on the MPE

When sending data to the channel, the producer first determine whether the channel is full. If channel is full, the producer cannot send a message to the channel, then it gives up the control right and let other coroutines run. If the channel is not full, the producer first reads the write pointer and then updates the value of write with CAS operation. If it succeeds, it means that no other coroutines successfully change the write value, a message can be sent to buffer according to the write pointer. Note that while other coroutines may operate on write values when current coroutine writes data to the buffer, data coverage will not occur because we have determined the write location in the buffer. In this way, we ensure the synchronization of channel message sending on the MPE.

3.2.2. Parallel Synchronization Mechanism on the CPE

While CAS can be used to realize the synchronization of parallel programs and ensure the correctness of communication on the MPE, it is not supported on the CPE. There is only one atomic operation supported on the CPE, which can modifies data. Its interface is as follows.

```
updt( _n_, _addr_)
```

This operation represents adding *_n_* to the data pointed by *_addr_*. Parallel synchronization of channel is more difficult to achieve on the CPE because the atomic operation changes data directly without comparison. This paper uses the mechanism shown below to synchronize channels, as shown in Figure 6.

```

1.   while (1){
2.       if (full (chan)){
3.           co_swap_out();
4.       }
5.       temp = chan->write;
6.       if (temp == chan->to_write){
7.           updt_addw(1,&(chan->write));
8.       } else {
9.           continue;
10.      }
11.      if (chan->write == temp + 1){
12.          //copy data here
13.          updt_addw (1,&chan->to_write);
14.          return 0;
15.      } else {
16.          updt_addw (-1,&chan->write);
17.          continue;
18.      }
19.  }

```

Figure 6. Message send with parallel synchronization on the CPE

In order to synchronize the writing of buffer using atomic operations, `to_write`, a comparison of the write pointer is introduced. When `to_write` is equal to `write`, it indicates that no coroutine is sending messages to the channel. When they are not equal, it indicates that a coroutine is sending. At the beginning, we read the value of variable `write`, save it in the variable `temp`, and compare it with the value of `to_write`. If they are not equal, it means that other producer has modified the value of the `write`. At this time, the `write` value should be read again. If they are equal, it means that other producer has finished sending to the channel, then this producer will modify the value of `write`. Since comparison and update cannot be done in one instruction, comparison and update may still be performed by two producers in the order of 6.-6.-7.-7., there is still a case where two producers have modified the value of variable `write`, so we read the value of variable `write` again and compare it with the value saved by the local variable `temp`. If the current value of variable `write` equals to `temp+1`, which indicates that only one atomic operation has been performed, message can be send to channel in next line, and the value of variable `to_write` can be updated to complete one message sending. If the value of variable `write` is not equal to `temp+1` at this time, it means that other threads have also made atomic updates, this producer should reduce the value of variable `write` by atomic update, let the `write` value revert to the state that was before this producer accessed. This send can be considered a failure, and we do it again from the beginning. In this way, we ensure that when multiple producers send data to the channel, at most one producer can find that after atomic operation, the value of variable `write` equal to the value of variable `temp+1`, and other producers will fail. Thus, the synchronization of messages in the channel is ensured.

Although the synchronization mechanism on the CPE can also ensure that data will not be overwritten or be read repeatedly, it is more complex than the CAS operation on the MPE, and has the possibility of invalid operation, so the performance loss is higher than that of the MPE.

3.2.3. Different Modes of Channels

Although using the synchronization mechanism can ensure the correctness of the messages in channel, it will also result in decreasing the communication efficiency. Therefore, in order to maximize the communication efficiency, this paper designs different communication modes for different number of producers and consumers. Different modes can be chosen according to the actual needs to maximize the efficiency of communication. There are four modes in total:

Single producer-single consumer: only one producer and one consumer. In this case, there is no synchronization, and the efficiency is the highest.

Single producer- multi consumer: only one producer, but multiple consumers. In this case, the consumer read buffer needs to be synchronized, but the producer can send messages directly.

Multi producer-single consumer: multiple producers, but only one consumer. In this case, the producer write buffer needs to be synchronized, and the consumer can receive messages directly.

Multi producer-multi consumer: multiple producers and multiple consumers. In this case, both reading and writing of buffer needs to be synchronized, which is also the default mode of channel.

3.3. Blocking and Wakeup Mechanism of Channel

In the process of communication, sometimes the program wants to communicate cannot communicate normally, for example, the producer cannot send message when the channel is full. At that time, the program has no choice but to wait. When it is implemented in multi-threaded mode, the mechanism of cyclic access or thread switching can be chosen. However, the thread switching consumes much system resources, which will lead to the performance degradation. But for the program based on coroutines, the switching consumes less resources, we choose to let the coroutine block and switch when the communication cannot be carried out. If a coroutine is blocked and switched off running queue, other coroutines is going on running, which reduces the time cost for waiting. When a producer sends messages to channel, it will first determine whether the channel buffer is full. If it is not full, it will send a message and continue to run. If it is full, the message cannot be sent, and the producer coroutines will enter a block, and the executor will transfer the execution right to other coroutines to run. The blocked coroutine will be recorded on the waiting queue of the channel. The blocked coroutine does not wake up automatically or be awakened by executor, but it wakes up when a consumer takes a message out of the channel so that the channel is no longer full. At that point, the blocked coroutine back to the running queue to continue run, and has a high probability successfully send messages. Similarly, when the channel is empty, the consumer coroutine will also be blocked and be awakened by a producer coroutine. This kind of mutual wake-up mechanism allows a program to directly give up the execution right in the case of unable to communicate, and let other coroutines run instead of waiting in a loop. It also does not consume a lot of system resources like thread switching, and effectively uses the operation ability of the processor.

4. EXPERIMENTAL RESULTS AND ANALYSIS

4.1. Performance Test of Channel

In order to understand the specific performance of channel communication, it is necessary to test the operation performance of channel under different conditions. This paper uses such a process to simulate the use of channel under real conditions:

First, a channel is created. In order to get the minimum time of one message sending and receiving, and to test the highest performance of channel, the capacity of channel in this experiment is large enough to accommodate all message data, so there will be no blocking. Then, the producer produces messages. In this test, a randomly generated integer value is used as the message data, and the message is sent to the channel by the producer many times, the average sending time is taken as the time of one message sending. Next, the consumer obtains data from the channel, and the average receiving time is taken as the time of one message receiving. Since channel has different modes, which will affect the competition between producers or consumers, we test channel performance under different conditions, which including different cores and different number of producers and consumers. And the result is shown in Table 1.

Table 1. Sending/Receiving time under different conditions.

number of producer/consumer	1	10	32
MPE send	0.13 μ s	0.22 μ s	0.22 μ s
MPE receive	0.12 μ s	0.23 μ s	0.22 μ s
CPE send	1.37 μ s	30 μ s	457 μ s
CPE receive	1.95 μ s	54 μ s	791 μ s

4.2. Analysis

It can be seen from Table 1 that the communication efficiency on the CPE is lower than that on the MPE, and with the increase of producers/consumers, the sending/receiving time for one message increase whether on the MPE or CPE, but the increase on the CPE is much higher than that on the MPE. The process time of one sending/receiving on the MPE is about the same when there are 10 and 32 producers/consumers, but on the CPE, the sending/receiving time of 32 producers/consumers is much longer than that of 10 producers/consumers.

There are two reasons why the communication efficiency of the CPE is lower than that of the MPE. First is that the speed accessing main memory from the CPE is lower than that of the MPE. Second, the synchronization mechanism on the CPE will cause much more decrease of efficiency when producer or consumer increases. More processes competing, higher the probability of invalid operation, then the average communication time increases.

5. CONCLUSIONS

In this paper, we design the producer-consumer mode inter-core channel communication based on the coroutine implementation on SW26010 processor. We design the data structure based on ring buffer, the synchronization mechanism based on different atomic operations of the MPE and CPE, and the mechanism of mutual wake-up between producers and consumers, so that the security and efficiency of communication are guaranteed. At last, we test and analyse the performance of channel, draw the conclusion that the performance of channel on the CPE is

lower than that on the MPE due to the lower efficiency of read/write to memory, and the channel performance will decrease when the number of producers and consumers increases.

This study provides an effective communication guarantee for the implementation of the coroutine on SW26010 processor, provides an efficient communication interface for the development of upper application, and improves the efficiency of program execution, and explores the communication capability of SW26010 processor. Because the performance of channel is mainly affected by the memory read/write efficiency and parallel synchronization, the future directions for research are to reduce the read/write to memory and reduce the competition between coroutines.

ACKNOWLEDGEMENTS

This work is supported by the National Key Research and Development Program of China under Grant 2018YFB1003601

REFERENCES

- [1] Fu, H., Liao, J., Yang, J., Wang, L., Song, Z., Huang, X., ... & Zhao, W. (2016). The Sunway TaihuLight supercomputer: system and applications. *Science China Information Sciences*, 59(7), 072001.
- [2] Duan, X., Xu, K., Chan, Y., Hundt, C., Schmidt, B., Balaji, P., & Liu, W. (2017, September). S-Aligner: Ultrascable Read Mapping on Sunway Taihu Light. In *2017 IEEE International Conference on Cluster Computing (CLUSTER)* (pp. 36-46). IEEE.
- [3] Wang, X., Liu, W., Xue, W., & Wu, L. (2018, February). swSpTRSV: a fast sparse triangular solve with sparse level tile layout on sunway architectures. In *Proceedings of the 23rd ACM SIGPLAN Symposium on Principles and Practice of Parallel Programming* (pp. 338-353).
- [4] Fang, J., Fu, H., Zhao, W., Chen, B., Zheng, W., & Yang, G. (2017, May). swdnn: A library for accelerating deep learning applications on sunway taihulight. In *2017 IEEE International Parallel and Distributed Processing Symposium (IPDPS)* (pp. 615-624). IEEE.
- [5] Bailes, P. A. (1985). A low-cost implementation of coroutines for C. *Software: Practice and Experience*, 15(4), 379-395.
- [6] Pauli, W., & Soffa, M. L. (1980). Coroutine behaviour and implementation. *Software: Practice and Experience*, 10(3), 189-204.
- [7] Hui-Ba, L. I. , Yu-Xing, P. , & Xi-Cheng, L. U. . (2008). A programming pattern for distributed systems. *computer engineering & science*.
- [8] Xu, X., & Li, G. (2012, October). Research on Coroutine-Based Process Interaction Simulation Mechanism in C++. In *Asian Simulation Conference* (pp. 178-187). Springer, Berlin, Heidelberg.
- [9] Zhang-juna, Y. A. O., Shu-yub, C. H. E. N., & Yaoa, L. U. (2012). Research and Implementation of High-performance Ring Buffer [J]. *Computer Engineering*, 8.
- [10] Feldman, S., & Dechev, D. (2015). A wait-free multi-producer multi-consumer ring buffer. *ACM SIGAPP Applied Computing Review*, 15(3), 59-71.
- [11] Bergauer, H., Jeitler, M., Kulka, Z., Mikulec, I., Neuhofer, G., Padrta, M., & Taurok, A. (1996). A 1-GHz Flash-ADC module for the tagging system of the CP-violation experiment NA48. *Nuclear*

Instruments and Methods in Physics Research Section A: Accelerators, Spectrometers, Detectors and Associated Equipment, 373(2), 213-222.

- [12] He, Z. (2012). On algorithm design and programming model for multi-threaded computing (Doctoral dissertation, Georgia Institute of Technology).
- [13] Michael, M. M. (2003, August). CAS-based lock-free algorithm for shared dequeues. In European Conference on Parallel Processing (pp. 651-660). Springer, Berlin, Heidelberg.

AUTHOR

Shaodi Li, postgraduate student of School of Software Engineering, University of Science and Technology of China. Research direction is parallel computing and communication.



© 2020 By AIRCC Publishing Corporation. This article is published under the Creative Commons Attribution (CC BY) license.

LINKING SOCIAL MEDIA POSTS TO NEWS WITH SIAMESE TRANSFORMERS

Jacob Danovitch

Institute for Data Science, Carleton University, Ottawa, Canada

ABSTRACT

Many computational social science projects examine online discourse surrounding a specific trending topic. These works often involve the acquisition of large-scale corpora relevant to the event in question to analyze aspects of the response to the event. Keyword searches present a precision-recall trade-off and crowd-sourced annotations, while effective, are costly. This work aims to enable automatic and accurate ad-hoc retrieval of comments discussing a trending topic from a large corpus, using only a handful of seed news articles.

KEYWORDS

Deep Learning, Natural Language Processing, Information Retrieval, Social Media, News Articles.

1. INTRODUCTION

Many computational social science projects examine online discourse surrounding a specific trending topic, such as political events, natural disasters, or sporting matches. These works often involve the acquisition of large-scale corpora relevant to the event in question to analyze aspects of the response to the event, often with a focus toward social media. However, existing methods for the acquisition of these events come with trade-offs.

Commonly, keyword searches are used [1], which present a choice between high precision (using narrow keywords and getting fewer but more accurate results) and recall (using broad keywords and getting many irrelevant results). One common method of keyword searching, specific to Twitter, is the use of hashtags. However, hashtag-only searches can lead to low recall [2]. Crowd sourcing is an effective way to filter corpora [3], though it can be expensive both monetarily as well as in terms of time spent. This work proposes a method for automatic and accurate ad-hoc retrieval of comments discussing a trending topic from a large corpus using only a handful of seed news articles. Using a Siamese architecture and triplet loss, we jointly embed news articles and social media posts with the objective of minimizing the distance between the embeddings of each article and its relevant posts. This allows the automatic filtering of corpora by selecting comments most similar to news articles describing the event or topic of interest. The asymmetric lengths of comments and news articles pose a challenge for Siamese architectures. We propose a novel solution using a sparse attention mechanism, which allows the network to attend only to the most relevant parts of the input, easing the asymmetry in length. We make our code publicly available on *GitHub*.

2. RELATED WORK

The specific task of matching articles and social media comments (used interchangeably with *posts*) has received limited attention, especially in recent years. Some early works focused on *social content alignment*, the task of aligning comments to specific sentences within articles. Latent Dirichlet Allocation [4], [5] and several extensions, such as the Document-Comment Topic Model [6], [7] and Specific-Correspondence LDA [8], were used to provide interpretable alignments of comments to the most relevant segments of a news article. However, binary classification with feature engineering was seen to outperform these methods [9].

Similar methods have been employed for the task of matching tweets to news articles. [10] proposes a graphical weighted matrix factorization approach while also contributing a large-scale dataset similar to ours. Recent work using this dataset proposes an interactive attention mechanism to match tweet-article pairs [11]. These works find the most relevant news article for a particular tweet, rather than vice versa. The intent of our work is more similar to [12], which identifies the most relevant tweet for a given news article using binary classifiers as well as semantic similarity.

Little has been done to apply more recent advancements in deep learning to this task. This is likely due to the large computational overhead in training over corpora of news articles, which consist of thousands of tokens each, as well as the inherent theoretical challenges these methods face in processing long documents. These challenges have inspired creative solutions, such as segmenting long documents into individual sentences, hierarchically processing each sentence, and performing an aggregation step [13]. Alternatively, [14] presents an approach using Graph Convolution Networks on *concept-interaction graphs* to match pairs of news articles. While this is an effective method, the approach is restricted to pairwise classification, which creates a combinatorial explosion of pairs. Our work uses a Siamese architecture to perform retrieval using only cosine similarity.

3. METHODOLOGY

3.1. Task definition

We use a large corpus of tweets which share links to news articles published by CNN and the New York Times [10]. The corpus contains 34,888 tweets which link to 12,704 unique articles. While the goal of the original study is to find the most relevant news article for a given tweet, we are interested in the reverse; finding the most relevant tweets for a given news article. We say that for each tweet-article pair (T, A) , T is *relevant* to A , and any other tweet T' not paired with A is *irrelevant*.

3.2. Notation

We refer to vectors in bold (\mathbf{x}), tensors in capitalized bold (\mathbf{X}), and scalars in standard font (x, X). We define an encoder as a deep neural network which maps a sequence of S word embeddings $[\mathbf{e}_1, \mathbf{e}_2, \dots, \mathbf{e}_S]$ to either an output sequence of D -dimensional hidden states $\mathbf{H} = [\mathbf{h}_1, \mathbf{h}_2, \dots, \mathbf{h}_S]$ (in the sequence-to-sequence case) or a single D -dimensional representation \mathbf{H} (in the sequence-to-vector case).

3.3. Objectives

We wish to use a Siamese network to jointly learn fixed-length embeddings for each (T, A) pair, minimizing the distance between them using triplet loss. Projecting A and T into a common latent space allows us to compare the similarity of documents from vastly different domains (short, informal tweets versus long, formal news articles). However, doing so requires an encoder capable of solving several challenges pertaining to document length.

Noise. News articles can be in the order of thousands of tokens, and they often discuss multiple different topics [7]. The asymmetric length of tweets relative to the articles suggests that tweets rarely discuss the entirety of the article's content, making much of the article irrelevant and perhaps even adding additional noise. As such, it would be useful for an encoder to be able to filter out this noise and focus on only the most important input tokens.

Efficiency. Using large batch sizes creates more informative triplets [15], which is constrained by the already-high memory usage of processing thousands of tokens at once. These concerns are accentuated by the computational demands of the attention mechanism. While attention is more effective than other methods for modelling long sequences, its $\mathcal{O}(n^2)$ complexity [16] will exhaust reasonable resources with such long documents. As such, we require an encoder capable of efficiently processing long documents without sacrificing quality in the process.

3.4. Blocking out the noise

We begin by confronting the theoretical challenges of modelling long documents, such as the ability to capture the long-range dependencies and focusing only on crucially important tokens. Attention-based architectures have shown to outperform alternative candidates for these challenges [17]. However, certain models such as BERT [18] can be computationally intensive and impose maximum token lengths, which prevents their use. An additional problem for attention-based models introduced by such long documents is that they may struggle to identify vital portions of the text. For example, consider the attention mechanism and its multi-headed extension [16]:

$$\begin{aligned} \text{Attention}(\mathbf{Q}, \mathbf{K}, \mathbf{V}) &= \text{softmax}(f(\mathbf{Q}, \mathbf{K}))\mathbf{V} \\ \mathbf{a}_i &= \text{Attention}(\mathbf{Q}\mathbf{W}_{Q_i}, \mathbf{K}\mathbf{W}_{K_i}, \mathbf{V}\mathbf{W}_{V_i}) \\ \text{MultiHeadAttention}(\mathbf{Q}, \mathbf{K}, \mathbf{V}) &= [\mathbf{a}_1; \mathbf{a}_2; \dots \mathbf{a}_h] \end{aligned}$$

Where the parameters $\mathbf{W}_{Q_i}, \mathbf{W}_{K_i}, \mathbf{W}_{V_i} \in \mathbb{R}^D$ are trainable and f is a function which computes the similarity between each entry in \mathbf{Q} and \mathbf{K} . One such function is $\text{cos}(\mathbf{Q}, \mathbf{K}) = \frac{\mathbf{Q}\mathbf{K}^T}{\|\mathbf{Q}\| \cdot \|\mathbf{K}^T\|}$, which is known as cosine attention [19]. Crucial to the attention operation is the softmax function:

$$\sigma(\mathbf{z})_i = \frac{e^{z_i}}{\sum_{j=1}^S e^{z_j}}$$

This produces an S -length vector with a sum of 1, where each z_i is a weight for each token in the input document. The operation $\text{softmax}(\cdot)\mathbf{V}$ is equivalent to taking a weighted average of each token embedding in \mathbf{V} . Note that softmax has full support (all $\sigma(\mathbf{z})_i > 0$), which means that even unimportant portions of the input document will still receive non-zero weight [20]. As we noted earlier, our documents are very long and many of the words could be unimportant to the output, which makes it highly difficult for softmax to filter them out without assigning any weights of precisely 0. In fact, we observe a negative correlation between S and $\mathbb{E}[\sigma(\mathbf{z})_i]$ - that is, as

documents grow *longer*, the expected weight of a given token *decreases*. We provide a brief proof in appendix A.

This is problematic, as it will be difficult for the most important tokens to stand out in such long sequences like news articles. As the value of each attention weight decreases, the distribution becomes more uniform, and the operation becomes equivalent to simply taking the mean over all $\mathbf{h}_i \in \mathbf{H}$, many of which should have been filtered out. To counter this problem, we look toward the growing family of sparse activation functions. Figure 1 demonstrates a comparison of self-attention using softmax versus one such sparse function, known as sparsemax[21]. While both activations identify important tokens in a sequence of 5, softmax approaches uniformity for the sequence of length 25 while sparsemax still identifies important tokens.



Figure 1. Self-attention applied to sequences of 5 and 25 random embeddings using softmax and sparsemax. As document length increases, softmax produces nearly uniform weights approaching 0, making self-attention equivalent to taking the mean over all embeddings.

In particular, we replace softmax with the α – entmax activation function, a controllably sparse alternative [22], and we use a unique trainable parameter α_h for each attention head h . This is known as adaptively sparse multi-head attention, which addresses our first objective by allowing each attention head to learn an optimal level of sparsity [20]. This allows each head to learn which segments of the input sequence to filter, reducing the noise introduced by long input documents.

3.5. Improving efficiency

Next, we address our second objective, which requests an encoder capable of efficiently processing long documents without sacrificing quality in the process. Irrespective of the activation function used, the $\mathcal{O}(n^2)$ complexity of a standard Transformer layer is prohibitively expensive for documents thousands of tokens long. As such, we require a way to model long-range dependencies more efficiently than a standard Transformer. For this, we use the Star Transformer, a simple and efficient extension of the standard Transformer capable of learning many of the same semantic relationships and long-range dependencies [23].

The Star Transformer is able to reduce the quadratic time complexity to linear time ($\mathcal{O}(n)$) by using a message-passing mechanism along a sliding window of embeddings. Given a sequence of input embeddings $[\mathbf{e}_1, \mathbf{e}_2, \dots, \mathbf{e}_n]$, we produce an output sequence of embeddings $[\mathbf{h}_1, \mathbf{h}_2, \dots, \mathbf{h}_n]$. Initially, each $\mathbf{h}_i = \mathbf{e}_i$, and a message-passing relay node \mathbf{s} is initialized as the mean of all \mathbf{e}_i . For each embedding \mathbf{e}_i , its immediate c neighbours and the relay node \mathbf{s} are used to form a new representation \mathbf{h}_i . This message-passing mechanism enables the learning of long-range dependencies in linear time, as each attention operation only considers the c immediate neighbors of each token (as well as the relay node).

$$\begin{aligned} \mathbf{C}_i &:= [\mathbf{h}_{i-c}; \dots; \mathbf{h}_i; \dots; \mathbf{h}_{i+c}; \mathbf{s}] \\ \mathbf{h}_i &:= \text{MultiHeadAttention}(\mathbf{C}_i, \mathbf{h}_i, \mathbf{h}_i) \end{aligned}$$

After all i operations, we then update the relay node as $\mathbf{s} := \text{MultiHeadAttention}(\mathbf{H}, \mathbf{s}, \mathbf{s})$ where $\mathbf{H} = [\mathbf{h}_1; \mathbf{h}_2; \dots; \mathbf{h}_n]$. The authors find that performing T iterations of these operations enables re-reading to more effectively capture long-range dependencies, though additional iterations only marginally improved performance in our experiments. To encode the output sequence \mathbf{H} to a fixed-length vector, we take the maximum over each embedding dimension and average it with the final state of the relay node, computed as $\frac{\max(\mathbf{H}) + \mathbf{s}}{2}$.

3.6. Siamese Architecture

Finally, we use our altered Star Transformer to jointly embed each tweet-article pair, represented as a tuple of word embedding sequences $([\mathbf{t}_1, \mathbf{t}_2, \dots, \mathbf{t}_m], [\mathbf{a}_1, \mathbf{a}_2, \dots, \mathbf{a}_n])$. Each are independently passed through the encoder, producing fixed-length vectors \mathbf{f}_t and \mathbf{f}_a . These embeddings are directly passed to the objective function, triplet loss [24], formulated as:

$$L = \max(0, \|\mathbf{f}_a - \mathbf{f}_t\|^2 - \|\mathbf{f}_a - \mathbf{f}_r\|^2 + \alpha)$$

Where \mathbf{f}_r is an irrelevant tweet mined using the multi-similarity method [25] and α is the margin. This minimizes the distance between the embeddings of articles and their relevant tweet(s). Figure 2 shows the t-Stochastic Neighbour Embedding (t-SNE) [26] projection of the learned embeddings for a sample of tweets which reference the top-10 most shared articles in the dataset. The result is that tweets referring to the same articles are tightly clustered in latent space. We call our resulting model the Adaptive Siamese Transformer (AST).

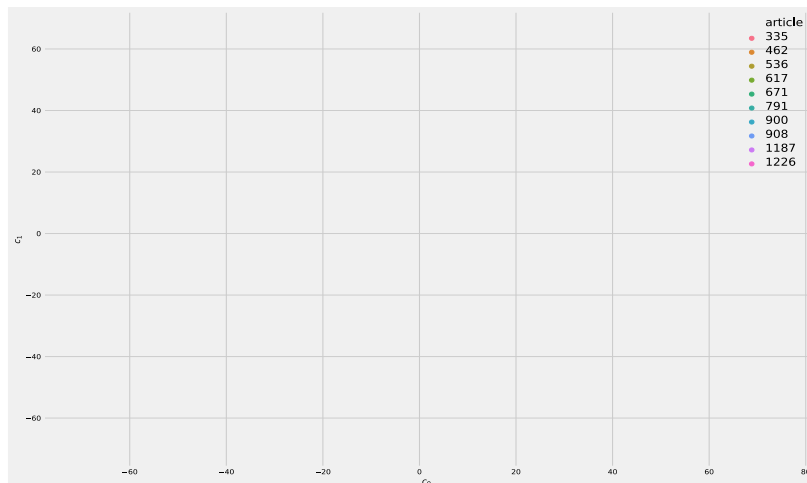


Figure 2. t-SNE projection of tweets about the most shared news articles.

4. EXPERIMENTAL RESULTS

4.1. Evaluation Criteria

The goal of our work is to enable the automatic filtering of a corpus of tweets using news articles as seeds. We assume that it is cheap to *collect* tweets, but expensive to *annotate* them, and that an ideal model identifies relevant tweets while returning as close to 0 false positives as possible. Precision, a common metric for many information retrieval tasks, reflects our wish to minimize the number of false positives. A model that retrieves exclusively relevant documents will have a precision of 100%. However, this could be achieved by simply returning a very small number of relevant documents. We ensure that a reasonable number of documents are returned by using r -Precision as our evaluation metric, which computes the precision after r documents are retrieved. We also report several other metrics for additional comparison.

4.2. Inference Process

For evaluation, we hold out approximately 3300 samples as our test set. The model returns an embedding for each news article \mathbf{f}_a and tweet \mathbf{f}_t . The relevance score of some \mathbf{f}_{a_i} to a given \mathbf{f}_{t_j} is defined as their cosine similarity.

4.3. Training Configuration

We train Siamese networks on a large dataset of tweet-article [10] pairs using three additional encoders as baselines, including Convolutional Neural Networks (CNN) [27], Gated Recurrent Units (GRU) [28], and Bidirectional GRUs (Bi-GRU) as benchmarks. Each network uses 300-dimensional pre-trained GloVe embeddings [29]. Triplet mining was performed using the `pytorch_metric_learning` library [30], and experiments were conducted with the AllenNLP library [31] using four NVIDIA V100 GPUs on Google Cloud Platform. All configuration details are available on GitHub.

4.4. Results

Table 1. r -Precision for each model at various thresholds.

r	CNN	GRU	Bi-GRU	AST
50	100.0	98.00	98.00	100.0
100	99.00	96.00	99.00	96.00
200	97.50	92.00	96.50	94.50
500	90.40	88.00	92.60	92.40
1000	84.80	79.80	83.70	84.80
2000	68.65	62.25	67.25	70.00
3000	55.53	49.93	54.27	57.90

Evaluation #1. We report the r -Precision for each baseline encoder, which is the precision after having retrieved r documents. For each r , we retrieve the r highest scoring tweet-article pairs by cosine similarity and compute the precision. This captures both the quality and quantity of documents retrieved by each model. All models decrease in precision as they retrieve more documents, as is expected [32]. The GRU-based framework quickly falters in performance, demonstrating the challenges recurrent models face with long sequences. Bi-directionality

appears to help, but the most competitive baseline was clearly the CNN-based framework. We posit that CNNs’ ability to identify the most important n-grams using global max pooling [33] provides the filtering ability we describe in our first objective. Our model performs the best at higher quantity thresholds, significantly outperforming the recurrent models. It is possible that the sliding-window approach of the Star Transformer could lead to similar behavior as CNNs, a possibility we leave to be examined in future work.

Table 2. Comparison of mAP, AUC-ROC, and mean r-Precision between models.

	mAP	AUC-ROC	mRP
GRU	43.53	96.03	76.68
Bi-GRU	47.58	96.05	80.29
CNN	49.81	97.09	81.05
AST	53.01	97.50	81.31

Evaluation #2. We also report **mean r-Precision (mRP)**, **Mean average precision (mAP)**, and **area under the Receiver-Operating Curve (AUC-ROC)**. **mRP** is simply the *r*-Precision over all thresholds in Table 2. **mAP** and **AUC-ROC** are calculated using the `scikit-learn` library [34]. Our model outperforms the three baselines in each metric.

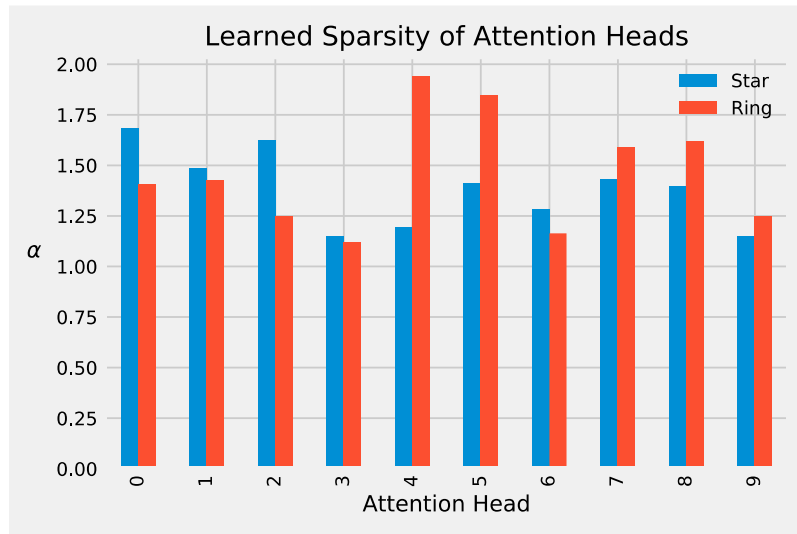


Figure 3. Learned α for each attention head.

Learned sparsity. Following the training process, we examine the α values learned by each attention head of the Star Transformer. Values closer to 1 will lead to attention weights closer to those produced by softmax, while values closer to 2 will be similar to sparsemax, and a value of 1.5 is equal to $1.5 - \text{entmax}[20]$. The star attention heads are used to update the relay node, while the ring attention heads are used at each context window. Overall, it appears that the ring attention heads learn a diverse set of alphas, allowing for varying levels of sparsity in the representations of each context window. Heads 4 and 5 approach sparsemax, while heads 3 and 6 remain relatively close to softmax. The α values for the star attention heads were more tightly bound, but heads 1 and 3 were still quite sparse, exceeding the sparsity of $1.5 - \text{entmax}$.

5. CASE STUDY

Finally, we present a case study applying our model to a corpus of tweets about a terrorist attack which took place in Toronto, Canada in April 2018. We computed the cosine similarity of 100 manually annotated tweets' embeddings to that of a news article written shortly after the attack. As shown in Figure 4 with a retrieval threshold of $\cos(\mathbf{f}_a, \mathbf{f}_t) \geq 0.7$, our model was able to minimize the number of false negatives without greatly diminishing the quantity of tweets retrieved.

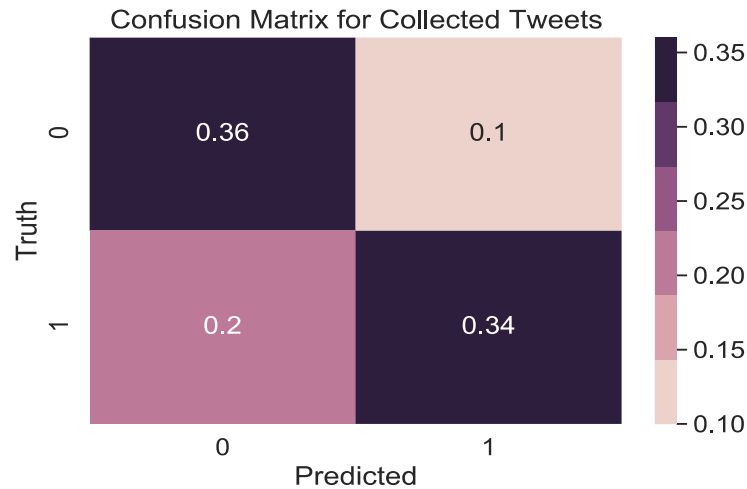


Figure 4. Of all tweets retrieved by our model, 36 were relevant while only 10 were irrelevant.

As seen in Table 4, sorting the tweets by cosine similarity showed results which may suggest that the model was able to learn which tweets are more relevant than others (as opposed to a binary notion of relevance), though we note these results are heavily anecdotal. We share these results to demonstrate potentially useful applications of our model. For example, a project which requires at least N relevant tweets and precisely 0 irrelevant tweets necessarily requires human annotations. Our model could significantly decrease the financial cost of collecting annotations by presenting the tweets in order of estimated relevance (cosine similarity), minimizing the quantity of tweets that must be shown to annotators until N relevant tweets are found.

Table 4. The most and least similar Tweets to a news article written after the attack.

Tweet	Score
Second, my thoughts and prayers go out to everyone in Toronto after the attack that left 10 dead and 16 injured! A d also, thank you so much for a...	0.9166
What a devastating Tragedy! Savagery of mankind has no bound! Deadly Toronto van driver: What we know about Alek Minassian http://bit.ly/2vFJfDx	0.8996
Everyone at Community Safety Net would like to express their deepest sympathies to all those affected by yesterday's events in Toronto #TorontoStr...	0.8841
What we know about Alek Minassian, the man charged in deadly Toronto van attack http://ow.ly/jZpd30jF9Jo	0.8838
Yesterday was a deeply sad day for the city of #Toronto and our hearts go out to the victims, the families and anyone affected by the tragic incid...	0.8686
⋮	⋮
Incel or MGTOW Facebook groups banned me from their Facebook groups all	0.4311

because they also hate not just women.	
Une pense pour le tragiquevnement Toronto	0.3877
Stay strong Canada - we are with you	0.3875
It is both wrong and unhelpful to cast the incel phenomenon as some kind of dark internet cult. This is garden variety misogyny and rape culture w...	0.3797

6. CONCLUSION

In conclusion, we present a novel approach to article-comment linking using a Siamese architecture and triplet loss. We encode pairs using Adaptive Star Transformers, an efficient Transformer using adaptively sparse attention to filter irrelevant information from the input sequences, which we show outperforms several other encoders in a Siamese framework. This model could allow other researchers to eliminate or vastly reduce the cost of filtering corpora.

7. ACKNOWLEDGEMENTS

Thank you to Kevin Musgrave for assistance using his `pytorch_metric_learning` library, and to Jorge Salazar for consultation on the proof regarding the softmax function and general proof-reading. This work was funded in part by the I-CUREUS research grant.

8. REFERENCES

- [1] B. Mazoyer, J. Cagé, C. Hudelot, and M. Viaud, "Real-time collection of reliable and representative tweets datasets related to news events," in Proceedings of the first international workshop on analysis of broad dynamic topics over social media (brodyn 2018) co-located with the 40th european conference on information retrieval (ECIR 2018), grenoble, france, march 26, 2018, 2018, vol. 2078, pp. 23–34 [Online]. Available: <http://ceur-ws.org/Vol-2078/paper2.pdf>
- [2] J. Letierce, A. Passant, J. Breslin, and S. Decker, "Understanding how twitter is used to spread scientific messages," Proceedings of the Web Science Conference (WebSci10): Extending the Frontiers of Society On-Line, 2010.
- [3] X. Lin, Y. Gu, R. Zhang, and J. Fan, "Linking news and tweets," in Australasian database conference, 2016, pp. 467–470.
- [4] D. K. Sil, S. H. Sengamedu, and C. Bhattacharyya, "ReadAlong: Reading articles and comments together," in WWW, 2011.
- [5] T. Hoang-Vu, A. Bessa, L. Barbosa, and J. Freire, "Bridging vocabularies to link tweets and news," in Proceedings of webdb, 2014.
- [6] L. Hou et al., "What users care about: A framework for social content alignment," IJCAI International Joint Conference on Artificial Intelligence, pp. 1401–1407, Aug. 2013.
- [7] L. Hou, J. Li, X.-L. Li, J. Tang, and X. Guo, "Learning to align comments to news topics," ACM Transactions on Information Systems (TOIS), vol. 36, no. 1, p. 9, 2017.
- [8] M. K. Das, T. Bansal, and C. Bhattacharyya, "Going beyond corr-lda for detecting specific comments on news & blogs," in Proceedings of the 7th acm international conference on web search and data mining, 2014, pp. 483–492, doi: 10.1145/2556195.2556231 [Online]. Available: <http://doi.acm.org/10.1145/2556195.2556231>
- [9] D. K. Sil, S. H. Sengamedu, and C. Bhattacharyya, "Supervised matching of comments with news article segments," in CIKM '11, 2011.
- [10] W. Guo, H. Li, H. Ji, and M. Diab, "Linking tweets to news: A framework to enrich short text data in social media," in Proceedings of the 51st annual meeting of the association for computational linguistics (volume 1: Long papers), 2013, pp. 239–249.
- [11] S. Zhao, Y. Huang, C. Su, Y. Li, and F. Wang, "Interactive attention for semantic text matching," arXiv preprint arXiv:1911.06146, 2019.

- [12] O. Demirsoz and R. Ozcan, "Classification of news-related tweets," *Journal of Information Science*, vol. 43, no. 4, pp. 509–524, 2017, doi: 10.1177/0165551516653082. [Online]. Available: <https://doi.org/10.1177/0165551516653082>
- [13] M. Chen, C. Meng, G. Huang, and C. Zaniolo, "Neural article pair modeling for wikipedia sub-article matching," *Lecture Notes in Computer Science*, pp. 3–19, 2019, doi: 10.1007/978-3-030-10997-4_1. [Online]. Available: http://dx.doi.org/10.1007/978-3-030-10997-4_1
- [14] B. Liu et al., "Matching article pairs with graphical decomposition and convolutions." 2018.
- [15] C.-Y. Wu, R. Manmatha, A. J. Smola, and P. Krahenbuhl, "Sampling matters in deep embedding learning," 2017 IEEE International Conference on Computer Vision (ICCV), Oct. 2017, doi: 10.1109/iccv.2017.309. [Online]. Available: <http://dx.doi.org/10.1109/ICCV.2017.309>
- [16] A. Vaswani et al., "Attention is all you need." 2017.
- [17] C. Raffel and D. P. W. Ellis, "Feed-forward networks with attention can solve some long-term memory problems." 2015.
- [18] J. Devlin, M.-W. Chang, K. Lee, and K. Toutanova, "BERT: Pre-training of deep bidirectional transformers for language understanding." 2018.
- [19] A. Graves, G. Wayne, and I. Danihelka, "Neural turing machines." 2014.
- [20] G. M. Correia, V. Niculae, and A. F. T. Martins, "Adaptively sparse transformers," *Proceedings of the 2019 Conference on Empirical Methods in Natural Language Processing and the 9th International Joint Conference on Natural Language Processing (EMNLP-IJCNLP)*, 2019, doi: 10.18653/v1/d19-1223. [Online]. Available: <http://dx.doi.org/10.18653/v1/d19-1223>
- [21] A. F. T. Martins and R. F. Astudillo, "From softmax to sparsemax: A sparse model of attention and multi-label classification." 2016.
- [22] B. Peters, V. Niculae, and A. F. T. Martins, "Sparse sequence-to-sequence models," in *Proceedings of the 57th annual meeting of the association for computational linguistics*, 2019, pp. 1504–1519, doi: 10.18653/v1/P19-1146 [Online]. Available: <https://www.aclweb.org/anthology/P19-1146>
- [23] Q. Guo, X. Qiu, P. Liu, Y. Shao, X. Xue, and Z. Zhang, "Star-transformer." 2019.
- [24] G. Chechik, V. Sharma, U. Shalit, and S. Bengio, "Large scale online learning of image similarity through ranking," *Journal of Machine Learning Research*, vol. 11, no. Mar, pp. 1109–1135, 2010.
- [25] X. Wang, X. Han, W. Huang, D. Dong, and M. R. Scott, "Multi-similarity loss with general pair weighting for deep metric learning." 2019.
- [26] L. van der Maaten and G. Hinton, "Visualizing data using t-sne," *Journal of machine learning research*, vol. 9, no. Nov, pp. 2579–2605, 2008.
- [27] Y. Kim, "Convolutional neural networks for sentence classification," *Proceedings of the 2014 Conference on Empirical Methods in Natural Language Processing (EMNLP)*, 2014, doi: 10.3115/v1/d14-1181. [Online]. Available: <http://dx.doi.org/10.3115/v1/D14-1181>
- [28] K. Cho et al., "Learning phrase representations using rnn encoder–Decoder for statistical machine translation," *Proceedings of the 2014 Conference on Empirical Methods in Natural Language Processing (EMNLP)*, 2014, doi: 10.3115/v1/d14-1179. [Online]. Available: <http://dx.doi.org/10.3115/v1/D14-1179>
- [29] J. Pennington, R. Socher, and C. D. Manning, "GloVe: Global vectors for word representation," in *Empirical methods in natural language processing (emnlp)*, 2014, pp. 1532–1543 [Online]. Available: <http://www.aclweb.org/anthology/D14-1162>
- [30] K. Musgrave, S.-N. Lim, and S. Belongie, "PyTorch metric learning," *GitHub repository*. https://github.com/KevinMusgrave/pytorch_metric_learning; GitHub, 2019.
- [31] M. Gardner et al., "AllenNLP: A deep semantic natural language processing platform," 2017.
- [32] C. D. Manning, C. D. Manning, and H. Schütze, *Foundations of statistical natural language processing*. 1999.
- [33] A. Jacovi, O. Sar Shalom, and Y. Goldberg, "Understanding convolutional neural networks for text classification," in *Proceedings of the 2018 EMNLP workshop BlackboxNLP: Analyzing and interpreting neural networks for NLP*, 2018, pp. 56–65, doi: 10.18653/v1/W18-5408 [Online]. Available: <https://www.aclweb.org/anthology/W18-5408>
- [34] F. Pedregosa et al., "Scikit-learn: Machine learning in Python," *Journal of Machine Learning Research*, vol. 12, pp. 2825–2830, 2011.

9. APPENDICES

9.1. A. Softmax Expectation

We will show that an increase in S , the length of a document, can be expected to diminish the weight of each token in the softmax step of the attention mechanism. To demonstrate a decrease in $\mathbb{E}[\sigma(\mathbf{z})_i]$ with S , we need only show an increase in the expectation on the denominator $\sum_{j=1}^S e^{z_j}$, which we refer to as expsum.

Using cosine attention, let $\mathbf{z} = \cos(\mathbf{Q}, \mathbf{K})$. Since $\cos(\cdot) \in [-1, 1]$, let each z_j be an independent random variable drawn uniformly from $\mathcal{U}(-1, 1)$. It follows that all $e^{z_j} \in [e^{-1}, e^1]$. The expectation on expsum then becomes:

$$\begin{aligned} \mathbb{E} \left[\sum_{j=1}^S e^{z_j} \right] &= \sum_{j=1}^S \mathbb{E}[e^{z_j}] \\ &= \sum_{j=1}^S \int_{-1}^1 \frac{1}{2} e^{z_j} \\ &= \sum_{j=1}^S \frac{e^2 - 1}{2e} \\ &= S \cdot \frac{e^2 - 1}{2e} \\ &\approx 1.1752 \cdot S \end{aligned}$$

This demonstrates that $\mathbb{E}[\text{expsum}]$ increases as a function of S . As stated previously, an increase in $\mathbb{E}[\text{expsum}]$ decreases $\sigma(\mathbf{z})_i$. This dictates that $\sigma(\mathbf{z})_i$ must decrease when S increases. Therefore, an increase in the length of a document will decrease the expected attention weight of each token. ■

AUTHOR

Jacob Danovitch is a senior undergraduate student at Carleton University in Ottawa, Canada, where he is supervised by professor Majid Komeili. In the summer, he is a data science intern with Microsoft Search, Assistant, and Intelligence (MSAI) in Seattle, USA.



HATE SPEECH DETECTION OF ARABIC SHORTTEXT

Abdullah Aref¹, Rana Husni Al Mahmoud²,
Khaled Taha³ and Mahmoud Al-Sharif³

¹Computer Science Department, Princess Sumaya
University for Technology, Amman, Jordan

²Computer Science Department, University of Jordan, Amman, Jordan

³Social Media Lab, Trafalgar AI, Amman, Jordan

ABSTRACT

The aim of sentiment analysis is to automatically extract the opinions from a certain text and decide its sentiment. In this paper, we introduce the first publicly-available Twitter dataset on Sunnah and Shia (SSTD), as part of a religious hate speech which is a sub problem of the general hate speech. We, further, provide a detailed review of the data collection process and our annotation guidelines such that a reliable dataset annotation is guaranteed. We employed many stand-alone classification algorithms on the Twitter hate speech dataset, including Random Forest, Complement NB, DecisionTree, and SVM and two deep learning methods CNN and RNN. We further study the influence of word embedding dimensions FastText and word2vec. In all our experiments, all classification algorithms are trained using a random split of data (66% for training and 34% for testing). The two datasets were stratified sampling of the original dataset. The CNN-FastText achieves the highest F-Measure (52.0%) followed by the CNN-Word2vec (49.0%), showing that neural models with FastText word embedding outperform classical feature-based models.

KEYWORDS

HateSpeech, Dataset, Text classification, Sentiment analysis.

1. INTRODUCTION

Hate speech is a crime that has been growing in recent years, not only in face-to-face interactions but also in online communication [1]. Social media platforms allow users to broadcast any sort of messages in these systems and to reach millions of users in a short period and at near zero cost [2]. The freedom available to social media users to express their opinions and the anonymity provided by these environments [1] made it easier to spread hate propaganda against individuals or groups [3], [4]. This provoked the need for automatic detection of hate speech contents shared across social media platforms [3], especially if such online contents can direct physical hate crimes [3].

The problem in hate speech is wide in nature and varies according to the type of hate speech (sexism, racism, religious hate speech, etc.). The absence of human annotated vocabulary that explicitly reveals the presence of hate speech, makes the available hate speech corpora sparse and noisy [5]. Even though, many studies have been conducted on automatic detection of hate speech,

only a few of them can result in high precision and recall rates [6], and the tools provided are scarce[1].

When compared to English, Arabic is considered an under-resourced language. The complexity and richness of Arabic morphology combined with the existence of different dialects add up more challenges to Arabic NLP research [7]. Despite the existence of many researches that investigated anti-social behaviours such as, abusive or offensive language and cyberbullying, a limited number of researches have contributed to hate speech detection in Arabic [6].

In this work, we address the hate speech between Sunnah and Shia, as part of the religious hate speech which is a sub problem of the general hate speech. In the absence of a labelled data-set for this purpose, we create Sunnah Shia Twitter Dataset (SSTD) analyse it using various well known machine learning approaches.

2. RELATED WORK

Several studies have been conducted with the goal of describing online hate speech and which groups are more threatening. Descriptive statistics about hate speech can be found in the literature [1]. including Racism [8], Sexism [9], Prejudice toward refugees [10], Homophobia [11], and General hate speech [2]. Other researchers focused on algorithms for hate speech detection and used text mining and machine learning for hate speech classification [1] such as [3] and [7]. Many text mining strategies have been adapted for automatic detection of hate speech[1].

Features representation for hate speech detection including distance metric are addressed in [12], dictionaries, Bag-of-words (BOW) [8], [13], N-grams [14], Profanity Windows [15], TF-IDF [16], part of-speech [17], Lexical Syntactic Feature-based [18], Rule Based [19], Topic Classification [20], Sentiment [21], Word Embeddings [22], Typed Dependencies [17], and Deep Learning [23]. A more in depth survey for features representation for hate speech detection can be found in [1]. In the litterateur, supervised, semi-supervised and unsupervised approaches machine learning classification algorithms were used for hate speech detection [6].

Deep learning models showed promising future text sentiment analysis [24]. Recurrent Neural Networks (RNN) were used in [25] with word frequency vectorization to implement the features. Convolutional Neural Networks (CNNs), Long Short-Term Memory Networks (LSTMs), and FastText, combined with numerous features like TFIDF and Bag of Words (BoW) vectors were used in [26] to detect racism and sexism, including. LSTM with random embeddings found to outperform other approaches [27].

Levantine Hate Speech and Abusive (L-HSAB) Twitter dataset introduced in [3] and two well known machine learning algorithms were evaluated. The results indicated the the multinomial NB outperforms SVM [3].

The problem of religious hatred in Arabic twitter was tackled in [7], and various deep learning algorithms were tested for this task including GRU RNN which were found to work better than LSTM with smaller datasets [6].

This work has two contributions: we address hate speech between Sunnah and Shia, in twitter and we created SSTD and applied various machine learning approaches on it.

3. WHAT IS HATE SPEECH?

A universal definition of Hate Speech was found to be difficult to derive. There are a variety of definitions by a number of international and organizations like the United Nations and the European Union, in addition to key NGO activist organizations. A survey of multiple definitions from different origins were presented in [1]. By studying common factors across most popular definitions and implementing practical, philosophical, cultural and technological considerations, a definition of Hate Speech was derived for the purpose of this study. It can be stipulated as follows:

” Any Pejoration or Threat Directed at a Group of Protected Attributes”.

Pejoration is articulated to be one or any combination of: a) expression or incitement to disdain b) expression or incitement to insult c) expression of belittling false generalization.

Threat is articulated to be one or any combination of: a) expression or incitement to violent action b) expression or incitement to isolate c) expression or incitement to hate.

4. METHODOLOGY

In this work we follow a methodology of six stages namely. 1) keywords selection, 2) collecting the dataset, 3) preprocessing 4) feature extraction, 5) model development, and 6) evaluation. Figure 1 shows the flow layout of these stages. The following subsections discuss each stage in more details.

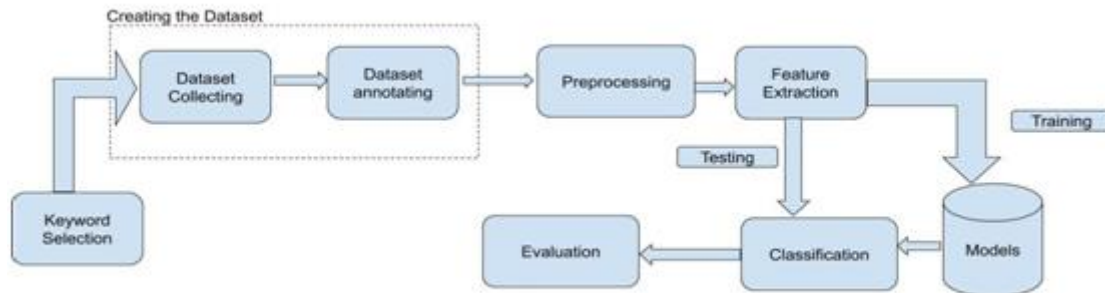


Figure 1. Methodology

4.1. Keywords selection

In doing research on the use of Twitter for hate speech targeting Sunnah and Shia, the first challenge is to collect a comprehensive (or at least representative) sample of tweets for the topic. To tackle this issue, one simple and straightforward solution is to concentrate on tweets that contain words that are likely to indicate hate speech combined with words that are likely to indicate one of the two groups

We created a set of words to work as our seeding list. The list words extracted from a set of the hate speech related documents [28]–[31]. There are around 365 words, appearing in these documents that were manually assessed and scored by one member of the team for being hate or not and the degree of hatred in these keywords. The selected keywords that had high score are presented in Table I. Keywords that related to Sunnah and Shia topic presented in Table II.

Table I: Keywords related to Sunnah and Shia with high score

Keyword	Transliteration	Keyword	Transliteration	Keyword	Transliteration
اجتثاث	Egthithath	دحابشه	Dahabshah	أخونجي	Ekhwanji
إرهابي	Erhabe	دواعش	Dawaesh	العدوان	Al Edwan
الحقد الشيعي	Al-Heqd Al Sha'abe	رخيص	Rakhees	الغن اليهود	Aleyn AlYahood
الحوثيون	Al Hotheon	زنادقة	Zanadeka	اللهم العن	AllahomAleyn
السنة النواصب	Al Sunnah Al Nawaswb	سعود	Souod	المشركين	Al Mushreken
الشرك	Al Sherk	شراميط	Sharameed	ايران	Iran
الشيعة ليسوا مسلمين	Al Sheialiso Muslimeen	شيعه	Sheia	الشيعة حمير اليهود	Al Sheia Hamer Al Yahood
العربان	Al Orban	ضد	Ded	أسبادك	Asyadak
القردة والخنازير	Al kerada and al khanazeer	عبيد	Abeed	أهل البدع	Ahl Albeda'a
المد الإيراني	Al Mad Al Irani	عملاء	Omala'a	أوغاد	Awgad
انفصالي	Enfesali	فاسدون	Fasedoon	آل سلول	Al Salol
أخذ عز يز مقتدر	Akhdaazizmuqtader	فاسقون	Faseqon	حاقد	Haked
أذرع	Athroey	قتل	Katal	حقارة	Haqara
أعداء	Aeyda'a	كافر	Kafer	حقير	Haqeer
أو باش	Awbash	كلاب	Kelab	خايس	Khaes
أولاد حرام	Awlad Al haram	لعن	Laa'an	خرا	Khara
تبا لكم	Taba'a Lak	لعنه	Laanah	خرى	Khara
حتالة	Huthala	ليبرالي	Lebraly	خونة	Khawana
حقد	Heked	مخنث	Mukhanath	شيطان	Sheitan
حمير	Hamer	ملحد	Mulhed	صفوي	Safawy
خائن	Khaen	نجس	Najas	عاهرة	Aahera
خرة	Kharah	نواصب	Nawaseb	عصابة	Aesaba
خوارج	Khawarej	وهابي	Wahabe	عميل	Ameel
خيانة	Kheana	يهودي	Yahodi	فاسدين	Fasedeen
إرهاب	Erhab	دحباشي	Dehbashi	فساد	Fasad
الإرهابيون	Al Erhabeon	رافضه	Rafeda	قذر	Kather
الحوثي	Al Hothe	زق	Zaq	كفر	Kafar
السنة الدواعش	Al Suna Al Dawaesh	سراق	Suraq	كلب	Kalb
السنة إرهابية	Al Sunaerhabia	سفلة	Safala	لعنة الله	La'anat Allah
مناقفون	Munafekon	وهابية	Wahabiah	لعين	Laeen
نصراني	Nasrane	و بنس المصير	Wabeas Al maseer	مجوس	Majoos
مرتزقة	Murtasaqah				

4.2. Creating the Dataset

The process of creating the dataset consists of two phases, collecting and annotating the dataset.

1) Dataset collection: Twitter offers several open, public data access options. Every approach has particular advantages and limitations. The researcher's aims to determine which approach is effective in a given context.

The standard Twitter APIs consist of REST APIs and Streaming APIs¹. Twitter provides Representational State Transfer (REST) search API for searching tweets from Twitter's search index. REST API provides seven days historical results. While the streaming API gives results from the point of the query. Streaming API can be used to track a specific query in real-time. Twitter search API has many limitations as mentioned on their web site². We created a number of queries that contain all concatenations of the hate speech keywords and group keywords of Tables I & II. We carried two searches, one on 30/9/2019 and the other on 5/10/2019. Due to twitter limitations in search API, it retrieved around 8220 tweets within the 7 days before search date. Our dataset tweets are date between 23/9/2019 and 5/10/2019.

To make our models, we select a dataset that contains 3235 tweets. The selected dataset was stratified sampling of the original dataset. Which means that each combination of the topic and groups tweets has the same ratio in sampled and original dataset.

Table II: Group keywords

Group	Transliteration	Group	Transliteration
الشيعة	Al Sheia	رافضي	Rafede
أهل السنة	Ahl Al Sunah	السلفيون	Al Salafeyon
سني	Suni	روافض	Rawafed
شيعي	Sheie	قتلة الحسين	Katalat Al Husien
وهابية	Wahabia	مجوس	Majos
سلفي	Salafi	مذهبي	Mathhabe
شيعية	Sheiah	صفوي	Safawe
طائفي	Taeefe	أبناء المتعة	Abna'a Al Muteyah
فرس	Furs	وهابي	Wahabe

2) Evaluation rules: The following evaluation rules were derived for improving the quality of labelling the individual tweets.

- Criticism directed at political regimes or states, is not to be considered hate speech, even if it was severe.
- Special consideration is applied to the context of insults directed at individuals, since some of it can be interpreted as hate speech.
- Consideration of the variety of grounds that Hate Speech is based upon across extended geographies (example: Arab West: Islamic vs. Secular, Arab East: Sunni vs. Shai).
- New terms that appear to be neutral in normal contexts, are found to be extremely pejorative against specific groups, are added to stop words list of hate speech.

- Cursing, is still a common practice in the Arab culture (as opposed to Western culture). It's important to distinguish between cursing as a common practice from cursing as a hate speech.
- Irony, metaphors and figurative speech can be used as a maneuver around hate speech, especially in countries that have strict legal liabilities against it.
- Special attention is paid to the religious terms that carry meanings of supplication to God, exclamation or expression of weakness - since all can be used as a religious cover to hate speech.
- Pejoration directed at women, even if done on cultural or social basis, is labeled as so with no leniency
- Special attention is paid in order not to constraint freedom of speech in the attempt to alleviate hate speech.
- Stigmatizing terms are found to be extremely pejorative to groups, and can't be interpreted in any positive form, hence they are labeled as hate speech wherever it appears (example: "Rawafid" for Shiis, "Irhabi" for Sunnis).
- Wherever a new word is found to be associated with Western Arab's hate speech, it is added to hate speech stop words.
- Political correctness is not to be mistaken with hate speech.
- Sole usage of controversial historical topics, is not to be considered hate speech. It must be associated with terms or incitements that indicate clear hate speech.
- Citation of hate speech, is not to be considered or labeled as hate speech.
- Extreme criticism to protected groups is to be considered non hate, if it's done only in generalized political context.
- In Arab culture, it's extremely important not to take everything at "face value", and dig down into understanding roots and deeper meanings of expressions used.

3) Data Annotation: We assigned the labelling task to two annotators; Khaled Taha³, and MamoudAl Sharief⁴.

We asked the annotators to judge each tweet and categorize them as either contains hate speech (HATE); or does not contain hate (Not Hate). The agreement between the two annotators was 0.85%. In a corpora for Hate Speech, annotator disagreement can be related to the fact that there are many rules to be applied on the tweet to indicate it as hate tweet. Therefore, any tweet is considered to be Hate if it is marked as Hate by at least one of the annotators. It is not uncommon to discard tweets with high disagreements among annotators. While some claim that this is done to remove noise from low annotator quality; this argument does not hold when considering that high rates of consensus annotator agreement are present in these datasets. This indicates that the issue is not weak annotators, but rather difficult data that are not in the predefined categories [32].

The resulting dataset contains the text of each tweet along with the adjudicated label. The distribution of the texts across the two classes is shown in Table III.

Table III: Hate Speech Identification dataset classes

Class Label	Number of tweets
Not Hate	2590
Hate	642

4.3. Data pre-processing

The text pre-processing phase includes a set of processes applied on the dataset. They mainly include: normalization of some Arabic letterforms, tokenization of words, stop-words removal and stemming.

- 1) **Normalization:** Generally, text pre-processing tasks attempt to reduce the noise using normalization. In this work, we employed the following normalization steps:
 - Remove non letters and special characters (\$,&,%,...)
 - Remove non Arabic letters
 - Replace initial $\bar{ا}$, $اِ$ or $أ$ with bare alef $ا$
 - Replace final $ة$ with $ه$
 - Remove $ال$ from the beginning of a word
 - Replace final $ي$ with $ى$
- 2) **Tokenization:** This step is used to analyze text linguistically. It breaks strings of characters, words, and punctuation marks into tokens during the indexing process.
- 3) **Stop Words removal:** Words that do not affect the meaning of the text usually referred to as Stop Words, such as prepositions. Every natural language has its own list of stop-words.
- 4) **Morphological analysis and stemming:** Arabic morphological analysis and root extraction are essentials for many Arabic applications such as information retrieval and data mining. In the literature adequate works tackling the problem of Arabic morphological analysis is given in [33]–[35]. Because of its nature, Arabic found to be very difficult to stem [36]. Mainly, there are two kinds of stemming algorithms in Arabic: a root-based approach, for example Khoja and Garside [37]; and stem-based (light stemming) approach [38]. In this work we apply light stemmer on the text.

4.4. Feature extraction

Feature extraction is a pre-processing step toward knowledge discovery and dimensionality reduction. In this stage, features (i.e. POSTs) were extracted from documents based on their calculated weights in the collection. In the literature, several features- extraction approaches were used [39]. In this work, we used the TF-IDF as a weighting scheme for feature selection. TF-IDF is used to determine the keywords that can identify or categorize some specific documents in a

collection. TF-IDF attempts to combine both the number of times the word t occurs in document d , referred to as $TF(t,d)$, with the inverse document frequency, referred to as $IDF(t)$ [40].

For each of the deep neural networks methods, we initialize the word embeddings with either Word2Vec embeddings or FastText embeddings that give better results compared with GloVe embedding.

For the Word2Vec and FastText model, it has been trained on SSTD using the skipgram model where the context window size was set to (10), and the vector size was set to (100). In addition to wordNgrams equals 6 for FastText model.

4.5. Evaluation measures

We compare the performance of all these methods based on a set of standard evaluation measurements (described next) with respect to the confusion matrix shown in Table 3. We have two class labels in the dataset namely Hate, Not Hate. The four possible outcomes of the confusion matrix are as follows:

A : A Not Hate Tweet is correctly classified as a Not Hate

B : A Not Hate Tweet is incorrectly classified as Hate

C : A Hate Tweet is incorrectly classified as a Not Hate

D : A Hate Tweet is correctly classified as a Hate

Table 3: Confusion Matrix

		Predicted	
		Not Hate	Hate
Actual	Not Hate	A(TN)	B(FP)
	Hate	C(FN)	E(TP)

Following is a description of the evaluation measures used to compare the performance of the different classification methods used in this study:

Basic measures

– Accuracy: Accuracy is a metric used to estimate how a classifier can correctly predict Hate, Not Hate instances for each class. It can be calculated as the ratio of correctly classified instances to the total number of instances, as given in Eq. 1 which is adapted from the general accuracy equation (32).

$$\text{Accuracy} = \frac{A+D}{A+B+C+D} \quad (1)$$

– Precision: Precision of a class C, where C is Not Hate, or Hate is the ratio of the correctly predicted to the total predicted samples and is calculated as in Eq. 2 which is adapted from the general macro precision equation (32).

$$\text{Precision} = \frac{TP}{(TP+FP)} \quad (2)$$

– Recall: Recall of a class C, where C is Not Hate, or Hate is the ratio of C instances that are correctly predicted to the total number of actual C instances. It can be calculated as in Eq. 3 which is adapted from the general macro recall equation (32).

$$\text{Recall} = \frac{TP}{(TP+FN)} \quad (3)$$

– F-Measure: F-Measure is a composition of Precision and Recall. It is a consistent average of the two metrics which is used as an accumulated performance score. F-Measure of a class C, where C is Not Hate, or Hate can be calculated as in Eq. 4 which is adapted from the general macro F-Measure equation (32).

$$\text{F-Measure} = \frac{2 * (\text{precision} * \text{Recall})}{(\text{Precision} + \text{Recall})} \quad (4)$$

Mainly we used two metrics to evaluate the performance of the developed classification model, namely, the precision and recall which can be summarized in F-measure, which is commonly used in the literature for imbalanced datasets as the accuracy measure is not of interest in similar cases.

5. EXPERIMENTS AND EVALUATION RESULTS

This section presents the experimental analysis of the performance of several well known classifiers over the created dataset.

5.1. Experiments setup

All experiments were conducted using a personal computer with Intel® core i5-5500U CPU @ 2.53GHz / 8 GB RAM. To conduct the experiments, we used Python and Anaconda framework. The Scikit-learn library was selected to implement the classification and to measure the machine learning algorithms' performance; we applied neural network classifiers using the Keras Python library.

5.2. Experiments

We evaluated the performance of several machine learning and deep learning algorithms including Random Forest [41], Complement NB [42], Decision Tree [43], support Vector Machine (SVM) [44], Convolutional Neural Network (CNN) [45], and Recurrent Neural Networks (RNN) [46].

In all experiments, all classification algorithms are trained using a random split of data (66% for training and 34% for testing). The two datasets were stratified sampling of the original dataset.

The testing dataset is unseen during training the model and the performance of the model is determined by predictions applied on the testing dataset.

Text of tweets used for our analysis of the first four classifiers, and TF-IDF used for feature extraction generate numerical features with bag-of-words strategy. We further study the influence of word embedding dimensions FastText [47] and word2vec [48] on deep learning algorithms; Manley CNN and RNN,

Table V: Classification results over Sunnah Shia Dataset. Best values are in bold typeface

	accuracy	Precision		Recall		F-Score	
		0	1	0	1	0	1
Random Forest	0.78	0.78	0.78	0.99	0.086	0.87	0.15
Complment NB	0.68	0.85	0.39	0.72	0.579	0.78	0.46
DecisionTree	0.74	0.84	0.46	0.83	0.46	0.83	0.46
SVM	0.8	0.81	0.64	0.95	0.29	0.88	0.4
cnn	0.8	0.83	0.62	0.93	0.39	0.88	0.48
Rnn	0.8	0.83	0.63	0.93	0.37	0.88	0.47
CNN+fasttext	0.71	0.88	0.42	0.71	0.69	0.79	0.52
Rnn+ fasttext	0.76	0.83	0.49	0.87	0.4	0.85	0.44
Cnn+word2vec	0.79	0.84	0.59	0.91	0.42	0.87	0.49
Rnn +word2vec	0.74	0.83	0.44	0.84	0.42	0.83	0.43

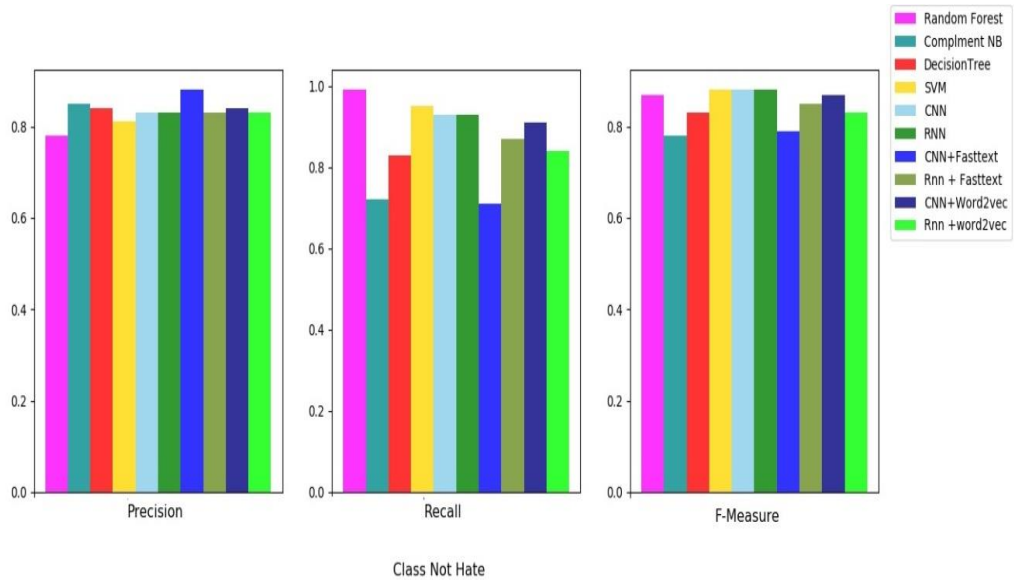


Figure3. The calculated measures for class Not Hate of all tested models

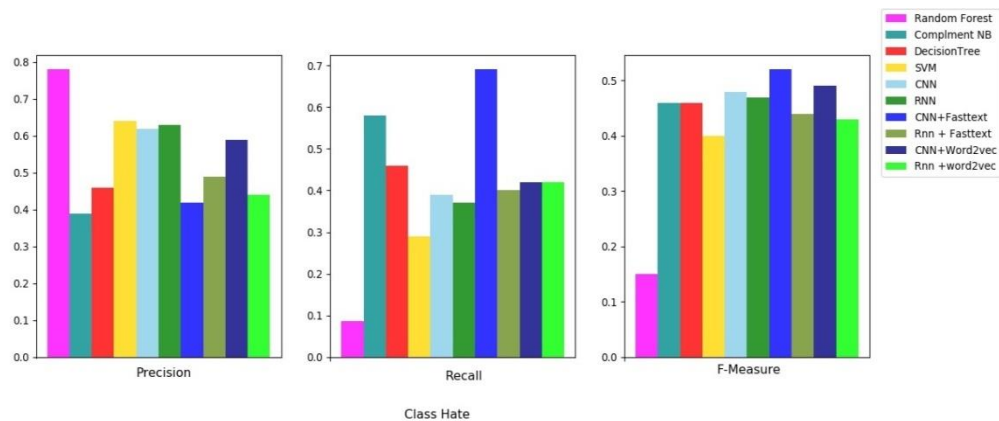


Figure4. The calculated measures for class Hate of all tested models

Experimental results are shown in Table V. As we are targeting the minority class improvement in learning from imbalanced data distributions, it is more important to improve the F-Measure for each class, than improving accuracy. Thus, we studied the behaviour of F-Measure in experiments. We can see from Table V that deep learning models based on CNN and RNN outperformed other models. Also we find that the use of FastText combined with CNN and RNN, outperforms CNN and RNN alone or combined with Word2vec.

Figure 3 and Figure 4 shows the overall performance of ten classification models tested over SSTD. They are reported in terms of Precision, Recall and F1-measure

Our first observation from Figure 3, is that there is no majority difference in precision for class "NOT Hate". Random Forest classifier outperformed all other models in recall measure. The highest F-Measure values achieved for "Not Hate" class when applying SVM, RNN and CNN models.

As presented in the Figure 4, CNN outperformed other algorithms with respect to F-Measure for Class "Hate". This agrees with the findings in [49] that CNN is a powerful tool to improve the prediction performance. CNN's first success in sentiment analysis was triggered by research on document classification [50], where CNN has demonstrated state-of-the-art results in document classification datasets, this performance has led to a rise in deep neural network sentiment analysis research [50].

The benefit of the FastText feature over Word2Vec is that it integrates subword information into the embedding learning process. Through the combination of learned ngram embeddings it can learn similar embedding for words sharing a common stem and also generate embedding for unseen words into the test set [51].

6. CONCLUSIONS AND FUTURE DIRECTIONS

In this paper, we introduced SSTD, a dataset targeting religious hate speech (Sunnah and Shia). To build the dataset, we retrieved many tweets from Twitter, and asked 2 annotators to manually label the tweets following a set of agreed on rules. The dataset combined 3232 tweets with 2 categories: "Hate" and "Not Hate". As hate speech annotation rely on several rules as well as the annotators' knowledge, experience, and assumptions, the agreement between annotators remains an issue. The performance of several well known machine learning and deep learning algorithms were analysed using the SSTD. The results indicated the outperformance of CNN over other

tested algorithms. A natural future step would involve building publicly-available datasets for hates speech targeting other Muslim groups such as Sufi and Muslim brotherhood as well as that targeting other religious groups such as The Copts and Orthodox and so on.

REFERENCES

- [1] P. Fortuna and S. Nunes, "A survey on automatic detection of hate speech in text," *ACM Computing Surveys (CSUR)*, vol. 51, no. 4, p. 85, 2018.
- [2] L. Silva, M. Mondal, D. Correa, F. Benevenuto, and I. Weber, "Analyzing the targets of hate in online social media," in *Tenth International AAAI Conference on Web and Social Media*, 2016.
- [3] H. Mulki, H. Haddad, C. B. Ali, and H. Alshabani, "L-hsab: A levantine twitter dataset for hate speech and abusive language," in *Proceedings of the Third Workshop on Abusive Language Online*, 2019, pp. 111–118.
- [4] N. Chetty and S. Alathur, "Hate speech review in the context of online social networks," *Aggression and violent behavior*, vol. 40, pp. 108–118, 2018.
- [5] N. Ousidhoum, Z. Lin, H. Zhang, Y. Song, and D.-Y. Yeung, "Multilingual and multi-aspect hate speech analysis," *arXiv preprint arXiv: . .*, 2019.
- [6] A. Al-Hassan and H. Al-Dossari, "Detection of hate speech in social networks: a survey on multilingual corpus," *Computer Science & Information Technology (CS & IT)*, vol. 9, no. 2, p. 83, 2019.
- [7] N. Albadi, M. Kurdi, and S. Mishra, "Are they our brothers? analysis and detection of religious hate speech in the arabictwittersphere," in *IEEE/ACM International Conference on Advances in Social Networks Analysis and Mining (ASONAM)*. IEEE, 2018, pp. 69–76.
- [8] I. Kwok and Y. Wang, "Locate the hate: Detecting tweets against blacks," in *Twenty-seventh AAAI conference on artificial intelligence*, 2013.
- [9] A. Jha and R. Mamidi, "When does a compliment become sexist? analysis and classification of ambivalent sexism using twitter data," in *Proceedings of the second workshop on NLP and computational social science*, 2017, pp. 7–16.
- [10] B. Ross, M. Rist, G. Carbonell, B. Cabrera, N. Kurowsky, and M. Wojatzki, "Measuring the reliability of hate speech annotations: The case of the european refugee crisis," *arXiv preprint arXiv: . .*, 2017.
- [11] V. Reddy, "Perverts and sodomites: Homophobia as hate speech in africa," *Southern African Linguistics and Applied Language Studies*, vol. 20, no. 3, pp. 163–175, 2002.
- [12] W. Warner and J. Hirschberg, "Detecting hate speech on the world wide web," in *Proceedings of the second workshop on language in social media*. Association for Computational Linguistics, 2012, pp. 19–26.
- [13] P. Burnap and M. L. Williams, "Us and them: identifying cyber hate on twitter across multiple protected characteristics," *EPJ Data Science*, vol. 5, no. 1, p. 11, 2016.
- [14] Z. Waseem and D. Hovy, "Hateful symbols or hateful people? predictive features for hate speech detection on twitter," in *Proceedings of the NAACL student research workshop*, 2016, pp. 88–93.
- [15] M. Dadvar, F. d. Jong, R. Ordelman, and D. Trieschnigg, "Improved cyberbullying detection using gender information," in *Proceedings of the Twelfth Dutch-Belgian Information Retrieval Workshop (DIR)*. University of Ghent, 2012.
- [16] K. Dinakar, R. Reichart, and H. Lieberman, "Modeling the detection of textual cyberbullying," in *fifth international AAAI conference on weblogs and social media*, 2011.
- [17] P. Burnap and M. L. Williams, "Hate speech, machine classification and statistical modelling of information flows on twitter: Interpretation and communication for policy decision making," 2014.
- [18] Y. Chen, Y. Zhou, S. Zhu, and H. Xu, "Detecting offensive language in social media to protect adolescent online safety," in *International Conference on Privacy, Security, Risk and Trust and International Confernece on Social Computing*. IEEE, 2012, pp. 71–80.
- [19] Y. Haralambous and P. Lenca, "Text classification using association rules, dependency pruning and hyperonymization," *arXiv preprint arXiv: . .*, 2014.
- [20] S. Agarwal and A. Sureka, "Characterizing linguistic attributes for automatic classification of intent based racist/radicalized posts on tumblr micro-blogging website," *arXiv preprint arXiv: . .*, 2017.

- [21] S. Liu and T. Forss, "New classification models for detecting hate and violence web content," in *International Joint Conference on Knowledge Discovery, Knowledge Engineering and Knowledge Management (IC K)*, vol. 1. IEEE, 2015, pp. 487–495.
- [22] N. Djuric, J. Zhou, R. Morris, M. Grbovic, V. Radosavljevic, and N. Bhamidipati, "Hate speech detection with comment embeddings," in *Proceedings of the th international conference on world wide web*. ACM, 2015, pp. 29–30.
- [23] S. Yuan, X. Wu, and Y. Xiang, "A two phase deep learning model for identifying discrimination from tweets." in *EDBT*, 2016, pp. 696–697.
- [24] L. Zhang, S. Wang, and B. Liu, "Deep learning for sentiment analysis: A survey," *Wiley Interdisciplinary Reviews: Data Mining and Knowledge Discovery*, vol. 8, no. 4, p. e1253, 2018.
- [25] G. K. Pitsilis, H. Ramampiaro, and H. Langseth, "Effective hate-speech detection in twitter data using recurrent neural networks," *Applied Intelligence*, vol. 48, no. 12, pp. 4730–4742, 2018.
- [26] P. Badjatiya, S. Gupta, M. Gupta, and V. Varma, "Deep learning for hate speech detection in tweets," in *Proceedings of the th International Conference on World Wide Web Companion. International World Wide Web Conferences Steering Committee*, 2017, pp. 759–760.
- [27] A. M. Founta, D. Chatzakou, N. Kourtellis, J. Blackburn, A. Vakali, and I. Leontiadis, "A unified deep learning architecture for abuse detection," in *Proceedings of the th ACM Conference on Web Science*. ACM, 2019, pp. 105–114.
- [28] N. Hamdi, "A guide to avoiding hate speech", The Egyptian Media Development Program., Tech. Rep., 2017
- [29] R. AbuJuma, "The dictionary of hatred and hatred in the Tunisian media", Monitoring Media For Group, 2013
- [30] Iraqi Media House, "Hate Dictionary", Tech. Rep., 2017
- [31] Syrian Center for Media and Freedom of Expression, "Study hate speech and incitement to violence in the Syrian media", Tech. Rep., 2017
- [32] K. Kenyon-Dean, E. Ahmed, S. Fujimoto, J. Georges-Filteau, C. Glasz, B. Kaur, A. Lalonde, S. Bhanderi, R. Belfer, N. Kanagasabai et al., "Sentiment analysis: It's complicated!" in *Proceedings of the Conference of the North American Chapter of the Association for Computational Linguistics: Human Language Technologies, Volume (Long Papers)*, 2018, pp. 1886–1895.
- [33] A. Pasha, M. Al-Badrashiny, M. T. Diab, A. El Kholy, R. Eskander, N. Habash, M. Pooleery, O. Rambow, and R. Roth, "Madamira: A fast, comprehensive tool for morphological analysis and disambiguation of arabic." in *LREC*, vol. 14, 2014, pp. 1094–1101.
- [34] I. A. Al-Sughaiyer and I. A. Al-Kharashi, "Arabic morphological analysis techniques: A comprehensive survey," *Journal of the American Society for Information Science and Technology*, vol. 55, no. 3, pp. 189–213, 2004.
- [35] A. Boudlal, A. Lakhouaja, A. Mazroui, A. Meziane, M. Bebah, and M. Shoul, "Alkhalil morpho sys1: A morphosyntactic analysis system for arabic texts," in *International Arab conference on information technology*. Benghazi Libya, 2010, pp. 1–6.
- [36] H. K. Aldayel and A. M. Azmi, "Arabic tweets sentiment analysis—a hybrid scheme," *Journal of Information Science*, vol. 42, no. 6, pp. 782–797, 2016.
- [37] S. Khoja and R. Garside, "Stemming arabic text," Lancaster, UK, Computing Department, Lancaster University, 1999.
- [38] L. S. Larkey, L. Ballesteros, and M. E. Connell, "Improving stemming for arabic information retrieval: light stemming and co-occurrence analysis," in *Proceedings of the th annual international ACM SIGIR conference on Research and development in information retrieval*, 2002, pp. 275–282.
- [39] V. Gupta and G. S. Lehal, "A survey of text summarization extractive techniques," *Journal of emerging technologies in web intelligence*, vol. 2, no. 3, pp. 258–268, 2010.
- [40] L.-P. Jing, H.-K. Huang, and H.-B. Shi, "Improved feature selection approach tfidf in text mining," in *Machine Learning and Cybernetics*, . *Proceedings. International Conference on*, vol. 2. IEEE, 2002, pp. 944–946.
- [41] L. Breiman, "Random forests," *Machine learning*, vol. 45, no. 1, pp. 5–32, 2001.
- [42] J. D. Rennie, L. Shih, J. Teevan, and D. R. Karger, "Tackling the poor assumptions of naive bayes text classifiers," in *Proceedings of the th international conference on machine learning (ICML-)*, 2003, pp. 616–623.
- [43] J. R. Quinlan, C . : programs for machine learning. Elsevier, 2014.

- [44] C. Cortes and V. Vapnik, "Support-vector networks," *Machine learning*, vol. 20, no. 3, pp. 273–297, 1995.
- [45] R. Collobert, J. Weston, L. Bottou, M. Karlen, K. Kavukcuoglu, and P. Kuksa, "Natural language processing (almost) from scratch," *Journal of machine learning research*, vol. 12, no. Aug, pp. 2493–2537, 2011.
- [46] K. Kawakami, "Supervised sequence labelling with recurrent neural networks," Ph. D. dissertation, PhD thesis. Ph. D. thesis, 2008.
- [47] P. Bojanowski, E. Grave, A. Joulin, and T. Mikolov, "Enriching word vectors with subword information," *Transactions of the Association for Computational Linguistics*, vol. 5, pp. 135–146, 2017.
- [48] T. Mikolov, K. Chen, G. Corrado, and J. Dean, "Efficient estimation of word representations in vector space," *arXiv preprint arXiv: 1301.3781*, 2013.
- [49] A. M. Alayba, V. Palade, M. England, and R. Iqbal, "A combined cnn and lstm model for arabic sentiment analysis," in *International Cross-Domain Conference for Machine Learning and Knowledge Extraction*. Springer, 2018, pp. 179–191.
- [50] B. Shin, T. Lee, and J. D. Choi, "Lexicon integrated CNN models with attention for sentiment analysis," in *Proceedings of the 17th Workshop on Computational Approaches to Subjectivity, Sentiment and Social Media Analysis*. Copenhagen, Denmark: Association for Computational Linguistics, Sep. 2017.
- [51] M. Schmitt, S. Steinheber, K. Schreiber, and B. Roth, "Joint aspect and polarity classification for aspect-based sentiment analysis with end-to-end neural networks," in *Proceedings of the Conference on Empirical Methods in Natural Language Processing*. Brussels, Belgium: Association for Computational Linguistics, Oct.-Nov. 2018.

TOPIC DETECTION FROM CONVERSATIONAL DIALOGUE CORPUS WITH PARALLEL LATENT DIRICHLET ALLOCATION MODEL AND ELBOW METHOD

Haider Khalid¹ and Vincent Wade²

¹School of Computer Science and Statistics, Trinity College Dublin, University of Dublin, Dublin, Ireland

²ADAPT Centre, Trinity College Dublin, University of Dublin, Dublin, Ireland

ABSTRACT

A conversational system needs to know how to switch between topics to continue the conversation for a more extended period. For this topic detection from dialogue corpus has become an important task for a conversation and accurate prediction of conversation topics is important for creating coherent and engaging dialogue systems. In this paper, we proposed a topic detection approach with Parallel Latent Dirichlet Allocation (PLDA) Model by clustering a vocabulary of known similar words based on TF-IDF scores and Bag of Words (BOW) technique. In the experiment, we use K-mean clustering with Elbow Method for interpretation and validation of consistency within-cluster analysis to select the optimal number of clusters. We evaluate our approach by comparing it with traditional LDA and clustering technique. The experimental results show that combining PLDA with Elbow method selects the optimal number of clusters and refine the topics for the conversation.

KEYWORDS

Conversational dialogue, latentDirichlet allocation, topic detection, topic modelling, text-classification

1. INTRODUCTION

Almost fifty years ago, ELIZA [16] was created as the first conversational software and considered as an intelligent chat-bot. It was intended to emulate psycho-therapist. Today, conversational systems emerging in many domains, ranging from ticket reservation to educational context. In recent years, many conversational systems have been introduced, such as Google Assistant, Amazon Alexa, Apple Siri, Microsoft Cortana. Conversational agents often restrict for task-oriented systems [8] to achieve a particular task but human conversational dialogue is however, too complex to be handled by a simple intent-based system [5]. The system requires more human conversational dialogues become more complicated to understand the context of the conversation and decide what to say next depends on anything more than the current user input. There are mainly four categories for intelligent conversational systems are task-oriented, answering the questions, social conversational system and purposeful conversational systems. Natural Language Understanding (NLU) is the central aspect of intelligent systems. In NLU tasks, we can extract meaning from words, sentences, paragraph and

a document. There is a series of hierarchy to extract the context of a conversation. At the dialogue utterance level, one of the most useful ways to understand the text is by analysing its topics and the context of the conversation.

In this paper, we combine the Parallel Latent Dirichlet Allocation (PLDA) Model with K-mean clustering technique. Clustering vocabulary of known similar words based on TF-IDF scores and Bag of Words (BOW) approach. In this approach, each dialogue converted as a document in the pre-processing data phase. Using the classical bag of words approach with TF-IDF weighting scheme dialogues are represented. The similarity measure is used for clustering the combination of document-to-document and document-to-cluster. Also, we use the elbow method for interpretation and validation of consistency within-cluster analysis to select the optimal number of clusters. In order to study the performance of semantic similarity between similar words, noise is removed from data pre-processing phase, we use precision, recall and F-measures for the evaluation and compared our results with traditional LDA and clustering technique.

In section 2, we describe topic detection challenges in a dialogue system. Also, how topic detection is different from the dialogue system as compared with topic detection from tweets, blogs and textual documents. Section 3, mentions the state of art-related work on topic detection and existing techniques for topic detection from textual data. Section 4, explains the proposed approach and methods used for the experiment. Section 5, provides the experimental results and the evaluation metrics together with the comparison between existing approaches and the proposed approach.

2. TOPIC DETECTION CHALLENGES IN DIALOGUE SYSTEMS

The significant difference between topic detection in textual documents/tweets and dialogue corpus is textual documents or tweets are stable data and not changing in context with different times. But conversational dialogues change the context of the conversation over time. For example, yesterday it was raining, and we collect the conversational data on weather information and train our system on this weather data. Today weather condition is different and when a user starts a conversation with the system and system detects the topic about the weather. System responses on the weather condition will be different according to today's weather conditions. In results, the system performs correctly according to the training mechanism, but the system will lose user engagement during the conversation.

The conversational dialogues are short text with irregular writing styles, abbreviations and synonyms. An incremental clustering technique helps to find similarities and topic detection in a temporal context [10]. Contextual topic modelling is also the main challenge in a conversational dialogue system. To create a coherent and engaging dialogue system, the context-aware topic classification method with dialogue act helps in unsupervised topic keyword detection [7]. Topic tracking in conversational dialogue [17], semantic similarity, making an evaluation, continuous state tracking, Multi-functional behaviour and more unsupervised learning [14] is also big challenges in dialogue systems.

3. RELATED WORK

The original idea of topic detection originated in 1996 as part of its broadcast news at the US Government Defence Advanced Research Projects Agency (DARPA) [2]. Detecting topics can be valuable as soon as possible to discover natural disasters [4, 9], helping political parties to predict election results [12] and companies to understand user opinions to improve marketing contents for better understanding of customers' needs [11]. One of the common representations is

describing each topic by a set of keywords. This set can be a weighted set of keywords, where weights represent the keywords and their importance in the topic.

Topic detection from textual data falls in three categories: document-pivot, feature-pivot approaches and probabilistic methods [1]. Firstly, document pivot method groups the individual documents according to the document similarity. Secondly, feature pivot method groups together the terms according to their co-occurrence features pattern. Lastly, probabilistic models treat the problem of topic detection as a probabilistic inference problem. Many techniques have been proposed for topic detection, including clustering, frequent pattern mining, matrix factorisation and exemplar-based topic detection. These existing approaches are used to detect topics from tweets [21], textual documents such as Wikipedia [15] and textual blogging [13]. Clustering involves the organizing of objects into meaningful groups known as a cluster. Objects in one cluster would likely be different from objects grouped under another cluster. The centroid is used as a representative for each cluster discovered, where the top t words (in terms of TF-IDF weights) are used as the keywords of this topic. To detect topics, each utterance in the dialogue is represented using TF-IDF scheme and the number of topics to be discovered is used as the number of clusters (k). The combination of k -means clustering and elbow method improves the efficiency and effectiveness of k -means performance in processing a large amount of data [6]. Incremental clustering with vector expansion extracts scores automatically and utilizes temporarily term similarities for online event detection in microblogs [18]. They use temporal context in microblog posts to detect similar terms by using incremental clustering techniques. When corpus contains closely related topics, then feature pivot approach to detect co-occurrence patterns simultaneously for a large number of terms perform better for textual topic detection [19].

In the human-machine conversation, an engaging and coherent response is possible if the context of the conversation is taking into account. Deep average network and attention deep average network explore various features to incorporate the context of the conversation and dialogue acts gain in topic classification accuracy by 35% and unsupervised keyword detection recall function by 11% [20]. The Latent Dirichlet Allocation (LDA) [3] idea was a mix of topics in which each topic performs as a latent multinomial variable characterized by a distribution of words over a defined vocabulary.

4. PROPOSED METHOD

In the previous work, there are multiple approaches for topic detection such as topic detection with clustering techniques, frequent pattern mining, exemplar-based approach, matrix factorisation and probabilistic models. In our approach, firstly, we combined term similarity analysis by analysing frequent pattern in the dataset to detect topics and k -means clustering to make clusters for all high-frequency words in topics. Secondly, LDA topic model combined with elbow method to select the optimal number of clusters. In the experiment, topic detection is divided into three sections. Data pre-processing, term similarity analysis with clustering and elbow method and topic detection with Parallel Latent Dirichlet Analysis (PLDA). Figure 1 shows the proposed method.

4.1. Data Pre-processing

For the experimental purpose, we use switchboard corpus. Switchboard is a set of approximately 2,400 two-sided telephone conversations between 543 speakers (302 male, 241 female) from all over the United States. We used total 2145 conversation and removed smaller conversations such as “uh-huh”, “okay”, “right”, “oh”, “um-hum” etc. In the experiment, we used unsupervised data, only the dialogue utterances.

- Markup Tag Filter: From the input column, removed all markup language tags.
- Stanford Tagger: assigns to each term of a document a part of speech (POS) tag.
- Punctuation Eraser: From the input documents, removed all the punctuation characters.
- Number filter: From the input documents, filtered all terms contains digits, including decimal separators ",", " or "." and possible leading "+" or "-".
- N Char Filter: Filters all terms contained in the input documents with less than the specified number N characters (we set the value 3).
- Stop Word Filter: Removed stop words and filtered all the input documents.
- Case Converter: In the input documents, convert all the term to lower or upper case.

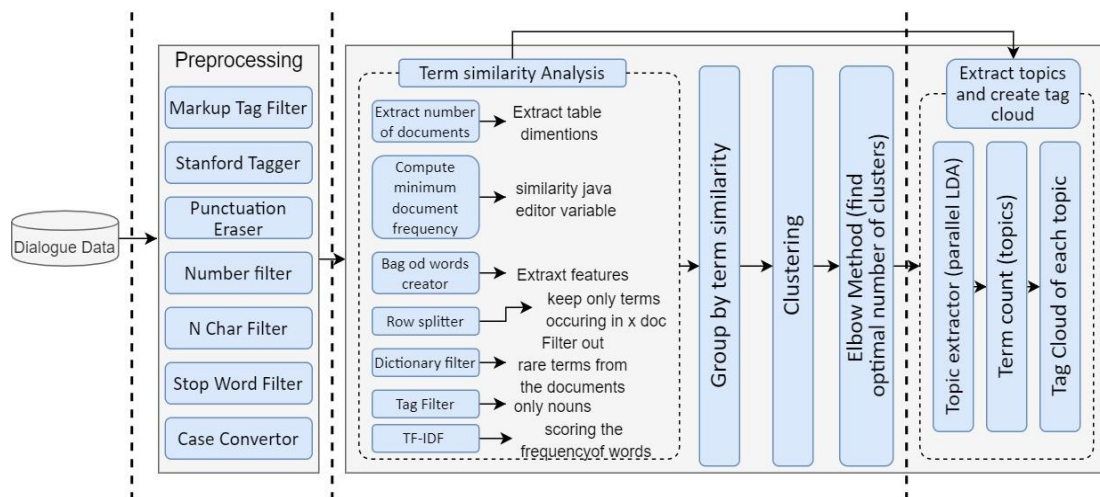


Figure 1. Proposed Method for Topic Detection

4.2. Term Similarity Analysis

The first challenge for topic detection within a conversational dialogue is to find the dialogue utterances that are similar in content, under the term similarity analysis. The dialogue is composed of utterances, and each utterance is considered as a single document. For each row, a document will be created and attached to that row to extract the number of rows for the table dimensions. The Bag of word (BoW) model is used to extract the features from each document. It collects the data in strings and designs the vocabulary of known words. TF-IDF scores the frequency of the words in the current document. It is also scoring of how rare the words are across documents. The concept of BoW and TF-IDF is necessary to train the PLDA model. Dictionary filter filters the high-frequency words from the documents. By applying simple k-means, an unsupervised machine learning algorithm that groups all the high-frequency words into k number of clusters. The elbow method helps the interpretation and validation of consistency within-cluster analysis and select the optimal number of clusters by fitting the model with a range of values for K.

4.3. Topic Extraction and making Tag Clouds

The LDA model defined as a generative probabilistic model for collections of discrete data such as text corpora. It imagines a fixed set of topics. Each topic represents a set of words. LDA's goal is to map all documents to relevant topics in such a way that those imaginary topics mostly capture the words in each document. The concept behind LDA is that each document can be represented through a topic distribution and each topic can be described through a word distribution, which is the premise of the 'bag of words'. In our approach LDA is taking input parallel from elbow method and term similarity based on BoW and TF-IDF to compute the topics.

5. EXPERIMENTAL RESULTS

To determine the optimal clusters in the corpus is the fundamental issue in the clustering technique. The elbow method looks the total within clusters sum of square (WSS) error and minimizes this to absolute value. The optimal number of clusters is defined as follows in the Figure 2:

1. To calculate the clustering algorithm (e.g., clustering of k-means) for different k values varies from 1 to 10. It also depends on the term similarity of word frequency value.
2. Calculate the total within-cluster sum of square (WSS) error value for each k.
3. Plot the elbow method WSS curve based on the number of clusters k.
4. The curve in the graph is generally considered an indication of the optimal number of clusters.

From the experimental results, there are a total of 20 optimal clusters, and each cluster contains a different number of similar items. The elbow method selects the optimal number of clusters in Figure 2 and decreases the sum of squared errors within the clusters in Figure 2.

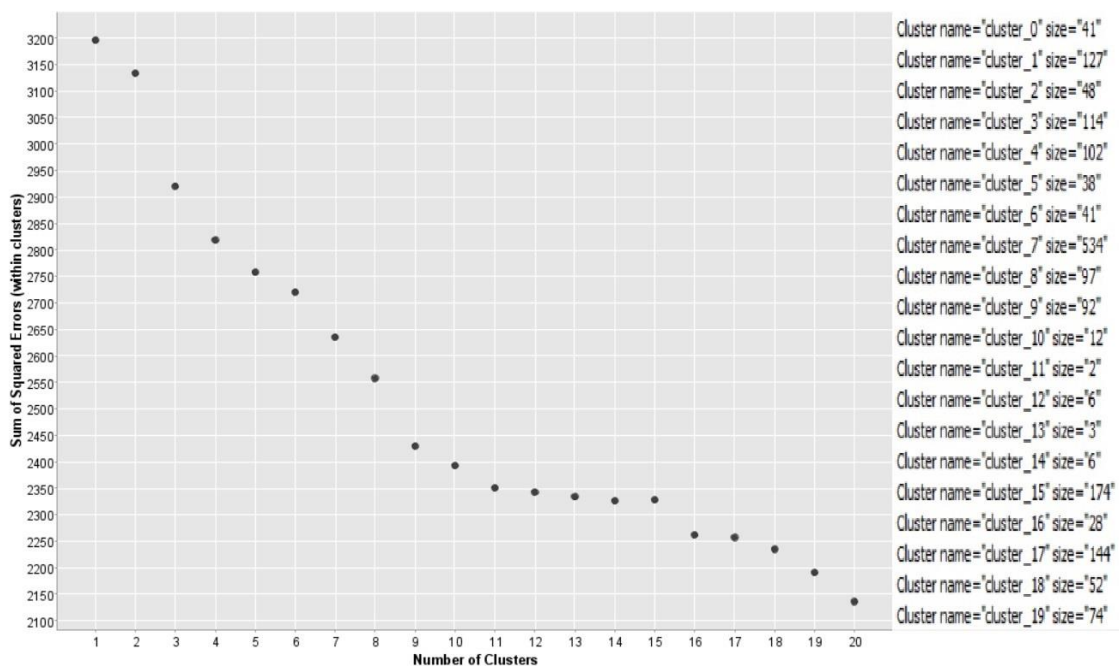


Figure 2. Optimal numbers of clusters from Elbow Method and WSS curve

The PLDA model detects the topics with parameters alpha is 0.5, beta 0.1 and sampling iteration 1000. The number of topics is 3, with ten words in each topic and representation of tag clouds in Figure 3.

Topic 0	Topic 1	Topic 2	Row ID	Image	Topic id
call	day	car	Row0#0		topic_0
car	dollar	feel	Row0#1		topic_1
care	house	change	Row0#2		topic_2
family	look	guess			
child	money	kid			
home	month	people			
course	pay	school			
job	time	sort			
kid	week	stuff			
lot	yeah	talk			

Figure 3. Representations of topics in tag clouds

We reformulated the problem in terms of standard information retrieval evaluation metrics:

$Precision = PP/PNr$, $Recall = PP/NP$, and

$F\text{-measures} = [2(precision)(recall)] / [(precision + recall)(PP)]$

Table 1. Performance comparison between different methods with alpha 0.5 and beta 0.1

Methods	Precision	Recall	F-measures
LDA	0.762	0.834	0.874
Clustering (K-means)	0.778	0.861	0.899
PLDA+Elbow method	0.846	0.931	0.915

6. CONCLUSIONS

On this work we proposed a topic detection approach combining with clustering, elbow method and PLDA model. The first step in a series of different approached to refine the dataset. Then the data is being used to extract similar features word and transform in to multiple clusters. The elbow method with clustering interprets and validates the consistency within the clusters and select optimal number of clusters. LDA is taking input parallel from elbow method and term similarity based on BoW and TF-IDF to compute the topics. We compare our approach with simple LDA model and clustering to evaluate precision, recall and F-measures.

ACKNOWLEDGEMENTS

This research was conducted with the financial support of the Science Foundation Ireland under grant agreement No. (13/RC/2106) at the ADAPT SFI Research Centre at Trinity College Dublin, University of Dublin, Ireland. The ADAPT SGI Centre for Digital Media Technology is funded by Science Foundation Ireland through the SFI Research Centre Programmes and is Co-funded under the European Regional Development Fund (ERDF) through grant #13/RC/2016.

REFERENCES

- [1] Nora Alkhamees and Maria Fasli. 2016. Event detection from social network streams using frequent pattern mining with dynamic support values. In 2016 IEEE International Conference on Big Data (Big Data). IEEE, 1670–1679.
- [2] James Allan. 2002. Introduction to topic detection and tracking. In *Topic detection and tracking*. Springer, 1–16.
- [3] David M Blei, Andrew Y Ng, and Michael I Jordan. 2003. Latent dirichlet allocation. *Journal of machine Learning research* 3, Jan (2003), 993–1022.
- [4] Paul S Earle, Daniel C Bowden, and Michelle Guy. 2012. Twitter earthquake detection: earthquake monitoring in a social world. *Annals of Geophysics* 54,6 (2012).
- [5] M Gašić, Dongho Kim, Pirros Tsiakoulis, Catherine Breslin, Matthew Henderson, Martin Szummer, Blaise Thomson, and Steve Young. 2014. Incremental on-line adaptation of pomdp-based dialogue managers to extended domains. In *Fifteenth Annual Conference of the International Speech Communication Association*.
- [6] Kalpana D Joshi and PS Nalwade. 2013. Modified K-Means for Better Initial Cluster Centres. *International Journal of Computer Science and Mobile Computing, IJCSMC* 2, 7 (2013), 219–223.
- [7] Chandra Khatri, Rahul Goel, Behnam Hedayatnia, Angeliki Metanillou, Anushree Venkatesh, Raefer Gabriel, and Arindam Mandal. 2018. Contextual topic modelling for dialog systems. In *2018 IEEE Spoken Language Technology Workshop (SLT)*. IEEE, 892–899.
- [8] Ryan Lowe, Nissan Pow, Iulian Serban, and Joelle Pineau. 2015. The ubuntu dialogue corpus: A large dataset for research in unstructured multi-turn dialogue systems. *arXiv preprint arXiv:1506.08909*(2015).
- [9] Onook Oh, Kyounghee Hazel Kwon, and H Raghav Rao. 2010. An Exploration of Social Media in Extreme Events: Rumor Theory and Twitter during the Haiti Earthquake 2010. In *Icic*, Vol. 231. 7332–7336.
- [10] Ozer Ozdakis, Pinar Karagoz, and Halit Oğuztüzün. 2017. Incremental clustering with vector expansion for online event detection in microblogs. *Social Network Analysis and Mining* 7, 1 (2017), 56.
- [11] Fuji Ren and Ye Wu. 2013. Predicting user-topic opinions in twitter with social and topical context. *IEEE Transactions on affective computing* 4, 4 (2013), 412–424.
- [12] Andranik Tumasjan, Timm O Sprenger, Philipp G Sandner, and Isabell M Welp. 2010. Predicting elections with twitter: What 140 characters reveal about political sentiment. In *Fourth international AAI conference on weblogs and social media*.
- [13] Xiaodong Wang and Juan Wang. 2013. A method of hot topic detection in blogs using N-gram model. *Journal of Software* 8, 1 (2013), 184–191.
- [14] Nigel G Ward and David DeVault. 2015. Ten challenges in highly-interactive dialog system. In *2015 AAAI Spring Symposium Series*.
- [15] Christian Wartena and Rogier Brussee. 2008. Topic detection by clustering keywords. In *2008 19th International Workshop on Database and Expert Systems Applications*. IEEE, 54–58.
- [16] Joseph Weizenbaum and others. 1966. ELIZA—a computer program for the study of natural language communication between man and machine. *Commun. ACM* 9, 1 (1966), 36–45.

- [17] Jui-Feng Yeh, Chen-Hsien Lee, Yi-Shiuan Tan, and Liang-Chih Yu. 2014. Topic model allocation of conversational dialogue records by Latent Dirichlet Allocation. In Signal and Information Processing Association Annual Summit and Conference (APSIPA), 2014 Asia-Pacific. IEEE, 1–4.
- [18] Ozer Ozdakis, Pinar Karagoz, and Halit Oğuztüzün. 2017. Incremental clustering with vector expansion for online event detection in microblogs. *Social Network Analysis and Mining* 7, 1 (2017), 56.
- [19] Georgios Petkos, Symeon Papadopoulos, Luca Aiello, Ryan Skraba, and Yiannis Kompatsiaris. 2014. A soft frequent pattern mining approach for textual topic detection. In Proceedings of the 4th International Conference on Web Intelligence, Mining and Semantics (WIMS14). 1–10
- [20] Chandra Khatri, Rahul Goel, Behnam Hedayatnia, Angeliki Metanillou, Anushree Venkatesh, Raefer Gabriel, and Arindam Mandal. 2018. Contextual topic modeling for dialog systems. In 2018 IEEE Spoken Language Technology Workshop (SLT). IEEE, 892–899.
- [21] A Castellanos, J Cigarrán, and Ana García-Serrano. 2017. Formal concept analysis for topic detection: a clustering quality experimental analysis. *Information Systems* 66 (2017), 24–42.

AUTHORS

Haider Khalid is an ADAPT PhD student at Trinity College Dublin, Ireland. His current research is focused on topic detection and topic modelling for dialog system with NLP. He holds a Master's degree in Software Engineering from Jiangsu University China, funded by Chinese Scholarship Council (CSC). Outside of the office, he likes sport, socializing with people and nature. He is also very interested in politics, technology and different cultures.



Professor Vincent Wade is Director of the ADAPT Centre for Digital Media Technology and holds the Professorial Chair of Computer Science (Est. 1990) in School of Computer Science and Statistics, Trinity College Dublin as well as a personal Chair in Artificial Intelligence. His research focuses on intelligent systems, AI and Personalisation. He was awarded Fellowship of Trinity College for his contribution to research and has published over three hundred and fifty scientific papers in peer reviewed international journals and conferences.

QUANTUM CRITICISM: A TAGGED NEWS CORPUS ANALYSED FOR SENTIMENT AND NAMED ENTITIES

Ashwini Badgajar¹, Sheng Cheng¹, Andrew Wang¹, Kai Yu¹,
Paul Intrevado² and David Guy Brizan¹

¹Department of Computer Science
University of San Francisco, San Francisco, CA, USA
²Department of Mathematics and Statistics
University of San Francisco, San Francisco, CA, USA

ABSTRACT

In this project, we continuously collect data from the RSS feeds of traditional news sources. We apply several pre-trained implementations of named entity recognition (NER) tools, quantifying the success of each implementation. We also perform sentiment analysis of each news article at the document, paragraph and sentence level, with the goal of creating a corpus of tagged news articles that is made available to the public through a web interface. Finally, we show how the data in this corpus could be used to identify bias in news reporting.

KEYWORDS

Content Analysis, Named Entity Recognition, Sentiment Analysis.

1. INTRODUCTION

Many of us implicitly believe that the news we consume is an important summary of the events germane to our lives. Regardless of how we divide ourselves—by demographics, political leaning, profession or other socioeconomic schism—we rely on trusted individual journalists and the news organizations to which they belong to distil stories and provide unbiased context.

There are several organizations that attempt to address this need. USAFacts.org is a non-profit organization and website which offers a non-partisan portrait of the US population, its government's finances, and government's impact on society. Similar sites and outlets have had the same mission, perhaps most prominently MIT's Data USA and the US government's data.gov. These efforts, however, largely deal with quarterly or bi-annual government reports, excluding day-to-day news analysis about business, politics, etc.

More timely news on these excluded topics can typically be found reported on by private news organizations, often funded by a subscription or ad-based model. There are, however, a subset of articles that are freely available to the public. News producers often promote selected articles through their real simple syndication (RSS) feeds, consumed by phone or web applications such as Feedly, NewsBlur and FlowReader, among others.

News organizations should be a reflection of the populations they represent. Yet, despite ease of access to news articles through RSS feeds, we find a dearth of resources supporting the analysis of said news articles, e.g., how the news is reported or how it may be affecting our lives over time. For example, observing climate change denial, one journalist from Vox, David Roberts, has named the current American philosophical divide “tribal epistemology,” specifically discussing the tribalism of information through the news [1]. While his presentation is compelling, the idea of tribal epistemology is largely delivered without an analysis of the news from sources which he critiques. Roberts’s lack of analysis could be the result of having no facile manner to find and analyse daily news articles from multiple sources in a single corpus.

In our survey of existing news corpora in Section 2, we find existing corpora lacking in one or more aspects, including cost, availability, coverage and/or analysis. We therefore create our own corpus, Quantum Criticism, to address these issues. Specifics of the tools and approaches we use to build our corpus are discussed in Section 3. We discuss the performance of our tools in Section 4. We aspire for our corpus to be used by journalists and for those in academic research to establish trends, identify differences, and affect change in news reporting and its interpretation. In Section 5, we demonstrate two ways in which our corpus can be used to uncover potential media bias.

2. RELATED WORK

We begin the Related Work section by highlighting existing corpora that have some coverage or analysis limitation, discussed in Section 2.1. Section 2.2 briefly reviews common tasks in natural language processing, as well as some of the available tools for accomplishing those tasks. Lastly, in Section 2.3, we explore several use-cases of existing news corpora.

2.1. Corpora

There are several outcomes of forming a news-based corpus. One may be the task of language modelling. Journalists and news organizations can be barometers of when a word gets introduced to a language. Another important use of news-based corpora is the derivation of larger social patterns from individual units of reporting.

The consumers of a news corpus must regard journalists and news organisations as imperfect messengers. As far back as 1950, White [2] demonstrated that the news we read is frequently collated by a set of “gate keepers” who filter candidate events. These gate keepers may have biases based on ideological (liberal or conservative) leanings, race or gender [3], economic interdependence [4] and geopolitical affiliation [5], likely only some of the many factors influencing a news story’s selection. One use of a properly constructed corpus could be the unearthing of selection bias or other biases.

Selection bias may be the result of the choices of not only the specific journalists but also the news organizations and their owners [6]. In a large-scale study based on articles from the GDELT database, [7] lays out the constraints under which the news organizations operate and quantify the selection bias of news organizations.

Prior to building our Quantum Criticism corpus, we considered a number of other corpora assembled from news articles, all appearing online. The Linguistic Data Consortium (LDC) has an extensive collection, including the New York Times corpus [8], which we use for validation of our tools (see Section 4). This corpus contains 1.8 million news articles from the New York Times over a period of more than 10 years, covering stories as diverse as political news and

restaurant reviews. Articles are provided in an XML format, with the majority of the articles tagged for named entities—persons, places, organizations, titles and topics—so that these named entities are consistent across articles.

The LDC also offer the North American News Corpus [9], assembled from varied sources, including the New York Times, the Los Angeles Times, the Wall Street Journal and others. The primary goals of this corpus are support for information retrieval and language modelling, so the count of “words”—almost 350 million tokens—is more important than the number of articles. Also offered by the LDC is the Treebank corpus [10], often called the Penn Treebank, which has been an important and enduring language modelling resource; see [11] for an early use of this corpus, and [12] for a more recent implementation.

Collectively, the LDC corpora and their like are excellent resources for news generated from a discrete number of sources during a particular period of time. Because of their volume of articles and tokens, and because they are mostly written in Standard American English, they are ideal for building language models from the period during which they were collected.

However, we find the aforementioned corpora broadly lacking in a number of areas, chiefly, in their static nature: these corpora do not continuously collect new articles. Depending on the research being conducted, researchers may require current articles as well as historic ones. We also find flaws in the tagging of the articles in the New York Times Annotated Corpus, however, leave the full treatment of this to Section 4. Finally, we find that processing these articles requires a non-trivial cost and effort. Finding articles in which a particular person, place or organisation is mentioned requires a search through a considerable number of articles, for which there are no additional tags.

In contrast to the offerings by the LDC, the Global Database of Events, Language and Tone [13], known as GDELT, has a dizzying array of tools for searching and analysing their corpus. With a public, no-cost access to articles from 1979 to present, albeit offered at a 48-hour delay, and a commitment to the continued collection of news from a wide variety of sources, GDELT’s offerings have resulted in insightful results, some of which are explored herein.

One criticism of GDELT by Ward et al. [14] is that the collection effort has been optimized for volume of news articles and speed of analysis through automated techniques, sacrificing the careful curation of articles. This results in the improper classification of articles, erring mostly toward false positives, i.e., presenting more news articles as related to an event than is warranted.

In terms of implementation, our Quantum Criticism corpus is closest to the News on the Web (NOW) Corpus, itself a public-facing version of the Corpus of Contemporary American English [15]. As of the time of this writing, this corpus reports containing 8.7 billion words from a number of American English sources, including such varied sources as the Wall Street Journal and tigerdroppings.com, the student newspaper of Louisiana State University.

While the diversity of our Quantum Criticism corpus is not as extensive as what we find in the NOW Corpus, our initial version of the Quantum Criticism corpus contains one non-American English source and allows the user to specify the source(s) for a query. We believe the power of our search and presentation makes our corpus a better analysis tool.

2.2. Overview of NLP Tools

We analyse news articles in two ways: through named-entity recognition and sentiment analysis. Our search tool exposes the results of these analyses simultaneously.

In free-form text, named-entity recognition (NER) seeks to locate and classify the names of (among other entities) people, organisations and locations. Although there are other possible categories of named entities, we selected these three classes based on available resources and commonality of model outputs. Three powerful and oft used NER tools include BERT (Bidirectional Encoder Representations from Transformers, [16]), which uses BIO tagging, CoreNLP [17], which offers both IO and BIO tagging, and spaCy [18], which employs IOB tagging.

2.3. Use Cases of Corpora

Using corpora and NLP tools, we can discover the biases of a journalist, a news organisation or the target audience of the news. The effects of biases can effect change on the political or sociological lives of a people. We see some interesting examples of these effects. While work by Rafail and McCarthy [19] stops short of the claim that some news organizations made the Tea Party—a small, right-leaning movement—a political force, there may be ample evidence to draw such a conclusion. The suggestion is that the news media simplified the message of the party so that it could be consumed by a wider audience, as well as amplified the coverage of the party's events beyond the size its supporters would normally warrant given their numbers.

A more pernicious effect may be seen in the coverage of the Persian Gulf “Crisis” and subsequent war of the early 1990s [20]. Here, the media was focused on stories which, among other effects, made readers inclined to favour military rather than diplomatic paths. In turn, this had an effect on the political leadership of the time. The authors also find an interesting effect wherein the selection bias for stories was proportional to public interest in such stories. Interestingly, work by Soroka et al. [21] suggests the opposite effect may be a force. Here, the “strength” of sentiment in social media reactions differ from the news media coverage in some economic news coverage. As a result, the contexts and degree to which public opinion affects news coverage or vice versa deserve additional study.

Systematic analysis of media coverage often involves framing the content from the point-of-view of the reader. A paper by An and Gower [22] discusses five frames (attribution of responsibility, human interest, etc.) and two “responsible parties” (individuals vs. organizations) in coverage of crises, finding that some frames are more common than others. Similarly, Trumbo [23] examines the differing reactions of scientists and politicians to climate change. While analysis approaches tend to focus on the content produced, work by Ribeiro et al. [24] examines the political leanings and demographics of the target audience through the advertising associated with the content. We see this kind of side-channel investigation as promising, especially if applied systematically to a large set of data.

Our Quantum Criticism corpus is designed with these types of analysis in mind. We tag each article for named entities and sentiment and expose this corpus to the public. We expect this corpus to have multiple purposes, including sociological research on influential people and organizations, “framing” news articles and assigning responsible parties, and the detection of selection bias and other biases in a media organization's coverage. We provide details on how each element of our pipeline is built, and quantify the performance using well-established metrics. We conclude by validating the tools employed and discussing two use cases for our corpus.

3. CORPUS AND DATA PROCESSING

The data used for our Quantum Criticism effort was collected, managed, and processed using a proprietary system designed to scrape, parse, store and analyse the content of news articles from a variety of sources. Several sentiment and named entity recognition tools were run against the collected news articles. We also implemented a custom entity resolution algorithm, providing a rich data set upon which to explore several hypotheses. A pictorial summary of the ingestion, analysis and storage pipeline is shown in Figure 1.



Figure 1: A Summary of the Ingestion, Analysis and Storage Pipeline

3.1. News Scraper

Several custom web scrapers were created for retrieving news articles from various online news organizations. All web scrapers were run every two hours to retrieve articles from the following five news sites: the Atlantic, the British Broadcasting Corporation (BBC) News, Fox News, the New York Times and Slate Magazine. Web scrapers continue to run every two hours in perpetuity, scraping additional news articles. Collectively, the web scrapers used each news organization's RSS feed as input, storing the scraped output into a custom database. Article URLs were used for disambiguation; where two scraped articles shared a URL, the most recently retrieved article replaced previous versions of articles.

As of November 2019, we collected a total of 105,000 news articles from five media organizations. Figure 2 depicts the number of cumulative articles scraped for each news organization over time. Even though articles from Fox News were regularly scraped four months later than other news sources, the number of articles scraped rose quickly, and now constitutes the news organization with the most scraped articles. Given the news scrapers run at regularly scheduled two-hour intervals for all news organization, this suggests that Fox News updates its RSS feed with new articles far more often than others, and the Atlantic updates its RSS feed far less frequently than others.

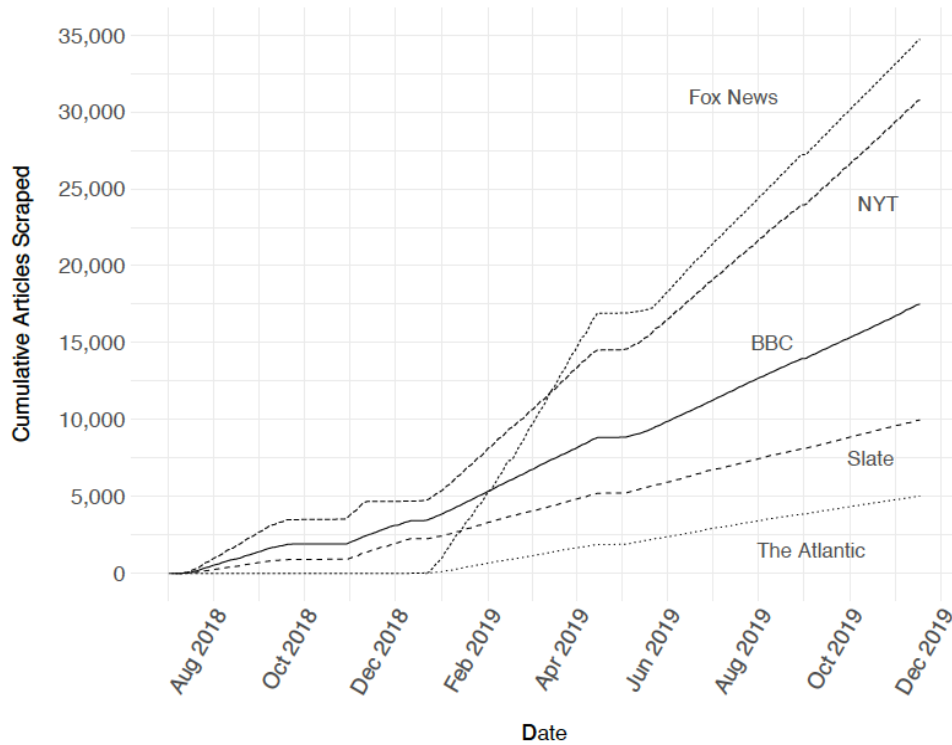


Figure 2: Cumulative Quantity of Articles Scraped by News Organization

3.2. Data and Database Management

All scraped data is stored in a MariaDB relational database. We considered a NoSQL database, especially one focused on storing documents, such as MongoDB; however, we found that a relational database was appropriate for the needs of this project.

We constructed many “primary” tables to support the scraped articles. The most important of these tables are the article, media (e.g., The Atlantic, BBC, etc. representing the news organization) and entity (a named person, location or organization) tables. To support modelling the many-to-many relationship between article and entity, we have one “join” table (article entity). To support the work in sentiment analysis and named entity recognition; we also created tables to store the outputs of the algorithms for these tasks. For sentiment analysis, we created a table called “sentiment. For named entity recognition, we created a table “entity.” Other tables in our schema are omitted for brevity. Courtesy of dbdiagram.io, a schema appears as Figure 3.

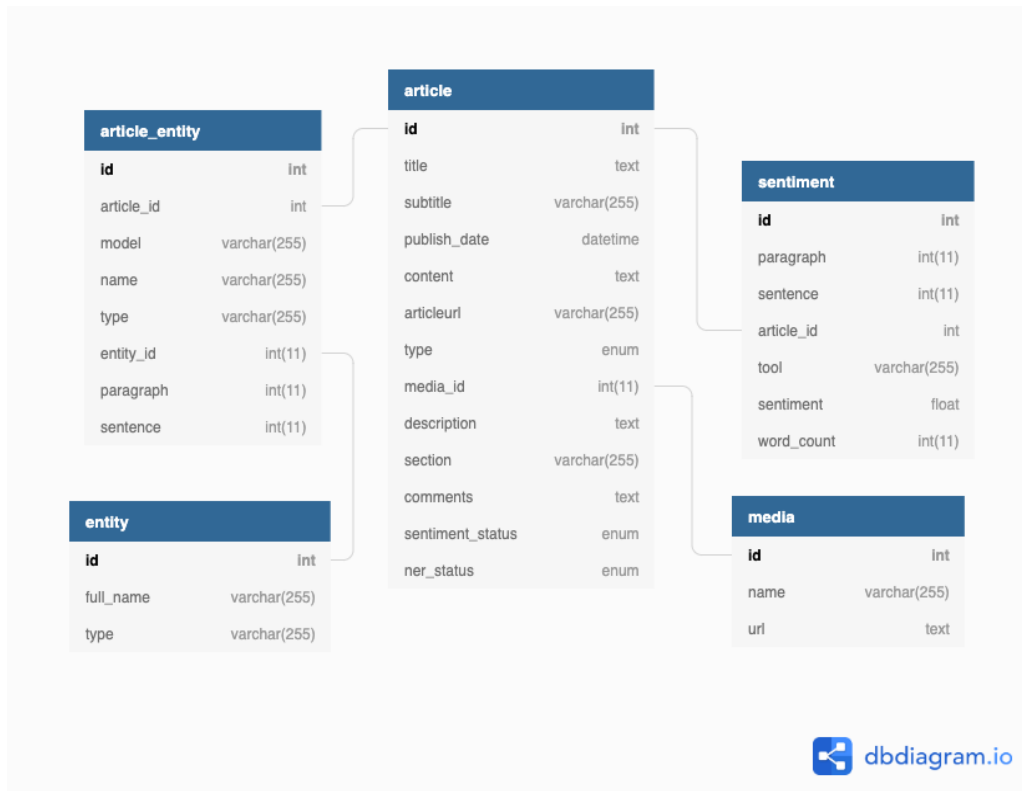


Figure 3: Schema for the Quantum Criticism Database

3.3. Sentiment Analysis

For each news article, we generated a sentiment score. We employed both the VADER (Valence Aware Dictionary and sentiment Reasoner) [25] module, as implemented in NLTK [26] in python, as well as CoreNLP sentiment analysis. Sentiment scores in VADER are continuous values between -1 (very negative) to +1 (very positive), with 0 representing neutral sentiment. Sentiment scores in CoreNLP are integer values between 0 (very negative) and 4 (very positive), with 2 representing neutral sentiment.

Sentiment analysis tools were run against each sentence and each paragraph in the article, as well as on the entire article. For example, if an article contained two paragraphs, where paragraph 1 contains two sentences and paragraph 2 contains one sentence, we would have calculated six different sentiment scores per sentiment analysis tool: one for each sentence (3), one for each paragraph (2), and one for the article (1). This deconstructed approach allows researchers to associate named entities with their associated sentiment at a quantum level. This granular level of sentiment may help disambiguate the sentiment of an article with respect to the named entities. For example, an article from a conservative news organization may be positive overall, however, it is likely to be more critical of more liberal politicians, organizations or causes mentioned therein, and more supportive of conservative organizations or causes. Our quantum approach to sentiment analysis allows researchers to parse sentiment at the sentence level and associate that sentiment with named entities, independently of the paragraph or article in the aggregate.

3.4. Named Entity Resolution

We employed eight named entity recognition (NER) models from CoreNLP, spaCy, and BERT packages to identify PERSONs, ORGANIZATIONs and LOCATIONs in news articles. While some models predict different NER categories, we sought only those entities which were tagged as above.

We store each NER model output individually in our database. In many articles, a named entity is referenced by a complete name or title, and subsequently, by a shortened version. For example, a recent New York Times Opinion article (Democrats’ Vulnerabilities? Elitism and Negativity) first refers to politician Alexandria Ocasio-Cortez by her full name, and then subsequently as Ocasio-Cortez. In order to connect references to the same named entity, we implemented a custom entity resolution algorithm. Owing to the highly structured manner in which we observed news articles were written, we expected to observe the pattern of an entity’s full name, followed by partial name. Our algorithm therefore matched any name extracted in an article as a substring, to the most recent instance of another name in the same article. Where a match occurred, the two names are determined to be the same entity. Such an entry is matched or created by category (PERSON, LOCATION, ORGANIZATION).

This process often failed for abbreviations such as the acronym F.B.I.—in reference to the Federal Bureau of Investigation—with periods left out, resulting in FBI. We therefore also created custom code to query a corpus of abbreviations and associate acronyms to their full names. Only full names were stored in the database. We label each such instance of the full name a resolved entity. The entity resolution algorithm is depicted in Figure 4. Entities are also resolved across articles in a similar manner.

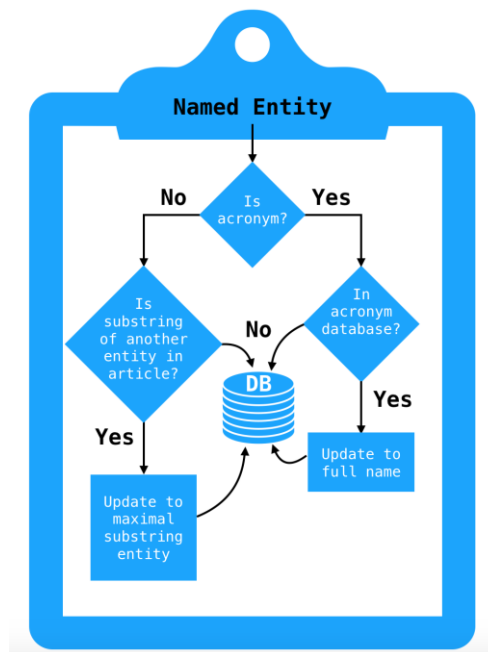
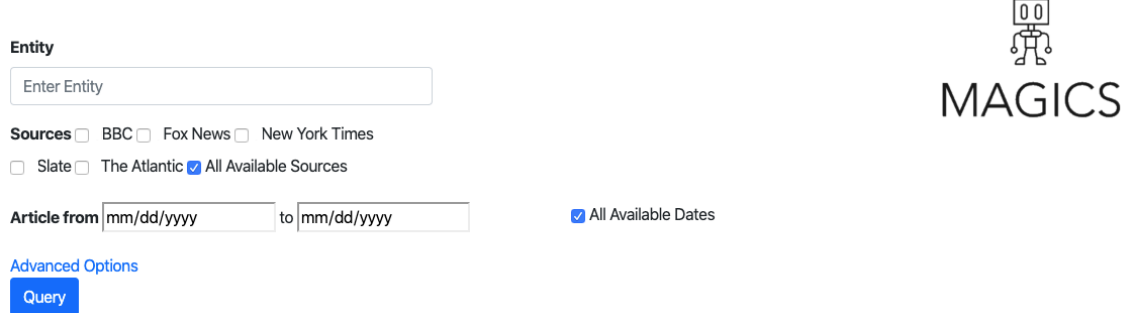


Figure 4: Pseudo-code for Named Entity Resolution Within a News Article

3.5. Web Interface

We designed and implemented a web interface for our corpus. Through this interface, a user can specify basic search criteria for the articles, specifically: the entity name, in whole or part, of the entity to be searched; the news source(s) to be searched from among those in our database; and the date or date range of the articles. (See Figure 5.)

Quantum Criticism: Search Tool



The screenshot shows a web interface for a search tool. At the top left, there is a section titled "Entity" with a text input field labeled "Enter Entity". Below this is a "Sources" section with several radio button options: BBC, Fox News, New York Times, Slate, The Atlantic, and All Available Sources (which is selected). To the right of the sources is a "MAGICS" logo featuring a stylized robot head. Below the sources is an "Article from" and "to" section with date input fields in the format "mm/dd/yyyy" and a checked checkbox for "All Available Dates". At the bottom left, there is a link for "Advanced Options" and a blue "Query" button.

Figure 5: Search Screen for Web Interface

Additionally, advanced search criteria—not shown in Figure 5 but available on the live web interface—allow the user to include additional filters for specific NER tools, the sentiment tools, and/or the level of granularity (article, paragraph or sentence) to be reported.

Upon executing a successful query, a small subset of the results is displayed so that the user may perform a quick validation. In addition, a link is provided to allow the user to download the full set of results in comma-separated value (CSV) format. Each row in the result set contains the fields listed in Table 1.

Table 1: Fields in the Result Set of the Web Interface

Field	Type	Notes
id	integer	Database table ID
entity	string	Full name of entity
entity id	int	Database table ID
type	Enum	PER, LOC or ORG
date	Date	Last modified date
url	String	Article's URL
NER tool	String	Name of the NER tool
paragraph	int	Possibly NULL or empty
sentence	int	Possibly NULL or empty
sentiment score	float	
sentiment tool	String	Name of the model
media name	String	"Fox News", "Slate," ...
media url	String	URL of the news org.

Notably absent from the columns in the result set are the contents of the article. This absence is deliberate. While recent legal rulings have suggested that distributing content produced by third parties is permissible, we are unsure about whether that ruling is the final word on this or whether the ruling applies globally. As a result, we provide the URL to the source article, allowing the user to download the content themselves.

4. VALIDATION

We employ well-studied tools with established performance benchmarks in our data ingestion and processing pipeline. In this section, we describe how we evaluated the performance of those tools. For the validations reported in this section, we used two news corpora: a historical New York Times corpus and our Quantum Criticism corpus of scraped news articles.

4.1. Named Entity Recognition Validation

We test the efficacy of our eight NER models across three different NER tools using two approaches. Firstly, we executed each of the models against the articles in the New York Times Annotated Corpus with a 1st of December publication date across all 20 years covered by the corpus. Secondly, we explore the fidelity of the NER tools by examining how well they identify the 538 members of the U.S. Congress (Senate and House of Representatives), as identified by Ballotpedia.

4.1.1. NER Tools vs. the LDC New York Times Corpus

To determine the fidelity of our results, we ran each NER model against the New York Times Annotated Corpus [8], for which named entities are provided as an adjunct list. The corpus contains 1.8 million articles from the New York Times from the years between 1987 and 2007.

While we found that the 4,713 articles from the 1st of December, 1987–2007 was a sufficiently ample volume from which to draw conclusions, we tested an additional ten months of data for the spaCy and CoreNLP models, finding no significant deviation from the results we report here.

For each of the articles published on the 1st of December, we determined the mean (and standard deviation) of the following in each article: the number of tokens per article: 587.2 (643.7); and the number of named entities identified by the models per article: 31.8 (43.9). For each of the models, we also computed the precision, recall and F1 score for each article. The BERT `bert.base.multilingual.cased` model generated the highest mean precision and mean F1 scores of 0.1753 and 0.2549, respectively, whereas the highest mean recall score was obtained from the CoreNLP `en-english.all.3class.distsim.crf.ser` model.

We observed a consistently low F1 score for all NER models, despite the variable number of entities identified by the classifiers. Some of this poor performance may be explained by the models' generation of improperly resolved entities in the body of the article. However, we believe that this poor performance can be largely attributed to errors in the labels of the source corpus.

To confirm this hypothesis, we examined several articles from the New York Time Annotated Corpus, and found disagreement with the named entities identified in the manual tagging of the corpus. Filtering for the named entity classes PERSON, LOCATION and ORGANIZATION in one of these examined articles, *Homicides Up in New York; Other Crimes Keep Falling*, we find

only three tags from the corpus: Cara Buckley, the article’s author; New York City, the location being reported; and the Federal Bureau of Investigation. These instances identified by the corpus are highlighted in blue. In contrast, one of the authors, a native English speaker who has performed several annotation tasks on other projects, identified several other named entities. These additional named entities are highlighted in yellow. Interestingly, two of the models we use, `bert.base.cased` and `bert.base.multilingual.cased`, added a spurious named entity label in this case, “Homicides.” We highlight this deviation in red.

In the articles we inspected, our annotator found that his identification is closer to the results we obtain from the NER models. Interestingly, BERT appears to exhibit a tendency toward combining tokens to form named entities (e.g., “Ms. Pickett” with “Fort Greene” to form “fort green pickett”), and toward listing names of people with family name first (e.g., “pickett, cheryl”); we converted to the surname-last ordering common in American English. While we believe the output of the BERT models is closer aligned to our expectations, it also clearly misidentified tokens (e.g., “homicides” in the above example) as named entities and misclassified named entities, commonly determining a person’s name to be a LOCATION instance.

Homicides Up in New York; Other Crimes Keep Falling

By CARA BUCKLEY JAN. 1, 2007

In New York City, rapes, robberies and assaults, among other crimes, continued to decline last year, prompting the Police Department’s top official to herald 2006 as a very good year. Homicides, however, climbed 10 percent in the city, reversing a much-hailed decrease.

“We’d like to see no homicides. The reality is we’re going to have them,” said Police Commissioner Raymond W. Kelly. “I think this is a very good year.”

He called the increase in killings in 2006 all but negligible compared with 1990, a year with one of the highest homicide rates in recent history. That year, crack-fueled violence soared, and 2,262 people were killed.

Last year there were 579 killings citywide as of Dec. 24, an increase of 52 homicides over the same period in 2005. Yet overall crime last year was down 5 percent. The number of reported rapes declined by 7.4 percent to 1,486, subway crime plunged 13 percent and auto theft fell 11.4 percent.

The police said the year’s jump in homicides was rooted largely in an unusually high number of “reclassified” deaths, deaths linked to injuries incurred in months or years past. There were 38 reclassified homicides in New York last year, compared with 21 in 2005.

New York’s overall fall in crime also contrasts with an increase nationwide. According to a report by the F.B.I., violent crime across the country rose 3.7 percent during the first half of the year. Dallas remained the country’s most violent city, with 3,985 crimes per 100,000 people, according to the midyear report, while New York ranked 10th with 1,187 per 100,000.

Myriad factors account for New York’s continuing decline in crime overall, the police and criminologists say. They cited more effective policing, shifting drug patterns and the lowest unemployment rate in 30 years.

Yet what is puzzling, one expert said, is that overall crime is dropping even as New York becomes an increasingly polarized city, with haves and have-nots often living side by side in luxury condominiums and public housing.

“Within a few blocks, people are living worlds apart,” said Andrew Karmen, a sociology professor at John Jay College of Criminal Justice and the author of “New York Murder Mystery: The True Story Behind the Crime Crash of the 1990s.”

“In theory, that should make the poor more dissatisfied and drive people to commit crimes,” he said. “But that doesn’t seem to be happening in New York.”

One possible explanation, Dr. Karmen said, is that the city is largely populated by immigrants, many of whom are driven by a determination to succeed.

Figure 6: Labels identified by the NY Times Corpus (blue) and additional labels identified by our annotator (yellow) and spurious labels identified by BERT (red)

Although our manual evaluation of the corpus was limited in scope, it does lead us to believe that named entities are generally under-reported by the corpus. We therefore concluded that the most

reliable metric in comparing our models to the corpus is recall. This allows us to treat each NER system as a detector, i.e., to determine what fraction of the entities in the articles' annotations are identified by the NER models.

4.1.2. NER Tools vs. the Quantum Criticism Corpus

Because we were unable to label an extensive set of articles, we have no ground truth for the performance of the NER tools against our corpus. Instead, we largely rely on the metrics of the NER tools against the NY Times Corpus for this. However, we are interested in determining the number or rate of misclassifications of entities.

For this, we used the 538 current members of the U.S. legislative branch (Congress) as identified by Ballotpedia. This list includes all members of the U.S. Senate and the U.S. House of Representatives. Of these, 372 (69%) are mentioned at least once in the articles we scraped. We examined these mentions as a way to assess the quality of the NER tools employed.

Looking across all eight NER tools from BERT, CoreNLP and spaCy, 96.9% of all entities resolved to the correct classification of PERSON. There were, however, some notable deviations. Two models however, one from spaCy and another from CoreNLP, consistently misidentified Congress people as ORGANIZATION instances, at a rate of 5.06% and 2.98%, respectively, as depicted in Figure 7. This behaviour may be, in part, attributed to the fact that Congresspeople often lead or participate in important organizations, and are therefore often conflated with them. For example, Nancy Pelosi, the former and current Speaker of the U.S. House of Representatives at the time of this writing, is often misidentified as an ORGANIZATION given her leadership role. Perhaps more interesting is the performance of the `english.conll.4class.distsim.crf.ser` model in CoreNLP, which misidentifies 7.76% of all Congresspeople.

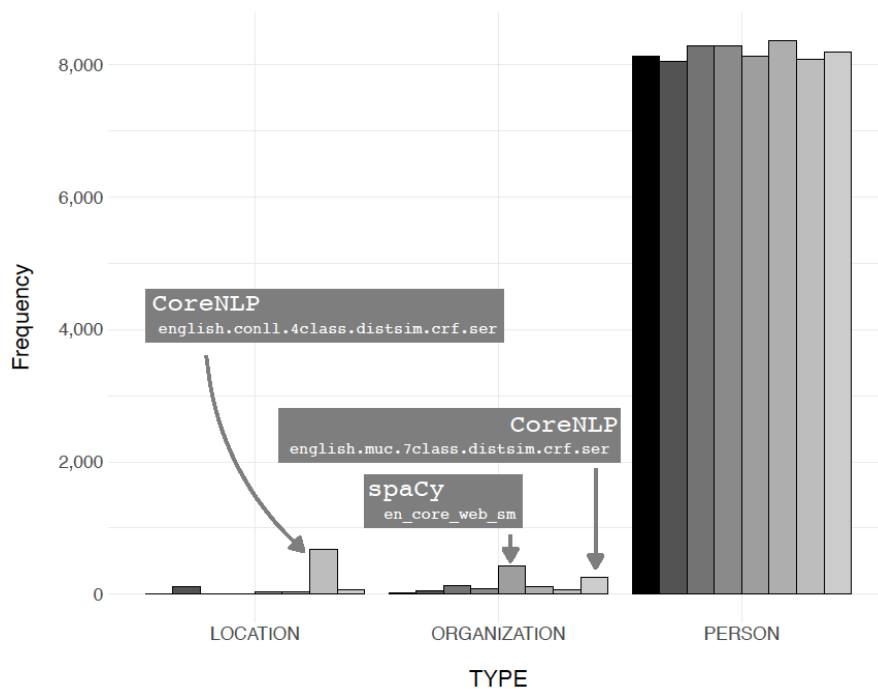


Figure 7: (Mis)Classification of PERSON Entities by NER Model

4.2. Entity Resolution Validation

Querying our scraped articles, we sought to explore how well our proprietary entity resolution algorithm worked to resolve the names of Congresspeople. We searched our scraped data using each space-separated or hyphen-separated token from the full names of members of Congress listed on Ballotpedia. These results were then manually checked to retain only valid references to the individuals in question.

To illustrate the above, we use Nancy Pelosi, who is the most-mentioned Congressperson in our database. Using the strings “%Nancy%” and “%Pelosi%” as our search criteria and removing unassociated entities (e.g., “Pino Pelosi”, “Nancy Reagan”, etc.), we identified thousands of references to 475 entities. “Nancy Pelosi” as a PERSON instance is the most common entity, with 1,915 scraped articles. “Pelosi,” misidentified as an ORGANIZATION 371 times, is the second most frequent occurrence. “Ms. Pelosi,” “Pelosi” and other variants are less frequent. Figure 8 shows the top ten entities for Nancy Pelosi along with the frequency with which they occur. We can measure the precision of our model with respect to an individual instance as the most frequent occurrence. In this case, Nancy Pelosi (PERSON) represents 53% of all the references to her.

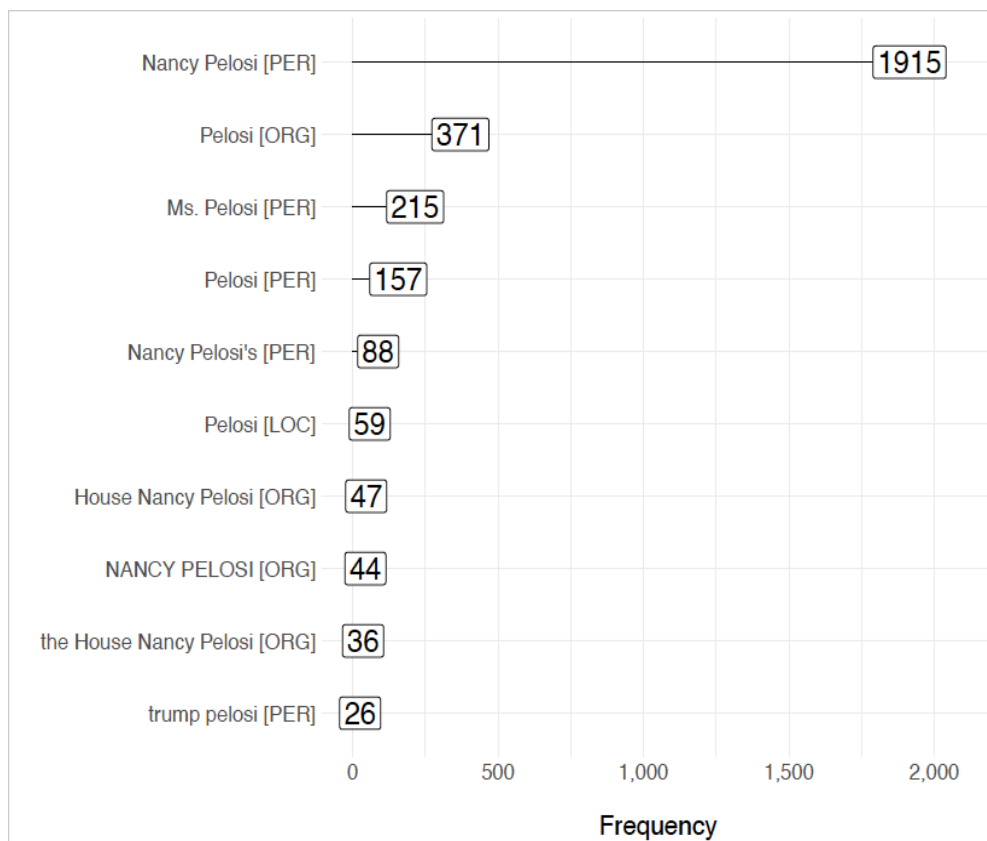


Figure 8: Frequency of Top 10 Entities Associated with “Nancy Pelosi”

Building on the above analysis, we sought to examine how often and what fraction of the time the ten most frequently-mentioned U.S. Congresspeople were correctly resolved by our ER algorithm. Figure 8 depicts the top ten ways in which “Nancy Pelosi” is resolved. “Nancy

Pelosi”, how-ever, is resolved a total of over 400 different ways, demonstrating room for improvement. Figure 9 depicts the number of different ways in which a Congressperson is resolved (x-axis), the cumulative sum of the number of times the name was resolved (y-axis), with a percentage, in square brackets, indicating the fraction of references attributed to the most frequent instance of the entity.

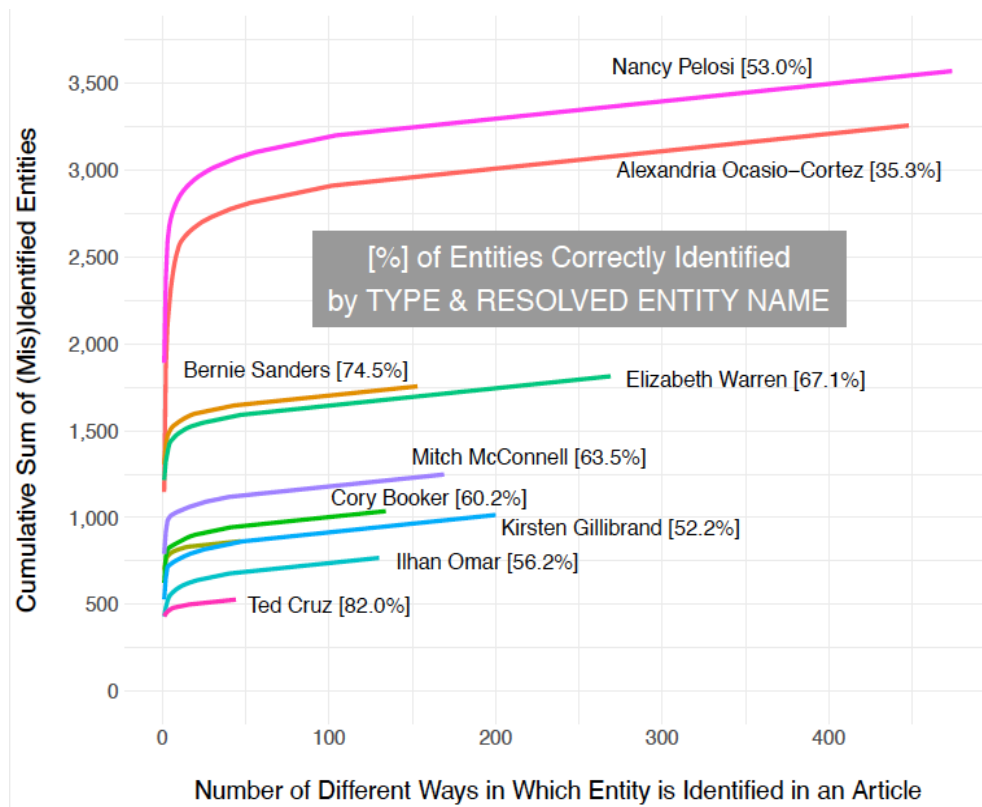


Figure 9: (Mis)Identification of Congresspeople

The many different entities for Congresspeople can be partly attributed to errors in NER models that associate extraneous characters and tokens with names. As discussed above, we also observed Congresspeople being associated with the incorrect labels of LOCATION or ORGANIZATION. Sporadic errors in the spelling of a Congressperson’s name from source articles also contributed to errors in this Entity Resolution step. For example, “Alexander OcasioCortez” [sic] appears as a misspelling of the representative.

5. CASE STUDIES

To demonstrate the power of our resource, we choose two case studies. The first study uses the locations mentioned in an article by different news organisations to expose a location bias. The second study demonstrates how a critical event on a given day can alter the sentiment ascribed to a politician by a news organization, and how our resources provides the high level of resolution necessary to detect said changes.

5.1. Location Bias

In seeking to determine whether news organizations have a geographic reporting bias, we plotted all named LOCATION entities and their frequencies for the Atlantic and Slate news articles between July, 2018 and June, 2019. The geomap, produced using OpenHeatMap, is depicted in Figure 10, and demonstrates that, despite having a larger volume of articles than the Atlantic, articles found in Slate produce fewer mappable locations.

Moreover, locations referenced are concentrated on the North American coast (Eastern and Western United States), the British Islands and Southern France. Counterintuitively, the smaller volume of articles from the Atlantic produce a larger number and wider variety of references to locations.

The location bias for Slate is not wholly unexpected. The first sentence in its description on Wikipedia is, “Slate is an online magazine that covers current affairs, politics, and culture in the United States.” We find a similar pattern for the other news organizations from which we scraped data. For example, the BBC shows a plurality of articles referencing the United Kingdom, Ireland, the USA, with several references to former British colonies (India, Australia, New Zealand, South Africa, etc.). These findings are a confirmation of [4].

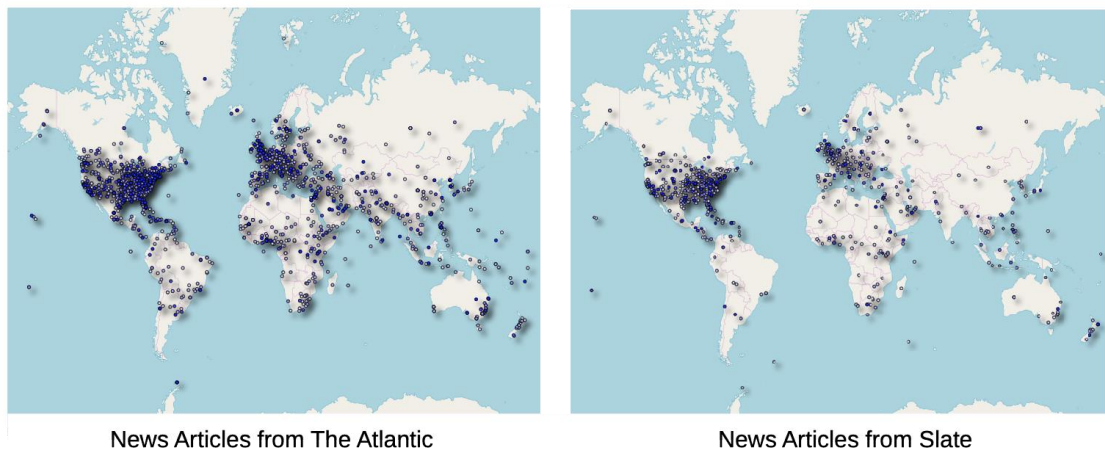


Figure 10: Locations Referenced by The Atlantic and Slate

5.2. Sentiment for José Serrano

Scouring left-leaning news organizations, we observed a peculiar pattern. When reporting on a left-leaning politicians—in America, typically, a Democrat—the sentiment associated with this reporting follows a pattern whereby the sentiment of the overall article is lower than that of the sentiment associated with paragraphs in which the politician in question is referenced, which itself has a lower sentiment than the sentence(s) in which the politician is mentioned. In sum, the more focus there is on the politician herself, the higher the sentiment. This has been shown to be true for several left-leaning politicians when querying the Quantum Criticism corpus. This rule, however, is violated, when a seminal event. For example, when José E. Serrano, Democrat representing the 15th district of New York announced his retirement, the overall sentiment of the article jumped to a value higher than either the paragraph-or sentence-level sentiment (see Figure

11), a change only detectable with the sentence-level of granularity provided by the Quantum Criticism corpus.

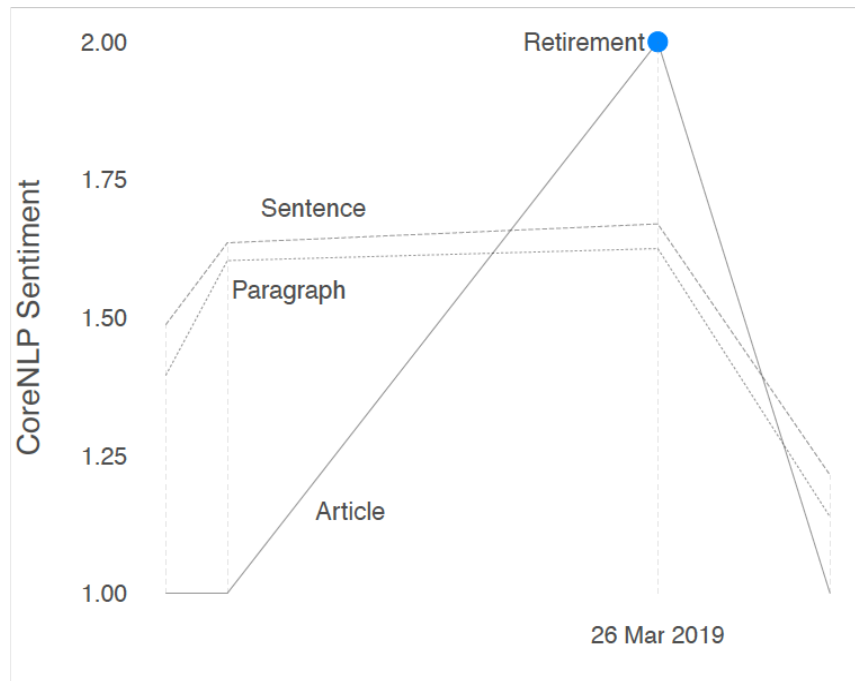


Figure 11: Sentiment for José E. Serrano at the Sentence, Paragraph and Article levels

6. CONCLUSION AND FUTURE WORK

We collected a database of news articles from five popular media organizations, placed each article in a pipeline to identify named entities and determined the affect of each named entity. We identified interesting patterns and confirmed a geographic selection bias found by other researchers. Collecting new news data every two hours, our platform shows great promise for future research, and will further benefit from additional iterations.

We aspire to make this tool even more useful through the addition of news articles from additional news sources. Because news is sometimes underreported by organizations—see Radiolab’s *Breaking Bongo* [27] for one unusual case—we will also consider adding selected tweets and other social media messages from individuals and organizations. We have already collected hundreds of thousands of candidate tweets which we have not yet filtered for relevance or made available. When coupled with better or customized tools for NER, sentiment and entity resolution, we believe this project has the potential to uncover a wide range of phenomena.

The addition of one or more frameworks for coding event data, such as CAMEO, COPDAB or others would also increase the usefulness of the tool. Such frameworks would allow comparison of the same set of events across different media outlets, communities and countries.

The authors acknowledge and thank culture critic Theodore Gioia, who originated the term Quantum Criticism and was a guide and inspiration for this work. Software Engineer Nikhil

Barapatre led the effort to produce the web interface. The authors would also like to thank the Machine learning, Artificial and Gaming Intelligence and, Computing at Scale (MAGICS) Lab at the University of San Francisco for supporting this research with mentorship and computational infrastructure.

REFERENCES

- [1] Roberts, D. (2017). Donald trump and the rise of tribal epistemology. Vox Media.
- [2] White, D. M. (1950). The “gate keeper”: A case study in the selection of news. *Journalism Bulletin*, 27(4):383–390.
- [3] Gruenewald, J., Pizarro, J., and Chermak, S. M. (2009). Race, gender, and the newsworthiness of homicide incidents. *Journal of criminal justice*, 37(3):262–272.
- [4] Wu, H. D. (2000). Systemic determinants of international news coverage: A comparison of 38 countries. *Journal of communication*, 50(2):110–130.
- [5] Huiberts, E. and Joye, S. (2018). Close, but not close enough? audiences’ reactions to domesticated distant suffering in international news coverage. *Media, Culture & Society*, 40(3):333–347.
- [6] Baum, M. A. and Zhukov, Y. M. (2019). Media ownership and news coverage of international conflict. *Political Communication*, 36(1):36–63.
- [7] Bourgeois, D., Rappaz, J., and Aberer, K. (2018). Selection bias in news coverage: learning it, fighting it. In *Companion of the The Web Conference 2018 on The Web Conference 2018*, pages 535–543. International World Wide Web Conferences Steering Committee.
- [8] Sandhaus, E. (2008). The new york times annotated corpus ldc2008t19.
- [9] Graff, D. (1995). North American news text corpus.
- [10] Marcus, M. P., Santorini, B., Marcinkiewicz, M. A., and Taylor, A. (1999). *Trebank-3*. Linguistic Data Consortium, Philadelphia, 14.
- [11] Bell, A., Jurafsky, D., Fosler-Lussier, E., Girand, C., Gregory, M., and Gildea, D. (2001). Form variation of english function words in conversation. Submitted manuscript.
- [12] Kann, K., Mohananey, A., Bowman, S., and Cho, K. (2019). Neural unsupervised parsing beyond english. In *Proceedings of the 2nd Workshop on Deep Learning Approaches for Low-Resource NLP (DeepLo 2019)*, pages 209–218.
- [13] Leetaru, K. and Schrod, P. A. (2013). Gdelt: Global data on events, location, and tone, 1979–2012. In *ISA annual convention*, volume 2, pages 1–49. Citeseer.
- [14] Ward, M. D., Beger, A., Cutler, J., Dickenson, M., Dorff, C., and Radford, B. (2013). Comparing gdelt and icews event data. *Analysis*, 21(1):267–97.
- [15] Davies, M. (2010). The corpus of contemporary american english as the first reliable monitor corpus of english. *Literary and linguistic computing*, 25(4):447–464.
- [16] Devlin, J., Chang, M.-W., Lee, K., and Toutanova, K. (2018). Bert: Pre-training of deep bidirectional transformers for language understanding. arXiv preprint arXiv:1810.04805.

- [17] Manning, C., Surdeanu, M., Bauer, J., Finkel, J., Bethard, S., and McClosky, D. (2014). The Stanford corenlp natural language processing toolkit. In Proceedings of 52nd annual meeting of the association for computational linguistics: system demonstrations, pages 55–60.
- [18] Honnibal, M. and Montani, I. (2017). spaCy 2: Natural language understanding with Bloom embeddings, convolutional neural networks and incremental parsing. To appear.
- [19] Rafail, P. and McCarthy, J. D. (2018). Making the tea party republican: Media bias and framing in newspapers and cable news. *Social Currents*, 5(5):421–437.
- [20] Iyengar, S. and Simon, A. (1993). News coverage of the gulf crisis and public opinion: A study of agendasetting, priming, and framing. *Communication research*, 20(3):365–383.
- [21] Soroka, S., Daku, M., Hiaeshutter-Rice, D., Guggenheim, L., and Pasek, J. (2018). Negativity and positivity biases in economic news coverage: Traditional versus social media. *Communication Research*, 45(7):1078–1098.
- [22] An, S.-K. and Gower, K. K. (2009). How do the news media frame crises? a content analysis of crisis news coverage. *Public Relations Review*, 35(2):107–112.
- [23] Trumbo, C. (1996). Constructing climate change: claims and frames in us news coverage of an environmental issue. *Public understanding of science*, 5:269–283.
- [24] Ribeiro, F. N., Henrique, L., Benevenuto, F., Chakraborty, A., Kulshrestha, J., Babaei, M., and Gummadi, K. P. (2018). Media bias monitor: Quantifying biases of social media news outlets at large-scale. In Twelfth Inter-national AAAI Conference on Web and Social Media.
- [25] Hutto, C. J. and Gilbert, E. (2014). Vader: A parsimonious rule-based model for sentiment analysis of social media text. In Eighth international AAAI conference on weblogs and social media.
- [26] Loper, E. and Bird, S. (2002). Nltk: The natural language toolkit. In Proceedings of the ACL-02 Workshop on Effective Tools and Methodologies for Teaching Natural Language Processing and Computational Linguistics - Volume 1, ETMTNLP '02, pages 63–70, Stroudsburg, PA, USA. Association for Computational Linguistics.
- [27] Adler, S. “Breaking Bongo,” Radiolab, 26 November, 2019. New York City: WNYC Studios. Available <https://www.wnycstudios.org/podcasts/radiolab/articles/breaking-bongo>. Accessed: 28 February, 2020.

VSMbM: A NEW METRIC FOR AUTOMATICALLY GENERATED TEXT SUMMARIES EVALUATION

Alaidine Ben Ayed^{1,3}, Ismaïl Biskri^{2,3} and Jean-Guy Meunier³

¹Department of Computer Science, Université du Québec à
Montréal (UQAM), Canada

²Department of Mathematics and Computer Science, Université du Québec à
Trois-Rivières (UQTR), Canada

³LANCI : Laboratoire d'ANalyse Cognitive de l'Information, Université du
Québec à Montréal (UQAM), Canada

ABSTRACT

In this paper, we present VSMbM; a new metric for automatically generated text summaries evaluation. VSMbM is based on vector space modelling. It gives insights on to which extent retention and fidelity are met in the generated summaries. Two variants of the proposed metric, namely PCA-VSMbM and ISOMAP VSMbM, are tested and compared to Recall-Oriented Understudy for Gisting Evaluation (ROUGE): a standard metric used to evaluate automatically generated summaries. Conducted experiments on the Timeline17 dataset show that VSMbM scores are highly correlated to the state-of-the-art Rouge scores.

KEYWORDS

Automatic Text Summarization, Automatic summary evaluation, Vector space modelling.

1. INTRODUCTION

1.1. Automatic Text Summarization

Automatic text summarization (ATS) is the process of creating a short, accurate, and fluent summary from a longer source text [1]. It has been a field of study for decades. [2] provides six reasons why we need ATS. Indeed; 1) Summaries reduce reading time, 2) they make the selection process easier when researching documents, 3) ATS improves the effectiveness of indexing, 4) ATS algorithms are less biased than human summarizers, 5) Personalized summaries are useful in question answering systems as they provide personalized information and 6) Using automatic or semi-automatic summarization systems enables commercial abstract services to increase the number of texts they are able to process. Note that automatically generated summaries should satisfy three criteria:

- Retention: It is a measure of how much the generated summary reports salient topics present in the original text.
- Fidelity: Does the summary accurately reflect the author's point of view?

- Coherence: To which extent, the generated extract is semantically meaningful?

There are mainly two subtasks of ATS [2]: 1) single text summarization: it uses only one source text to build the summary, 2) multi text summarization: it uses a bunch of source texts to create the final output. In both cases, evaluating the generated summaries is still a challenging research area.

In the next two section, we make a short state of the art of most relevant proposed protocols for automatically generated text summarization. Then, we present key features which make the originality of our work.

1.2. Related Work

Evaluating automatically generated summaries is not an effortless task. In the last two decades, significant advances have been made in this research field. Therefore, various evaluation measures have been proposed. SUMMAC [3], DUC (Document Understanding Conference) [4] and TAC (Text Analysis Conference) [5] are the main evaluation campaigns led since 1996. Note that the evaluation process can be led either in reference to some ideal models or without reference [6]. ROUGE (Recall-Oriented Understudy for Gisting Evaluation) is the most used metric for automatically generated abstracts evaluation. Summaries are compared to a reference or a set of references (human-produced summaries) [7]. Note that there are five variants of the ROUGE metric: 1) ROUGE-N [8]: it captures the overlap of N-grams between the system and reference summaries, 2) ROUGE-L [9]: it gives statistics about the Longest Common Subsequence (LCS), 3) ROUGE-W: a set of weighted LCS-based statistics that favors consecutive LCSes, 4) ROUGE-S [10]: a set of Skip-bigram (any pair of words in their sentence order) based co-occurrence statistics. COVERAGE is another metric which has been used in DUC evaluations. It gives an idea on to which extent peer summary conveys the same information as a model summary [11]. RESPONSIVENESS has also been used in focused-based summarization tasks of DUC and TAC evaluation campaigns [11]. It ranks summaries in a 5-point scale indicating how well the summary satisfied a set of needed information criteria. The pyramid evaluation approach uses Summarization Content Units (SCUs) to calculate a bunch of weighted scores [12]. A summary containing units with higher weights will be affected a high pyramid score. A SCU has a higher weight if it appears frequently in human-generated summaries. Fresa is another metric [13]. It is the state-of-the-art technique for evaluating automatically generated summaries without using a set of human-produced reference summaries. It computes a variety of divergences among probability distributions. Recently, [14] proposed a new implementation of the ROUGE protocol without human-built model summaries. The new summary evaluation model (ASHuR) extracts most informative sentences of the original text based on a bunch of criteria: the frequency of concepts, the presence of cue-words, sentence length, etc. Then, the extracted set of sentences will be considered as the model summary. [15] gives an overview of challenging issues related to summary evaluation

1.3. Originality of our work

Most of the above described metrics only focus on the overlap of N-grams between the original text and the generated summary. In other words, they reflect the coverage ratio meanwhile they don't give insights on to which extent fidelity is met, i.e. if a long source text contains six concepts and a first summary focuses on the four last most important ones, it will be assigned a higher score than another summary focusing on the most important two concepts present in the original text. In this case retention is met. However, it is not the case for the fidelity criterion

In this paper we present a new vector space modelling-based metric for automatic text summaries evaluation. The proposed metric gives insights on to which extent both retention and fidelity are met. We assume that fidelity is met if we assign higher weights to text units related to most important concepts reported in the original text. The next section describes technical and mathematical details of the proposed metric. The third one describes conducted experiments and obtained results. Conclusion and future work are exposed in the fourth section.

2. VECTOR SPACE MODELLING BASED METRIC (VSMbM) FOR AUTOMATICALLY GENERATED TEXT SUMMARIES EVALUATION

From a computational point of view, the main idea is to project the original text onto a lower dimensional space that captures the essence of concepts present in it. Unitary vectors of the latter space are used to compute the two proposed *VSMbM* metrics. Mathematical and implementation details of *PCA-VSMbM* and *ISOMAP-VSMbM* will be expanded in the coming two subsections.

2.1. The *PCA-VSMbM*

First, source text is segmented onto m sentences. Then a dictionary of all nouns is constructed and filtered in order to remove all generic nouns. Text is then represented by an $m \times z$ matrix, where m is the number of segments and z is the number of unique tokens. Next the conceptual space is being constructed. It will be used later to compute the *PCA-VSMbM* metric.

2.1.1. Construction of the conceptual space

Each sentence S_i is represented by a column vector ζ_i . ζ_i is a vector of Z components. Each component represents the *tf-idf* of a given word. Afterwards, mean concept vector τ is computed as follows:

$$\tau = \frac{1}{m} \sum_{i=1}^m \zeta_i \quad (1)$$

Note that each ζ_i should be normalized to get rid of redundant information. This is performed by subtracting the mean concept:

$$\Theta_i = \zeta_i - \tau \quad (2)$$

In the next step, the covariance matrix is computed as follows:

$$C = \frac{1}{m} \sum_{n=1}^m \Theta_n \Theta_n^T = AA^T \quad (3)$$

Where $A = [\Theta_1, \dots, \Theta_m]$. Note that C in (3) is a $z \times z$ matrix and A is a $z \times m$ matrix. Eigen concepts are the eigenvectors of the covariance matrix C . They are obtained by performing a singular value decomposition of A :

$$A = U.S.V^T \quad (4)$$

Where dimensions of matrix U , S and V are respectively $z \times z$, $z \times m$ and $m \times m$. Also, U and V are orthogonal ($UU^T = U^T U = Id_z$ and $VV^T = V^T V = Id_m$). In addition to that;

- Columns of V are eigenvectors of $A^T A$.
- Columns of U are eigenvectors AA^T .
- Squares of singular values s_k of S are eigenvalues λ_k of AA^T and $A^T A$.

Note that $m < z$. So, eigenvalues λ_k of AA^T are equal to zero when $k > m$ and their associated eigenvectors are not necessary. So, matrix U and S can be truncated, and, dimensions of U , S and V in (4) become respectively $z \times m$, $m \times m$ and $m \times m$. Next, conceptual space is being constructed by K eigenvectors associated to the highest K eigenvalues:

$$\Xi_k = [U_1, U_2, \dots, U_k] \quad (5)$$

Each projected sentence onto the conceptual space is represented as a linear combination of K eigenconcepts:

$$\Theta_i^{proj} = \sum_k C_{\Theta_i}(k) U_k \quad (6)$$

Where $C_{\Theta_i}(k) = U_k^T \Theta_i$ is a vector providing coordinates of the projected sentence in the conceptual space.

2.1.2. Computation of the PCA-VSMbM score

The goal here is to find out to which extent selected sentences to be part of the generated summary are expressing the main concepts of the original text. Thus, each vector ζ_i representing a given sentence S_i is normalized by subtracting the mean concept τ : $\Theta_q = \zeta_i - \tau$. Then it is projected onto the newly constructed conceptual space:

$$\Theta_q^{proj} = \sum_k C_{\Theta_q}(k) U_k \quad (7)$$

Next, the Euclidean distance between a given concept q and any projected sentence is defined and computed as follows:

$$d_i(\Theta_q^{proj}) = \|\Theta_q^{proj} - \Theta_i^{proj}\| \quad (8)$$

Next, Retention-Fidelity matrix is constructed as follows: First, we fix a window size W . In the bellow example, W is set to 4. The first line gives the index of the four sentences having the smallest distances to the vector encoding the first most important concept. The second line gives the same information related to the second most important concept. Also, the order of a given sentence in each window W depends on its distance to a given concept. For instance, the first sentence is the best one to encode the first most important concept while the 8th sentence is the last one to encode the same concept in a window of four sentences.

$$\begin{array}{c}
 \text{Distance (concept)} \\
 \xrightarrow{\hspace{1.5cm}} \\
 \begin{array}{c}
 1 \\
 2 \\
 3 \\
 4 \\
 5
 \end{array}
 \left(
 \begin{array}{cccc}
 1 & 6 & 9 & 8 \\
 1 & 22 & 13 & 11 \\
 10 & 22 & 6 & 1 \\
 22 & 2 & 1 & 11 \\
 9 & 11 & 2 & 8
 \end{array}
 \right)
 \end{array}
 \begin{array}{l}
 \\
 \\
 \\
 \text{Concept importance} \\
 \downarrow
 \end{array}$$

Next, the *Retention* score of each sentence being projected in the conceptual space is defined as follows: it's equal to the number of times it occurs in a window of size W when taking in consideration the most important K concepts. The main intuition behind it, is that a given sentence having a height *Retention* score should encode as much as possible the K most important concepts expressed in the original text.

$$R_{kw}(s) = \frac{1}{k} \sum_{i=1}^k \alpha_i \quad (9)$$

$\alpha_i = 1$ if the sentence S occurs in the i^{th} window. If not, it is equal to zero.

Now, the *PCA-VSMbM* score is defined as shown in the tenth equation as the averaged sum of the retention coefficients of summary sentences. Note that every retention coefficient is weighted according to the sentence's position in a given window of size W . The main intuition behind it is that, single units (sentences) of a given summary whose *PCA-VSMbM* score is high should encode the most important concepts expressed in the original text. So, they should have minimal distances $d_i(\Theta_q^{proj}) = \|\Theta_q^{proj} - \Theta_i^{proj}\|$ in equation 8. In other words, the *PCA-VSMbM* score gives insights on to which extent extracted sentences encode concepts present in the original text while taking in consideration the importance degree of each concept

$$PCA_{VSMbM}_{kw}(s) = \frac{1}{p} \frac{1}{k} \sum_{j=1}^p \sum_{i=1}^k \alpha_i \left[1 + \frac{1 - \psi_i}{w} \right] \quad (10)$$

p is the number of extracted sentences to construct the summary, $\alpha_i = 1$ if a sentence s occurs in the i^{th} window. If not, it is equal to zero. ψ_i is the rank of s in the i^{th} window.

2.2. The ISOMAP-VSMbM

In the *ISOMAP-VSMbM*, we rather use the geodesic distance. The *ISOMAP-VSMbM* approach consists in constructing a k -nearest neighbor graph on n data points each one representing a sentence in the original space. Then, we compute the shortest path between all points as an estimation of geodesic distance D^G . Finally, we compute the decomposition K in order to construct Ξ_k previously defined in equation 5 where:

$$K = \frac{1}{2} H D^G H \quad (11)$$

H is centering matrix; $H = Id - \frac{1}{n} e e^T$ and $e = [1, 1, \dots, 1]^T$. T is an $n \times 1$ matrix. Note that the decomposition of K is not always possible in the sense that there is no guarantee that K is a

positive semidefinite matrix. We deal with this case by finding out the closest positive semidefinite matrix to K . Then we decompose it. Next we proceed the same way we proceeded previously with $PCA-VSMbM$. $ISOMAP-VSMbM$ is defined as $PCA-VSMbM$ in equation 10.

3. EXPERIMENTS AND RESULTS

3.1. Dataset

The *Timeline17* dataset is used for experiments [16]. It consists of 17 manually created timelines and their associated news articles. They mainly belong to 9 broad topics: BP Oil Spill, Michael Jackson Death (Dr. Murray Trial), Haiti Earthquake, H1N1 (Influenza), Financial Crisis, Syrian Crisis, Libyan War, Iraq War, Egyptian Protest. Original articles belong to news agencies, such as BBC, Guardian, CNN, Fox news, NBC News, etc. The contents of these news are in plain text file format and noise filtered.

3.2. Results and discussion

In order to evaluate the proposed metric, we compute the Pearson's correlation between $VSMbM$ and $ROUGE$ (Recall-Oriented Understudy for Gisting Evaluation) scores. Note that Pearson's correlation coefficient measures the statistical correlation, between two signals. Thus, we assume that all the computed scores with a given evaluation approach constitute a signal. Then, we compare obtained averaged *Rouge-1* and $PCA/ISOMAP-VSMbM$ scores when using both human-made and automatically generated summaries [17] [18]. Results of the described above experiments are reported in Table 1 and Table 2.

Table 1: Pearson's correlation between $VSMbM$ and $ROUGE$ scores.

	ROUGE-1	ROUGE-2	ROUGE-S
PCA-VSMbM	0.79	0.88	0.89
ISOMAP-VSMbM	0.81	0.89	0.91

Table 2: Average $ROUGE-1$, $ISOMAP-VSMbM$ and $PCA-VSMbM$ scores when using handmade summaries and automatically made ones by MEAD and ETS summarizers.

	MEAD	ETS	Human ms
ROUGE-1	0.207	0.206	0.211
ISOMAP-VSMbM	0.204	0.205	0.205
PCA-VSMbM	0.189	0.201	0.203

Obtained results in Table 1 show that the $VSMbM$ scores are highly positively correlated to the $ROUGE$ scores. Indeed, the proposed metric can give a high score when the $ROUGE$ protocol for summary evaluation does. It gives a low score in the inverse case. Also, the $ISOMAP-VSMbM$ outperforms $PCA-VSMbM$. Indeed, when using the $PCA-VSMbM$, we assume that we are dealing with a linear dimensional reduction problem (which is not totally true regarding the high dimensionality) and we use Euclidian distance. Meanwhile, with the $ISOMAP-VSMbM$, we use the geodesic distance since we assume that we are dealing with a nonlinear dimensionality reduction problem. Results of Table 2 lead to the same conclusions when using both human-made and automatically generated summaries. Note that, the $VSMbM$ protocol do not only check

whether the generated summary reports salient topics present in the original text or not. It also gives insights on to which extent fidelity is met by focusing on the most important ones.

4. CONCLUSION AND FUTURE WORK

In this paper, we presented a new metric for automatically generated text summaries evaluation. The proposed metric is based on vector space modelling. It gives insights on to which extent retention and fidelity are met. Conducted experiments on the Timeline17 dataset show that scores of the proposed metric are highly positively correlated to those produced by *ROUGE*: the standard metric for *ATS* evaluation. To deal with the decomposition problem of K in equation 11, we are currently implementing a Locally Linear Embedding version of our *VSMbM* metric (*LLE-VSMbM*). Next, we will test our metric with bigger size and multilingual corpora, and we will compare its performance to more *ATS* evaluation metrics.

ACKNOWLEDGEMENTS

The authors would like to thank Natural Sciences and Engineering Research Council (NSERC) of Canada for financing this work.

REFERENCES

- [1] Gambhir, Mahak; Gupta, Vishal. Recent automatic text summarization techniques: a survey, *TheArtificial Intelligence Review*; Dordrecht Vol. 47, N 1: 166. DOI:10.1007/s10462-016-9475-9, 2017
- [2] Torres-Moreno, Juan-Manuel, *Automatic Text Summarization*, London, Wiley 2014
- [3] I. Mani, G. Klein, D. House, L. Hirschman, T. Firmin, and B. Sundheim, "Summac: a text summarization evaluation," *Natural Language Engineering*, vol. 8, no. 1, pp. 43–68, 20028
- [4] P. Over, H. Dang, and D. Harman, "DUC in context," *IPM*, vol. 43, no. 6, pp. 1506–1520, 2007.
- [5] *Proceedings of the Text Analysis Conference*. Gaithersburg, Maryland, USA: NIST, November 17-19, 2008.
- [6] K. Sparck Jones and J. Galliers, *Evaluating Natural Language Processing Systems, An Analysis and Review*, ser. *Lecture Notes in Computer Science*. Springer, 1996, vol. 1083.
- [7] Lin, Chin-Yew. 2004. *ROUGE: A Package for Automatic Evaluation of Summaries*. In *Proceedings of the Workshop on Text Summarization Branches Out (WAS 2004)*, Barcelona, Spain, July 25 - 26, 2004.
- [8] Lin, Chin-Yew and E.H. *Automatic Evaluation of Summaries Using N-gram Cooccurrence Statistics*. In *Proceedings of Language Technology Conference (HLT-NAACL)*, Edmonton, Canada, 2003.
- [9] Lin, Chin-Yew and Franz Josef Ochs. 2004a. *Automatic Evaluation of Machine Translation Quality Using Longest Common Subsequence and Skip Bigram Statistics*. In *Proceedings of the 42nd Annual Meeting of the Association for Computational Linguistics (ACL 2004)*, Barcelona, Spain, July 21 - 26, 2004.
- [10] Lin, Chin-Yew and Franz Josef Ochs. 2004a. *Automatic Evaluation of Machine Translation Quality Using Longest Common Subsequence and Skip-Bigram Statistics*. In *Proceedings of the 42nd Annual Meeting of the Association for Computational Linguistics (ACL 2004)*, Barcelona, Spain, July 21 - 26, 2004.
- [11] P. Over, H. Dang, and D. Harman, "DUC in context," *IPM*, vol. 43, no. 6, pp. 1506–1520, 2007.
- [12] A. Nenkova and R. J. Passonneau, "Evaluating Content Selection in Summarization: The Pyramid Method," in *HLT-NAACL*, 2004, pp. 145–152.
- [13] Juan Manuel Torres Moreno, Horacio Saggion, Iria da Cunha, Eric SanJuan, and Patricia Velázquez-Morales, *Summary Evaluation with and without References*, *Polibits* (42), 2010
- [14] Alan Ramirez-Noriega, Reyes Juarez-Ramirez Samantha Jimenez, Sergio Inzunza, Ashur: *Evaluation of the relation summary-content without human reference using rouge*, *Computing and Informatics*, Vol. 37, 509–532, doi: 10.4149/cai 2018 2 509, 2018

- [15] Elena Lloret, Laura Plaza, and Ahmet Aker. 2018. The challenging task of summary evaluation: an overview. *Lang. Resour. Eval.* 52, 1, 101-148. DOI: <https://doi.org/10.1007/s10579-017-9399-2>, March 2018
- [16] Tran G. B., Tran T.A., Tran N.K., Alrifai M. and Kanhabua N.: Leverage Learning to rank in an optimization framework for timeline summarization. In TAIA workshop, SIGIR 13, 2013
- [17] D. R. Radev, T. Allison, S. Blair-Goldensohn, J. Blitzer, A. ĀGelebi, S. Dimitrov, E. DrĀabek, A. Hakim, W. Lam, D. Liu, J. Otterbacher, H. Qi, H. Saggion, S. Teufel, M. Topper, A. Winkel, and Z. Zhang. Mead - a platform for multidocument multilingual text summarization. In Proceedings of LREC'04, 2004
- [18] R. Yan, X. Wan, J. Otterbacher, L. Kong, X. Li, and Y. Zhang. Evolutionary timeline summarization: a balanced optimization framework via iterative substitution. In Proceedings of SIGIR'11, pages 745–754, 2011.

AUTHORS

Alaidine Ben Ayed is a PhD. candidate in cognitive computer science at Université du Québec à Montréal (UQAM), Canada. His research focuses on artificial intelligence, natural language processing (Text summarization and conceptual analysis) and information retrieval.



Ismail Biskri is a professor in the Department of Mathematics and Computer Science at the Université du Québec à Trois-Rivières (UQTR), Canada. His research focuses mainly on artificial intelligence, computational linguistics, combinatory logic, natural language processing and information retrieval



Jean Guy Meunier PhD. is a research professor at UQAM, co-director of the Cognitive Information Analysis Laboratory (LANCI), member of the Institute of Cognitive Sciences at UQAM and member of the Centre for Research in Digital Humanities (CRHN), full member of the International Academy of Philosophy of Science (Brussels).



FREE-TEXT AND STRUCTURED CLINICAL TIME SERIES FOR PATIENT OUTCOME PREDICTIONS

Emilia Apostolova PhD¹, Joe Morales², Ioannis Koutroulis, MD PhD³ and
Tom Velez, PhD, JD²

¹Language.ai, Chicago, IL, USA

²Computer Technology Associates, Ridgecrest, CA, USA

³Children's National Health System, Washington, DC, USA

ABSTRACT

While there has been considerable progress in building deep learning models based on clinical time series data, overall machine learning (ML) performance remains modest. Typical ML applications struggle to combine various heterogenous sources of Electronic Medical Record (EMR) data, often recorded as a combination of free-text clinical notes and structured EMR data. The goal of this work is to develop an approach for combining such heterogenous EMR sources for time-series based patient outcome predictions. We developed a deep learning framework capable of representing free-text clinical notes in a low dimensional vector space, semantically representing the overall patient medical condition. The free-text based time-series vectors were combined with time-series of vital signs and lab results and used to predict patients at risk of developing a complex and deadly condition: acute respiratory distress syndrome. Results utilizing early data show significant performance improvement and validate the utility of the approach.

KEYWORDS

Natural Language Processing; Clinical NLP; Time-series data; Machine Learning; Deep Learning; Free-text and structured data; Clinical Decision Support; ARDS; COVID-19

1. INTRODUCTION

Deep Learning utilizing Electronic Medical Record (EMR) data for medical diagnosis/outcome predictions is an active and promising field of research. The interest in the topic has been spurred by the combination of a number of contributing factors. On one hand, there is the availability and sheer abundance of EMR data: in the US alone, the Centers for Disease Control and Prevention report more than 800 million physician office visits annually, most associated with digital EMR data [1]. This, combined with the practical significance of medical AI, advances in deep learning, and the availability of powerful and inexpensive computing resources, has led to an abundance of clinical prediction models derived to predict various medical outcomes with limited clinical success [2,3].

More recently, the utility of time-series EMR data has been explored for improved deep learning predictions, as traditional ML on the entire time series is often infeasible as each data point would be handled as a separate feature introducing dimensionality problems. Patient visit EMR data, such as vital signs, lab results, clinical notes, etc., is typically time-stamped, and, intuitively,

human experts often base their judgments on the temporal relations of various variables. For example, a time series showing non-improving respiratory rate values, despite medical interventions, may serve as a sign of clinical deterioration, as well as other outcomes (e.g. mortality risk). Recently, time-series-based ML effort attempts to learn such temporal clinical knowledge and multi-task inference using a clinical time series benchmark dataset [4,5], derived from the publicly available Medical Information Mart for Intensive Care (MIMIC-III) database [6]. The dataset contains time series data for 17 selected clinical variables containing more than 31 million clinical events. The benchmark tasks consist of in-hospital mortality prediction, decompensation prediction, length-of-stay prediction, and phenotype classification. Harutyunyun et al. [4] also built several baseline ML models on the benchmark, including several LSTM-based models.

The clinical time series benchmark was also used on the task of medical diagnosis code prediction. Inspired by the success of embeddings combined with recurrent networks in NLP, Lipton et al. [7] built an LSTM-based diagnosis prediction model utilizing 13 time series variables used to predict 128 common diagnosis codes. More recently, [8] developed an attention model outperforming the LSTM models on a number of the MIMIC time series benchmark tasks. The performance of the proposed time-series-based ML models, however, is quite limited. For example, the best achieved F1-scores on the multi-label diagnosis task described by Harutyunyun et al. [4] are 0.29 and 0.15, micro and macro F1-scores respectively. Human expert diagnosis coding significantly outperforms the proposed models simply because clinicians have access to additional patient data (outside the time series of 13 vital signs and lab results variables), that provides rich patient medical context. In particular, clinicians have access to the clinical free-text notes, that include information such as the patient medical history, family history, the reason for the visit, signs, symptoms, findings, social history, etc.

2. TASK DEFINITION

The goal of this study is to better approximate the clinical information used by human experts, by combining time series structured data (lab results and vital signs), with time series free text data (clinical notes). In particular, we focus on the early identification (within 24 hours of admission) of patients at risk of developing ARDS (Acute Respiratory Distress Syndrome). The condition is characterized by the development of acute dyspnea at rest, hypoxemia, and alveolar infiltrates on chest imaging within hours to days of an inciting event such as viral pneumonia. ARDS is a significant cause of morbidity and mortality in the USA and worldwide [9,10] and is the principal cause of COVID-19 associated mortality.

In a reported Wuhan case series, among the 201 patients with confirmed COVID-10, 41.8% developed ARDS and among these patients 52.4% died. It has been reported that in general ARDS caused by COVID-19 results in 2.3% mortality rate of diagnosed cases [11]. Early recognition can limit the propagation of lung injury and significantly improve patient outcomes [12]. Similar to other acute conditions, predicting ARDS is a difficult task even for human experts, as the condition is often confounded by cardiogenic factors, and, at the same time, is highly heterogeneous [13] and COVID-induced ARDS is atypical. ARDS involves the interaction of multiple risk factors, past history, and current conditions, signs, and symptoms, and thus structured time series data, without access to the free-text patient context will be insufficient in judging ARDS outcomes.

3. RELATED WORK

The literature related to this study falls into two categories: combining free-text and structured EMR data for clinical outcome predictions, and machine learning with clinical time series data.

A large volume of literature on combining structured and free-text EMR data pre-processes the free-text data by applying some information extraction (IE) technique, typically medical concept detection [14,15,16]. The majority of approaches extract UMLS or SNOMED-CT concepts from free-text with their negation status with various off-the-shelf tools [15, 17, 18, 19, 20].

More recently, Miotto et al. [21] built Deep Patient representations utilizing structured EMR variables and notes converted to a set of concepts using traditional methods. Shickel et al. [3] present a survey of various deep learning techniques, the majority of which focus on structured EMR data. In addition, a number of deep learning studies explore pre-training on diagnosis and procedure code embeddings [22,23,24].

In terms of utilizing time series data, deep learning techniques have been explored extensively, typically focusing only on structured EMR data. In addition to the studies focusing on LSTM and transformer architectures for clinical time series described in Section Introduction [4,7,8], a number of studies explore clinical time series for patient outcome prediction. For example, Choi et al. [25] develop a temporal model using recurrent neural networks (RNN) and time-stamped structured EMR data. Similarly, Lipton et al. [26] explore the modeling of missing time series data with RNNs. Choi, et al. [27] developed a reverse time attention model, so that recent clinical visits are likely to receive higher attention. Razavian et al. [28] built multi-task disease onsets prediction utilizing LSTM and CNN on common lab test results. Nguyen et al. [29] built a CNN model using coded EMR data, combined with coded time separators, such as [1-3 months], [6-12 months], etc. Xu et al. [30] developed a recurrent multi-channel attention model combining various clinical sources of time-series records including waveform and numeric data.

The main contribution of this work is the low-dimensional vector space representation of free-text, that can be combined with structured EMR data in the context of time-series based clinical outcome prediction.

4. METHOD

4.1. Dataset

Clinical encounter data of adult patients was extracted from the MIMIC3 Intensive Care Unit (ICU) database [6]. MIMIC3 consists of retrospective ICU encounter data of patients admitted into Beth Israel Deaconess Medical Center from 2001 to 2012. MIMIC3 includes time series data recorded in the EMR during encounters (e.g. vital signs/diagnostic laboratory results, free text clinical notes, medications, procedures, etc.). The dataset contains data associated with over 58,000 ICU visits, including over 2 million free-text clinical notes.

For this study, in accordance with previous literature [31], we identified ARDS for adult patients older than 18 years with ICD-9 codes for severe acute respiratory failure and use of continuous invasive mechanical ventilation, excluding those with codes for acute asthma, COPD and CHF exacerbations. This resulted in 4,624 ARDS cases from a total of 48,399 adult ICU admissions. The ICU mortality rate in this population was approximately 59%.

4.2. Structured Data Time Series

Time series data was collected over the first 24 hours of ICU admission. The first 24-hour timeframe was chosen, as it has been reported that ARDS develops at a median of 30 hours after hospital admission [32]. Thus, a 24-hour window provides for the gathering of enough data,

while at the same time is early enough for real-time clinical decision support (CDS). Time series were created in 4-hour windows (averaging values if more than one present).

Utilizing clinical knowledge and ML experiments on the dataset, we identified the most informative vital and lab result variables in the context of ARDS outcome predictions. They include 'Bicarbonate', 'Systolic blood pressure (noninvasive)', 'Tidal Volume (set)', 'Partial pressure of carbon dioxide (arterial)', 'Monocytes', 'Partial pressure of oxygen', 'Lactate dehydrogenase', 'Urine output', 'Calcium (total)', 'Mean corpuscular hemoglobin concentration', 'Lymphocytes', 'Respiratory rate', 'Glasgow coma scale verbal response', 'Minute Volume', 'Phosphate', 'Respiratory rate (total)', 'Heart Rate', 'Mean Airway Pressure', 'PEEP set', 'Diastolic blood pressure (noninvasive)', as well as 'age' and 'bmi'.

4.3. Free-text Data Time Series

In addition to structured data, we also included time-series of time-stamped clinical notes. In particular, we focused on nursing notes, as they are available early (within 24 hours), unlike, for example, discharge notes available at the end of the patient stay. Nursing notes also contain a comprehensive summary of the patient history and present condition. Similarly to the structured data time series, free-text time series were created in 4-hour windows. Ideally, we would like the free-text notes to be converted to a low dimensional vector space, semantically representing the overall patient medical condition, including medical history and present illness and symptoms.

It has been noted that clinicians viewing properly coded patient diagnosis codes (ICD9 and ICD10 codes) are typically capable of deducing the overall condition, history, and risk factors associated with a patient [33]. Diagnosis codes are used to describe information, such as current diagnoses, signs and symptoms, history and chronic conditions, past and current treatments / procedures, age group and/or susceptibilities, expected outcome, patient social history, the reason for the visit, etc. Intuitively, the totality of patient's diagnosis codes represent a meaningful medical summary of the patient. However, real-time CDS systems, such as predicting ARDS outcome within 24 hours of admission, won't have access to the full set of the patient's ICD codes, which are typically entered at a later time.

At the same time, it has been suggested that the medical code co-occurrence of diagnosis can be exploited to generate low-dimensional representations of ICD codes [22-24] that may facilitate EMR data-based exploratory analysis and predictive modeling [33-35]. Building upon this work, we built a deep learning model trained to predict the patient's ICD code embeddings from nursing notes and thus create a low dimensional vector space semantically representing the overall patient medical condition: *Patient Context Vectors* (PCV).

The full set of MIMIC3 nursing notes (1,081,176 free-text notes) were used as a pre-training step in a model trained to predict the patient's averaged ICD-code embeddings: PCVs. The optimum size of the ICD-code embedding vectors was determined to be 50. Experiments with two deep learning networks were performed. In both cases, the architectures utilized were similar to typical deep learning text classification networks, with the difference that the target prediction is not probabilities on a set of categories (soft-max loss function), but an ICD-code embedding vector (multi target regression with mean squared error loss function). In both cases, the input texts were truncated/padded to a length 400 tokens, the last linear layer of size 50 used loss function of mean squared error, the Adam optimizer was used with batch size of 32, trained on 3 epochs. A word-level CNN model [36], consisting of a convolutional, max Pooling layers, followed by 2 hidden layers of size 500 achieved a mean squared error of 0.18 on the test set. A fine-tuned Bert base model [37] achieved a mean squared error of 0.13 on the test set. Both models were used to

convert test notes into to a low dimensional vector space (PCVs of size 50), semantically representing the overall patient medical condition.

4.4. Time-series ARDS Predictions

Time series data was collected from 6 four-hour windows following ICU admission. Each time series step contains values from 20 structured variables and nursing notes represented as PCVs of size 50, i.e. each time series step contains a total of 70 variables, with a total of 6 time series per visit. The representation is analogous to text classification representations, with word embeddings of size 70 and text length of size 6. All structured variables were normalized, and missing values were replaced with an indicator variable. A basic LSTM network was trained with an LSTM layer of size 200, followed by a dense layer with binary cross-entropy loss. The network used the Adam optimizer, LSTM-layer 0.3 dropout and L2 regularizer. Instances were weighted to accommodate for the unbalanced dataset (4,624 ARDS cases from a total of 48,399 adult ICU admissions). 10-fold cross-validation results are shown in Table 1.

Table 1. 10-fold cross-validation results for predicting ARDS outcomes from 6 time series steps (within 24 hours of admission). Structured: Structured data representing 20 vital signs and lab results; Structured + CNN PCV: Structured data and Patient Context Vectors of size 50 pre-trained using word-level CNN on all MIMIC3 nursing notes; Structured + Bert PCV: Structured data and Patient Context Vectors of size 50 pre-trained using Bert base model fine-tuning on all MIMIC3 nursing notes.

Time Series Data	Precision	Recall	F1-score
Structured	30.6	64	41.4
Structured + CNN PCV	36.3	65	46.6
Structured + Bert PCV	38.6	66	48.7

Results suggest that including free-text time-series data significantly outperforms predictions based exclusively on structured lab and vital signs. The addition of the CNN and the Bert-based models outperformed the baseline LSTM using only structured data by 5.2 and 7.3 F1-score absolute percent points respectively. Not surprisingly, the transformer-based Bert pre-trained model outperformed the word-level CNN results (by 2.1 F1-score absolute percent points). It is not clear how the results compare to human expert performance, as the outcome variable is based on subsequent ARDS outcome, and not on human judgements made within 24 hours of admission. It is likely that human expert ARDS predictions utilizing early admission data might also exhibit relatively low F-scores, as ARDS is an extremely challenging condition, requiring knowledge and inference based on complex geno- and pheno-type interactions.

5. CONCLUSIONS

This study focused on combining time-series lab results and vital signs EMR data, with free-text clinical notes time series attempting to capture patient medical context information. Our end goal was to predict early (within 24 hours) the development of an acute condition (ARDS), a task that is challenging even for clinical experts as it requires thorough knowledge and understanding of the patient's geno- and pheno-type, combined with the temporal monitoring of various tests and signs. Results suggest that the encoding and addition of the information present in free-text notes improved substantially the overall model performance.

REFERENCES

- [1] P. Rui and T. Okeyode, "National ambulatory medical care survey: 2016 national summary tables," 2016.
- [2] A. Adibi, M. Sadatsafavi, and J. Ioannidis, "Validation and utility testing of clinical prediction models: Time to change the approach," *Jama*, 2020. [Online]. Available: <https://doi.org/10.1001/jama.2020.1230>
- [3] B. Shickel, P. J. Tighe, A. Bihorac, and P. Rashidi, "Deep ehr: a survey of recent advances in deep learning techniques for electronic health record (ehr) analysis," *IEEE journal of biomedical and health informatics*, vol. 22, no. 5, pp. 1589–1604, 2018.
- [4] H. Harutyunyan, H. Khachatrian, D. C. Kale, G. V. Steeg, and A. Galstyan, "Multitask learning and benchmarking with clinical time series data," arXiv preprint arXiv:1703.07771, 2017.
- [5] H. Harutyunyan, H. Khachatrian, D. C. Kale, G. Ver Steeg, and A. Galstyan, "Multitask learning and benchmarking with clinical time series data," *Scientific data*, vol. 6, no. 1, pp. 1–18, 2019.
- [6] A. E. Johnson, T. J. Pollard, L. Shen, H. L. Li-wei, M. Feng, M. Ghassemi, B. Moody, P. Szolovits, L. A. Celi, and R. G. Mark, "Mimic-iii, a freely accessible critical care database," *Scientific data*, vol. 3, p. 160035, 2016.
- [7] Z. C. Lipton, D. C. Kale, C. Elkan, and R. Wetzell, "Learning to diagnose with lstm recurrent neural networks," arXiv preprint arXiv:1511.03677, 2015.
- [8] H. Song, D. Rajan, J. J. Thiagarajan, and A. Spanias, "Attend and diagnose: Clinical time series analysis using attention models," in *Thirty-second AAAI conference on artificial intelligence*, 2018.
- [9] J. Ma'ca, O. Jor, M. Holub, P. Sklienka, F. Burs'a, M. Burda, V. Janout, and P. Ševc'ík, "Past and present ards mortality rates: a systematic review," *Respiratory care*, vol. 62, no. 1, pp. 113–122, 2017.
- [10] G. Bellani, J. G. Laffey, T. Pham, E. Fan, L. Brochard, A. Esteban, L. Gattinoni, F. Van Haren, A. Larsson, D. F. McAuley et al., "Epidemiology, patterns of care, and mortality for patients with acute respiratory distress syndrome in intensive care units in 50 countries," *Jama*, vol. 315, no. 8, pp. 788–800, 2016.
- [11] Z. Wu and J. M. McGoogan, "Characteristics of and important lessons from the coronavirus disease 2019 (covid- 19) outbreak in china: summary of a report of 72 314 cases from the chinese center for disease control and prevention," *Jama*, 2020.
- [12] E. Fan, L. Del Sorbo, E. C. Goligher, C. L. Hodgson, L. Munshi, A. J. Walkey, N. K. Adhikari, M. B. Am- ato, R. Branson, R. G. Brower et al., "An official american thoracic society/european society of intensive care medicine/society of critical care medicine clinical practice guideline: mechanical ventilation in adult patients with acute respiratory distress syndrome," *American journal of respiratory and critical care medicine*, vol. 195, no. 9, pp. 1253–1263, 2017.
- [13] C. M. Shaver and J. A. Bastarache, "Clinical and biological heterogeneity in acute respiratory distress syndrome: direct versus indirect lung injury," *Clinics in chest medicine*, vol. 35, no. 4, pp. 639–653, 2014.
- [14] S. DeLisle, B. South, J. A. Anthony, E. Kalp, A. Gundlapalli, F. C. Curriero, G. E. Glass, M. Samore, and T. M. Perl, "Combining free text and structured electronic medical record entries to detect acute respiratory infections," *PloS one*, vol. 5, no. 10, p. e13377, 2010.
- [15] H. Zheng, H. Gaff, G. Smith, and S. DeLisle, "Epidemic surveillance using an electronic medical record: an empiric approach to performance improvement," *PloS one*, vol. 9, no. 7, p. e100845, 2014.
- [16] E. Ford, J. A. Carroll, H. E. Smith, D. Scott, and J. A. Cassell, "Extracting information from the text of electronic medical records to improve case detection: a systematic review," *Journal of the American Medical Informatics Association*, vol. 23, no. 5, pp. 1007–1015, 2016.
- [17] A. V. Gundlapalli, B. R. South, S. Phansalkar, A. Y. Kinney, S. Shen, S. Delisle, T. Perl, and M. H. Samore, "Application of natural language processing to va electronic health records to identify phenotypic characteristics for clinical and research purposes," *Summit on translational bioinformatics*, vol. 2008, p. 36, 2008.
- [18] R. J. Carroll, A. E. Eyler, and J. C. Denny, "Naïve electronic health record phenotype identification for rheumatoid arthritis," in *AMIA annual symposium proceedings*, vol. 2011. American Medical Informatics Association, 2011, p. 189.

- [19] S.Karnik, S.L.Tan, B.Berg, I.Glurich, J.Zhang, H.J.Vidaillet, C.D.Page, and R.Chowdhary, "Predicting atrial fibrillation and flutter using electronic health records," in *Engineering in Medicine and Biology Society (EMBC), 2012 Annual International Conference of the IEEE*. IEEE, 2012, pp. 5562–5565.
- [20] A. N. Ananthkrishnan, T. Cai, G. Savova, S.-C. Cheng, P. Chen, R. G. Perez, V. S. Gainer, S. N. Murphy, P. Szolovits, Z. Xia et al., "Improving case definition of crohn's disease and ulcerative colitis in electronic medical records using natural language processing: a novel informatics approach," *Inflammatory bowel diseases*, vol. 19, no. 7, pp. 1411–1420, 2013.
- [21] R. Miotto, L. Li, B. A. Kidd, and J. T. Dudley, "Deep patient: an unsupervised representation to predict the future of patients from the electronic health records," *Scientific reports*, vol. 6, p. 26094, 2016.
- [22] Y. Choi, C. Y.-I. Chiu, and D. Sontag, "Learning low-dimensional representations of medical concepts," *AMIA Summits on Translational Science Proceedings*, vol. 2016, p. 41, 2016.
- [23] E. Choi, M. T. Bahadori, E. Searles, C. Coffey, M. Thompson, J. Bost, J. Tejedor-Sojo, and J. Sun, "Multi-layer representation learning for medical concepts," in *Proceedings of the 22nd ACM SIGKDD International Conference on Knowledge Discovery and Data Mining*. ACM, 2016, pp. 1495–1504.
- [24] D. Kartchner, T. Christensen, J. Humpherys, and S. Wade, "Code2vec: Embedding and clustering medical diagnosis data," in *Healthcare Informatics (ICHI), 2017 IEEE International Conference on*. IEEE, 2017, pp. 386–390.
- [25] E. Choi, M. T. Bahadori, A. Schuetz, W. F. Stewart, and J. Sun, "Doctor ai: Predicting clinical events via recurrent neural networks," in *Machine Learning for Healthcare Conference, 2016*, pp. 301–318.
- [26] Z. C. Lipton, D. C. Kale, and R. Wetzel, "Modeling missing data in clinical time series with rnns," *arXiv preprint arXiv:1606.04130*, 2016.
- [27] E. Choi, M. T. Bahadori, J. Sun, J. Kulas, A. Schuetz, and W. Stewart, "Retain: An interpretable predictive model for healthcare using reverse time attention mechanism," in *Advances in Neural Information Processing Systems, 2016*, pp. 3504–3512.
- [28] N. Razavian, J. Marcus, and D. Sontag, "Multi-task prediction of disease onsets from longitudinal laboratory tests," in *Machine Learning for Healthcare Conference, 2016*, pp. 73–100.
- [29] P. Nguyen, T. Tran, N. Wickramasinghe, and S. Venkatesh, "Deepr: A convolutional net for medical records," *IEEE journal of biomedical and health informatics*, vol. 21, no. 1, pp. 22–30, 2017.
- [30] Y. Xu, S. Biswal, S. R. Deshpande, K. O. Maher, and J. Sun, "Raim: Recurrent attentive and intensive model of multimodal patient monitoring data," in *Proceedings of the 24th ACM SIGKDD International Conference on Knowledge Discovery & Data Mining, 2018*, pp. 2565–2573.
- [31] C. Bime, C. Poongkunran, M. Borgstrom, B. Natt, H. Desai, S. Parthasarathy, and J. G. Garcia, "Racial differences in mortality from severe acute respiratory failure in the united states, 2008–2012," *Annals of the American Thoracic Society*, vol. 13, no. 12, pp. 2184–2189, 2016.
- [32] G. Shari, M. Kojicic, G. Li, R. Cartin-Ceba, C. T. Alvarez, R. Kashyap, Y. Dong, J. T. Poulouse, V. Hrasevich, J. A. C. Garza et al., "Timing of the onset of acute respiratory distress syndrome: a population-based study," *Respiratory care*, vol. 56, no. 5, pp. 576–582, 2011.
- [33] E. Apostolova, T. Wang, T. Tschampel, I. Koutroulis, and T. Velez, "Combining structured and free-text electronic medical record data for real-time clinical decision support," in *Proceedings of the 18th BioNLP Workshop and Shared Task, 2019*, pp. 66–70.
- [34] T. Bai, A. K. Chanda, B. L. Egleston, and S. Vucetic, "Ehr phenotyping via jointly embedding medical concepts and words into a unified vector space," *BMC medical informatics and decision making*, vol. 18, no. 4, p. 123, 2018.
- [35] E. Apostolova, A. Uppal, J. Galarraga, I. Koutroulis, T. Tschampel, T. Wang, and T. Velez, "Towards reliable ards clinical decision support: Ards patient analytics with free-text and structured emr data," *AMIA Summits on Translational Science Proceedings*, vol. 2019, 2019.
- [36] Y. Kim, "Convolutional neural networks for sentence classification," *arXiv preprint arXiv:1408.5882*, 2014.
- [37] J. Devlin, M.-W. Chang, K. Lee, and K. Toutanova, "Bert: Pre-training of deep bidirectional transformers for language understanding," *arXiv preprint arXiv:1810.04805*, 2018.

AUTHORS

Emilia Apostolova, Ph.D.

Dr. Apostolova has extensive experience in Natural Language Processing and Machine Learning and has developed a number of information extraction and text categorization systems in the biomedical, financial, and legal domains. She has been an NIH Researcher and a Master – Natural Language Processing / Machine Learning at the Deloitte Innovation Lab. Dr. Apostolova received her BA/MA in Linguistics / English Literature from Sofia University St. Kliment Ohridski, MS Computer Science from Loyola University Chicago, and PhD Computer Science / Natural Language Processing from DePaul University.



Joe Morales

Joe Morales began his career as a nuclear submarine officer, serving onboard USS Alabama (SSBN-731) where he made six strategic deterrent patrols. After completion of his Navy service, Joe returned home to Colorado Springs and embarked on career in software development. Joe is now a software leader with 25 years experience leading teams in the design, development, and fielding of software systems in a variety of domains for commercial and government customers. He has extensive expertise in data analytics and processing, machine learning, modeling and simulation, and cloud-based architectures. Joe received his BS in Computer Science from the US Naval Academy and Masters of Information and Data Science from the University of California, Berkeley.



Ioannis Koutroulis, MD

Ioannis Koutroulis, M.D., is originally from Greece, where he attended medical school and received a Ph.D. in infectious diseases. He completed residency training in New York and a fellowship in Philadelphia at St. Christopher's Hospital for Children and Drexel University College of Medicine. At that time, he also completed an MBA in healthcare management and finance. While at Drexel, Dr. Koutroulis served as the course director of pathophysiology for second year medical students. He has published work on sepsis, atopic dermatitis, obesity and asthma. Dr. Koutroulis is currently the Co-Director, Urgent Care Fellowship and an Emergency Medicine Physician at Children's National Hospital.



Tom Velez, PhD, JD

Dr. Tom Velez is an accomplished entrepreneur, aerospace engineer, mathematician and computer scientist with over 40 years of experience in the development of complex technology-intensive systems in the aerospace, intelligence, military, and healthcare industries. His current interest and passion is directed at the effective utilization of advanced information systems technologies in support of outcomes-focused, patient-centered chronic disease care quality. Dr. Velez received a B.S. in Mathematics from Iona College, M.S. in Mathematics and Computer Science from Adelphi University; Ph.D. in Applied Mathematics from Georgetown University and J.D., Magna Cum Laude from the University of Baltimore.



A NOVEL BIT ALLOCATION ALGORITHM IN MULTI-VIEW VIDEO

Tao Yan¹, In-Ho Ra², Deyang Liu³, Jiajun Hong¹,
Jingyu Feng¹ and Shaojie Hou¹

¹School of Information Engineering, Putian University, Putian, China

²School of Computer, Information and Communication Engineering, Kunsan
National University, Gunsan, South Korea

³School of Computer and Information, Anqing Normal University,
Anqing 246000, China

ABSTRACT

The difficulty of rate control for Multi-view video coding(MVC) is how to allocate bits between views. The results of our previous research including the bit allocation among viewpoints uses the correlation analysis among viewpoints to predict the weight of each viewpoint. But when the scene changes, this prediction method will produce a lot of errors. Therefore, this article avoids this situation happening through scene detection. The core of the algorithm is to first divide all images into 6 types of encoded frames according to the structural relationship between disparity prediction and motion prediction, and improve the binomial rate distortion model, and then perform inter-view, frame layer, and basic unit based on the encoded information. Layer bit allocation and code rate control. In this paper, a reasonable bit rate is allocated between viewpoints based on the encoded information, and the frame layer bit rate is allocated using frame complexity and time-domain activity. Experimental simulation results show that the algorithm can effectively control the bit rate of MVC, while maintaining efficient coding efficiency, compared with the current MVC using JVT with fixed quantization parameters.

KEYWORDS

MVC, Quantization parameters, Bit allocation, Rate distortion model, Basic unit layer.

1. INTRODUCTION

3DTV / FTV system has broad application prospects in many aspects such as digital entertainment, virtual reality, 3D reconstruction, 3D monitoring, expo exhibition, medical treatment, education and so on. However, there are still many key technical problems in signal processing of 3DTV / FTV systems. The relevant international standards have not yet been developed, which is a very challenging and pioneering research field.[1-2] .

The multi-view video is compressed and sent to the channel for transmission and then decoded at the decoder. It is stored or displayed according to user needs. In the entire process of encoding → transmission → decoding, how to solve the compressed multi-view video data Adapt to the coding rate control problem of the channel. If this problem cannot be solved, the coded stream is directly sent to the channel for transmission, which will cause the channel or congestion or idle, which will greatly reduce the channel utilization.

Previous video compression standards such as MPEG-2, MPEG-4, H.263, H.264 [3-6], etc. have been given code rate control models. However, the multi-view video encoding reference software JMVC of JVT currently has no effective rate control algorithm [7]. The MVC code rate control algorithm must not only reasonably allocate the code rate in time to prevent buffer overflow, but also perform reasonable code rate allocation among the various viewpoints to ensure the video quality balance between the viewpoints. Many scholars at home and abroad have begun to study the rate control of multi-view video coding [8-14]. Multi-view video coding is very complicated. I can first optimize multi-view video coding and extend the constraint relationship between the sports field and parallax field in stereo video to multi-view video coding. The acquisition cameras are corrected and synchronized, and they are arranged in parallel on the same horizontal straight line at equal intervals. In this way, only parallax in the horizontal direction appears in the system, which can better simulate the stereo vision system of the human eye.

Therefore, this paper first analyzes the problems of existing video rate control algorithms and proposes a rate control algorithm for multi-view video. Experimental simulation results show that the algorithm in this paper can maintain efficient encoding efficiency while effectively controlling the bit rate of multi-view video encoding.

2. RATE CONTROL ALGORITHM FOR MULTI-VIEW VIDEO

Multi-view video coding sets more B-pictures in order to improve the coding efficiency. The MPEG organization provides relevant requirements for multi-view video coding. The main requirements are: higher compression rate, lower coding and decoding complexity, and reasonable code rate control. Taking this as the guiding direction of MVC research, researchers have carried out a lot of work in recent years, and some results or suggestions have been submitted to the MPEG organization. Therefore, the bit-rate control of multi-view video coding should increase the bit-rate control of B-frames. Based on previous studies [12], [13], the key point of this paper is how to make a reasonable bit rate allocation among various views according to the requirements of multi-view video coding to ensure the balance of video quality between views. The key steps of the algorithm are as follows:

In the rate control algorithm in this paper, let $T_{GGOP}(sn_{i,0})$ denote the total number of bits allocated to the i th GGOP, and use the weight w_k to indicate the importance of the viewpoint k . A larger w_k indicates that the viewpoint is more important. The total number of bits allocated to the GOP_k at the k -th viewpoint in GGOP is given by equation (1)

$$T_{GOP}(n_{k,0}) = T_{GGOP}(sn_{i,0}) \cdot w_k \quad (1)$$

According to the number of remaining bits $T_{GOP}^*(k-1)$ of the previous GOP_{k-1} , the number of bits finally allocated by the current GOP_k is:

$$T_{GOP}(n_{k,0}) = T_{GGOP}(sn_{i,0}) \cdot w_k + T_{GOP}^*(k-1) \quad (2)$$

$w_k (k=1,2,L, N_{view})$ initial value is set to 1,

$$w_k = \frac{\frac{1}{N_{view}} \cdot \sum_{j=0}^{N_{view}-1} C(S_j, S_k)}{\sum_{k=0}^{N_{view}-1} \frac{1}{N_{view}} \cdot \sum_{j=0}^{N_{view}-1} C(S_j, S_k)} \quad j, k \in \{0, 1, \dots, N_{view} - 1\} \quad (3)$$

$$w_0 = \max\{w_0, w_1, w_2\}, \quad w_1 = \min\{w_0, w_1, w_2\}, \quad w_2 = \text{mid}\{w_0, w_1, w_2\} \quad (4)$$

Frames with smaller time-domain activities require smaller bits; frames with larger time-domain activities require more bits. Using the time-domain activity of the previous frame, the MAD of the previous frame, and the time-domain activity of the current frame to predict the complexity of the current frame. The target bit of the current frame is shown in formula (5):

$$T_r(j) = T'_r(j-1) \cdot \frac{FD(j)}{\frac{1}{j-1} \sum_{k=1}^{j-1} \Theta \cdot FD(k)} \quad (5)$$

In the formula, $FD(j)$ and $FD(j-1)$ represent the time-domain activity of the j -th and $j-1$ frames, respectively.

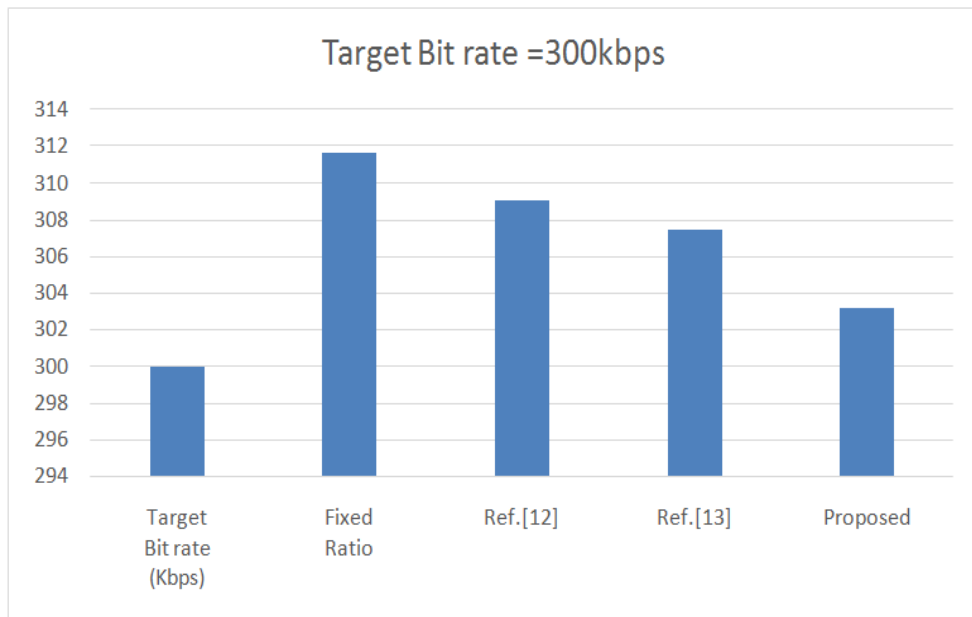
A new GoP encoding will begin after the scene switch frame. This paper refers to previous research results. GoP target bit T_{GoP} is set in the method as follow:

$$T_{GoP} = \chi \cdot N_{GoP} \times \left(R_{picAvg} + \frac{R_{picAvg} \times N_{coded} - R_{coded}}{SW} \right) \quad (6)$$

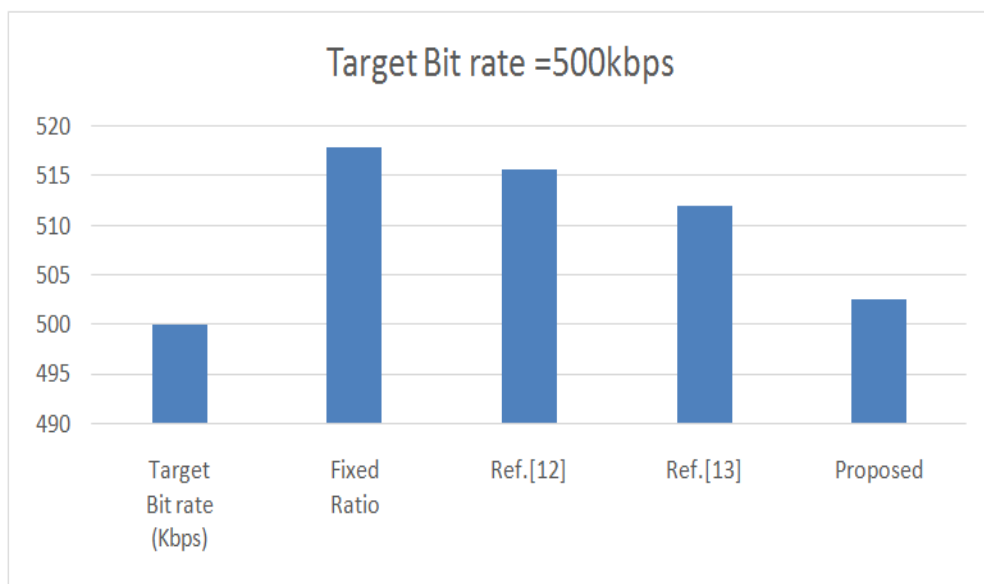
In the formula: N_{GoP} represents the size of GoP; R_{picAvg} is the target bit rate; N_{coded} is the number of encoded frames; SW is the size of the smoothing window; R_{coded} is the number of bits consumed by the encoded frame. The remaining number of bits of the GoP terminated early and the number of bits consumed by the coding scene switching frame need to be calculated.

3. EXPERIMENTAL RESULTS

In order to verify the performance advantage of the algorithm in terms of coding efficiency, this paper uses the test sequences *Rena*, *Ballroom*, *Exit*, *Flamenco2*, and *Vassar* provided by MERL, KDDI and Nagoya University / Tanimoto Lab for experimental analysis. *Newspaper-balloons* sequence is a combination of *Newspaper* sequence and *balloons* sequence. The other sequences are also synthesized by two sequences. The *Newspaper-balloons'* sequence is obtained by resampling the *Newspaper-balloons* sequence. The other sequences are similar.



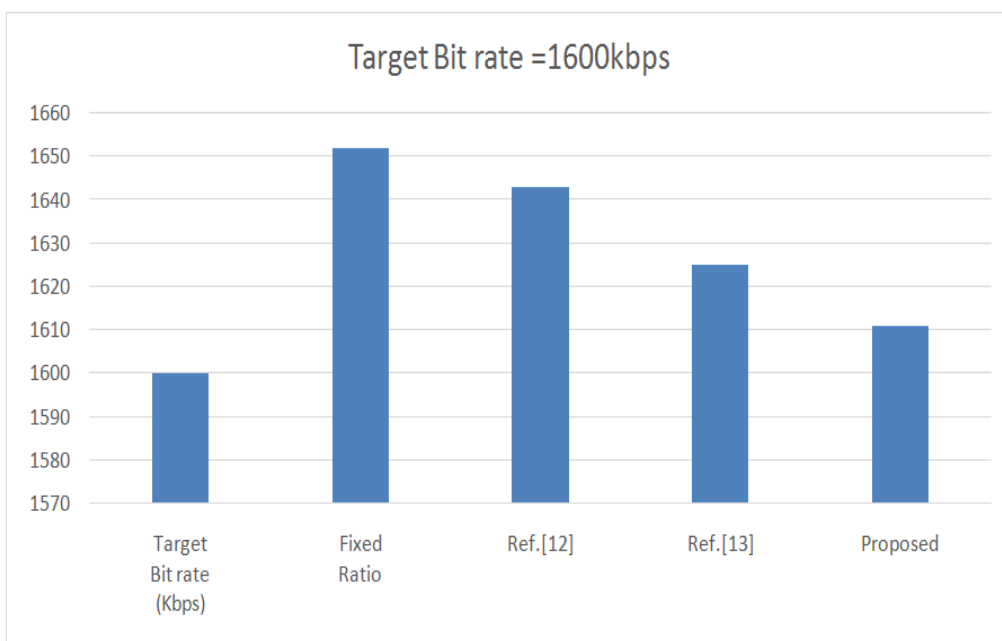
(a)



(b)



(c)



(d)

Fig. 1 The experimental results of the sequence Rena-Ballroom.

Table. 1 Simulation results

Sequence		Target Bit rate (Kbps)	Actual generated bits (kbps)				Rate control error (%)			
			Fixed Ratio	Ref.[12]	Ref.[13]	Proposed	Fixed Ratio	Ref.[12]	Ref.[13]	Proposed
VGA	Rena-Ballroom'	300	311.67	309.09	307.5	303.18	3.89	3.03	2.5	1.06
		500	517.95	515.6	511.95	502.55	3.59	3.12	2.39	0.51
		800	829.2	822.72	814	804.16	3.65	2.84	1.75	0.52
		1600	1652	1642.88	1624.96	1611.04	3.25	2.68	1.56	0.69
	Exit-Flamenco2'	300	309.09	308.79	309.3	306.33	3.03	2.93	3.1	2.11
		500	514.3	514.1	509	501.4	2.86	2.82	1.8	0.28
		800	826.32	825.52	819.84	810	3.29	3.19	2.48	1.25
		1600	1659.84	1643.36	1633.44	1614.56	3.74	2.71	2.09	0.91
	Ballroom-Exit'	300	309.15	306.57	303.36	302.04	3.05	2.19	1.12	0.68
		500	516.4	514.25	513	508	3.28	2.85	2.6	1.6
		800	823.12	818.96	814.88	804.56	2.89	2.37	1.86	0.57
		1600	1651.84	1647.04	1635.2	1609.12	3.24	2.94	2.2	0.57
	Vassar-Flamenco2'	300	310.71	309.99	307.71	304.38	3.57	3.33	2.57	1.46
		500	518.15	513.85	511.7	507.35	3.63	2.77	2.34	1.47
		800	820.48	819.04	815.76	809.92	2.56	2.38	1.97	1.24
		1600	1651.2	1642.24	1634.72	1632.64	3.2	2.64	2.17	2.04
HD	Newspaper-balloons'	300	311.49	308.97	306.63	307.23	3.83	2.99	2.21	2.41
		500	517.05	514.85	512	509.2	3.41	2.97	2.4	1.84
		800	826.16	825.04	817.84	811.04	3.27	3.13	2.23	1.38
		1600	1650.08	1650.08	1638.24	1617.12	3.13	3.13	2.39	1.07
Average							3.32	2.85	2.19	1.18

As can be seen from Fig. 1, experimental results with target bits of 300, 500, 800, and 1600. As can be seen from Table 1, rate control for multi-view video coding based on Ref. [12], which is previous research results. Although it can maintain high coding efficiency, the code rate control deviation is relatively large and the average code rate the control error is 3.32%. The method in this paper controls the output bit rate of multi-view video coding more accurately. In most cases, the error between the actual bit rate and the target bit rate can be controlled at about 1.18% or lower. Among them, Flamenco2 and Ballroom sequence code rate control deviation is relatively large, the main reason is that the scene is relatively fierce, the use of coded information for inter-view bit allocation, easily lead to inaccurate bit allocation between views. As can be seen from Table 1 and Figure 2, compared with JMVC, the decoded image PSNR can be improved by 0.05-0.12dB; and compared with Ref. [12], the decoded image PSNR can be improved by 0.07-0.16dB.

4. CONCLUSION

This paper proposes a bit rate control algorithm for multi-view video coding based on a binomial model. Based on the encoded information, a reasonable bit rate allocation is made between viewpoints, and the frame layer bit rate is allocated using frame complexity and time domain activity. Establish a framework for continuous encoding of multiple viewpoints to achieve continuous encoding of multiple viewpoints: The multi-view video encoding reference model JMVM (Joint Multiview Video Model) provided by JVT (Joint Video Team) implements encoding from viewpoint to viewpoint, that is After the encoding of the current viewpoint is completed, the parameter configuration needs to be performed again when encoding the next viewpoint. Obviously, the reference model cannot perform simultaneous encoding of multiple viewpoints. Experimental results show that the actual bit rate can track the target bit rate while maintaining the coding efficiency.

ACKNOWLEDGMENTS

This work was supported by Natural Science Foundation of China (Grants No. 61741111, 61801006); This work was supported by Program for New Century Excellent Talents in Fujian Province University; This work was supported by the National Research Foundation of Korea(NRF) grant funded by the Korea government (MSIP) (No.2016R1A2B4013002); in part by Natural Science Foundation of Fujian (Grants No. 2019J01816); in part by Natural Science Foundation of Jiangxi (Grants No. 20181BAB202011); Putian University's Initiation Fee Project for Importing Talents for Scientific Research (Grants No. 2019003); This work was supported in part by the Key Project on Anhui Provincial Natural Science Study by Colleges and Universities under Grant KJ2018A0361.

REFERENCES

- [1] E. M. El-Bakary, W. El-Shafai, S. El-Rabaie, O. Zahran, M. El-Halawany, F. E. Abd El-Samie, Proposed enhanced hybrid framework for efficient 3D-MVC and 3D-HEVC wireless communication[J], *Multimedia Tools and Applications*, Vol. 78, No. 11, pp. 14173–14193, June 2019
- [2] Jianjun Lei, Jinhui Duan, Feng Wu, Nam Ling, and Chunping Hou. Fast mode decision based on grayscale similarity and Inter-view correlation for depth map coding in 3D-HEVC[J], *IEEE Transactions on Circuits and Systems for Video Technology*, Vol. 28, No. 3, 706-718, March 2018
- [3] Jingyao Xu, Mai Xu, Yanan Wei, Zulin Wang, and Zhenyu Guan, Fast H.264 to HEVC Transcoding: A Deep Learning Method [J], *IEEE Transactions on Multimedia*, Vol. 21, No. 7, 1633-1645, July 2019
- [4] Pan F, Li Z G, Lim K. A study of MPEG-4 rate control scheme and its implementations. *IEEE Transactions on Circuits and System for Video Technology*[J], 2003, 13(5):440-446.
- [5] Corbera, J., R. and Lei, S., M., “A frame-layer bit allocation for H.263+,” *IEEE Trans. Circuits Syst. Video Technol*, 10(7), 1154-1158 (2000).
- [6] R. Atta and M. Ghanbari, “Low-Complexity joint temporal-quality scalability rate control for H.264/SVC,” *IEEE Transactions on Circuits and Systems for Video Technology*, Vol.28, No. 9, pp. 2331-2344, September 2018

- [7] Joint Video Team of ITU-T VCEG and ISO/IEC MPEG. WD 1 Reference software for MVC (JMVC) 1.0, Doc. JVT-AA212, CH, Geneva, April, 2012.
- [8] Naito S, Matsumoto S. 34/35 Mbps 3D-HDTV digital coding scheme using a modified motion compensation with disparity vectors, VCIP, SPIE, USA, 1999, pp: 1082-1089.
- [9] Woo W, Ortega A. Optimal blockwise dependent quantization for stereo image coding. IEEE Transactions on Circuits and Systems for Video Technology[J], 1999, 9(6):861-867.
- [10] Z Zhao, L Shen, Q Hu, Z Zhang. "Algorithm optimization based on the complexity of HEVC rate control," Chinese Journal of Optoelectronics Laser, Vol.25, No.9, pp. 1715-1720, September 2014
- [11] S. Park, D. Sim. An efficient rate-control algorithm for multi-view video coding. The 13th IEEE International Symposium on consumer Electronics[C], Kyoto, Japan, 2009: 115-118.
- [12] T Yan, P An, L Shen, Q Zhang, and Z Zhang, "Rate control algorithm for multi-view video coding based on correlation Analysis", the International Symposium on Photonics and Optoelectronics (SOPO), pp. 1-4, Wuhan, China, August 2009.
- [13] T Yan, P An, L Shen, Z Li, H Wang, and Z Zhang, "Frame-layer bit allocation for multi-view video coding based on frame complexity estimation," Journal of Shanghai university, vol.14, no. 1, pp. 50-54, February 2010.
- [14] J. Ribas-Corbera, S. M. Lei, A frame-layer bit allocation for H.263+, IEEE Trans. Circuits Syst. Video Technol[J], vol.10, no.7, 2000: 1154-1158.

A SEMI-SUPERVISED LEARNING APPROACH TO FORECAST CPU USAGES UNDER PEAK LOAD IN AN ENTERPRISE ENVIRONMENT

Nitin Khosla¹ and Dharmendra Sharma²

¹Assistant Director – Performance Engineering, Dept. of Home Affairs, Australia

²Professor – Computer Science, University of Canberra, Australia

ABSTRACT

The aim of a semi-supervised neural net learning approach in this paper is to apply and improve the supervised classifiers and to develop a model to predict CPU usages under unpredictable peak load (under stress conditions) in a large enterprise applications environment with several hundred applications hosted and with large number of concurrent users. This method forecasts the likelihood of extreme use of CPU because of a burst in web traffic mainly due to web-traffic from large number of concurrent users. This model predicts the CPU utilization under extreme load (stress) conditions. Large number of applications run simultaneously in a real time system in an enterprise large IT system. This model extracts features by analysing the work-load patterns of the user demand which are mainly hidden in the data related to key transactions of core IT applications. This method creates synthetic workload profiles by simulating synthetic concurrent users, then executes the key scenarios in a test environment and use our model to predict the excessive CPU utilization under peak load (stress) conditions. We have used Expectation Maximization method with different dimensionality and regularization, attempting to extract and analyse the parameters that improves the likelihood of the model by maximizing and after marginalizing out the unknown labels. With the outcome of this research, risk mitigation strategies were implemented at very short duration of time (3 to 4 hours) compared to one week taken in the current practice. Workload demand prediction with semi-supervised learning has tremendous potential in capacity planning to optimize and manage IT infrastructure at a lower risk.

KEYWORDS

Semi-supervised learning, Performance Engineering, Stress testing, Neural Nets, Machine learning applications.

1. INTRODUCTION

With the new emerging IT technologies, usages data centre applications in cloud have grown tremendously in the past decade to cater high user expectations. It is observed at many instances the web-traffic or number of hits increases exponentially to a particular IT applications within a very short span of time (called as internet traffic burst). As a results the CPU utilization of the system increases drastically and has adverse impact of the performance of the IT systems and it slows down the enterprise application system [6][14].

At many instances, the IT system crashes because the IT system cannot sustain the excessive load under the peak load (stress) conditions. Sometimes the critical applications, providing services to the public, e.g. air tickets booking, emergency hospital services, custom clearances at airports,

etc. halt suddenly. These systems crash random and many times it happens due to unpredictable high load or high volume of internet traffic. This results in adversely impacting the productivity and the system performance degrades. In large enterprise organizations, it is found that many times the system alerts are not observed and practically it is not feasible to take any remedial actions e.g. load balancing, etc. Some key transactions become irresponsive and the IT systems are unable to process transactions requests because of extremely high transaction rate which peaks randomly. Managing the keys applications to run 24/7 at a high efficiency level is always constant challenge between productivity, functionality and resource management [8]. Sometimes it is observed that very little or no memory is available for the critical applications to run it leads to a system crash. When transactions are being generated through internet traffic in a wide area distributed network where the network latency and bandwidth are key factors impacting the performance of applications, the scenario become even more complex [4][6].

Main objective of this research paper is to develop and demonstrate the use of a semi-supervised neural net approach to predict the usages of CPU utilization under unpredictable high volume of internet traffic under peak load conditions. To achieve this the work load patterns of the system are observed and analysed for a long period of time (one / two years). Then critical work-load profiles are extracted, which are hidden in the data generated by the key transactions of the crucial applications. Profile data is collected to observe the CPU utilization under peak load conditions (extremely high volume of web traffic) using data mining techniques.

2. RESEARCH QUESTION

Patters of CPU utilization at different time periods (during last one year) were studied and analysed by collecting data from profile points which were configured at different instances in the system. Load profiles were plotted and analysed to identify patterns. The CPU utilization and work load variations were used to develop test scenarios for the validation tests. These tests were conducted in the test environment. This helped us to identify the issues related in estimating a peak load in a test environment. We used this information to forecast the likelihood of this peak load in real world (production) environment. Using semi-supervised neural nets model we have developed a forecasting model to predict the CPU performance under peak load (stress conditions) in an enterprise environment.

2.1. Complex Integrated Environment

Public service departments of big size incorporates different types of system architectures which includes some old applications (legacy) and some developed recently e.g. smart mobile applications, video and face recognition in a cloud computing set-up, etc. We collected the experimental data from a large and complex integrated environment with more than 300 servers where many of them were distributed across multiple geographical locations (countries). Validation were performed in a test environment (called as pre-production environment), which represents a subset of the whole enterprise set-up containing and contains all applications with the most recent releases (builds) but with limited data set. This test environment was also used to represent a set-up with all applications of the department which are distributed in more than 52 overseas posts across the world.

2.2. IT Performance Issues

Computer applications are generally developed upon business specifications and are demand driven. The business specifications are mainly dependent upon the user requirements which keep changing over a period of time. There are some critical limitations when we evaluate and

measure the performance of IT applications or performance of key transactions in the current practices, such as -

- Reliability Issues: System behaviour predictions e.g. response time, performance, etc., under high volume of traffic are not reliable and consistent
- Robustness Issues: Lack of a robust practical approach which can provide useful results in short time frames. It is mainly due to the unpredictable and dynamic web traffic
- Risk Based Approach: IT performance testing (Load and Stress) are mainly done on the critical (high priority) transactions or on the high-risk areas only because testing each and every scenario or their combinations is extremely time consuming and costly. So, the performance tests are designed and performed on -
 - Key transactions (high risk) which has critical impact
 - Important functions which could impact people, important services or have financial implications

3. FEATURE EXTRACTION

We collected raw data of key transactions from their data logs / files which were created at fixed periodic intervals thought a day over one year period. Profile points stored data continuously on pre-defined time intervals. These profile points were configured at different layers in the IT infrastructure. Different types of transactional data representing key transactions was captured e.g. transaction time responses, CPU utilization, memory used, bandwidth utilization, etc. and this was used for analysis, training and validation purposes.

Performance testing experiments (load and stress) for validation were performed in an IT test environment which represented a production like environment (representing a real work scenario). This test environment was configured and integrated with other systems in such a way that it simulated the real-world transaction behaviour. Monitoring of the identified transactions were done using the profile points which gathered the response-time data during the server-response paths (server to client and client to server). Analysis of data, identification of work-load patterns helped to improve our predictive model to forecast critical peaks considering the dynamic nature and variability of the load patterns [13].

3.1. Identifying Work Load Patterns

Workload patterns are dynamic and last for very short time span. Some patterns are different from the normal behaviour of a CPU. Many workload patterns are repeated at periodic instances due to some internal processes. We created a virtual traffic in a test environment to generate these type of workload patterns. We have captured transactions and relevant data for last one year with the help of profile data points. These profile (data capturing) points were configured at different threads, nodes and layers of the applications in the integrated test environment. We studied these patterns and analysed the CPU behaviour and patterns.

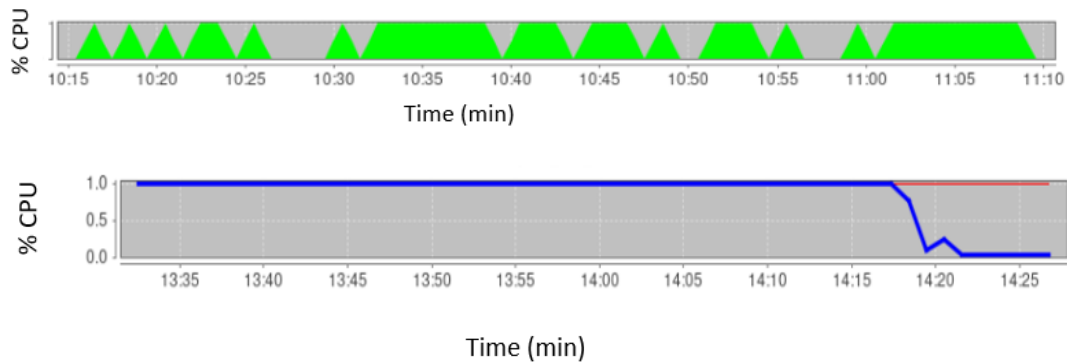


Figure 1. CPU workload pattern (% CPU Utilization), approx. 2500 hits per minute.

The above Figure 1 shows a CPU work-load pattern which follows a cyclic sequence. While in the second graph, the % CPU utilization drops suddenly about 12% from 95%. The key transactions response times were very high when the CPU usages were 95% and the system responded slowly during the peak load spikes. We captured the data during the peak intervals where we observed a typical pattern e.g. a higher CPU utilization for a longer duration of time, clearly shows an abnormal behaviour of CPU utilization. We have also collected some data related to memory, disk usages, database hits, network bandwidth, etc. during the peak CPU utilization periods and did some analytics to find insights from these patterns for predictive modelling. Hierarchical dependence and the impact of secondary transactions are out-of-scope and will be investigated as an extension to current work.

It was noticed that the cumulative CPU usages generally follows a cyclic behaviour for some transactions. These patterns can be represented by a time series consisting of a cyclic component.

4. SEMI SUPERVISED LEARNING MODEL

We used a labelled based semi-supervised learning approach to train our model and used labelled data initially along with some amount of unlabelled data [12]. There are some advantages associated with this research work such as -

- a) We can optimise efficiency in terms of time and accuracy by predicting results which could provide alerts to avoid failures
- b) A scalable predictive approach
- c) A model simulating analogies of work-load patterns based upon data sets captured from different profile points

Assumptions: To develop a practical implementation of the semi-supervised learning approach to work, we have assumed some assumptions e.g. when two distinct points d_1 , d_2 are close enough, then there might be respective outputs y_1 , y_2 . These assumptions helped to develop a practical model for a known number of training data sets to predict a set of infinitely number of test-cases which are mainly unseen or unpredictable [11].

We have also used some labelled data points such as - effort, time, tools and resources. In view of the potential implementation of the outcome of this research work, the semi-supervised learning

along with forced-training method [3][7] has provided some useful outcomes because it is based upon -

- i) Assumptions of forced regularization can reduce the training time
- ii) Learning of data set with both labelled and unlabelled data

We can take the feature vector x (1 D) as represented by $d \times 1$ and it represents the % CPU utilization of the system under test simulating the production environment. Let x is represented by $j \times d$ matrix which is a feature matrix of the labelled data samples. Let x_u be the matrix of Dimension $U \times d$ of unlabelled data samples. Let w denotes the weight vector of our classifier and y be the $L \times 1$ vector with labels encoded between the range of $\{0, 1\}$ showing the features of % CPU usages. The loss function in our classifier is defined as –

$$L_s(w) = \sum_{i=1}^j (x_i^T w - y_i)^2 + \mu \|w\|^2 \quad (1)$$

Where μ is the weight decay L2 regularization. This is used to improve the performance of the model for unseen data.

When we minimize of the above objective function, the weight is given by -

$$w = (X^T X + \mu I)^{-1} X^T Y \quad (2)$$

An updated object is labelled with a threshold of $\frac{1}{2}$ -

$$c_w(w) = \begin{cases} 1, & x^T w > \frac{1}{2} \\ 0, & otherwise \end{cases} \quad (3)$$

A variable u is introduced in the objective function (eq. 1) and this includes the unlabelled objects. Therefore, the updated objective function can be defined as –

$$L_u(w, u) = \left\| X_c w - \begin{pmatrix} y \\ u \end{pmatrix} \right\|^2 + \mu \|w\|^2 \quad (4)$$

Where X_c is the concatenation of X and X_u

Once we take the gradient (slope) of the function (eq. 4) and minimize labelling, each of the label representing the % CPU utilization can be projected within $\{0, 1\}$.

5. EXPERIMENTAL SET UP AND VALIDATION METHODOLOGY

We designed and implemented the following experiment set-up to execute of experiments in the test environment –

- i) Virtual User Generator: to simulate critical end-user business processes or transactions
- ii) Controller: to manage, control and monitor the execution of tests with specific ramping up and ramping down slopes

- iii) Load Generators: configured on servers to generate virtual user load. It simulates work-load patterns with large number of virtual users generating web-traffic hits simulating work-load patterns like web-traffic bursts

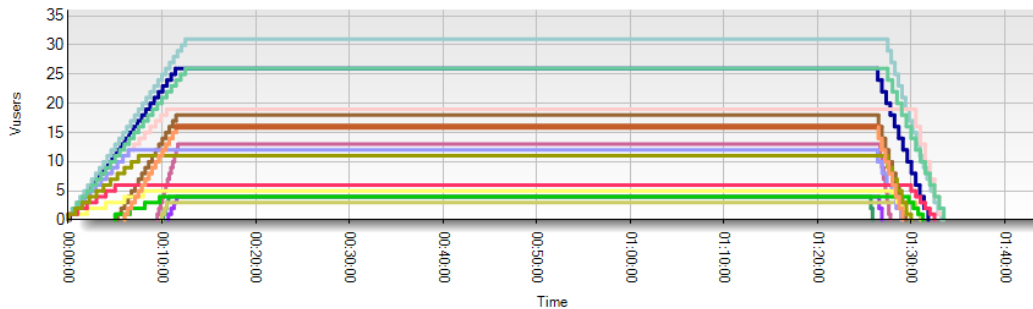


Figure 2. Load profile (ramp up and ramp down slopes) with virtual users

The above Figure 2 shows a work load profile of a group of virtual users (under peak load conditions) with different slopes of ramp up and ramp down times. This simulates real work user's type scenario. This set up was used for validation of our results in the test environment.

Limitations: Different virtual users have different ramping up slopes. It is assumed that these virtual users represent real time users but the actual ramp-up could have slightly different gradient and randomness.

Our validation methodology and experiments incorporated simulated work-load patterns showing burst in traffic at pre-defined intervals in the complex enterprise test environment. Then we collected respective transactional data. The test environment contained a sub-set of full production data which represents large data associated with the integrated applications in real word environment. Over 215 real applications, fully functional, were installed and configured in the test environment representing the real applications environment. This process included –

- i) Data collection, features extraction, analysis of workload demand patterns
- ii) Generate synthetic workloads patterns in the test environment
- iii) Execute stress tests in the test environment with large number of virtual users just as a real world scenario
- iv) Confirmation of results by gathering data from different profile points configured at application threads, nodes and layers
- v) Train the model using labelled based semi-supervised learning approach (deep learning paradigm with Expected Maximization) [7],
- vii) Forecast the likelihood of excessive CPU usages due to burst in the internet traffic [4][6].

6. PREDICTING TRENDS

To forecast a trend in the identified load patterns we have worked out the aggregate demand difference of each occurrence of the pattern from the original workload and compared them. We have used the modified exponential smoothing (ETS) algorithm with ETS point approximation where point-predicts are equal to the medians of the predict distributions [12].

Figure 3(a) shows the results of a semi-supervised neural network model (using EM). This is used to predict the % CPU usages under burst of internet traffic (web based) [9][10]. This model is now part of the monitoring process to continuously evaluate the demand patterns, as shown in Figure 3(b). This model provides information to system architects to set up alarms to take remedial actions e.g. re-allocation of IT resources for efficiency and to avoid a system crash or failure.

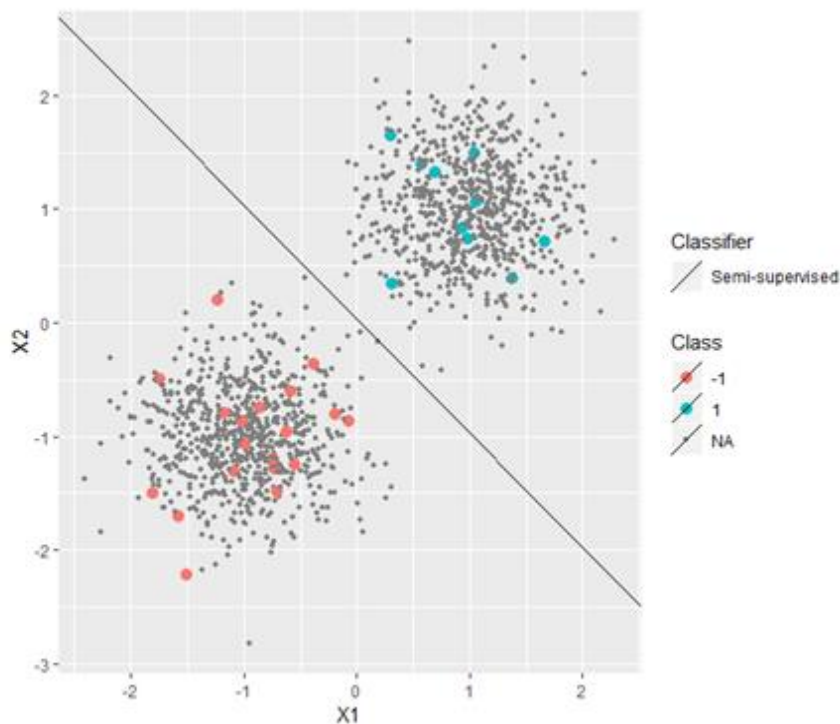


Figure 3 (a) Semi-supervised learning classifier (1 year data set)

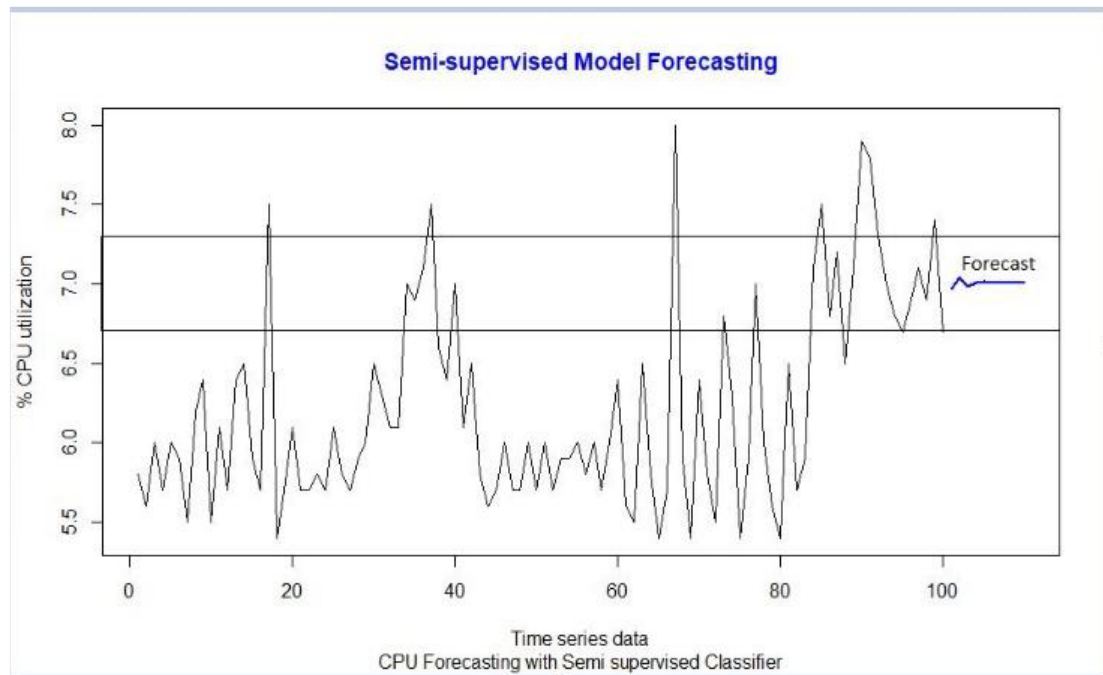


Figure 3(b) % CPU usages with peak load of internet traffic

Table 1 shows a comparison of % error loss with some relevant classifiers where our modified semi supervised model (EM based) has shown minimum loss.

Table 1: Comparison of % Mean Squared Loss with two data sets of peak load

Learning Algorithms	Data set730	Dataset1460
Least Square Classifier	13.05464	12.65698
EM Least Square Classifier	12.19138	11.79293
EM Semi supervised	11.93027	11.74969

7. CONCLUSION

We have designed and implemented a novel practical approach to predict % CPU utilization under the circumstances of unpredictable burst in web based in a complex and highly integrated environment (test or pre-production) where over 230 IT applications were live. Thousands of virtual users were used to generate a dynamic user-load under stress conditions. Our integrated enterprise environment had a distributed system with more than 300 servers serving more than 500 clients concurrently. Using our updated semi-supervised neural network approach (EM), the proposed methodology predicts and identifies the sharp increase in % CPU utilization in a complex enterprise IT infrastructure. Data analytics enabled the system architects and IT system capacity planners to distribute the load appropriately at different servers. The outcome of this research has mitigated the risk of potential failure and improved the system performance and outcomes. The mitigation strategies were implemented at very short duration of time (3 to 4 hours) compared to about 1 - 2 weeks taken in the current practice. Validation of our results were done in an integrated test environment and alerts generated as soon as the CPU utilization of the combined server's crosses 75% threshold critical limit. This validated that our proposed methodology to predict excessive % CPU utilization worked effectively. In addition, we have found that this research is beneficial for our department in planning future IT capacity, optimizing IT resources in the complex IT enterprise IT environment. As a result of this research,

the load balancing was appropriately balanced and database server capacities were shared to handle unexpected web traffic.

8. FUTURE WORK

As further work, we are working on developing a hierarchical semi-supervised learning model to extract patterns while considering the impact of different parameters e.g. memory, hard -disk failures, network latency, etc. and are trying to design an efficient semi-supervised learning approach for predictive modelling.

REFERENCES

- [1] Avital Oliver, Augustus Odena, Colin Raffel, Ekin D Cubuk, et, 2018. 6th International Conference on Learning Representations, ICLR, “Realistic Evaluation of Semi-supervised Learning Algorithms”, Vancouver, BC, Canada.
- [2] Chao Yu, Dongxu Wang, Tianpei Yang, 2018. PRICAI - Proceedings Part-1, “Adaptive Shaping Reinforcement Learning Agents vis Human Reward”, Springer.
- [3] Yuzong Liu, Katrin Krichhoff, 2013. Interspeech , “Graph Based Semi-supervised Learning for Phone and Segment Classification”, France.
- [4] Xishun Wang, Minjie Zhang, Fenghui Ren, 2018 PRICAI Proceedings Part-1, “DeepRSD: A Deep Regression Method for Sequential Data”, Springer.
- [5] Danilo J Rezende, Shakir Mohamed, Daan Wierstra, 2014. Proceedings of the 31st International Conference on Machine Learning, “Stochastic Backpropagation and Approximate Inference in Deep Generative Models”, Beijing, China.
- [6] Daniel Gmach, Jerry Rolia, Ludmila Cherkasova, Alfons Kemper, 2007. IEEE 10th International Symposium on Workload Characterization, “Workload Analysis and Demand Prediction of Enterprise Data Center Applications”, Boston, USA.
- [7] Diederik P. Kingma, Danilo J Rezende, Shakir Mohamad, Max Welling, 2014. Proceedings of Neural Information Processing Systems (NIPS), “Semi-supervised Learning with Deep Generative Models”, Cornell University, USA.
- [8] Kennedy John, Satran Michael, 2018. Microsoft Windows Documents, “Preventing memory leaks in Windows Applications”.
- [9] Kingma Diederik, Rezende Danilo, Mohamed Shakir, Welling M, 2014. Proceedings of Neural Information Processing Systems (NIPS), “Semi-supervised Learning with Deep Generative Models”.
- [10] H. Zhao, N. Ansari, 2012. Journal of Computing and Information Technology, 20(1). “Wavelet Transform Based Network Traffic Prediction: A Fast Online Approach”.
- [11] L. Nie, D. Jiang, S. Yu, H. Song; 2017. IEEE Wireless Communication and Networking Conference, “Network Traffic Prediction Based on Deep Belief Network in Wireless Mesh Backbone Networks”, USA.
- [12] M.F. Iqbal, M.Z. Zahid, D. Habib, K. John, 2019. Journal of Computer Networks and Communications Volume, “Efficient Prediction of Network Traffic for Real Time Applications”

- [13] A. Sankar, X. Zhang, K. Chen-Chuan Chang; 2019; Proceeding of the IEEE 2019/ACM International Conference on Advances in Social Network Analysis and Mining ASONAM; “Meta-GNN: metagraph neural network for semi-supervised learning in attributed heterogenous information networks”.
- [14] T. Miyato, S. Maeda, M. Koyama, S. Ishii; 2019; IEEE Transactions on Pattern Analysis and Machine Intelligence (Vol 41, Issue 8, Aug 2019); “Virtual Adversarial Training: A Regularization Method for Supervised and Semi-Supervised Learning”.

AUTHOR

Nitin Khosla Mr Khosla has worked about 15 years as Asst. Professor at MNIT in the Department of Electronics and Communication Engineering before moving to Australia. He acquired Master of Philosophy (Artificial Intelligence) from Australia, Master of Engineering (Computer Technology) from AIT Bangkok and Bachelor of Engineering (Electronics) from MNIT. His expertise is in Artificial Intelligence (neural nets), Software Quality Assurance and IT Performance Engineering. Also, he is a Certified Quality Test Engineer, Certified Project Manager and a Quality Lead Assessor. During last 14 years, he worked in private and public services in New Zealand and Australia as a Senior Consultant in Software Quality. Currently he is Asst. Director in Australian Federal Government in Performance and Capacity Management and leading multiple IT projects.



ADVANCED RATE CONTROL TECHNOLOGIES FOR MVC

Tao Yan¹, In-Ho Ra², Na Song¹, Yu Youhao¹,
Zhicheng Wu¹ and Zhongyu Shi¹

¹School of Information Engineering, Putian University, Putian 351100, China

²School of Computer, Information and Communication Engineering,
Kunsan National University, Gunsan 54150, South Korea

ABSTRACT

After analyzing the research status and existing problems of multi-view video coding and bit rate control, we found that in addition to achieving higher coding efficiency, scalability characteristics, and quality consistency, reasonable bit rate control is urgent. What needs further research. The paper proposes a multi-view video coding rate control algorithm based on the quadratic rate distortion (RD) model is presented. There are already many rate control algorithms. However, the testing work is very important, and different sequences need to be tested to effectively judge the effectiveness of the algorithm. Experimental simulation results show that the algorithm can effectively control the bit rate of multi-view video coding, while maintaining efficient coding efficiency, compared with the current MVC using JVT with fixed quantization parameters.

KEYWORDS

MVC(multi-view video coding), Rate control, Bit allocation, Basic unit layer.

1. INTRODUCTION

From the perspective of information theory, video compression is to remove the redundancy in video information, that is, to retain uncertain information and remove certain information. Video coding is an important part of digital video processing. Its main purpose is to represent video information with as few bits as possible while ensuring a certain reconstructed image quality. In video compression coding, how to effectively remove information redundancy is the main research issue. After decades of development, there have been many methods to eliminate information redundancy.

Although MVC is the extension of JM (Joint Model) of H.264, it has more picture types and estimation methods for disparity and motion vectors. Differing from the motion estimation, disparity estimation makes the H.264 rate control strategy incompatible. However, current most rate control algorithms concentrate on 2D video which are not suit for multi-view video coding(2-4). New MVC rate control strategy should allocate the appropriate bits temporally to avoid the overflow of buffer while it should also allocate bits between inter views to keep the quality of each view totally equal.

There are already many rate control algorithms(5-11). However, the testing work is still very heavy, and different sequences need to be tested to effectively judge the effectiveness of the algorithm. This reduces the change in lighting and ensures that in the left and right images, the same image block of the same object has the same gray value. However, in practical applications, the geometric characteristics of parallel optical axes cannot be accurately realized. In practical applications, since the left and right cameras cannot be exactly the same, two important deviations occur. First of all, it is difficult to ensure that the bottom edges of the imaging areas of the two cameras are collinear, or even accurate to within one pixel. Second, after digitization, the variance and mean of the pixel gray levels of the left and right images cannot be completely equal. Both of these points can be accomplished with a technique called camera calibration. Because of the fact that multi-view video has three or more views and more complicated bit allocation and rate control strategies are needed for it, it is not reasonable to continuedly adopt rate control model for stereoscopic video coding with two views to multi-view video. The MVC rate control algorithms are being preliminarily developed recently and most of the researchers have just studied the binocular stereo video. The stereo vision imaging system theoretically requires two cameras to have identical optical characteristics.

2. STRUCTURE OF RATE CONTROL

Multi-view video is a technique in which an object or a scene is recorded using several synchronous cameras from different positions, disparity-compensated prediction together with motion-compensated prediction are exploited to reduce all kinds of redundancy. Using the JVT MVC encoder, our rate control algorithm has 4 layers, GOP (the group of group of pictures), GOP, Frame and Basic-Unit. GOP, Frame and Basic-Unit are conformable to JVT-G012. GOP_k is the kth view in a GOP and there are N_{view} GOP in a GOP if let N_{view} denote the number of views.

3. RATE CONTROL ALGORITHM FOR MVC

Our algorithm adopts the fluid-flow traffic model, HRD (hypothetical reference decoder) and linear prediction model of MAD (the mean absolute difference). The main procedures of the test algorithm are described as follows:

This section also uses the previous algorithm. In terms of frame level rate control of JVT-G012, the target bit rate for each frame is determined according to the target buffer level, the predefined frame rate, the available channel bandwidth, the actual buffer occupancy and the remaining bits, in which residual energy is not considered, as a result, the above scheme generally occurs skipped frame and quality degradation. Lei proposed an optimal bit allocation scheme based on residual energy for coding frame as follows,

$$T(j) = \frac{MAD_j}{MAD_a} \cdot \frac{(T - \sum_{m=1}^M C_m)}{M} + C_j \quad (1)$$

where T denotes total bit budget for M frames, C_j and C_m denotes bit budget used for non-texture information of j th frame and m th frame, respectively, MAD_j denotes mean absolute

difference for j th frame, MAD_a denotes the average value of mean absolute difference for all frames. From formula (1), it is obvious that the more target bits should be assigned to those frames with larger MAD_j and C_j value. The proposed rate control scheme replaces M with $N(i)$, then T denotes bit number assigned for x th view, $T_{GOP}(n_{x,0})(x=1,2,\dots, N_{view})$.

In multi-view video coding, in order to determine coded block pattern for macro-block, quantization level should be given in advance, however, quantization level is determined before mode decision when no residual coefficients are generated needed for current frame, and residual energy used to implement target bit allocation for frame layer could not be obtained. To settled the problem, Shen¹² proposed a method to predict current frame coding complexity on the basis of mean absolute difference for the previous frame, temporal activity for current frame and temporal activity for the previous frame. Frame difference between two adjacent frames is applied to define temporal activity for frames, temporal activity for j th frame is defined as follows:

$$FD(j) = \frac{1}{X \cdot Y} \cdot \sum_{x=0}^X \sum_{y=0}^Y |I_j(x, y) - I_{j-1}(x, y)| \quad (2)$$

where X , Y denotes the number of luminance samples in the horizontal direction and vertical direction, respectively, x and y denote indexes of luminance samples in the horizontal direction and vertical direction, respectively, $I_j(x, y)$ and $I_{j-1}(x, y)$ denote the luminance values of pixels in position (x, y) in current frame and previous frame.

Based on target bit allocation technique illustrated in equation (2), target bit number allocated for $(j-1)^{\text{th}}$ frame is given by:

$$T'_r(j-1) = \left[\frac{MAD_{j-1}}{MAD_a} \cdot \left(\frac{T_{GOP}(n_{x,0})}{N(i)} - C_a \right) + C_{j-1} \right] \quad (3)$$

where MAD_{j-1} is mean absolute difference for j th frame, MAD_a is the average value of mean absolute difference of all encoded frames for the current group of pictures, C_a is the average value of non-texture information of all coded frames for the current group of pictures.

It is confirmed that those frames with larger temporal activity need more bits, and vice versa. Thus, we improve the target bit allocation method as illustrated in equation (4) in terms of mean absolute difference and temporal activity for previous frame, temporal activity for current frame, to predict current frame coding complexity. The target bits for current frame is computed as follows.

$$T_r(j) = T_r'(j-1) \cdot \frac{\sum_{l=1}^L W(l) \cdot 2^n}{\sum_{l=1}^L \chi \cdot \frac{FD(l-1)^2}{\frac{1}{L-1} \cdot \sum_{k=1}^{L-1} FD(k)^2} \cdot W(l) + \sum_{l=1}^L \gamma \cdot W_B(l) \cdot (2^n - 1)} + T_j + \psi \quad (4)$$

where $FD(j)$ and $FD(j-1)$ represent temporal activity for j^{th} frame and $(j-1)^{\text{th}}$ frame, respectively. χ , γ and ψ are adjustment parameters, which are obtained through a large number of experiments.

After each frame been encoded, $T_{GGOP}(sn_{i,j})$ will be refreshed as follows:

$$T_{GGOP}(sn_{i,j}) = T_{GGOP}(sn_{i,j-1}) - A(sn_{i,j-1}) \quad (5)$$

where, $A(sn_{i,j-1})$ denotes the real number of bits of the $(j-1)^{\text{th}}$ frame in the i^{th} GGOP.

3. EXPERIMENT RESULT

This article basically uses existing algorithms for testing. There are already many rate control algorithms. However, the testing work is still very heavy, and different sequences need to be tested to effectively judge the effectiveness of the algorithm. We carried out experiments using several sequences with different image properties, which include Akko& kayo, Rena, Vassar1, flameon2. The Flameco2' sequence is obtained by resampling the Flameco2 sequence. The other sequences are similar.

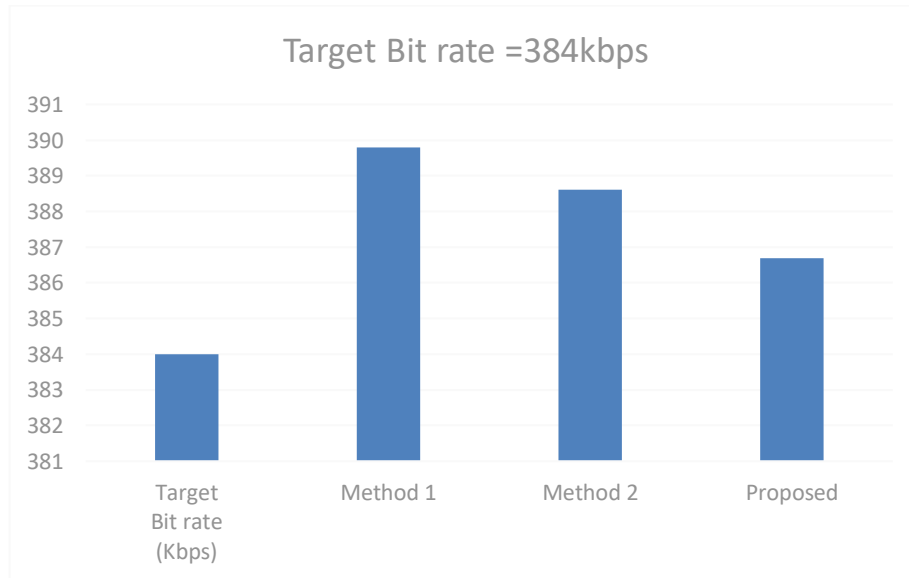


Figure 1 Experimental results

Table. 1 Simulation Results

Sequence	Target bits / (kbps)	Actual bits / (kbps)			Error/(%)		
		Method 1	Method 2	Algorithm used	Method 1	Method 2	Algorithm used
Flameco2'	256	259.07	258.07	258.02	1.20%	0.81%	0.79%
	392	396.78	395.72	395.33	1.22%	0.95%	0.85%
	512	521.48	520.12	519.05	1.85%	1.59%	1.38%
Vassar1'	256	258.15	258.82	257.79	0.84%	1.10%	0.70%
	392	400.9	399.51	395.21	2.27%	1.92%	0.82%
	512	523.96	518.66	515.19	2.34%	1.30%	0.62%
Akko&Kayo	384	389.8	388.61	386.69	1.51%	1.20%	0.70%
	512	518.14	517.89	516.25	1.20%	1.15%	0.83%
	768	774.91	774.14	772.84	0.90%	0.80%	0.63%
Rena'	256	260.76	259.3	258.33	1.86%	1.29%	0.91%
	392	396.61	395.37	394.76	1.18%	0.86%	0.70%
	512	516.35	516.1	514.65	0.85%	0.80%	0.52%
Aveg.					1.43%	1.15%	0.79%

Table 1 illustrates the coding results of the test rate control scheme, which demonstrates that the test scheme can efficiently control the bit rate with an average rate control error of 0.79%. We take note of that when the target bit rate is 512kbps, the Flameco2 sequence has larger rate control error, which is due to that the disparity is larger and movement is intense so that results in large error in bit allocation and MAD prediction. In our experiment, both modeled scene and real scene are used for evaluate validity of the test method.

4. CONCLUSION AND FUTURE WORK

There is still not much work on MVC RC. After analyzing the disadvantages and character of MVC, we propose a MVC-RC algorithm based on the quadratic RD model after analyzing the

character of MVC. It maintains the constant quality by distributing bit rate among different views rationally based on correlation analysis. Experimental results show that the test algorithm can control the bit rate accurately. When a scene changes, an effective video scene detection method needs to be further considered to ensure that the algorithm can quickly and accurately detect the video scene. Scene change detection is an issue to be considered in the future.

ACKNOWLEDGEMENTS

This work was supported by Natural Science Foundation of China (Grants No. 61741111, 61801006); This work was supported by Program for New Century Excellent Talents in Fujian Province University; This work was supported by the National Research Foundation of Korea(NRF) grant funded by the Korea government (MSIP) (No.2016R1A2B4013002); in part by Natural Science Foundation of Fujian (Grants No. 2019J01816); in part by Natural Science Foundation of Jiangxi (Grants No. 20181BAB202011); This work was supported in part by the Key Project on Anhui Provincial Natural Science Study by Colleges and Universities under Grant KJ2018A0361. Putian University's Initiation Fee Project for Importing Talents for Scientific Research (Grants No. 2019003).

REFERENCES

- [1] K. Muller, H. Schwarz, D. Marpe et al., "3D high-efficiency video coding for multi-view video and depth data," *IEEE Transactions on Image Processing*, vol.22,no.9,pp.3366–3378,2015.
- [2] D. K. Kwon, M. Y. Shen, and C. J. Kuo. Rate control for H.264 video with enhanced rate and distortion models. *IEEE Transactions on Circuits and Systems for Video Technology*, 2013, 5, 517-529.
- [3] Y. Liu, Z. G. Li, and Y. C. Soh. Rate control of H.264/AVC scalable extension. *IEEE Transactions on Circuits and Systems for Video Technology*, 2004, 1, 116-121.
- [4] L. Q. Shen, Z. Liu, Z. Y. Zhang. Frame-level bit allocation based on incremental PID algorithm and frame complexity estimation. *Journal of Visual Communication and Image Representation*, 2009, 1, 28-34.
- [5] Joint Video Team of ITU-T VCEG and ISO/IEC MPEG. WD Reference software for MVC , San Diego, USA, 19–26, 2006.
- [6] J. Yang, X. Z. Fang, and H. K. Xiong. A joint rate control scheme for H.264 encoding of multiple video sequences. *IEEE Transaction on Consumer Electronics*, 2015, 2, 667-673.
- [7] J. E. Lim, J. Kim, K. N. Ngan, and K. H. Sohn. Advanced rate control technologies for 3D-HDTV. *IEEE Transactions on Consumer Electronics*, 2003, 4, 1498-1507.
- [8] Pan F, Li Z G, Lim K. A study of MPEG-4 rate control scheme and its implementations. *IEEE Transactions on Circuits and System for Video Technology*[J], 2003, 13(5):440-446.
- [9] Bruno Boessio Vizzotto, Bruno Zatt, Muhammad Shafique, Sergio Bampi. A model predictive controller for frame-level rate control in multiview coding[C]. 2012 IEEE International Conference on Multimedia and Expo, Melbourne, Australia, 2012, 485- 490 .

[10] Li Z G, Pan F, Lim K P, Feng G N. Adaptive basic unit layer rate control for JVT [C]// JVT-G012, the 7th Meeting, Pattaya, Thailand. 2003: 7–14.

[11] J. Y Xu, M. Xu, Y. A Wei, Z. L. Wang, and Z. Y. Guan, “Fast H.264 to HEVC Transcoding: A deep learning method,” *IEEE Transactions on Multimedia*, Vol. 21, No. 7, pp. 1633-1645, July 2019.

© 2020 By AIRCC Publishing Corporation. This article is published under the Creative Commons Attribution (CC BY) license.

OVERSAMPLING LOG MESSAGES USING A SEQUENCE GENERATIVE ADVERSARIAL NETWORK FOR ANOMALY DETECTION AND CLASSIFICATION

Amir Farzad and T. Aaron Gulliver

Department of Electrical and Computer Engineering, University of Victoria, PO
Box 1700, STN CSC, Victoria, BC Canada V8W 2Y2

ABSTRACT

Dealing with imbalanced data is one of the main challenges in machine/deep learning algorithms for classification. This issue is more important with log message data as it is typically very imbalanced and negative logs are rare. In this paper, a model is proposed to generate text log messages using a SeqGAN network. Then features are extracted using an Autoencoder and anomaly detection is done using a GRU network. The proposed model is evaluated with two imbalanced log data sets, namely BGL and Openstack. Results are presented which show that oversampling and balancing data increases the accuracy of anomaly detection and classification.

KEYWORDS

Deep Learning, Oversampling, Log messages, Anomaly detection, Classification

1. INTRODUCTION

Logs are commonly used in software systems such as cloud servers to record events. Generally, these unstructured text messages are imbalanced because most logs indicate that the system is working properly and only a small portion indicate a significant problem. Data distribution with a very unequal number of samples for each label is called imbalanced. The problem of imbalanced data has been considered in tasks such as text mining [1], face recognition [2] and software defect prediction [3].

The imbalanced nature of log messages is one of the challenges for classification using deep learning. In binary classification, there are only two labels, and with imbalanced data, most are normal (denoted major) logs. The small number of abnormal (denoted minor) logs makes classification difficult and can lead to poor accuracy with deep learning algorithms. This is because the normal logs dominate the abnormal logs. Oversampling and undersampling are two methods that can be used to address this problem. In undersampling, the major label samples are reduced so the number is similar to the minor label samples. A serious drawback of

undersampling is loss of information [4]. In oversampling, the number of minor label samples is increased so it is similar to the number of major label samples. Recently, a generative adversarial network (GAN) [5] was proposed for generating images and showed good results in generating data which is similar to actual data such as with image captions [6]. GANs are able to generate more abstract and varied data than other algorithms [7].

In this paper we propose a model to deal with imbalanced log data by oversampling text log messages using a Sequence Generative Adversarial Network (SeqGAN) [8]. The resulting data is then used for anomaly detection and classification with Autoencoder [9] and Gated Recurrent Unit (GRU) [10] networks. An Autoencoder is a feed-forward network that has been shown to be useful for extracting important information from data. Autoencoders have been applied to many tasks such as probabilistic and generative modeling [11] and representation learning [12]. A GRU is a Recurrent Neural Network (RNN) which has been employed in tasks such as sentiment analysis [13] and speech recognition [14]. The proposed model is evaluated using two labeled log message data sets, namely BlueGene/L (BGL) and Openstack. Results are presented which show that the proposed model with oversampling provides better results than the model without oversampling.

The main contributions of this paper are as follows.

1. A model is proposed for log message oversampling for anomaly detection and classification.
2. The proposed model is evaluated using two well-known data sets and the results with and without oversampling are compared.

The rest of the paper is organized as follows. In Section 2 the Autoencoder, GRU and SeqGAN architectures are presented and the proposed model is described. The experimental results and discussion are given in Section 3. Finally, Section 4 provides some concluding remarks.

2. SYSTEM MODEL

In this section, the Autoencoder, GRU and SeqGAN architectures employed are given along with the proposed network model.

2.1. Autoencoder Architecture

An Autoencoder is a feed-forward multi-layer neural network with the same number of input and output neurons. It is used to learn a more efficient representation of data while minimizing the corresponding error. An Autoencoder with more than one hidden layer is called a deep Autoencoder [15]. A reduced dimension data representation is produced using encoder and decoder hidden layers in the Autoencoder architecture. Backpropagation is used for training to reduce the loss based on a loss function. Figure 1 shows the Autoencoder architecture with an input layer, two hidden layers, and an output layer.

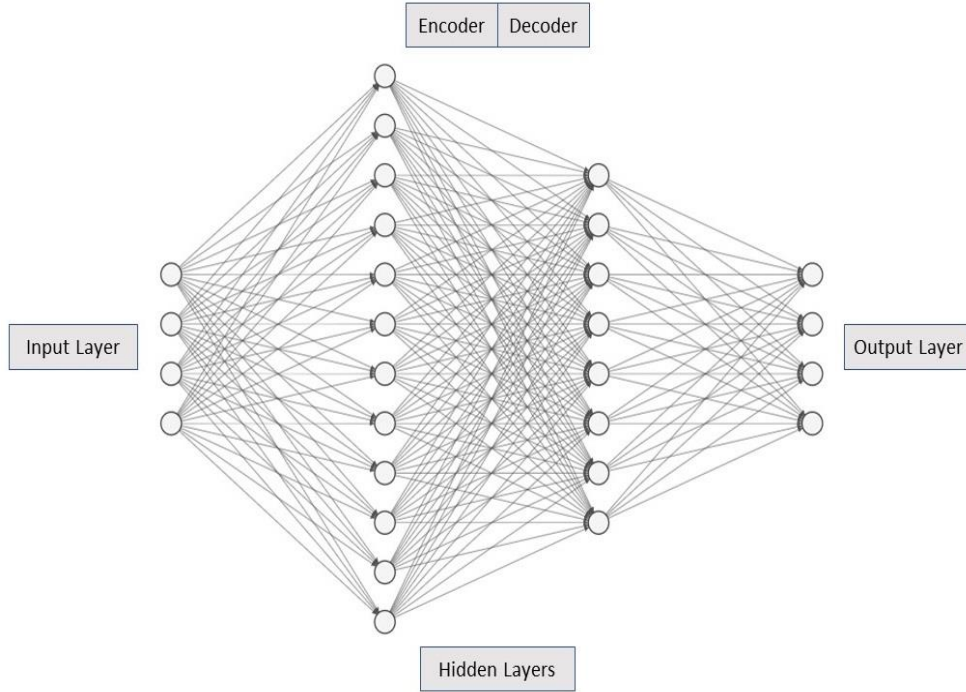


Figure 1. Autoencoder architecture with an input layer, two hidden layers, and an output layer.

2.2. GRU Architecture

A Gated Recurrent Unit (GRU) is a type of RNN network which is a modified version of an LSTM network [16]. It has a reset gate and an update gate. The reset gate determines how much information in a block should be forgotten and is given by

$$r_t = \sigma(W_r x_t + U_r h_{t-1} + b_r), \quad (1)$$

where b_r is the bias vector, σ is the sigmoid activation function and W_r and U_r are the weight matrices. The update gate decides how much information should be updated and can be expressed as

$$z_t = \sigma(W_z x_t + U_z h_{t-1} + b_z), \quad (2)$$

where W_z and U_z are the weight matrices and b_z is the bias vector. The block output at time t is

$$h_t = z_t \odot h_{t-1} + (1 - z_t) \odot \tanh(W_h x_t + U_h (r_t \odot h_{t-1}) + b_h), \quad (3)$$

where b_h is the bias vector and W_h and U_h are the weight matrices. A GRU block is shown in Figure 2.

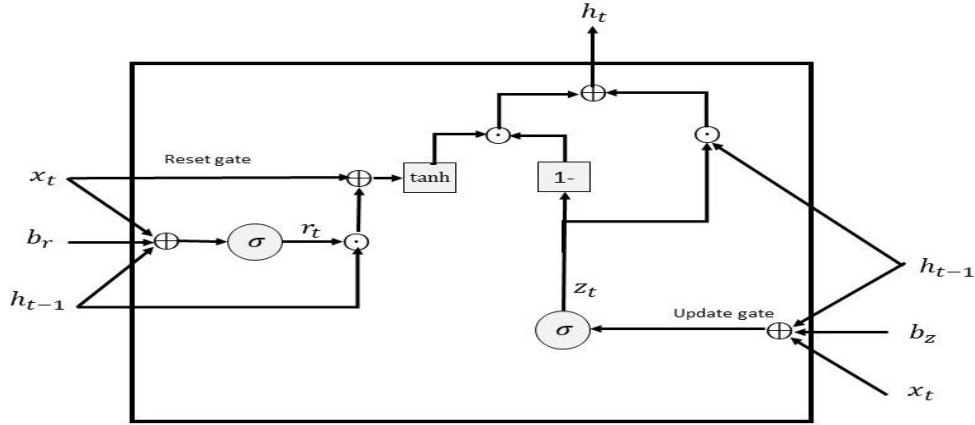


Figure 2. A GRU block with reset gate, update gate, and tangent hyperbolic and sigmoid activation functions.

2.3. SeqGAN Architecture

A SeqGAN consists of a Generator (G) and a Discriminator (D). The Discriminator is trained to discriminate between real data (sentences) and generated sentences. The Generator is trained using the Discriminator using the reward function with policy gradient [17]. In SeqGAN, the reward for a sentence is computed and the Generator is regulated using the reward with reinforcement learning. Generator G_θ is trained with a real data set to produce a sentence

$$Y_{1:T} = \{y_1, \dots, y_t, \dots, y_T\}, y_t \in Y,$$

where Y is the vocabulary of candidate words. This should produce a sentence that is close to real data. This is a reinforcement learning problem which considers G_θ to produce an action a (next word y_t) given the state s (previously generated words $Y_{1:t-1}$). SeqGAN trains the Discriminator D_ϕ as well as the Generator G_θ . D_ϕ is trained to discriminate between real data and data generated from G_θ . Words are generated by G_θ each time step but D_ϕ only computes rewards for full sentences. Hence, the rewards for intermediate states are estimated using Monte Carlo (MC) search and are given by

$$Q_{D_\phi}^{G_\theta} = (s = Y_{1:t-1}, a = y_t) = \quad (4)$$

$$\begin{cases} \frac{1}{N} \sum_{n=1}^N D_\phi(Y_{1:T}^n), Y_{1:T}^n \in MC(Y_{1:t}; N) & \text{if } :t < T, \\ D_\phi(Y_{1:t}) & \text{if } :t = T, \end{cases}$$

where $Q_{D_\phi}^{G_\theta}$ is the action-value function which is the expected reward from the Discriminator, T is the sentence length and N is the number of the sentences in the MC search, $Y_{1:T}^n$ is the n th sentence in the MC search, and $D_\phi(Y_{1:T}^n)$ is the probability of the n th sentence being denoted real by the Discriminator. After the reward is computed, the Generator G_θ is updated via the policy gradient which is the gradient of the objective function and is given by

$$\begin{aligned} & \nabla_\theta J(\theta); \quad \frac{1}{T} \sum_{t=1}^T \sum_{y_t \in Y} \nabla_\theta G_\theta(y_t | Y_{1:t-1}) Q_{D_\phi}^{G_\theta}(Y_{1:t-1}, y_t) \\ &= \frac{1}{T} \sum_{t=1}^T \mathbb{E}_{y_t: G_\theta(y_t | Y_{1:t-1})} [\nabla_\theta \log G_\theta(y_t | Y_{1:t-1}) Q_{D_\phi}^{G_\theta}(Y_{1:t-1}, y_t)], \end{aligned} \quad (5)$$

$$\theta \leftarrow \theta + \alpha \nabla_\theta J(\theta), \quad (6)$$

where α is the learning rate. SeqGAN updates the Discriminator and Generator until the stopping criteria are satisfied. An LSTM, GRU or other RNN network for the Generator and a Convolutional Neural Network (CNN) network for the Discriminator have been shown to provide good results for classification tasks [8].

The SeqGAN architecture is shown in Figure 3. The orange circles denote words in real sentences and the blue circles denote words in generated sentences. First, the Generator is pretrained with real data using the cross-entropy loss function which minimizes the negative log-likelihood. Then it is used to generate data and the Discriminator is pretrained with both generated and real data. The MC search parameters (β) are set to be the same as the Generator parameters (θ). As shown on the right, an MC search is used to compute the reward for an intermediate state. This search generates N complete sentences from the current state. A reward is computed for each sentence and averaged as the intermediate reward except in the last time step where the reward is obtained from the Discriminator. The input of each time step is the output of the previous time step and the next word is obtained via a multinomial distribution over the log softmax of the GRU output. Then the Generator is trained with the policy gradient. Finally, the updated Generator is used to generate data and the Discriminator is trained with both the generated and real data.

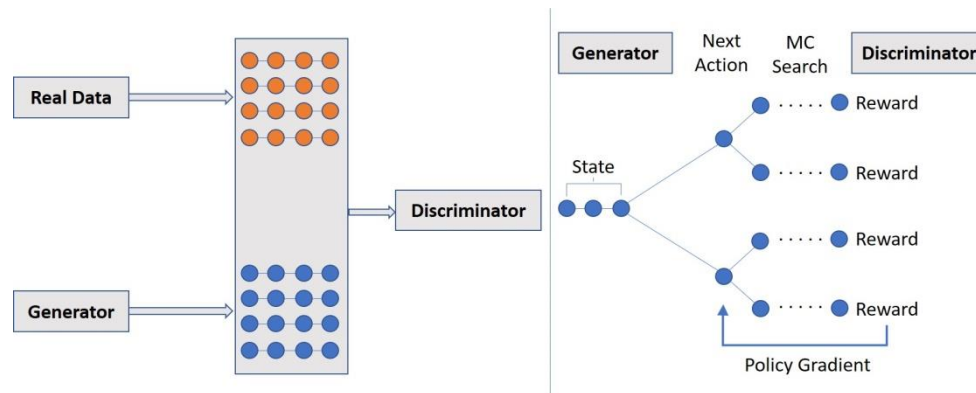


Figure 3. The SeqGAN architecture. The Discriminator on the left is trained with real data and data generated using the Generator. The Generator on the right is trained using the policy gradient. The reward is computed by the Discriminator and this is used to determine the intermediate action values for the MC search.

2.4. Proposed Model

The proposed model has three steps. The first is generating log messages using SeqGAN for oversampling. The log messages are divided into two data sets, positive labeled data (normal) and negative labeled data (abnormal). Additional negative labeled data is generated using the negative labeled data set. The initial negative data set is split into sets (the Openstack data set is split into two sets and the BGL data set is split into seven sets), and fed into the SeqGAN separately. This ensures better convergence and provides different negative log messages. Further, the network speed is faster which is important with data generation. A CNN is used in the SeqGAN for the discriminator and a GRU as the generator. The GRU has one hidden layer of size 30 with the ADAM optimizer and the batch size is 128. The generated negative log messages are concatenated with the original negative data and similar messages are removed. The resulting data set is balanced with similar numbers of positive and negative data.

The second step is the Autoencoder which has two networks (positive and negative) with three hidden layers (two encoder layers and one decoder layer). The encoder layers have 400 (with L1 regularizer) and 200 neurons and the decoder layer has 200 neurons. The output layer has 40 neurons which is the same size as the input layer. The positive labeled data is fed into the positive Autoencoder. Note that this network is trained with just positive label data. The maximum number of epochs is 100 and the batch size is 128. Dropout with probability 0.8 and early stopping is used to prevent overfitting. Categorical cross-entropy loss with the ADAM optimizer is used for training. The network output is labeled as positive. The negative labeled data which has been oversampled is fed into the negative Autoencoder and the network output is labeled as negative. The two sets of labeled data are then concatenated, duplicates are removed and Gaussian noise with zero mean and variance 0.1 is added to avoid overfitting [18].

The final step is the GRU network for anomaly detection and classification. First, the concatenated data set is divided into training and testing sets with 5% for training and 95% for testing, and these sets are shuffled. The training set is then divided into two sets with 5% for training and 95% for validation. The data is fed into the GRU hidden layer of size 100 and is classified using softmax activation. 10-fold cross-validation is used in training with a maximum of 100 epochs and a batch size of 128. Dropout with probability 0.8 and early stopping is used to

prevent overfitting. Categorical cross-entropy loss with the ADAM optimizer is used for training. The proposed model is shown in Figure 4.

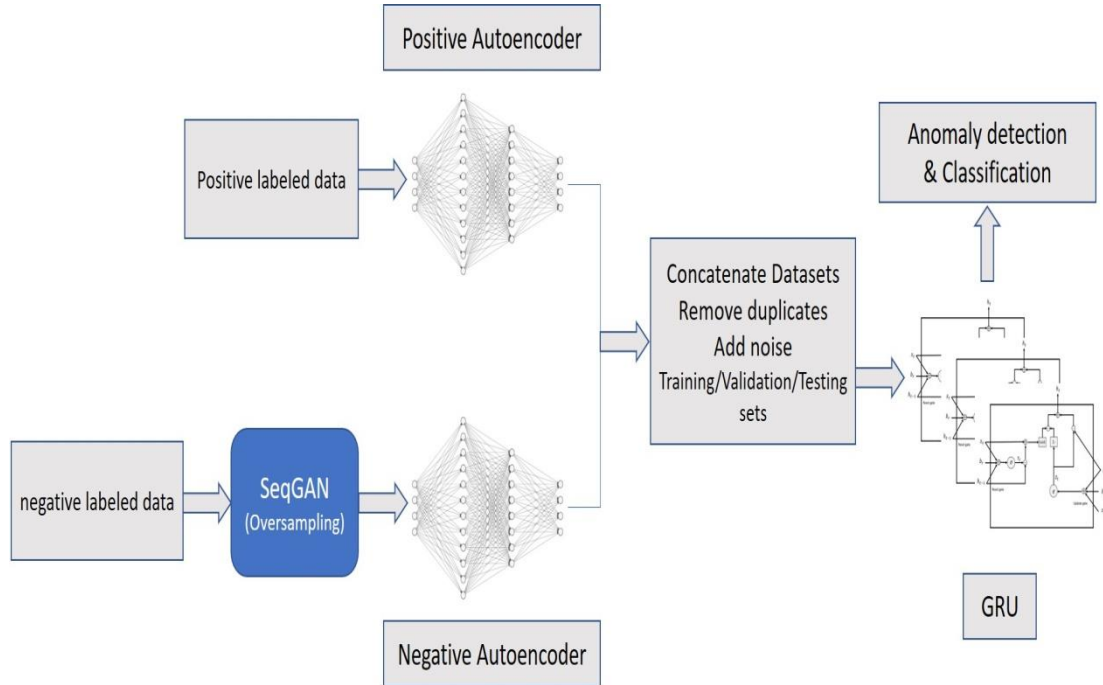


Figure 4. The proposed model architecture with SeqGAN for oversampling log messages, two Autoencoder networks and a GRU network for anomaly detection and classification.

3. RESULTS

In this section, the proposed model is evaluated with and without SeqGAN oversampling using the BGL and Openstack data sets. Four criteria are used to evaluate the performance, namely accuracy, precision, recall, and F-measure. Accuracy is the fraction of the input data that is correctly predicted and is given by

$$A = \frac{T_p + T_n}{T_p + T_n + F_p + F_n}, \quad (7)$$

where T_p is the number of positive instances predicted by the model to be positive, T_n is the number of negative instances predicted to be negative, F_p is the number of negative instances predicted to be positive, and F_n is the number of positive instances predicted to be negative. Precision is given by

$$P = \frac{T_p}{T_p + F_p}, \quad (8)$$

and recall is

$$R = \frac{T_p}{T_p + F_n}. \quad (9)$$

The F-measure is the harmonic mean of recall and precision which can be expressed as

$$F = \frac{2 \times P \times R}{P + R}. \quad (10)$$

All experiments were conducted on the Compute Canada Cedar cluster with 24 CPU cores, 125 GB memory and four P100 GPUs with Python in Keras and Tensorflow. We did not tune the hyperparameters of the proposed model so the default values were used for all data sets. For each data set, the average training accuracy, average validation accuracy, average training loss, testing accuracy, precision, recall, and F-measure were obtained. Tables 1 and 2 give the results for the BGL and Openstack data sets without and with SeqGAN oversampling, respectively.

3.1. BGL

The BlueGene/L (BGL) data set consists of 4,399,503 positive log messages and 348,460 negative log messages (without oversampling). From this data set, 11,869 logs are used for training, 225,529 for validation and the remaining 4,510,565 for testing with approximately 95% positive and 5% negative messages in each group. Without oversampling, the average training accuracy is 97.8% and average validation accuracy is 98.6% with standard deviations of 0.02 and 0.01, respectively, in 10-fold cross-validation. The average training loss is 0.07 with a standard deviation of 0.01. The testing accuracy is 99.3% with a precision of 98.9% for negative logs and 99.3% for positive logs, and recall of 91.6% and 99.9% for negative and positive logs, respectively. The F-measure is 95.1% and 99.6% for negative and positive logs, respectively.

Oversampling of the negative log messages with SeqGAN increased the number in the BGL data set to 4,137,516 so the numbers of positive and negative log messages are similar. From this data set, 21,342 logs are used for training, 405,508 for validation and the remaining 8,110,169 for testing with similar numbers of positive and negative log messages in each group. The average training accuracy is 98.3% and average validation accuracy is 99.3% with a standard deviation of 0.01 in 10-fold cross-validation. The average training loss is 0.05 with a standard deviation of 0.01. The testing accuracy is 99.6% with a precision of 99.8% for negative logs and 99.4% for positive logs, and recall of 99.3% and 99.8% for negative and positive logs, respectively. The F-measure is 99.6% for both negative and positive logs. The accuracy levels are better than the 98% obtained with the LogSig algorithm and the BGL data set [19]. The average precision, recall and F-measure with oversampling are 99.6%, 99.5%, and 99.6%, respectively, which are better than the values of 99%, 75%, and 85%, respectively, with SVM supervised learning and 83%, 99% and 91%, respectively, with unsupervised learning [20].

3.2. Openstack

The Openstack data set without oversampling consists of 137,074 positive log messages and 18,434 negative log messages. From this data set, 6,608 logs are used for training, 1,167 for validation and the remaining 147,733 for testing with approximately 95% positive and 5% negative messages in each group. Without oversampling, the average training accuracy is 98.4% and average validation accuracy is 97.2% with a standard deviation of 0.01 in 10-fold cross-validation. The average training loss is 0.05 with a standard deviation of 0.01. The testing accuracy is 98.3% with a precision of 97.9% for negative logs and 98.3% for positive logs, and recall of 87.1% and 99.8% for negative and positive logs, respectively. The F-measure is 92.2% and 99.0% for negative and positive logs, respectively.

Oversampling of the negative log messages with SeqGAN increased the number in the Openstack data set to 154,202. From this data set, 12,378 logs are used for training, 2,185 for validation and the remaining 276,713 for testing with similar numbers of positive and negative log messages in each group. With oversampling, the average training accuracy is 98.0% and average validation accuracy is 98.7% with a standard deviation of 0.01 in 10-fold cross-validation. The average training loss is 0.06 with a standard deviation of 0.01. The testing accuracy is 98.9% with a precision of 99.6% for negative logs and 98.2% for positive logs, and recall of 98.4% and 99.5% for the negative and positive logs, respectively. The F-measure is 99.0% and 98.8% for negative and positive logs, respectively. The accuracy levels are better than the 87.1% obtained with the IPLoM algorithm and the Openstack data set [21]. The average precision, recall and F-measure with oversampling are 98.9%, 99.0%, and 98.9%, respectively, which are better than the 94%, 99% and 97% obtained with the Deeplog network [22].

Table 1. Results without oversampling for the BGL and Openstack data sets (numbers in parenthesis are standard deviation). Positive labels are denoted by 1 and negative labels by 0.

Data set	Average Training Accuracy	Average Validation Accuracy	Average Training Loss	Testing Accuracy	Label	Precision	Recall	F-measure
BGL	97.8%	98.6%	0.07	99.3%	0	98.9%	91.6%	95.1%
	(0.02)	(0.01)	(0.01)		1	99.3%	99.9%	99.6%
Openstack	98.4%	97.2%	0.05%	98.3%	0	97.9%	87.1%	92.2%
	(0.01)	(0.01)	(0.01)		1	98.3%	99.8%	99.0%

Table 2. Results with oversampling using SeqGAN for the BGL and Openstack data sets (numbers in parenthesis are standard deviation). Positive labels are denoted by 1 and negative labels by 0.

Data set	Average Training Accuracy	Average Validation Accuracy	Average Training Loss	Testing Accuracy	Label	Precision	Recall	F-measure
BGL	98.3%	99.3%	0.05	99.6%	0	99.8%	99.3%	99.6%
	(0.01)	(0.01)	(0.01)		1	99.4%	99.8%	99.6%
Openstack	98.0%	98.7%	0.06%	98.9%	0	99.6%	98.4%	99.0%
	(0.01)	(0.01)	(0.01)		1	98.2%	99.5%	98.8%

3.3. Discussion

The proposed oversampling with SeqGAN provided good results for both the BGL and Openstack data sets. It is evident that oversampling significantly improved the model accuracy for negative log messages. For the BGL data set, the precision, recall and F-measure after oversampling increased from 98.9% to 99.8%, 91.6% to 99.3% and 95.1% to 99.6% which are 0.9%, 7.7% and 4.5% higher, respectively. For the Openstack data set, the precision, recall and F-measure after oversampling increased from 97.9% to 99.6%, 87.1% to 98.4% and 92.2% to 99.0% which are 1.7%, 11.3% and 6.8% higher, respectively. These results show that data balancing should be considered with deep learning algorithms to improve the accuracy, especially for small numbers of minor label samples. The proposed model was evaluated with two data sets for anomaly detection and classification with only a small portion (less than 1%) used for training. This is an important result because deep learning algorithms typically require significant amounts of data for training. Note that good results were obtained even though the hyperparameters were not tuned.

The first step in the proposed model where logs are oversampled with a SeqGAN network is the most important. These networks have been shown to provide promising results in generating text such as poems [23]. The concept of generating data is similar to that for oversampling. It was surprising that duplication in the oversampled log data was not high (less than 5%). As a consequence, after removing duplicates there was a significant amount of data available for anomaly detection and classification using deep learning. The second step which extracts features from the data using an Autoencoder is also important. The Autoencoder output is very suitable for use with an RNN based algorithm such as a GRU for anomaly detection and classification. The results obtained show that the proposed model can provide excellent results even when the data is imbalanced.

4. CONCLUSIONS

In this paper, a model was proposed to address the problem of imbalanced log messages. In the first step, the negative logs were oversampled with a SeqGAN network so that the numbers of positive and negative logs are similar. The resulting labeled logs were then fed into an Autoencoder to extract features and information from the text data. Finally, a GRU network was used for anomaly detection and classification. The proposed model was evaluated using two log message data sets, namely BGL and Openstack. Results were presented which show that oversampling can improve detection and classification accuracy. In the future, other text-based GAN networks such as TextGAN and MaliGAN can be used for oversampling.

REFERENCES

- [1] T. Munkhdalai, O.-E. Namsrai and K. H. Ryu, “Self-training in Significance Space of Support Vectors for Imbalanced Biomedical Event Data”, *BMC Bioinformatics*, vol. 16, no. S7, pp. 1-8, 2015.
- [2] Y.-H. Liu and Y.-T. Chen, “Total Margin Based Adaptive Fuzzy Support Vector Machines for Multiview Face Recognition”, in *IEEE International Conference on Systems, Man and Cybernetics*, pp. 1704–1711, 2005.
- [3] M. J. Siers and M. Z. Islam, “Software Defect Prediction using A Cost Sensitive Decision Forest and Voting, and A Potential Solution to the Class Imbalance Problem”, *Information Systems*, vol. 51, pp. 62-71, 2015.
- [4] N. V. Chawla, “Data Mining for Imbalanced Datasets: An Overview”, in *Data Mining and Knowledge Discovery Handbook*, pp. 853–867, Springer, 2005.
- [5] I. Goodfellow, J. Pouget-Abadie, M. Mirza, B. Xu, D. Warde-Farley, S. Ozair, A. Courville and Y. Bengio, “Generative Adversarial Nets”, in *International Conference on Neural Information Processing Systems*, pp. 2672–2680, MIT Press, 2014.
- [6] D. Li, Q. Huang, X. He, L. Zhang and M.-T. Sun, “Generating Diverse and Accurate Visual Captions by Comparative Adversarial Learning”, *arXiv e-prints*, arXiv:1804.00861, 2018.
- [7] L. Liu, Y. Lu, M. Yang, Q. Qu, J. Zhu and H. Li, “Generative Adversarial Network for Abstractive Text Summarization”, *arXiv e-prints*, p. arXiv:1711.09357, 2017.
- [8] L. Yu, W. Zhang, J. Wang and Y. Yu, “SeqGAN: Sequence Generative Adversarial Nets with Policy Gradient”, in *AAAI Conference on Artificial Intelligence*, pp. 2852–2858, 2017.
- [9] D. E. Rumelhart, G. E. Hinton and R. J. Williams, “Parallel Distributed Processing: Explorations in the Microstructure of Cognition”, in *Parallel Distributed Processing: Explorations in the Microstructure of Cognition, Vol. 1*, D. E. Rumelhart, J. L. McClelland and C. PDP Research Group, Eds., pp. 318–362, MIT Press, 1986.
- [10] K. Cho, B. Merriënboer, C. Gulcehre, D. Bahdanau, F. Bougares, H. Schwenk and Y. Bengio, “Learning Phrase Representations Using RNN Encoder–Decoder for Statistical Machine Translation”, in *Conference on Empirical Methods in Natural Language Processing*, pp. 1724–1734, 2014.

- [11] D. J. Rezende, S. Mohamed and D. Wierstra, “Stochastic Backpropagation and Approximate Inference in Deep Generative Models”, in *International Conference on Machine Learning*, vol. 32, pp. II–1278–II–1286, 2014.
- [12] I. Higgins, L. Matthey, A. Pal, C. Burgess, X. Glorot, M. Botvinick, S. Mohamed and A. Lerchner, “Beta-VAE: Learning Basic Visual Concepts with a Constrained Variational Framework”, in *International Conference on Learning Representations*, 2017.
- [13] M. Kuta, M. Morawiec and J. Kitowski, “Sentiment Analysis with Tree-Structured Gated Recurrent Units”, in *Text, Speech, and Dialogue, Lecture Notes in Computer Science*, pp. 74–82, Springer, 2017.
- [14] K. Irie, Z. Tüske, T. Alkhouli, R. Schlüter and H. Ney, “LSTM, GRU, Highway and a Bit of Attention: An Empirical Overview for Language Modeling in Speech Recognition”, in *Interspeech*, pp. 3519–3523, 2016.
- [15] Y. LeCun, Y. Bengio, and G. Hinton, “Deep Learning”, *Nature*, vol. 521, no. 7553, pp. 436–444, 2015.
- [16] S. Hochreiter and J. Schmidhuber, “Long Short-Term Memory”, *Neural Comput.*, vol. 9, no. 8, pp. 1735–1780, 1997.
- [17] R. S. Sutton, D. McAllester, S. Singh and Y. Mansour, “Policy Gradient Methods for Reinforcement Learning with Function Approximation”, in *International Conference on Neural Information Processing Systems*, pp. 1057–1063, MIT Press, 1999.
- [18] H. Noh, T. You, J. Mun and B. Han, “Regularizing Deep Neural Networks by Noise: Its Interpretation and Optimization”, in *Advances in Neural Information Processing Systems*, (I. Guyon, U. V. Luxburg, S. Bengio, H. Wallach, R. Fergus, S. Vishwanathan, and R. Garnett, eds.), vol. 30, pp. 5109–5118, Curran Associates, 2017.
- [19] P. He, J. Zhu, S. He, J. Li and M. R. Lyu, “An Evaluation Study on Log Parsing and Its Use in Log Mining”, in *IEEE/IFIP International Conference on Dependable Systems and Networks*, pp. 654–661, 2016.
- [20] S. He, J. Zhu, P. He and M. R. Lyu, “Experience Report: System Log Analysis for Anomaly Detection”, in *IEEE International Symposium on Software Reliability Engineering*, pp. 207–218, 2016.
- [21] J. Zhu, S. He, J. Liu, P. He, Q. Xie, Z. Zheng and M. R. Lyu, “Tools and Benchmarks for Automated Log Parsing”, in *International Conference on Software Engineering: Software Engineering in Practice, International Conference on Software Engineering: Software Engineering in Practice*, pp. 121–130, 2019.
- [22] M. Du, F. Li, G. Zheng and V. Srikumar, “DeepLog: Anomaly Detection and Diagnosis from System Logs through Deep Learning”, in *ACM Conference on Computer and Communications Security*, pp. 1285–1298, 2017.
- [23] X. Wu, M. Klyen, K. Ito and Z. Chen, “Haiku Generation using Deep Neural Networks”, *The Association for Natural Language Processing*, pp. 1–4, 2017.

AUTHORS

Amir Farzad received the Masters degree in computer engineering (minor: artificial intelligence) from Shahrood University of Technology, Shahrood, Iran, in 2016. He is currently a Ph.D. student in the Department of Electrical and Computer Engineering, University of Victoria, Victoria, BC, Canada. His research interests include machine learning, deep learning and natural language processing.



Thomas Aaron Gulliver received the Ph.D. degree in electrical engineering from the University of Victoria, Victoria, BC, Canada, in 1989. From 1989 to 1991, he was a Defence Scientist with the Defence Research Establishment Ottawa, Ottawa, ON, Canada. He has held academic positions at Carleton University, Ottawa, and the University of Canterbury, Christchurch, New Zealand. He joined the University of Victoria, in 1999, and is currently a Professor with the Department of Electrical and Computer Engineering. His research interests include information theory and communication theory, algebraic coding theory, cryptography, multicarrier systems, smart grid, intelligent networks, cryptography, and security. He became a Fellow of the Engineering Institute of Canada in 2002 and a Fellow of the Canadian Academy of Engineering in 2012.



INDUSTRIAL DUCT FAN MAINTENANCE PREDICTIVE APPROACH BASED ON RANDOM FOREST

Mashaal Maashi, Nujood Alwhibi, Fatima Alamr, Rehab Alzahrani,
Alanoud Alhamid and Nourah Altawallah

Department of Software Engineering, College of Computer and
Information Sciences, King Saud University, Riyadh, Kingdom of Saudi Arabia

ABSTRACT

When manufacturers equipment encounters an unexpected failure, or undergo unnecessary maintenance pre-scheduled plan, which happens for a total of millions of hours worldwide annually, this is time-consuming and costly. Predictive maintenance can help with the use of modern sensing technology and sophisticated data analytics to predict the maintenance required for machinery and devices. The demands of modern maintenance solutions have never been greater. The constant pressure to demonstrate enhanced cost-effectiveness return on investment and improve the competitiveness of the organization is always combined with the pressure of improving equipment productivity and keep machines running at the maximum output. In this paper, we propose maintenance prediction approach based on a machine learning technique namely random forest algorithm. The main focus is on the industrial duct fans as it is one of the most common equipment in most manufacturing industries. The experimental results show the accuracy, reliability of proposed Predictive Maintenance approach.

KEYWORDS

Predictive Maintenance, Maintenance, Random Forest, Duct Fan, Machine Learning & Artificial Intelligence

1. INTRODUCTION

Only 18% of manufacturers equipment fail due to its age, while 82% of failures occur randomly [1]. These unexpected failures cost the industrial manufacturers an estimated \$50 billion each year [2].

Maintenance organizations across industries are at different stages of maturity with different maintenance approaches. Some may be running scheduled maintenance checks based on estimates or Original Equipment Manufacturers (OEM) recommendations, while others may utilize statistics-based programs individually tailored to each fixed asset. These Preventative Maintenance (PM) programs does not accommodate with the latest industry revolution (industry 4.0) [3], which stands for predicting future failures in assets before occurring. Predictive Maintenance (PdM) offers the potential to optimize maintenance tasks in a real time, prevent

David C. Wyld et al. (Eds): ITCSE, NLCA, ICAIT, CAIML, ICDIPV, CRYPIS, WiMo - 2020

pp. 177-184, 2020. CS & IT - CSCP 2020

DOI: 10.5121/csit.2020.100516

unexpected failures, maximizing the useful life of the equipment while still avoiding disruption to operations. Also, this approach promises cost savings over preventive maintenance programs.

In recent years, several studies have been reported that used machine learning techniques to accurately predict the abnormality and remaining useful life of equipment. Chigurupati et al[4] used the Support Vector Machine (SVM) model with a Gaussian Kernel for their approach with a dataset containing 14 hardware samples. Paolanti and Romeo et al[5] Investigated the machine learning approaches for PdM. The study used Decision Forest (DF) classifier algorithm for predicting different machine states with accuracy of 95% on a dataset containing 530731 record. Mathew and Toby et al[6] constructed machine learning models based on the datasets from turbo fan engine data from the Prognostics Data Repository of NASA. The data collected from the engine has 21 sensors to collect different measurements related to the engine state at runtime. The study used ten different algorithms and compared between them. The random forest algorithm generated the least error.

In this work, the authors propose a maintenance prediction approach for industrial duct fans. The proposed method consists of three phases: the data collection phase, the data preparation phase and finally the training and prediction phase. The prediction phase consists of building a classifier to predict the abnormality and building a regression model to predict the remaining useful life.

The rest of the paper is organized as follows. Section 2 presents the proposed approach. Section 3 discusses the experimental results of the proposed approach. Finally, Section 4 provides concluding remarks.

2. THE PROPOSED APPROACH

The prediction approach proposed has a workflow as shown in Figure 1. The workflow consists of three phases: data collection phase, data preparation phase and predictive modelling phase. The extracted features from the collected data are used to build the abnormality classifier and the remaining-useful life regressor. Each of these stages is discussed with more details in the following subsections.

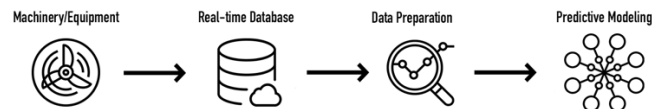


Figure 1. Predictive maintenance workflow

2.1. Data Collection

In the data collection process, MPU-6050 sensor was used to collect the data, it contains an inexpensive 3-axis accelerometer and a temperature sensor [7]. The MPU-6050 is attached to the industrial duct fan to collect the vibration and temperature data as the fan running to predict when the fan failure. Then it sends these data to the Raspberry Pi which sends the data with timestamp to a real-time database.

The output readings are sent to the real-time database every 5 seconds. The data contains the sensor ID, timestamp, x, y and z from the 3-axis accelerometer and the temperature in Celsius. The data was collected for normal and abnormal conditions. For the abnormal conditions, the authors considered some of the modes for simulating failure: increasing the temperature, deform the fan's blades shape, obstructing the movement of the fan's blades and finally simulating failure by blocking the airflow. Table 1 shows each factor with its normal and abnormal data which were taken from Duct fan model user manual [11], it's associated with failure simulation/experiment.

The authors conduct a set of experiments in order to collect accelerometer and temperature data in failure modes. each experiment has duration of 15 to 20 minutes. Table 2 shows each experiment along with its start time, when it end and the caption of losing if it happens. Losing data happens due to voltage source is unconnected to the power. Three fan faults are shown in Figure 2 as an example.

Table 1. Duct Fan Condition

Factor		Normal Data		Abnormal Data		Failure Simulation/ Experiment
		Min	Max	Below	Above	
Temperature	Ambient	—	60 / 140	—	(+) 60° c	Increase the temperature of the room
Motion Accelerometer	External	Normal vibration data readings	Normal vibration data readings	Abnormal vibration data readings		Blocking the airflow
						Blade shape deformation
						Tape on blades

Table 2. Experimental Results of Failure Simulation

Failure Simulation/ Experiment	Start Time	Losing Data	Return Sending	End Time	Duration	Sensor	Success
	H.M.S	H.M.S	H.M.S	H.M.S	(Min)		
Increase the temperature of the room	22.32.49	22.32.49	22.39.22	23.08.58	15	MPU 0001	yes
Blocking the airflow	22.08.10	22.10.05	22.16.36	22.29.37	15	MPU 0001	yes
Blade shape deformation	21:29:40.	21:44:20.	21:49:50.	21:56:51	20	MPU 0002	yes
Tape on blades	17:59:08	-----	-----	18:19:15	20	MPU 0002	yes

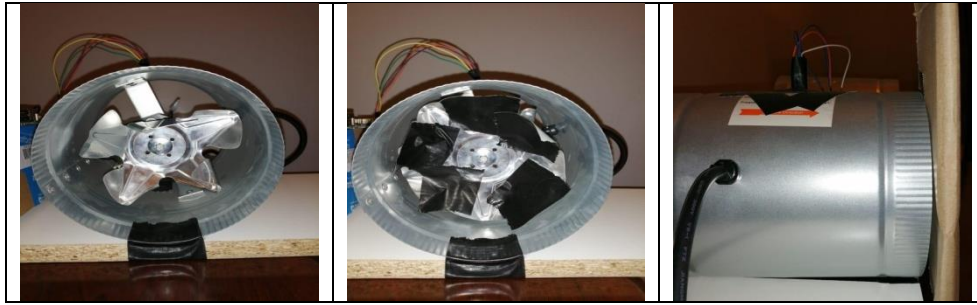


Figure 2. Faults on duct fan.

2.2. Data Preparation

The authors collect 10,963 records from the data collection process; the data needs to be transformed into a format conducive for Machine Learning. The most common is a data frame where rows represent examples to predict or learn from, and columns represent variables including features and targets. The target variables the authors considered were Abnormality and Remaining Useful Life. The collected data were split into training and testing set. The training set contains a known output and the model learns on this data in order to be generalized to other data. The authors have the test dataset (or subset) in order to test our model's prediction on this subset

2.3. Predictive Model

Our goal was ultimately to predict machine failures. The binary classification is viably used for predictive maintenance, being able to estimate the abnormality that the equipment has an abnormal behaviour or not. The regression models in predictive maintenance are used to calculate the remaining useful life of an asset, and it is defined as the amount of time during which the asset remains operational before the next failure occurs. The aim is to find a model that calculates the remaining useful life of each new example as a continuous number.

Random Forest algorithm (RF) [10] was applied to predict the outcomes, it is an ensemble learning method, It operates by constructing a set of decision trees at training time and outputting the mean prediction of the individual trees [8][9]. Decision trees are indeed ideal candidates for ensemble methods since they usually have low bias and high variance, making them very likely to benefit from the averaging process.

The random forests algorithm (for both classification and regression) is worked as follows:

- 1- Draw n bootstrap samples from the original data.
- 2- For each of the bootstrap samples, grow an un-pruned classification or regression tree, with the following modification: at each node, rather than choosing the best split among all predictors, randomly sample m of the predictors and choose the best split from among those variables.
- 3- Predict new data by aggregating the predictions of the n trees (i.e., majority votes for classification, average for regression).

The structures of random forests classifiers and regressor are illustrated in Figures 3 and 4 respectively.

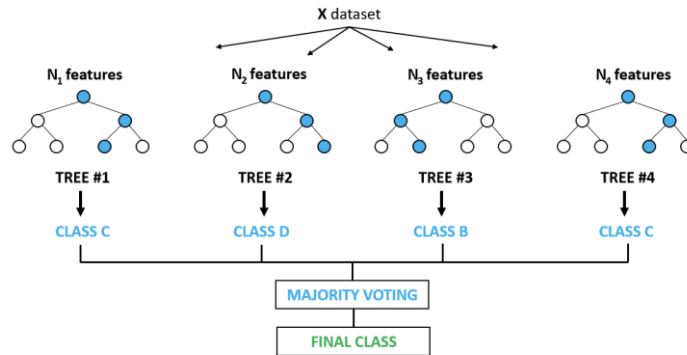


Figure 3. Random forest classifier. Adopted from [12]

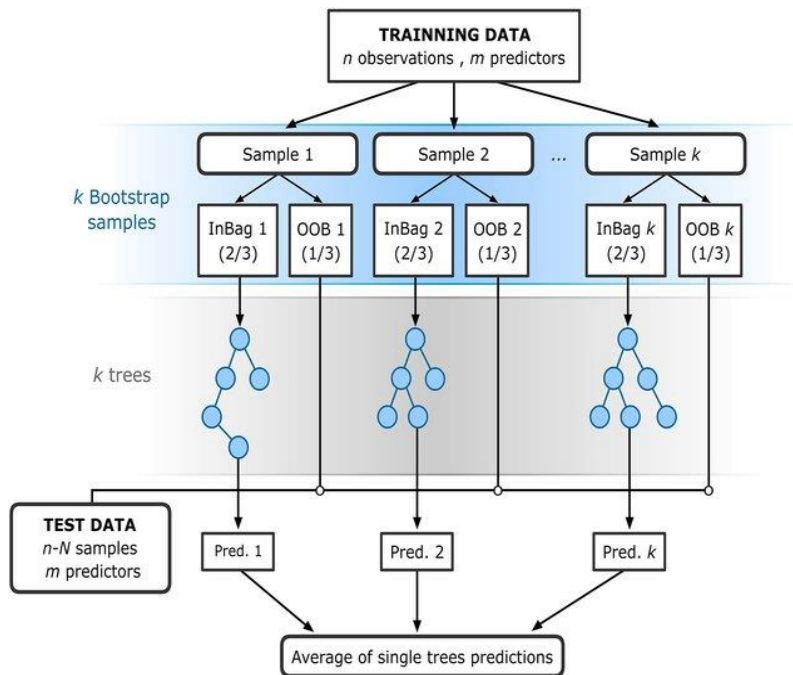


Figure 4. Random forest regressor. Adopted from [13]

2.4. Evaluation Measurements

The authors used the accuracy evaluation metric of the classification model by using the formula:

$$\text{Accuracy} = \frac{\text{true positives} + \text{true negatives}}{\text{total samples}} \tag{1}$$

The authors used the Root Mean Squared Error (RMSE) metric in order to evaluate the

regression model , where y_i is predicted value and y_i^{\wedge} is actual value by using the formula:

$$\text{RMSE} = \sqrt{\frac{1}{n} \sum_{i=1}^n (y_i - y_i^{\wedge})^2} \quad (2)$$

3. COMPUTATIONAL RESULTS

In this section, performance evaluation results of the prediction model are presented. The models were evaluated using the collected data which contains 10,963 records. The dataset was divided into training and testing dataset. The training dataset which is used in the training step includes 70% of the records and the remaining 30% is used in the testing step. According to performances metrics that used to evaluate the random forest classifier and regressor, the abnormality classifier achieved an average accuracy of 99% while the RMSE of the regressor approach achieved a value of 80.

The authors reassured that the models do not overfit by creating validation dataset and compare the model prediction against the validation labels. Figure 5 shows the model that was trained and validated on the training data. The graph produces two complexity curves, one for training and one for validation. The model does not seem to suffer from high variance and both have a high score, so the performance seems reasonably good.

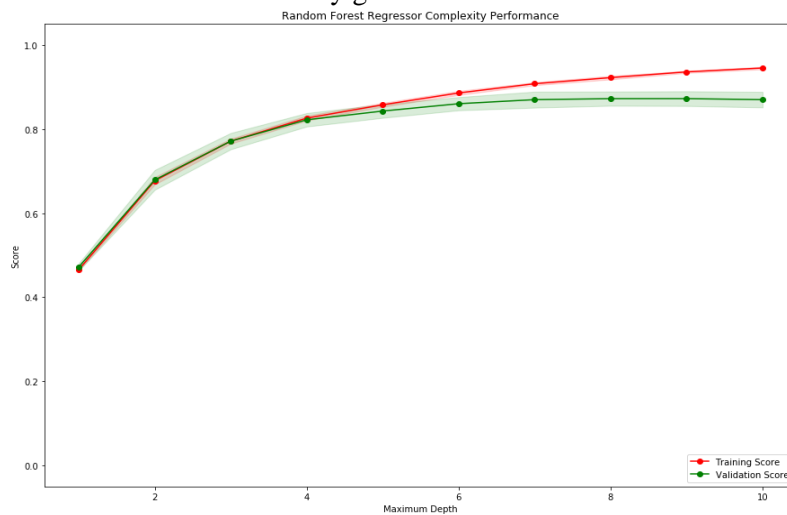


Figure 5. Complexity Performance.

4. CONCLUSION

In this paper, the authors demonstrated the potential of Machine Learning techniques on enhancing the operations of equipment and a methodology based on PdM machine learning approach on a duct-fan machine is presented. The methodology has been implemented in a real experimental environment and data has been collected by various sensors. Future work will go in the direction of having more robust dataset, investigating different fault scenarios, exploring a different set of features and add more relevant sensors.

ACKNOWLEDGEMENTS

The authors extend their appreciation to the Deanship of Scientific Research at King Saud University for funding this work through the Undergraduate Research Support Program, Project no. (URSP – 4 –19 – 121)

REFERENCES

- [1] Arcweb.com. (2018). Enterprise Asset Management (EAM) Market Size, Trends, Analysis, Forecast | ARC Advisory Group. [Online] Available: <https://www.arcweb.com/market-studies/enterprise-asset-management> [Accessed: 15- Dec- 2019].
- [2] Emerson-Unlocking Topn Performance. (2017). Paid Program: How Manufacturers Achieve Top Quartile Performance. [Online] Available: <https://partners.wsj.com/emerson/unlocking-performance/how-manufacturers-can-achieve-top-quartile-performanc> [Accessed: 15- Dec- 2019].
- [3] M. Mulders and M. Haarman, "Predictive Maintenance 4.0 Predict the unpredictable", PwC.In, 2017.[Online]. Available: <https://www.pwc.nl/nl/assets/documents/pwc-predictive-maintenance-4-0.pdf>. [Accessed: 15- Dec- 2019].
- [4] A. Chigurupati, R. Thibaux, and N. Lassar.“Predicting hardware failure using machine learning”.Annual Reliability and Maintainability Symposium, IEEE, 2016.
- [5] M. Paolanti, L. Romeo, A. Felicetti, A. Mancini, E. Frontoni, and J. Loncarski. “Machine Learning approach for Predictive Maintenance in Industry 4.0”. International Conference on Mechatronic and Embedded Systems and Applications, IEEE, 2018.
- [6] V. Mathew, T. Toby, V. Singh, B.M. Rao, and M.G. Kumar. “Prediction of Remaining Useful Lifetime (RUL) of turbofan engine using machine learning”.International Conference on Circuits and Systems, IEEE, 2018.
- [7] MPU 6050 Datasheet, [Online]. Available:<https://octopart.com/mpu-6050-invensense-19505926#> .[Accessed November. 2, 2019]
- [8] C. Jennings, D. Wu, J. Terpenney, "Forecasting obsolescence risk and product life cycle with machine learning", IEEE TRansactions on Components Packaging and Manufacturing Technology, vol. 6, no. 9, pp. 1428-1439, 2016.
- [9] W. Lin, Z. Wu, L. Lin, A. Wen, J. Li, "An ensemble random forest algorithm for insurance big data analysis", IEEE Access, vol. 5, pp. 16568-16575, 2017
- [10] L. Breiman, "Random Forests", Machine Learning , vol. 45, pp. 5-325, 2011
- [11] iPower-Booster-Inline-Exhaust-Grounded, [Online]. Available:<https://www.amazon.com/iPower-Booster-Inline-Exhaust-Grounded/dp/B008N4QIZG> .[Accessed November. 2, 2019]
- [12] "Random Forest Classifier – Machine Learning | Global Software Support", Globalsoftwaresupport.com, 2019. [Online]. Available:<https://www.globalsoftwaresupport.com/random-forest-classifier-bagging-machine-learning/>. [Accessed: 19- Mar- 2019]

- [13] V. Rodriguez-Galiano, M. Sanchez-Castillo, J. Dash, P. Atkinson and J. Ojeda-Zujar, "Modelling interannual variation in the spring and autumn land surface phenology of the European forest", *Biogeosciences*, vol. 13, no. 11, pp. 3305-3317, 2016

AUTHORS

Mashaal S. Maashi, She received the B.Sc. degree in computer Science from King Abdulaziz University, Jeddah, Saudi Arabia, in 2005, the M.Sc. degree in Computer Science from Glamorgan University, Wales, United Kingdom in 2009, and the Ph.D. degree in Computer Science from University of Nottingham, Nottingham, United Kingdom in 2014. She is currently an assistant professor in the Department of Software Engineering, College of Computer Science and Information sciences, King Saud University, Saudi Arabia. Her main research areas are, machine learning, artificial intelligence, evolutionary computation, optimization, intelligent computing and their applications. She is Editor of the International Journal of Computational & Neural Engineering (IJCNE). And Lead Editor for special issue theme "Computational Engineering" in IJCNE. She a board member for Global 2019 Congress on Computer Engineering. She a member in Technical Program Committee TPC of many International Conferences including: Evolutionary Computing (MIC-Evolu 2019), Computer Science and Engineering (MIC-Computing-19), Big Data and Security (ICBDS 2019) and Future Communications and Computing (MIC-FutureCom 2020).



CLASSIFICATION OF COMPUTER HARDWARE AND PERFORMANCE PREDICTION USING STATISTICAL LEARNING AND NEURAL NETWORKS

Courtney Foots¹, Palash Pal², Rituparna Datta¹ and Aviv Segev¹

¹Department of Computer Science, University of South Alabama,
Mobile, USA

²University Institute of Technology, Burdwan University, India

ABSTRACT

We propose a set of methods to classify vendors based on estimated central processing unit (CPU) performance and predict CPU performance based on hardware components. For vendor classification, we use the highest and lowest estimated performance and frequency of occurrences of each vendor in the dataset to create classification zones. These zones can be used to list vendors who manufacture hardware that satisfy given performance requirements. We use multi-layered neural networks for performance prediction, which accounts for nonlinearity in performance data. Several neural network architectures are analysed in comparison to linear, quadratic, and cubic regression. Experiments show that neural networks can be used to obtain low prediction error and high correlation between predicted and published performance values, while cubic regression can produce higher correlation than neural networks when more data is used for training than testing. The proposed methods can be used to identify suitable hardware replacements.

KEYWORDS

Computer Hardware, Performance Prediction and Classification, Neural Networks, Statistical Learning, Regression

1. INTRODUCTION

Computer performance is measured in relation to computational time and valuable work produced and is partly determined by hardware components such as the amount of memory and processor speed [1]. For this study, we are interested in specifically the central processing unit (CPU), which directly affects a computer's performance.

Computer performance prediction can be useful from several perspectives. If an accurate prediction is obtained, it can assist in detecting counterfeit hardware as well as viruses, spyware, Trojans, and other types of malware. Malware and counterfeit components can decrease performance or cause performance instability. There is a plethora of security measures that can be adopted to prevent malicious programs from being downloaded and remove them when they have been downloaded [2, 3]. There are also many novel ways of detecting counterfeit hardware [4, 5]. Thus, methods of detecting malware and counterfeits based on computer performance are useful and part of highly relevant topics in the technology field today.

We can also classify the vendor by the quality of their hardware. Each vendor produces hardware that operates at different standards. These differences could be due to differences in the intellectual property used, as well as the cost point of the hardware. Classifying the hardware based on performance can assist in determining which vendor sells hardware components that will maximize the average performance of the computer. It can also assist in identifying potential hardware replacements that will match the original performance standards.

We propose a set of methods to (1) classify the hardware manufacturer based on estimated CPU performance and (2) predict computer performance based solely on estimated CPU performance using a multi-layered neural network in comparison to regression techniques.

The outline of the rest of this paper is as follows. Section 2 provides a brief overview of related work in the domain of computer performance prediction and computer hardware classification. Section 3 explains the proposed set of methods. Section 4 details our experiments and results. Section 5 presents our conclusions.

2. RELATED WORK

On the topic of classification, Kar et al. [6] proposed a pattern classification model that uses quantitative and qualitative measurements to guide decision making in relation to vendor selection. This tool would assist its user by providing a robust analysis of the supplied collection of vendors so that they may choose the best vendor. In our method, we chose to classify vendors based on quantitative estimated CPU performance data only.

In the discussion of data analysis, Alexander et al. [7] presented a new methodology for analyzing computer performance data using nonlinear time series analysis techniques. The motivation was the concept that computers are deterministic nonlinear dynamic systems. Thus, the previous performance analyses in which computers were considered to be linear and time invariant are not representative of the nature of the actual testing conditions. In our method, we address the same issue of the nonlinearity of our performance data and use neural networks as accommodation.

Hardware performance prediction is a well-studied topic. Lopez et al. [8] explored a way to predict computer performance based on hardware component data without needing simulation. They used a deep learning model to generate a benchmark score for a given hardware configuration, then used multiple neural networks and principal component analysis to predict performance in comparison to the corresponding benchmarks. Neural network and linear regression techniques have been used to predict performance in multiprocessor systems [9]. Similarly, machine learning has been used to predict the performance of multi-threaded applications with various underlying hardware designs [10]. Girard et al. [11] designed a tool to predict the performance of avionic graphic hardware, which is used by engineers to determine the optimal hardware architecture design before manufacturing. Adjacent to the topic of predicting performance, Kang [12] used hardware performance to analyze the microeconomics of buying and leasing computers.

The dataset used in this study has previously been used for detecting scientific anomalies using probability density estimators [13] and fitting linear models in high dimensional spaces [14].

3. PROPOSED SET OF METHODS

3.1. CPU Performance Dataset Description

We aim to classify and predict the performance of CPUs based on a set of ten parameters from an opensource dataset [15]. This dataset contains 209 entries, representing a variety of vendors and models of CPUs. Though the data was donated in 1987, the attributes provided still work well with the scope of our study and are used as test data for the proposed method. The ten parameters of the dataset are listed below:

1. Vendor name
2. Model name
3. Machine cycle time in nanoseconds
4. Minimum main memory in kilobytes
5. Maximum main memory in kilobytes
6. Cache memory in kilobytes
7. Minimum channels in units
8. Maximum channels in units
9. Published relative performance
10. Estimated relative performance from original article [16]

Parameters 1 and 10 are used for vendor classification. Parameters 3 through 9 are used for performance prediction. Parameter 2 is not used in this study. Parameter 10 was calculated using linear regression by Ein-Dor and Feldmesser [16].

3.2. Proposed Classification Method for Hardware Vendors

The highest and lowest estimated performance values are recorded for each vendor, along with the frequency of occurrences of each vendor in the dataset. This information is used to create classification zones. Each zone is labeled with a range of relative performance. The goal is to produce a guide such that given a performance requirement, a list of vendors that manufacture hardware that meet the requirement can be produced.

3.3. Proposed Prediction Method for Hardware Performance

Input parameters 3 through 8 are used to predict the performance of the CPUs. Then, parameter 9 is used with our predicted performance value to calculate the Mean Squared Error (MSE) of the prediction and the correlation between predicted and published performance values. The MSE of the prediction provides insight on the level of accuracy of the prediction in relation to the published performance value. The correlation reflects the percentage of similarity between the predicted and published performance values.

The following is the standard formula used to calculate the MSE for a dataset of n CPUs, where p_i is the predicted performance and p_i' is the published performance:

$$MSE = \frac{1}{n} \sum_{i=1}^n (p_i - p_i')^2$$

To determine the correlation of the predicted and published performance values, we used the Pearson correlation formula to find the correlation coefficient and the significance level of the

correlation. The correlation coefficient r is calculated as follows, with the values m representing the mean of the predicted and published values:

$$r = \frac{\sum_{i=1}^n (p_i - m_{p_i})(p_i' - m_{p_i'})}{\sqrt{\sum_{i=1}^n (p_i - m_{p_i})^2 \sum_{i=1}^n (p_i' - m_{p_i'})^2}}$$

The significance level of the correlation is ascertained by first calculating the t value as follows:

$$t = \frac{r}{\sqrt{1 - r^2}} \sqrt{n - 2}$$

Then, the corresponding significance level is determined using the t distribution table with a degree of freedom of $n - 2$. If the significance level is less than 5%, then the correlation between the predicted and published performance values is considered to be significant.

Since the performance of a CPU is affected by other hardware components, there is no perfect or absolute formula to predict its performance. The scatterplot matrix between the inputs and output of our dataset is shown in Figure 1. From this figure, we can see that the relationship between the input variables and the output variable is random and nonlinear. As a result, we use multilayered neural networks, which are suited for random nonlinear input and output relationships.

Specifically, the performance predictions are acquired using various architectures of a multilayered feed forward network with six inputs and one output. When selecting architectures for our tests, we aimed for a variety of hidden layers to determine the level of versatility of the neural network in producing quality results. The inputs to the neural network are the previously discussed parameters. The output is the predicted performance, which is used with parameter 9 to calculate the MSE and correlation values.

We can use regression analysis for the prediction since CPU performance is a continuous measurement. Specifically, we use linear, quadratic, and cubic regression to model the input and output relationship of this dataset and predict performance. The input and output values for each of these are the same used for the neural network.

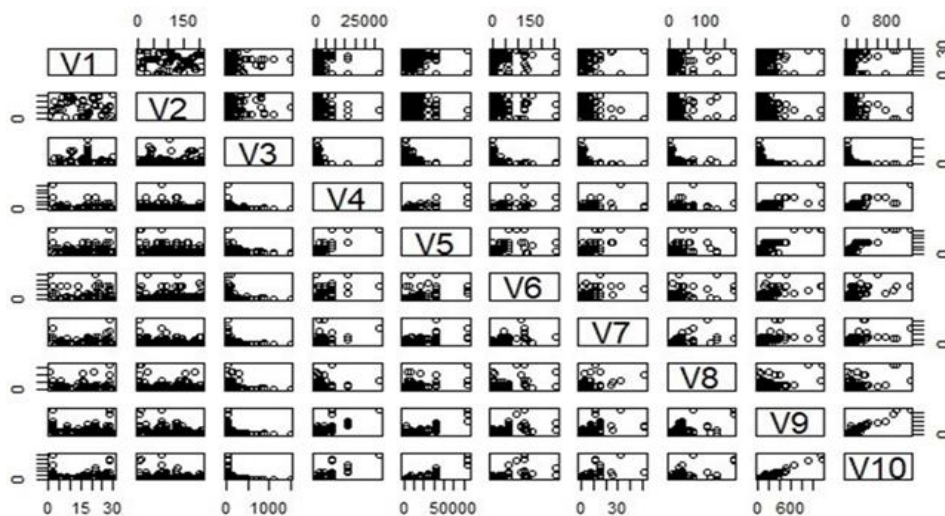


Figure 1. Scatterplot matrix of input and output variables for CPU performance data

4. EXPERIMENTS AND RESULTS

4.1. Vendor Classification Based on Estimated CPU Performance

The classification task is performed with the vendor names and estimated relative performances of each CPU in the dataset. The dataset contains 209 entries with 30 different vendors, out of which the highest and lowest performance values for each vendor as well as the frequency of occurrences of each vendor are tabulated in Table 1.

Table 1: Highest and lowest relative performance values along with frequency of occurrence of each vendor from the CPU performance dataset

Vendor	Highest Performance	Lowest Performance	Frequency
Amdahl	1238	132	9
Sperry	978	24	13
NAS	603	29	19
Siemens	382	19	12
IBM	361	15	32
NCR	281	19	13
Adviser	199	199	1
Honeywell	181	20	13
Gould	157	75	3
CDC	138	23	9
IPL	128	30	6
Burroughs	124	22	8
BASF	117	70	2
Magnuson	88	37	6
Cambex	74	30	5
DG	72	19	7
Nixdorf	67	21	3
Perkin-Elmer	64	24	3
BTI	64	15	2
HP	54	18	7
DEC	54	18	6
Prime	53	20	5
Harris	53	18	7
Wang	47	25	2
Stratus	41	41	1
Formation	34	34	5
Microdata	33	33	1
C.R.D	28	21	6
Apollo	24	23	2
Four-Phase	19	19	1

The classification result is shown in Figure 2. According to the results, the vendors can be classified into five zones. Each zone represents a performance standard, with Zone I being the lowest relative performance of 200 or less, and Zone V being the highest relative performance of

1000 or more. If the desired relative performance is less than 200, any vendor can be chosen. If the performance requirement is from 200 – 400, any one of NCR, IBM, Siemens, NAS, Sperry, or Amdahl can be chosen. The vendors NAS, Sperry, or Amdahl can be chosen for a performance requirement from 400 – 600. The vendors Sperry or Amdahl can be chosen for a performance requirement from 600 – 1000. Last, only Amdahl can be chosen for performance requirements more than 1000.

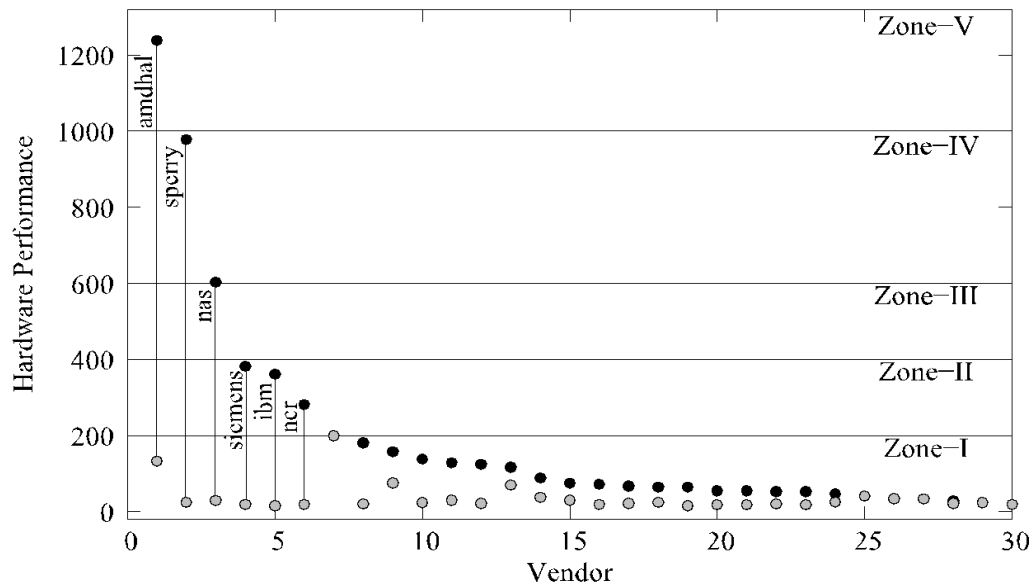


Figure 2. Classification of vendors based on estimated relative performance for CPU performance prediction

4.2. Computer Performance Prediction Based on Hardware Components

After scaling the data using Min-Max scaling, we construct several multilayered neural network architectures with various numbers of hidden layers. In Tables 2 through 5, the training-testing percentages represent the proportion of the dataset that was used for training and testing, respectively. The sequences of architecture values represent the number of neurons in each layer of the neural network. The scaled MSE and correlation of the predictions are calculated for each neural network architecture at each training-testing ratio. We also calculate the MSE and correlation of the predictions using linear, quadratic, and cubic regression analysis. All correlation coefficients have a significance value less than 5%, except for quadratic regression at 62.5% - 37.5% training-testing ratio. Therefore, the correlation coefficients between predicted and published performances for this study do have significance.

For all training-testing ratios, the lowest MSE values are produced by the neural network. For training-testing ratios 62.5% - 37.5% and 65% - 35%, the highest correlation values are produced by the neural network. For training-testing ratio 67.25% - 32.75%, the highest correlation value is produced by cubic regression, with the neural network outperforming linear and quadratic regression. For training-testing ratio 70% - 30%, the highest correlation values are produced by cubic and quadratic regression, with the neural network outperforming only linear regression.

Table 2: The MSE and predicted-published performance correlation for CPU performance prediction with 62.5% - 37.5% training-testing ratio

Training-Testing	Method	Architecture	Scaled	Correlation	Significance
62.5% - 37.5%	Neural Network	6 - 3 - 1	0.00357	0.913	2.2 e-16
		6 - 4 - 2 - 1	0.00387	0.909	2.2 e-16
		6 - 4 - 3 - 2 - 1	0.00307	0.924	2.2 e-16
		6 - 5 - 4 - 3 - 2 - 1	0.00369	0.914	2.2 e-16
	Regression	Linear	0.00629	0.848	2.2 e-16
		Quadratic	0.02555	0.136	0.2326
		Cubic	0.01549	0.898	2.2 e-16

Table 3: The MSE and predicted-published performance correlation for CPU performance prediction with 65% - 35% training-testing ratio

Training-	Method	Architecture	Scaled	Correlation	Significance
65% - 35%	Neural Network	6 - 3 - 1	0.00190	0.956	2.2 e-16
		6 - 4 - 2 - 1	0.00209	0.951	2.2 e-16
		6 - 4 - 3 - 2 - 1	0.00359	0.915	2.2 e-16
		6 - 5 - 4 - 3 - 2 - 1	0.00197	0.958	2.2 e-16
	Regression	Linear	0.00470	0.884	2.2 e-16
		Quadratic	0.00260	0.940	2.2 e-16
		Cubic	0.00242	0.944	2.2 e-16

Table 4: The MSE and predicted-published performance correlation for CPU performance prediction with 67.25% - 32.75% training-testing ratio

Training-Testing	Method	Architecture	Scaled	Correlation	Significance
67.25% - 32.75%	Neural Network	6 - 3 - 1	0.00284	0.934	2.2 e-16
		6 - 4 - 2 - 1	0.00223	0.954	2.2 e-16
		6 - 4 - 3 - 2 - 1	0.00342	0.920	2.2 e-16
		6 - 5 - 4 - 3 - 2 - 1	0.00220	0.952	2.2 e-16
	Regression	Linear	0.00500	0.884	2.2 e-16
		Quadratic	0.00757	0.910	2.2 e-16
		Cubic	0.00685	0.961	2.2 e-16

Table 5: The MSE and predicted-published performance correlation for CPU performance prediction with 70% - 30% training-testing ratio

Training-	Method	Architecture	Scaled	Correlation	Significance
70% - 30%	Neural Network	6 - 3 - 1	0.00351	0.898	2.2 e-16
		6 - 4 - 2 - 1	0.00332	0.886	2.2 e-16
		6 - 4 - 3 - 2 - 1	0.00414	0.880	2.2 e-16
		6 - 5 - 4 - 3 - 2 - 1	0.00348	0.867	2.2 e-16
	Regression	Linear	0.00355	0.850	2.2 e-16
		Quadratic	0.00386	0.922	2.2 e-16
		Cubic	0.01415	0.936	2.2 e-16

The best performing methods, architectures, and training-testing ratios are compared in Figure 3 with respect to lowest MSE and in Figure 4 with respect to highest correlation. It is clear from Figure 3 that the lowest MSE overall is obtained using architecture 6-3-1 with a training-testing ratio of 65% - 35%. Figure 4 shows that the highest correlation overall is obtained using cubic regression with a 67.25% - 32.75% training-testing ratio. A plot of the published vs. predicted CPU performance by the neural network with 65% - 25% training-testing ratio and 6-3-1 architecture is shown in Figure 5, and the best performing neural network architecture is shown in Figure 6. There appears to be no correlation between the number of hidden layers in the architecture of a neural network and the relative performance of the neural network.

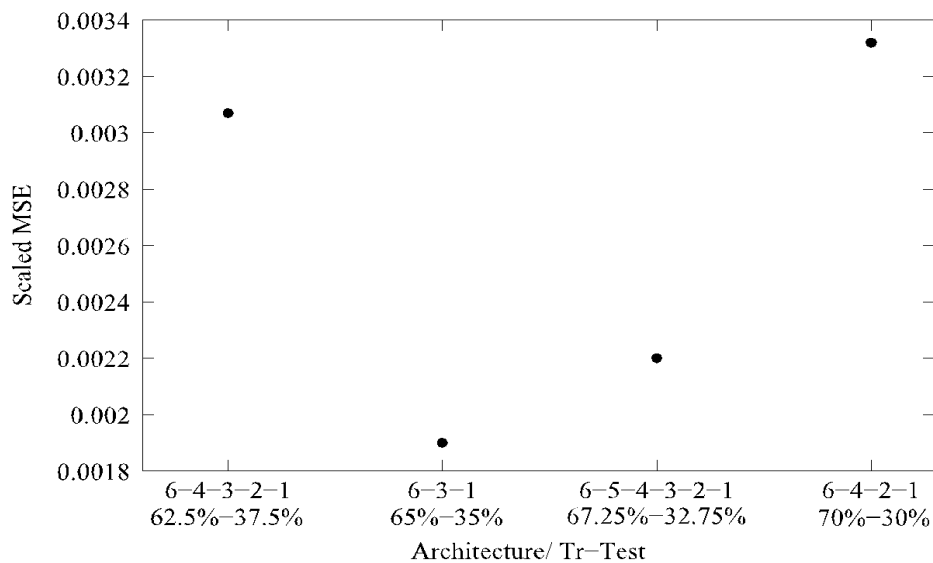


Figure 3. Comparison of architectures along with training testing ratio with respect to scaled Mean Squared Error for CPU performance prediction

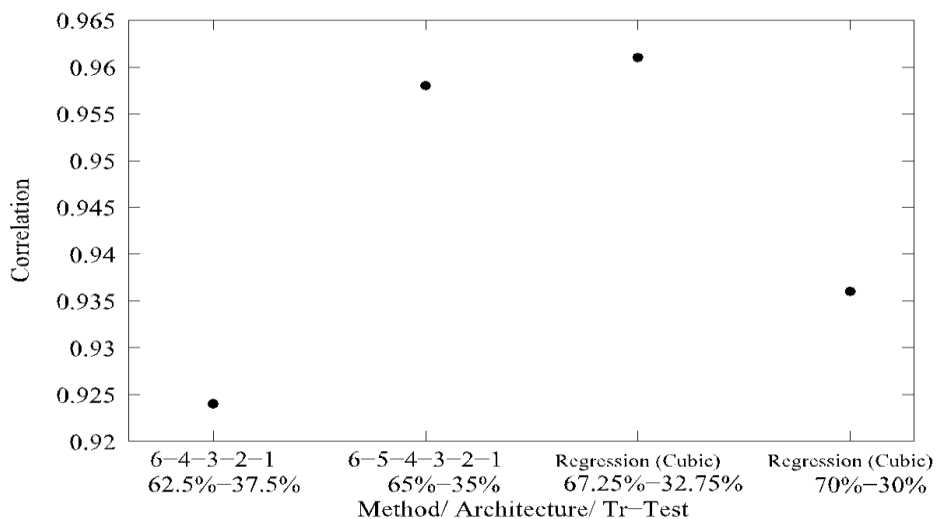


Figure 4. Comparison of methods and architectures along with training testing ratio with respect to correlation for CPU performance prediction

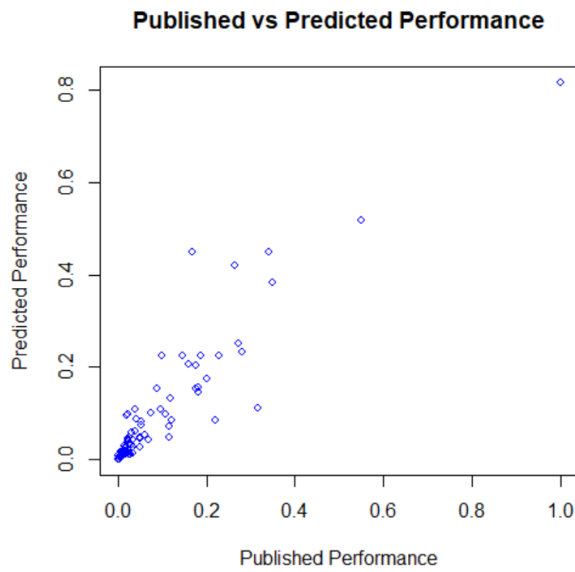


Figure 5. Plot of the published vs. predicted CPU performance for neural network with 65% - 25% training-testing ratio and 6-3-1 architecture

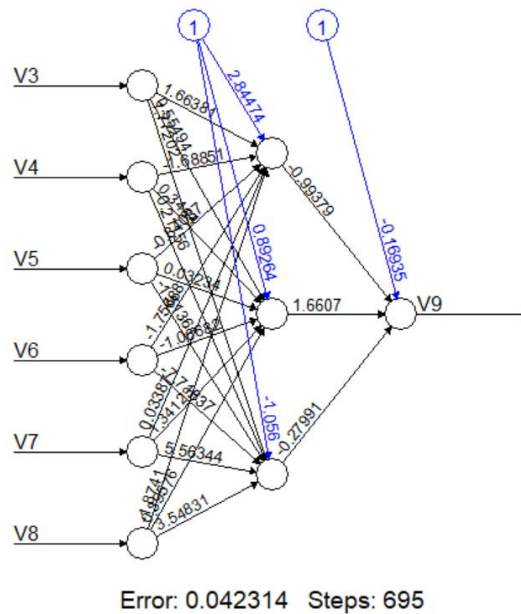


Figure 6. Graphical representation of the 6-3-1 neural network architecture

5. CONCLUSIONS

In this paper, both classification and prediction tasks are performed to analyze the performance of CPUs documented in our test dataset. The classification study shows that 30 vendors can be successfully classified into 5 performance zones. Each zone provides information about the relative performance capabilities of the vendors' hardware. Performance prediction is generated using neural network and regression techniques which accommodate the random, nonlinear relationship between input and output variables. Among all prediction results, the neural network with 65% training - 35% testing ratio and 6-3-1 architecture performs the best in terms of having

the lowest scaled MSE. However, the performance of cubic regression with 67.25% training - 32.75% testing ratio is found to be best in terms of the highest correlation. The numerous experiments with varying architectures and training-testing ratios show that the obtained results are robust. The results from our Pearson correlation analysis show that the correlations between the predicted and published performance values are significant.

The results from our performance prediction study show that neural networks can be used to obtain lower prediction error and often higher significant correlation between predicted and published values. However, cubic regression may have better predicting capabilities than a neural network when a higher percentage of the data is used for training. While this does reiterate our initial observation that there is no perfect or absolute method of predicting CPU performance, this study can be extended to analyze how hidden layers in the architecture of the tested neural networks affect their predicting capabilities. The prediction method can be also used on current hardware performance data to determine if neural networks outperform regression for a more robust range of experimental structures.

Our classification result shows that other than Zone-V, a given required performance can be obtained by more than one vendor. While this result does show that suitable replacement hardware can be found using this method, it also implies that hardware configuration can be copied or tampered with while still having nearly the same performance as the original configuration. To alleviate this drawback, the work will be extended to detect counterfeit hardware by a more thorough analysis and comparison of computer hardware performance

ACKNOWLEDGEMENTS

The work is supported by the Industry Advisory Board (IAB) of an NSF Industry–University Cooperative Research Center (IUCRC), United States under Grant DFII-1912-USA.

REFERENCES

- [1] Lilja, D. (2005) *Measuring Computer Performance: A Practitioner's Guide*, University of Minnesota, Cambridge University Press.
- [2] Aslan, O. & R. Samet (2020) "A Comprehensive Review on Malware Detection Approaches" *IEEE Access*, Vol. 8, pp 6249 - 6271.
- [3] Bakhshinejad, N. & A. Hamzeh (2020) "Parallel-CNN Network for Malware Detection," *IEEE Information Security*, Vol. 14, Issue 2, pp 210 - 219.
- [4] Wang, X., Y. Han, & M. Tehranipoor (2019) "System-Level Counterfeit Detection Using On-Chip Ring Oscillator Array," *IEEE Transactions on Very Large Scale Integration (VLSI) Systems*, Vol. 27, Issue 12, pp 2884 – 2896.
- [5] Chattopadhyay, S., P. Kumari, B. Ray, R. Chakraborty (2019) "Machine Learning Assisted Accurate Estimation of Usage Duration and Manufacturer for Recycled and Counterfeit Flash Memory Detection," *2019 IEEE 28th Asian Test Symposium (ATS)*, Kolkata, India, pp. 49-495.
- [6] Kar, A., A. Pani, B. Mangaraj, & S. De (2011) "A Soft Classification Model for Vendor Selection," *International Journal for Information and Education Technology*, Vol. 1, No. 4, pp 268 - 272.
- [7] Alexander, Z., T. Mytkowicz, A. Diwan, & E. Bradley (2010) "Measurement and Dynamical Analysis of Computer Performance Data" *Springer, Berlin, Heidelberg*, Lecture Notes in Computer Science, Vol. 6065, pp 18-29.

- [8] Lopez, L., M. Guynn, & M. Lu (2018) "Predicting Computer Performance Based on Hardware Configuration Using Multiple Neural Networks," *IEEE*, 17th IEEE International Conference on Machine Learning and Applications (ICMLA).
- [9] Ozisikyilmaz, B., G. Memik, & A. Choudhary (2008) "Machine Learning Models to Predict Performance of Computer System Design Alternatives," *IEEE*, 37th IEEE International Conference on Parallel Processing.
- [10] Agarwal, N., T. Jain, & M. Zahran (2019) "Performance Prediction for Multi-threaded Applications," *International Workshop on AI-assisted Design for Architecture*.
- [11] Girard, S., V. Legault, G. Bois, & J. Boland (2019) "Avionics Graphics Hardware Performance Prediction with Machine Learning," *Scientific Programming*.
- [12] Kang, Y. (1989) "Computer hardware performance: production and cost function analyses," *Communications of the ACM*, Vol. 32, No. 5, pp 586–593.
- [13] Pelleg, D. (2004) "Scalable and Practical Probability Density Estimators for Scientific Anomaly Detection," School of Computer Science, Carnegie Mellon University.
- [14] Wang, Y. (2000) "A New Approach to Fitting Linear Models in High Dimensional Spaces," Department of Statistics, University of Auckland.
- [17] Ein-Dor, P. & J. Feldmesser, Donor: W. Aha (1987) *Computer Hardware Data Set*, UCI Machine Learning Repository, <https://archive.ics.uci.edu/ml/datasets/Computer+Hardware>.
- [16] Ein-Dor, P. & J. Feldmesser (1987) "Attributes of the Performance of Central Processing Units: A Relative Performance Prediction Model," *Communications of ACM*, Vol. 30, pp 308-317.

AUTHORS

Courtney Foots is researching as an undergraduate student at the University of South Alabama, studying computer science and mathematics. Her research interests include counterfeit hardware detection, applications of artificial intelligence, and optimization.



Palash Pal received a bachelor's degree in Technology from University Institute of Technology, Burdwan University, West Bengal, India.

Rituparna Datta is working as a Computer Research Associate-II in the Department of Computer Science, University of South Alabama. Prior to that, he was an Operations Research Scientist in Boeing Research & Technology (BR&T), BOEING, Bangalore.



Aviv Segev is working as an Associate Professor at the Department of Computer Science, University of South Alabama. His research interest is looking for the DNA of knowledge, an underlying structure common to all knowledge, through analysis of knowledge models in natural sciences, knowledge processing in natural and artificial neural networks, and knowledge mapping between different knowledge domains.



SAFETY HELMET DETECTION IN INDUSTRIAL ENVIRONMENT USING DEEP LEARNING

Ankit Kamboj and Nilesh Powar

Advanced Analytics Team, Cummins Technologies India Pvt. Ltd, Pune, India

ABSTRACT

Safety is of predominant value for employees who are working in an industrial and construction environment. Real time Object detection is an important technique to detect violations of safety compliance in an industrial setup. The negligence in wearing safety helmets could be hazardous to workers, hence the requirement of the automatic surveillance system to detect persons not wearing helmets is of utmost importance and this would reduce the labor-intensive work to monitor the violations. In this paper, we deployed an advanced Convolutional Neural Network (CNN) algorithm called Single Shot Multibox Detector (SSD) to monitor violations of safety helmets. Various image processing techniques are applied to all the video data collected from the industrial plant. The practical and novel safety detection framework is proposed in which the CNN first detects persons from the video data and in the second step it detects whether the person is wearing the safety helmet. Using the proposed model, the deep learning inference benchmarking is done with Dell Advanced Tower workstation. The comparative study of the proposed approach is analysed in terms of detection accuracy (average precision) which illustrates the effectiveness of the proposed framework.

KEYWORDS

Safety Helmet Detection, Deep Learning, SSD, CNN, Image Processing

1. INTRODUCTION

The application of video surveillance is vast and multi-dimensional, from online facial expression to traffic signal rule break and even to health sectors. The monitoring of violations of wearing safety helmet in industrial environment involves a lot of manual effort hence the need of having an automatic surveillance system is of utmost importance. Deep learning and its applications in computer vision made a breakthrough due to its computational process, as well as accuracy of the detection of a target object but implementing the model for detection in real time is sometimes challenging if we are testing the model on low power device like raspberry pie. In this scenario, the state-of-the-art deep learning one stage object detection methods like SSD [1] (Single Shot Multi Box Detector) and Yolo [2] (You Only Look Once) are useful. Even though the model will run faster but there would certainly be a trade-off between speed and accuracy and SSD models doesn't provide good performance on small objects but for large objects, they provide competitive performance in comparison to other deep learning models. [3] SSD are often combined with lightweight feature extractors like MobileNet and they have different usage of depth wise separable convolution in comparison to traditional CNNs. [4]

In this paper we have proposed a novel and practical approach of detecting safety helmets by optimizing the performance of SSD MobileNet model for smaller size objects. The proposed approach utilizes application of two CNN models one after the other, first the SSD model is used

for detecting persons from a video data and then the SSD model identifies whether the person is wearing the safety helmet.

The rest of the paper is organized in the following manner: Section II describes the literature review and related work. Data pre-processing and methodology of novel safety detection algorithm are explained in Section III. Experimental evaluation and results are presented in Section IV. Finally, the paper ends with conclusions and future work in Section V.

2. LITERATURE REVIEW AND RELATED WORK:

Object detection involves both object classification and localization, which requires identification of bounding box around the object that needs to be detected. It is problem of not determining whether an object is in an image but also its location. To predict the coordinates of bounding box we need x and y coordinates for the centre, height and width of the rectangle.

There are many research papers regarding image classification which are based on only feature space. To extract features for object recognition, HOG (Histogram of gradients), SIFT (Scale-invariant feature transform) and Haar-like features are used. [5]. It is very difficult to design a reliable feature extractor by human considering different illumination, backgrounds and appearances of an object. The initial work on implementing object detection algorithms was seen in 2001 using Haar cascade classifiers used by Viola-Jones in their face detection algorithm by minimizing computation time. Haar Cascades takes series of cascaded classifiers using Haar features and then uses a sequence of steps to identify a face and even though they are fast with decent accuracy but are difficult to develop, train and optimize. [6] Yet there are drawbacks for this method as detection of tilted or turned faces is not that effective and is also sensitive to lighting conditions. [7]

For any deep learning computer vision task there are sequence of steps that needs to be followed. Firstly, we need to collect visual input composed of images or videos from an imaging device like camera. Then each image needs to be passed through a pre-processing step like noise reduction, colour correction, scaling to enhance the quality and detail of the image. Then the area of interest needs to be selected in an image by annotating each frame so that the model could be trained with relevant features. Some of the images that are kept for testing the model are fed to trained model that could recognize the object of interest and it does so with a certain probability. The input for a CNN is an image and output are the distribution of class scores from which we can get the predicted class for that image. The CNN is made up of series of layers that learn to extract relevant features out of any image such that each layer finds progressively more and more complex features. The backbone of CNN is convolutional layer, where a sequence of many image filters is applied which are also called as convolutional kernels. The filters may have extracted the features like edges of objects or colours that distinguish the different classes of image. As the CNN trains, it updates the weights that define the image filters in this convolutional layer using backpropagation. The result is classifier with convolutional layers that have learned to filter images to extract distinguishing features. [5]

Neural Networks take extremely long time to train, even if you use GPU. Deep learning researchers these days are committed to openness. We can take an existing pretrained neural network and its weights which is called transfer learning. [8] Then by doing some fine tuning we make the network for completely new problems. e.g. we can take SSD MobileNet trained on COCO data and use it on totally new data. [9] We can further do fine tuning of pretrained weights using backpropagation which would eventually result in better accuracy. One major advantage of transfer learning is that when you don't have enough data for model training.

Single shot multi box detector: SSD is the real milestone in computer vision as before this object detection algorithms were slow and require multiple stages, but with SSD we can get real time performance. As depicted in Figure 1, a feature extractor VGG16 is used. The name VGG stands for visual geology group, which is the research group that invented it and is one of the main benchmarks in image classification algorithms. The SSD object detection algorithm has two main steps, one is to extract the feature maps and other is the convolution filters application to detect objects. Instead of thinking of entire CNN as the state-of-the-art feature extractor, we can think of each subpart of CNN as feature extractor. We therefore take output from multiple parts of CNN and let them do their own object detection. The aspect scores and default object positions are uniquely defined such that while prediction, the SSD network produces scores for the existence of each object class in each default box and generates a change to box for a better match of their object shape. Instead of creating a single grid, SSD create several grids with different scales and feature maps of different resolutions are used to predict object of different scales. [1]

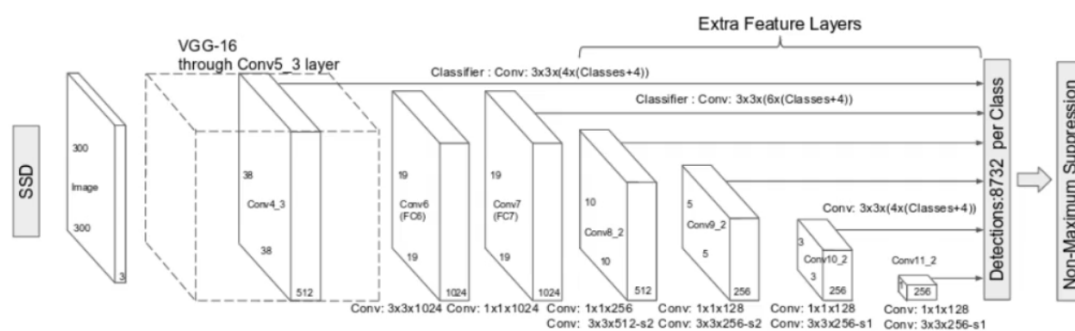


Figure 1: Single Shot Multibox Detector: SSD architecture. Reprinted from [1]

3. SAFETY HELMET DETECTION SYSTEM

3.1. Data Preprocessing

3.1.1. Data Preparation

The videos are collected from areas in industrial environment where safety compliance of wearing helmet is mandatory. We have considered footages from cameras installed at different locations to build a robust set of images. Our main objective is to recognize persons without helmet therefore video footages having persons with and without helmet are considered for analysis. The cameras are installed at the entrance of restricted zones and the experiment is conducted such that a person must face towards the camera while entering the hazardous zones. The cameras are placed at head level elevation from the ground (roughly 6 feet) to have videos with proper alignment of person's head for better detection of helmet. The videos are taken from cameras with resolution (1920*1080) with frame rate of 25 frames per second.

3.1.2. Data Annotation

In our data, proper annotation plays a major role. Annotations are metadata which describes the position of an object in the image. For an image classification algorithm, annotation is not at all necessary as the output only says about the class of the image (i.e. if the object is in that image or not) but in object detection algorithms it is necessary to train an algorithm with the exact position of the object in images.

For annotation we have used a Python library called labeling which helps to annotate an image manually (makes a bounding box outside the object in the frame) with multiple classes and

multiple objects for a frame. Every single object when annotated, it makes a .xml file which contains its four co-ordinates in the frame along with its given class in it (in PASCAL VOC format). For multiple object in a frame with different class, it just follows same rule and add the co-ordinates and classes of the other object in a new line of the .xml file. It is important to annotate properly otherwise it would result in underfitting or overfitting the model for the data and would detect wrong objects or even would not detect objects at all.

3.2. Methodology

In the novel safety helmet detection system as shown in Figure 2 and Figure 3, first CNN detects persons from the video data and then the second CNN detects whether the person is wearing the safety helmet. The detection system consists of four steps: a) SSD algorithm for person detection b) Cropping the precited images of persons c) Manually annotating the cropped images d) Implementing SSD algorithm for helmet detection.

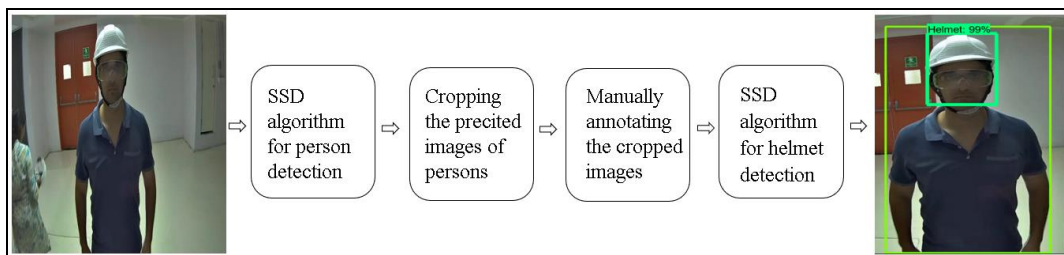


Figure 2. Safety helmet detection system

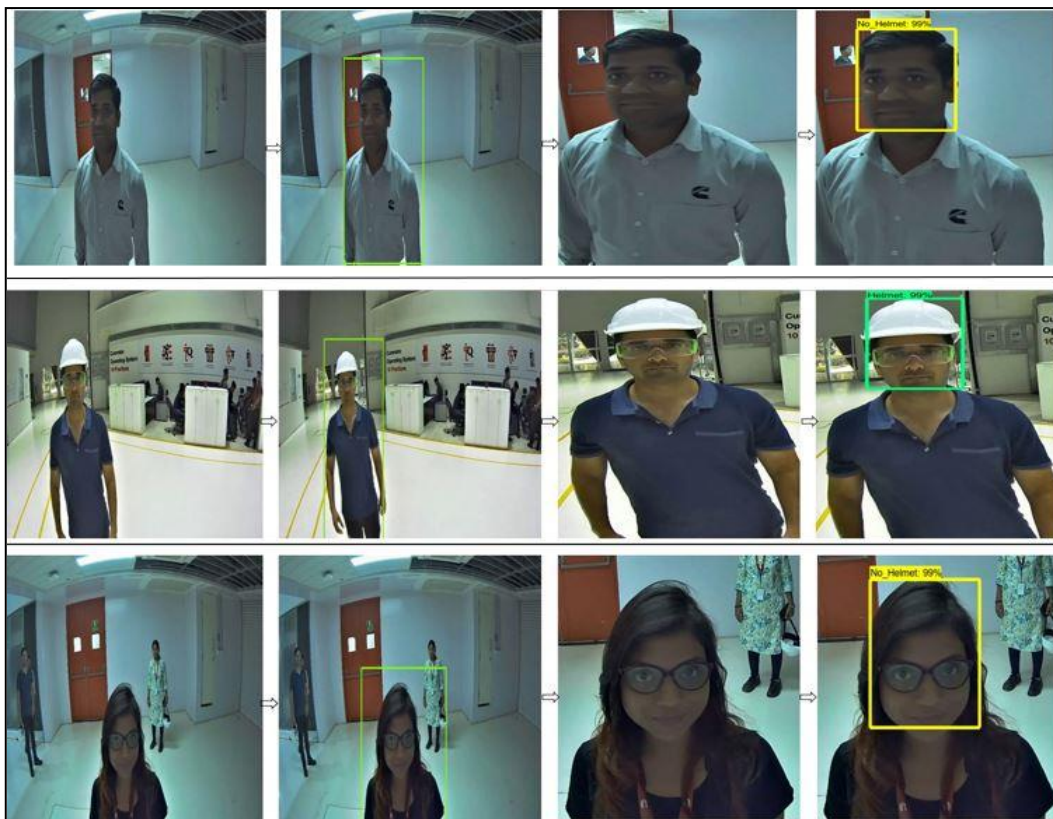


Figure 3. Safety helmet detection system

3.2.1. SSD Algorithm for Person Detection

In object detection problem it is beneficial to identify object of interest within in image to lower down false positives in predictions. Also, smaller the region to search for an object, lesser will be the processing time for a detection algorithm. [10]

We have used here SSD MobileNet object detection algorithm that is pretrained on coco dataset and implemented on the TensorFlow deep learning software platform. Even though SSD is state-of-art deep learning object detection model, there are many advancements in feature extractor for SDD (like VGG, ResNet or MobileNet). The model SSD-mobilenet-v1-coco with the weights pretrained on COCO data is used at the first step for detecting persons. There are 80 classes in COCO dataset which is widely used for benchmarking performance of deep learning algorithms. [9] The model is further modified to detect only the person class.

3.2.2. Cropping the Precited Images of Persons

While running the SSD person detection algorithm we have simultaneously cropped the images of predicted class around the bounding box in an image. SSD performs well even with a simple extractor like MobileNet but it is challenging task when it comes for detection of small objects. [3] Also, the SSD algorithm used here needs to have input images of size of 300*300(height: 300 width: 300), hence to improve the detection accuracy the cropped images with dimensions lesser than 160*160 are discarded for further processing as they would be of lower quality after resizing to fixed shape resizer of 300*300.

3.2.3. Manually Annotating the Cropped Images

Annotating bounding box on any visible object makes it recognizable for machines and data of annotated images is used in training deep learning algorithm to learn patterns of the object of interest. Further manual annotations are done for all the cropped images using Python library called labeling by drawing bounding boxes around the object of interest.

Here we have labelled two classes: “Helmet”: for persons wearing the safety helmet and “No_Helmet” otherwise. If multiple persons are present in a single image, both the classes are annotated in that image and the bounding boxes are drawn for only for the head area as shown in figure. Fig.4. The rectangular coordinates of annotated objects are stored in a .xml file along with its class in PASCAL VOC format and these later act as ground truth values for while training CNN in the next step of helmet detection.

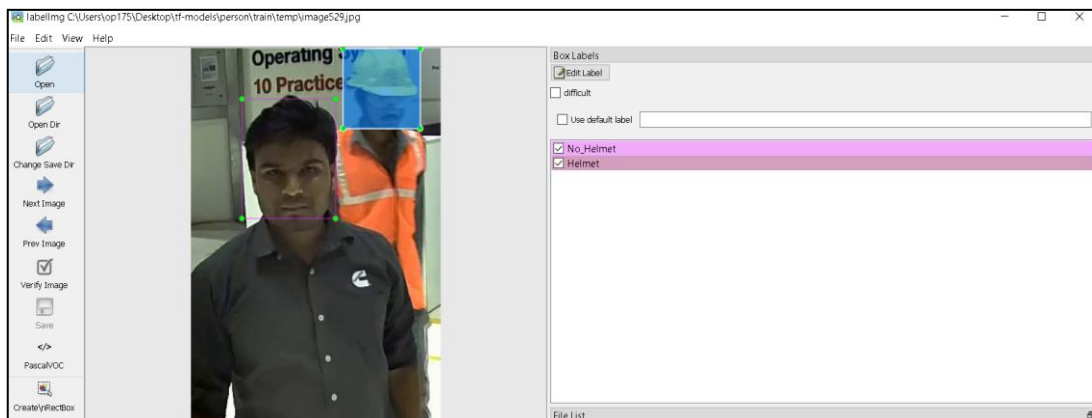


Figure 4. Manual Annotations in Labelimg

3.2.4. Implementing SSD Algorithm for Helmet Detection

The SSD MobileNet algorithm (SSD-mobilenet-v1-coco) with the weights pretrained on COCO data is then used as second CNN for detections of two classes: Helmet and No_Helmet. In computer vision, model that is trained on large benchmark dataset to provide a solution for a similar problem and hence providing more accurate models with lesser time is called pretrained model and the process is called transfer learning. The transfer learning helps to learn the patterns of new dataset by further fine tuning of pretrained weights using backpropagation.

4. EXPERIMENTAL EVALUATION AND RESULTS

4.1. Literature Review of Evaluation Metrics

Mean Average Precision(mAP) is the most widely used evaluation metrics for object detection problem. [11] The Area under curve (AUC) curve fails when to check the performance of an object detection algorithm as the curve goes up and down in zigzag manner. Even when comparing two graphs become very hard. To get rid of this problem an 11 points interpolation is done to summarize precision vs recall curve by taking average of the precision values at different recall values in $[0,0.1,0.2, \dots, 0.9,1]$, where $\rho_{interp}(r)$ is the maximum precision value at that point.

$$\text{Average Precision} = \frac{1}{11} \sum_{r \in \{0,0.1,\dots,1\}} \rho_{interp}(r) \quad (1)$$

$$\text{Precision} = \frac{\text{total number of correct detection}}{\text{total number of detection}} \quad (2)$$

$$\text{Recall} = \frac{\text{total number of correct detection}}{\text{total no. of target detect ground truth}} \quad (3)$$

If C is number of classes (in our case C=2 (Helmet and No_Helmet)), mAP is calculated by

$$\text{mAP} = \frac{\sum_{c=1}^C \text{average Precision}(c)}{C} \quad (4)$$

4.2. Model Hyperparameters

There is no predefined rule to select some of the parameters of any deep learning model. That's why tuning certain hyper parameters play a vital role in deploying such a model. How a deep network will train itself solely depends on these hyperparameters. Below we have discussed about certain optimization hyper-parameters some model hyper-parameters as they are flexible to the deployer of the algorithms and setup before training. These parameters affect the runtime of the model as these are the core features indicates convergence criteria or stopping criteria of the algorithm.

4.2.1. Number of Steps

The steps parameter indicates the number of training steps to run over data. Here we have kept 69,744 i.e. approx.(70k) steps for model training.

4.2.2. Learning Rate and Decaying Rate

When learning rate is very low the model takes much more time to converge again if it's too high the point of convergence may be missed. Taking into consideration these ideas, we have taken the default learning rate values for SSD_mobilenet_vi_coco and started training with an initial exponential decaying learning rate of .004, the decay steps are 800720 and decay factor is .95.

4.2.3. IoU (Intersection over Union)

IOU is a function that is used for both object localization in non-max suppression and evaluating the object detection algorithm. It is computed by the given formula, where intersection and union of area refers to the intersection and union of two bounding boxes. IOU value greater than 0.5 is a benchmark result. More IOU implies better accuracy. Here we have used IoU ratio as 0.5, i.e. when the predicted bounding box and the ground truth box overlap more than 50%, the predicted box has been considered as a correct result.

$$\text{IoU} = \frac{\text{size of the intersection area}}{\text{size of union area}} \quad (5)$$

4.3. Experimental Results

We have used advanced workstation for running this model, which has Intel(R) Xeon(R) Gold 6148 CPU @2.40Ghz, 384 GB RAM and 16 GB NVIDIA Quadro P5000 GPU on Windows10. The versions of few important libraries are: Python:3.6.8, Tensorflow:1.13.1, Numpy:1.16.2, open-cv:4.1.0, PIL: 6.0.0, Cuda 10: V10.0.130, CUDNN: 7.4.1. For evaluating the performance of the model, we have the dataset of cropped images from person detection model. The dataset consists of 5773 images, among which (4043 images) are in training set, (865 images) are in testing set and (865 images) are in validation set. The deep learning inference benchmarking is done on the above-mentioned workstation and it took around 17 hours for 69,744 steps of training the model.

The graphs of experimental results are taken from TensorBoard, which is a visualization software to analyse, debug and understand the flow of tensors and different performance metrics. In TensorFlow we have two basic components: operations and tensors. [12] When a model is created, it consists of set of operations and data or tensors are feed into the model and then the tensors will flow between operations until you get the output tensor.

TensorBoard are mainly used to write summaries to visualize learning and we have used the detection evaluation metrics used by COCO. [13] As depicted in Figure 5, it is a plot of mean Average Precision(mAP) at 50% IOU. On the x axis we have number of steps used for training and on the y axis we have the value of mAP. In the starting of training, the mAP has a sharp rising slope till 10k iterations, after that there is slight gradual increase till 35k(approx.) iterations and post that the accuracy is stagnant with very less significant change.

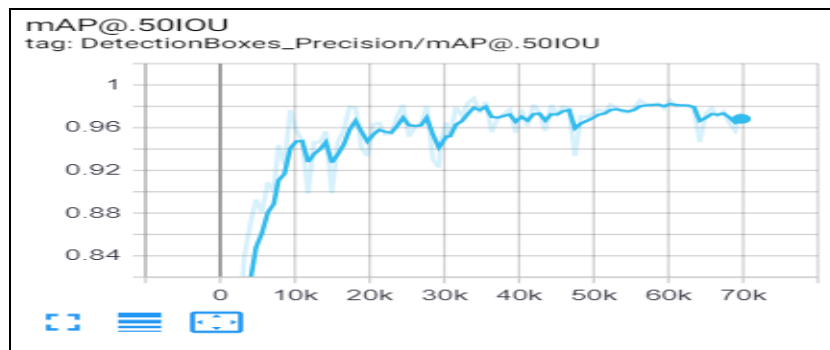


Figure 5. mean Average Precision(mAP) at 50% IOU

In the next Figure 6, it demonstrates the Average Recall (AR) given for 1 detection per image (AR@1), 10 detections per image (AR@10) and 100 detections per image (AR@100). [13]. On the x axis we have number of steps used for training and on the y axis we have the value of AR, for example, AR@10 would imply that for a single image we take 10 highest confidence predictions and then calculate the metrics on those 10 detections. Since in our dataset after the output of person detection algorithm, most of the time we have only one ground truth object per image and hence we have similar curves for all AR@1, AR@10 and AR@100.

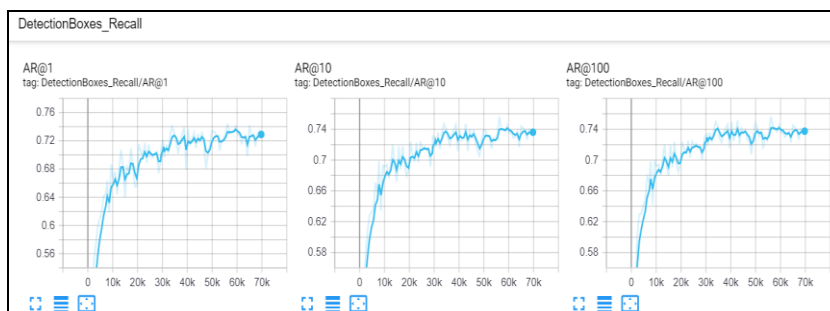


Figure 6. Average Recall with 1,10 & 100 detections per image

The training loss and validation loss are shown in Figure 7 and Figure 8 respectively. Here on the x axis we have number of steps used for training and on the y axis we have the loss value. As depicted in Training loss, we observe that the loss is decreasing at faster till 10k training iterations and beyond that there is gradual decrease in training loss. Visualizing the validation loss, we notice that loss decreased till 10k training steps, then there are some fluctuations in loss and it gradually decreases till 35k training steps which is further shows increasing trend till 70k.

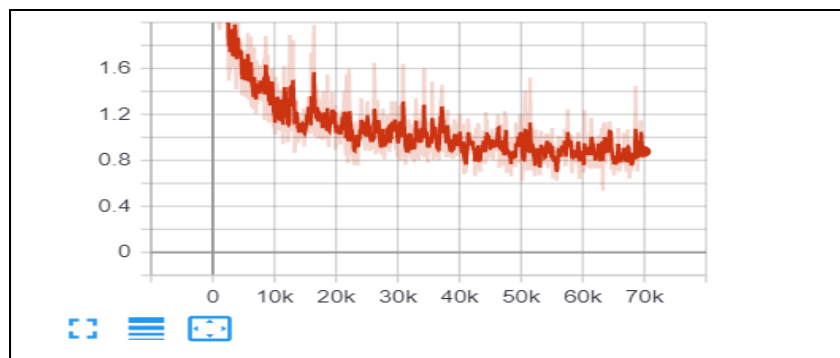


Figure 7. Training Loss wrt no. of training steps

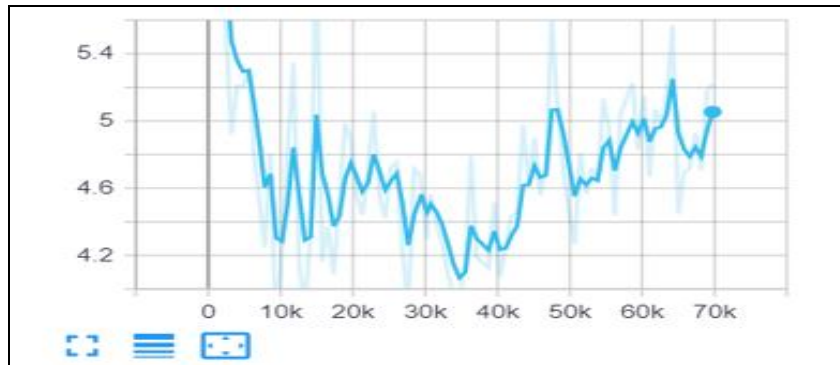


Figure 8. Validation Loss wrt no. of training steps

Based on the Figures 5, 6 & 8, it is observed that the number of training steps should be near to 35k as the model might be overfitting the data if we are moving further with the number of training steps. We might need to fine tune the model hyper parameters or add more samples for training and validation using data augmentation techniques. [14]

To evaluate how well the model has trained, there is a specific functionality of images tab in TensorBoard Figure 9. It shows the bounding box detections on images in validation set and for each image detections are shown in left side and ground truth are shown in right side to compare the results and so the title of image “Detections_Left_Groundtruth_Right”. The slider located on the top can be used to go backward and forward in number of training steps used to train the model and hence to analyse the training progression about how the predicted detection bounding box is changing w.r.t change in number of steps in training.



Figure 9. Bounding box detections in left and ground truth in right for images in validation set

5. CONCLUSIONS AND FUTURE WORK

In this paper we have demonstrated the safety helmet detection system to identify whether workers in industrial environment are wearing helmet or not. For better detection accuracy and to reduce false positives in predictions the persons are detected first using pretrained SSD MobileNet model on coco dataset. The predicted images are further cropped and annotated to pass through another SSD MobileNet algorithm for helmet detection.

Comparison of the proposed two stage SSD detection system is done with one step SDD for detection of person with and without Helmet on the same training data and model hyperparameters and further the performance is evaluated on same test data. The mAP@.5IOU for the proposed detection system converges to .96 with an increase in the number of training steps while for the one step SSD detection algorithm it only converges to .7 which proves that comparatively the proposed detection system provides an approximate 37% increase in model accuracy. The experimental results have illustrated that our approach is efficient and effective for helmet detection.

The future work for this paper is to tune different hyperparameters by debugging TensorBoard graphs and to optimize the model. To make a robust algorithm and detector, augmentation plays a key role. Most of the computer vision and deep learning algorithms need more data to train. If the set of training images consist of different angles and different sizes of the object, it automatically enhances the performance. [14] Using the proposed model, the deep learning inference benchmarking needs to be done with Raspberry Pie and Nvidia Jetson for its practical implementation. Further for accounting violations of wearing safety helmets, the algorithm will provide real time monitoring system where the images with No_Helmet predicted class are stored for further inspection, which would henceforth promote awareness of safety among workers.

In this experimentation the cameras are installed at the entrance, which has a narrow passage and each person is instructed to face towards the camera while entering the restricted zone area. One of the limitations of this detection system it that it cannot detect occlusions with multiple persons coming in front of camera at the same time. Since person detection is the first step in the proposed two-stage detection system and occlusions with multiple persons will not provide us precise cropped images of workers.

REFERENCES

- [1] W. Liu, D. Anguelov, D. Erhan, C. Szegedy, S. E. Reed, C. Fu, and A.C. Berg. SSD: single shot multibox detector. In Computer Vision ECCV 2016 - 14th European Conference, Amsterdam, The Netherlands, October 11-14, 2016, Proceedings, Part I, pages 21–37, 2016. [Online]. Available: <https://arxiv.org/abs/1512.02325>
- [2] J. Redmon, S. K. Divvala, R. B. Girshick, and A. Farhadi. You only look once: Unified, real-time object detection. In 2016 IEEE Conference on Computer Vision and Pattern Recognition, CVPR 2016, Las Vegas, NV, USA, June 27-30, 2016, pages 779–788, 2016. [Online]. Available: <https://arxiv.org/abs/1506.02640>
- [3] J. Huang, A. Fathi, V. Rathod, I. Fischer and C. Sun. Speed/accuracy trade-offs for modern convolutional object detectors. In Computer Vision and Pattern Recognition (cs.CV), April 2017, vol arXiv:1611.10012. [Online]. Available: <https://arxiv.org/abs/1611.10012>

- [4] A. Howard, W. Wang, M. Zhu, T. Weyand, B. Chen and D. Kalenichenko. MobileNets: Efficient Convolutional Neural Networks for Mobile Vision Applications. *Computer Vision and Pattern Recognition (cs.CV)*, April 2017, vol arXiv:1704.04861. [Online]. Available: <https://arxiv.org/abs/1704.04861>
- [5] Z.Q. Zhao, P. Zheng, S.T. Xu and X. Wu. Object Detection with Deep Learning: A Review. *IEEE Transactions on neural networks and learning systems*, April 2019, vol arXiv:1807.05511. [Online]. Available: <https://arxiv.org/abs/1807.05511>
- [6] P. Viola and M. Jones. Rapid Object Detection using a Boosted Cascade of Simple Features. *Computer vision and pattern recognition* 2001. [Online]. Available: <https://www.cs.cmu.edu/~efros/courses/LBMV07/Papers/viola-cvpr-01.pdf>
- [7] K. Aashish and A. Vijayalakshmi. Comparison of Viola-Jones and Kanade-Lucas-Tomasi Face Detection Algorithms. *Oriental Journal of Computer Science and Technology*, March 2017, ISSN : 0974-6471 Online ISSN : 2320-8481. [Online]. Available: <http://www.computerscijournal.org/vol10no1/comparison-of-viola-jones-and-kanade-lucas-tomasi-face-detection-algorithms>
- [8] K. Židek, P. Lazorík, J. Pitel and A. Hošovský. An Automated Training of Deep Learning Networks by 3D Virtual Models for Object Recognition. *Symmetry*, April 2019, 11(4), 496. [Online]. Available: <https://doi.org/10.3390/sym11040496>
- [9] T.Y Lin, J. Hays, M. Maire, S. Belongie, L. Bourdev and R. Girshick. Microsoft COCO: Common Objects in Context. *Computer Vision and Pattern Recognition*, February 2015, vol arXiv:1405.0312 . [Online]. Available: <https://arxiv.org/abs/1405.0312>
- [10] R. Silva, K. Aires and R. Veras. Helmet Detection on Motorcyclists Using Image Descriptors and Classifiers. *27th SIBGRAPI Conference on Graphics, Patterns and Images*, August 2014. [Online]. Available: <https://ieeexplore.ieee.org/document/6915301>
- [11] Z. Zou, Z. Shi, Y. Guo and J. Ye. Object Detection in 20 Years: A Survey. *IEEE TPAMI*, May 2019, arXiv:1905.05055. [Online]. Available: <https://arxiv.org/abs/1905.05055>
- [12] A. Mobiny. How to Use TensorBoard? *ITNEXT*, June 2018. [Online]. Available: <https://itnext.io/how-to-use-tensorboard-5d82f8654496>
- [13] COCO Common object in context, Evaluate tab. [Online]. Available: <http://cocodataset.org/#detection-eval>
- [14] C. Shorten and T. M. Khoshgoftaar. A survey on Image Data Augmentation for Deep Learning, *Journal of Big data*, July 2019, 6, Article number: 60 (2019). [Online]. Available: <https://journalofbigdata.springeropen.com/articles/10.1186/s40537-019-0197-0>

AUTHORS

Ankit Kamboj received his bachelor's in engineering from LNMIIT, India in 2014 and his Masters in Operations Research from Indian Statistical Institute, Kolkata, India in 2017. He has over 3+ years' experience in the field of Applied Statistics, Machine Learning and Computer Vision. Mr Kamboj is working as a Senior Data Scientist in Cummins. Recent efforts involve Multivariate Time Series Forecasting, proactive engine failure prediction using Machine Learning and attrition risk prediction.



Nilesh Powar received his bachelor's in engineering from University of Bombay, India in 1999, his M.S. in Computer Engineering from Wright State University in 2002, and a PhD in Electrical and Computer Engineering in 2013 from the University of Dayton. He has over 20+ years' experience in field of image processing, machine learning, statistical pattern recognition and system integration. Dr Powar worked in the US as Distinguished Research Scientist for University of Dayton Research Institute, Dayton, OH, USA. Currently he leads the Advanced Analytics team for Cummins - India as a Director. Recent efforts involve data analytics for die casting, predictive analysis for supply chain management and video summarization using deep learning.



RATE CONTROL BASED ON SIMILARITY ANALYSIS IN MULTI-VIEW VIDEO CODING

Tao Yan¹, In-Ho Ra², Deyang Liu³, Deli Chen¹,
Yu Youhao¹, and Shaojie Hou¹

¹School of Information Engineering, Putian University, Putian 351100, China

²School of Computer, Information and Communication Engineering, Kunsan
National University, Gunsan 54150, South Korea

³School of Computer and Information, Anqing Normal University,
Anqing 246000, China

ABSTRACT

As with previous single-view video coding, in order to promote the application of multi-view video coding, multi-view video coding also needs to study the appropriate rate control algorithm. Bit rate control has always been a difficult research topic in multi-view video coding. In multi-view video coding, there are 6 types of coded image, so the previous rate control algorithm for single-view video cannot be directly applied to multi-view video coding. The bit rate control is divided into a four-layer structure for bit rate control of multi-view video coding. Among them, the frame-layer code rate control considers the layer B frame and other factors to allocate the code rate, and the basic unit-layer code rate control uses different quantization parameters according to the content complexity of the macroblock. The average error between the actual bit rate and the target bit rate of the bit rate control algorithm can be controlled by 2.39%.

KEYWORDS

Multi-view video coding, Rate control, Bit allocation, Basic unit layer

1. INTRODUCTION

The main work of 3DAV in the early days was the analysis of 3DAV requirements, including the definition of 3DAV application scenarios, including panoramic video, multi-view video and interactive 3D video. Among them, the multi-view video is taken by multiple cameras from different angles. It contains multiple viewpoint images in the same scene, and the viewpoints are highly correlated. Therefore, in addition to usually using spatial-temporal redundancy to achieve coding purposes as in 2D video, it is more important to eliminate spatial prediction redundancy between different viewpoints. Multi-view video coding often requires more complex and efficient coding technology and higher compression efficiency than single-view video coding such as H.264 / AVC, MPEG-2. 3DTV / FTV (Three-dimensional television / Free-view television) will become the next-generation television technology after high-definition television (HDTV) [1-2]. But multi-view video coding (MVC) is still immature, and it is still a long way from the

application. The bit allocation and bit rate control of MVC, in particular, are key issues for transmission and applications.

In practical applications, bit rate control is one of the main key technologies. It is one of the most important technologies in video coding. Any video compression standard that leaves the bit rate control will be limited in its application. The previous video compression standards such as MPEG-2, MPEG-4, H.263, H.264, MVC, etc. have given a rate control model [3-6]. Compared with the previous video compression standards, the rate control of MVC The bit rate control is mainly to allocate a reasonable bit rate between the viewpoints to ensure the balance of the video quality between the viewpoints.

As with previous single-view video coding, in order to promote the application of multi-view video coding, multi-view video coding also needs to study the appropriate rate control algorithm. Bit rate control has always been a difficult research topic in multi-view video coding. In multi-view video coding, there are 6 types of coded image, so the previous rate control algorithm for single-view video cannot be directly applied to multi-view video coding. There have been many research results on bit rate control[7-9]. At present, the multi-view video coding rate control algorithm not only needs to reasonably allocate the bit rate in each frame in time to prevent buffer overflow, but also needs to allocate a reasonable bit rate between the viewpoints to ensure the balance of video quality between viewpoints. Therefore, an efficient multi-view video encoding bit rate control algorithm needs to be developed.

To this end, based on JMVC, a multi-view video rate control module is added in this article. The core of the algorithm is based on the analysis of the existing video bit rate control algorithms, according to the characteristics of multi-view video coding and the requirements of its bit rate control, to improve the traditional quadratic rate distortion model, and propose a multi-view video-oriented basic unit Layer rate control algorithm. Experimental simulation results show that compared with JMVC [10] which currently uses fixed quantization parameters, the algorithm in this paper can effectively control the bit rate of multi-view video coding while maintaining efficient coding efficiency.

2. MULTI-VIEW VIDEO CODING RATE CONTROL ALGORITHM

The rate control of single-view video coding is, in essence, the rate control of I and P frames, and the rate control of B frames is not performed. The QP value of B frames is simply based on the adjacent I frames and P The QP value of the frame or two adjacent P frames is determined. When the number of B frames between adjacent I frames and P frames or two adjacent P frames is large, the accuracy of the rate control will change. Very poor. For compatibility with H.264, the bit allocation and bit rate control proposed in this paper is based on the bit rate control algorithm of JVT-G012. The bit rate model adopts our previous research results [11]. The MVC code rate control algorithm is divided into four layers. Among them, GOP code rate control is mainly based on the correlation between viewpoints to allocate reasonable code rates among various views. Frame layer code rate control mainly considers the impact of hierarchical B frames Allocation code rate, basic unit layer code rate control uses different quantization parameters according to the content complexity of the macroblock. The main algorithm is as follows:

The I frame and the first $T(j)$ frame of the first GOP in each GGOP, and the first P frame of other GOPs are coded with QP_0 . There is no need to allocate target bits, and other B frames (or P frames) target allocate bits B is weighted by T_r and T_{buf} ,

$$T(j) = \beta \cdot T_r(j) + (1 - \beta) \cdot T_{buf}(j) \quad (1)$$

Where β is a fixed value, its typical value is 0.5 when there are no B frames, and 0.9 when there are B frames; where the allocation of T_{buf} for the current frame depends on the current target buffer overflow degree Tbl , similar to the previous algorithm. The methods are:

$$T_{buf}(j) = \gamma \cdot (Tbl(j) - B_c(j-1)) + \frac{u(j)}{F_r} \cdot \left\{ \frac{\sum_{l=1}^L W(l) \cdot 2^n}{\sum_{l=1}^L \Theta \cdot W(l) + \sum_{l=1}^L W_B(l) \cdot (2^n - 1)} - 1 \right\} \quad (2)$$

Where γ is a fixed value, its typical value is 0.75 when there is no B frame, otherwise it is 0.25. Represents the time layer where the current frame is located, $w(l)$ represents the weight of the complexity of each frame, and $W_B(l)$ represents the weight of the B frame. For the value method, see Ref. [13].

The allocation of T_r in the current frame in formula (6) depends on the number of bits remaining in the current GOP and at a certain time layer in FIG. 1.

$$T_r(j) = T_{GOP}(n_{k,j}) \cdot W_b(n_{k,j}) \quad (3)$$

In the formula, $T_{GOP}(n_{k,j})$ is the remaining bits of the current GOP, and $W_b(n_{k,j})$ is the weight of the current frame. The initial value of $W_b(n_{1,j})(j=1,2,\dots,N(i))$ is set to 1. After each GOP is encoded, it needs to be refreshed at the post-encoding stage. Let $A_{GOP}(n_{k-1,0})$ be the number of bits actually used to encode the $k-1$ th GOP of the i th GGOP. $A(j)$ represents the number of bits actually used in the j frame encoding, and the weight $W_b(n_{k-1,j})(j=1,2,\dots,N(i))$ of the current frame is given by equation (8)

$$W_b(n_{k-1,j}) = \frac{A(j)}{A_{GOP}(n_{k-1,0})} \quad (4)$$

$W_b(n_{k,j})$'s linear prediction model is:

$$W_b(n_{k,j}) = \beta_{k1} \cdot W_b(n_{k-1,j}) + \beta_{k2} \quad (5)$$

Among them, β_{k1} and β_{k2} are univariate regression coefficients, and the initial values are set to 1 and 0. After each GOP encoding is completed, it needs to be refreshed in the post-encoding stage. $T_{GGOP}(sn_{i,j})$ represents the number of remaining bits of the GGOP after the i frame of the j GGOP is encoded. This paper uses existing algorithms. The main ideas are as follows: Using H.264 / AVC Visa Baseline Tool to perform similarity analysis on video images to obtain the consistency of macroblocks is only possible using statistical features, and DCT coefficients are more suitable for image similarity than pixel brightness Sexual requirements. The macro block contains a part of the nose and lips. We refer to the results of previous research. It can be seen that if most of the subblocks obtain the same SAC value (dark part), the two blocks can match. Therefore, SAC is suitable for statistical matching of images, that is, the results are consistent with the error

concealment strategy of this paper. According to the statistical matching conditions of the sub-blocks, the similarity measure Δf_k for a certain block is defined as:

$$\Delta f_k = \sum_k \theta \cdot (SAC_k^{I_{i-1}} - SAC_k^{I_i}), I_i \in Z \quad (6)$$

Among them, $\delta(\cdot)$ is the δ function and I_i is the current frame. The similarity Δf_k represents the number of sub-blocks with the same statistical characteristics, and has the following conclusions. If $\Delta f_i < T_{AC}(= \delta \times T_{\max})$, then I_i and I_{i-1} are not similar; otherwise, I_i and I_{i-1} are similar. Therefore, it can be determined that the current frame I_i is a scene switching frame; if I_i and I_{i-1} are not similar, there is a scene switching frame between I_i and I_{i-1} , I_i is not a scene switching frame, and if there is no switching frame between them, I_i is a scene switching frame for the scene. σ is a certain similarity measure.

3. EXPERIMENTAL TESTS

In order to verify the effectiveness of the proposed multi-view video coding bit allocation and rate control algorithm, we used the test sequences which include Kendo-Dancer, Poznanstreet-Gtfly, Gtfly-Kendo, Poznanstreet-Dancer, and Dancer-Race1. The test platform is Intel (R) Core (TM) Duo CPU 2.66GHz (dual), 1.96GB memory. The Gtfly-Kendo' sequence is obtained by resampling the Gtfly-Kendo sequence. The other sequences are similar. Table 1 shows the experimental results of the proposed algorithm compared with the two fixed bit allocation algorithms.

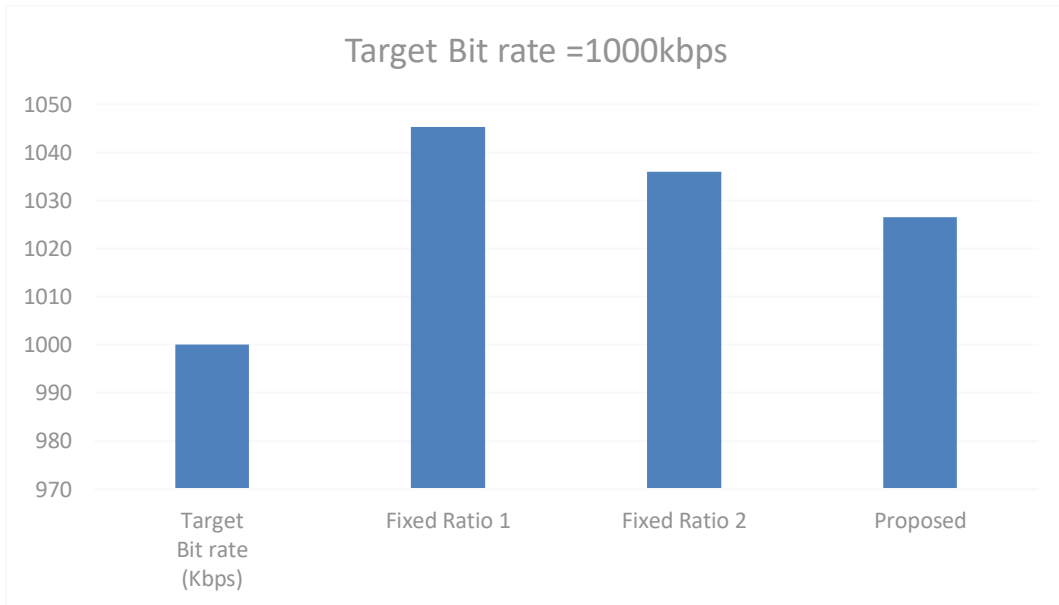


Table 1 Simulation Results

Sequence		Target Bit rate (Kbps)	Actual generated bits (kbps)			Rate control error (%)		
			Fixed Ratio 1	Fixed Ratio 2	Proposed	Fixed Ratio 1	Fixed Ratio 2	Proposed
HD	Gtfly-Kendo'	1000	1045.30	1036.00	1026.60	4.53	3.60	2.66
		2000	2096.40	2075.80	2028.20	4.82	3.79	1.41
		3000	3148.20	3076.50	3063.60	4.94	2.55	2.12
	Kendo-Dancer'	1000	1046.30	1044.00	1030.10	4.63	4.40	3.01
		2000	2082.40	2070.00	2033.60	4.12	3.50	1.68
		3000	3143.70	3107.40	3073.50	4.79	3.58	2.45
	Poznanstreet- Gtfly'	1000	1036.90	1027.20	1015.80	3.69	2.72	1.58
		2000	2091.00	2068.00	2054.00	4.55	3.40	2.70
		3000	3119.10	3097.80	3062.10	3.97	3.26	2.07
	Poznanstreet- Dancer'	1000	1049.30	1035.70	1031.60	4.93	3.57	3.16
		2000	2091.40	2068.80	2045.40	4.57	3.44	2.27
		3000	3125.40	3098.10	3082.20	4.18	3.27	2.74

Table 1 shows the experimental results of the proposed algorithm compared with the two fixed bit allocation algorithms. The JMVC algorithm without bit rate control uses a fixed quantization value for multi-view video encoding. The bit rate obtained when the fixed quantization value is used is the target bit rate of the bit rate control algorithm.

Table 1 shows the simulation results of code rate control for multi-view video coding. As can be seen from Table 1, compared with the two fixed bit allocation algorithms, rate control algorithm in this paper has a smaller code rate deviation, and the code rate error can be controlled at 2.39%. The main reason for this is that we not only perform reasonable bit allocation between viewpoints, but the basic unit layer code rate control uses different quantization parameters for code rate control according to the content complexity of the macroblock.

4. CONCLUSION

In the future, we consider the use of the relationship between the distortion of the video and the bit rate and the complexity of the video frame to optimize the allocation of the bit rate between the frames. In view of the large number of scene switches that may occur in the video frame, a scene switch detection based on non-connected points. The algorithm, combined with improved adaptive GOP packet technology, further improves the rate control performance. In videos where scenes change, the adaptive GOP grouping technology is used to eliminate the effects of scene switching and improve coding performance.

ACKNOWLEDGEMENTS

This work was supported by Natural Science Foundation of China (Grants No. 61741111, 61801006); This work was supported by Program for New Century Excellent Talents in Fujian Province University; This work was supported by the National Research Foundation of Korea(NRF) grant funded by the Korea government (MSIP) (No.2016R1A2B4013002); in part by Natural Science Foundation of Fujian (Grants No. 2019J01816); in part by Natural Science Foundation of Jiangxi (Grants No. 20181BAB202011); Putian University's Initiation Fee Project for Importing Talents for Scientific Research (Grants No. 2019003); This work was supported in part by the Key Project on Anhui Provincial Natural Science Study by Colleges and Universities under Grant KJ2018A0361.

REFERENCES:

- [1] P Ren, X Zhang, H Bi, H Sun, and N Zheng, "Toward an Efficient Multiview Display Processing Architecture for 3DTV," *IEEE Transactions on Circuits and Systems II: Express Briefs*, vol.64, no. 6, pp. 705 - 709, June 2017
- [2] C Yang, P An, L Shen, and D Liu, "Adaptive Bit Allocation for 3D Video Coding," *Circuits, Systems, and Signal Processing*, vol. 36, no. 5, pp. 2102-2124, May 2017
- [3] Jinag M Q, Yi X Q, Ling N. Improved frame-layer rate control for H.264 using MAD ratio. *Proceedings of IEEE International Symposium on Circuits and Systems[C]*, Vancouver, Canada, 2004. 813-816.
- [4] R. Atta and M. Ghanbari, "Low-Complexity joint temporal-quality scalability rate control for H.264/SVC," *IEEE Transactions on Circuits and Systems for Video Technology*, Vol.28, No. 9, pp. 2331-2344, September 2018
- [5] Li Z G, Pan F, Lim K P, Feng G N. Adaptive basic unit layer rate control for JVT. *JVT-G012,7Th meeting[C]*, Pattaya, Thailand, 2003 ,7-14.
- [6] L. Q. Shen, K. Li, G. R. Feng, P. An , and Z.Liu, "Efficient intra mode selection for depth-map coding utilizing spatiotemporal, inter-component and inter-view correlations in 3D-HEVC," *IEEE Transactions on Image Processing*, Vol. 27, No. 9, pp. 4195-4206, September 2018
- [7] Naito S, Matsumoto S. 34/35 Mbps 3D-HDTV digital coding scheme using a modified motion compensation with disparity vectors, *VCIP, SPIE, USA, 1999*, pp: 1082-1089.
- [8] Y. Z Zhang and C. Lu, "High-performance algorithm adaptations and hardware architecture for HEVC intra encoders," *IEEE Transactions on Circuits and Systems for Video Technology*, Vol.29, No. 7, pp. 2138-2145, July 2019.

- [9] S. Park, D. Sim. An efficient rate-control algorithm for multi-view video coding. The 13th IEEE International Symposium on consumer Electronics[C], Kyoto, Japan, 2012: 115-118.
- [10] T Yan, P An, L Shen, Q Zhang, and Z Zhang, "Rate Control Algorithm for Multi-view Video Coding Based on Correlation Analysis", *the International Symposium on Photonics and Optoelectronics (SOPO)*, pp. 1-4, Wuhan, China, August 2009
- [11] T Yan, P An, L Shen, Z Li, H Wang, and Z Zhang, "Rate control algorithm based on frame complexity estimation for MVC", *SPIE International Conference on Visual Communications and Image Processing*, pp. 77-85, Huang Shan, An Hui, China, July 2010
- [12] J. Yang, X. Z. Fang and H. K. Xiong. A joint rate control scheme for H.264 encoding of multiple video sequences. *IEEE Transaction on Consumer Electronics*, Vol. 51, No. 2, May, 2005.

TPM Based Design for Enhanced Trust in SaaS Services

Mustapha Hedabou ^{1,2} , Ali Azougaghe ³ , Ahmed Bentajer ⁴

¹ School of Computer and Communication Sciences
University Mohammed VI Polytechnic, Benguerir. Morocco

²Dept. Computer Science. ENSA de Safi
University Cadi Ayyad, Marrakch. Morocco

³ ENSIAS Mohammed V University in Rabat, Morocco

⁴ ENSA School of Tetouan
Abdelmalek Essaadi University, Morocco

Abstract. On the past decade, Trusted Platform Modules (TPM) have become a valuable tool for providing a high level of trust on locally executing software. Indeed, in addition to its availability on most commodity computers, TPM are totally free of cost unlike other available Hardware-Based devices while they offer the same level of security. Enhancing trust in SaaS services regarding the security and the privacy of the hosted SaaS application services can turn out to be a pertinent application scope of TPM. In this paper we present a design for a trusted SaaS model that gives cloud users more confidence into SaaS services by leveraging TPM functionalities combined with a trusted source code certifying authority facility. In our design, the cloud computing provider hosting the SaaS services acts as a root of trust by providing final cloud users insurance on the integrity of the SaaS application service running on its platform. A new mechanism of multisignature is developed for computing a join signature of SaaS service software by the trusted authority and TPM. A prototype implementation of the proposed design shows that the integrity of SaaS application service before and after it was launched on a cloud provider platform is guaranteed at low cost.

Keywords. Cloud computing, SaaS services, TPM, trust, Code source certification, Mutlisignature schemes.

1 Introduction

Cloud computing services demand is booming because they can reduce the cost and complexity of owning and managing computers and networks. Customers have no investment in information technology infrastructure, purchase hardware, or buy software licences because these charges are covered by cloud providers. On other hand, they can

benefit from rapid return on investment, rapid deployment, and customization. Moreover, specialized cloud providers in a particular area (such as e-mail) can bring advanced services that a single company can not provide. Cloud computing is often considered efficient because it allows organizations to devote their resources only to innovation and product development.

Nowadays, cloud services are widely used by businesses. More than 3 millions businesses have adopted Google Apps, Google's cloud e-mail, calendar and collaboration solutions for businesses. This rate is expanding at 3000 users a month [19].

Despite its potential benefits, many chief executives and IT manager are not willing to lost the control of their data by offloading it to cloud computing platforms. Their main concerns are about the confidentiality and privacy of their data. Their apprehension is amply justified because cloud provider employees can either accidentally or intentionally tamper with the hosted data. This violation can take place without the knowledge of the data's owner.

Many efforts have been done by cloud services providers in order to Strengthen the trust of users by reducing the threat of the insider attacks. For example, they protect and restrict access to the hardware facilities, adopt strict accountability and auditing procedures, and reducing the number of staff who have access to critical components of the infrastructure [16]. Nevertheless, cloud providers employees with administrator privileges can still have access to cloud users data and tamper with it.

To establish more confidence in their services, cloud providers have defined the specification for the widely implemented Trusted Platform Module (TPM) [18, 11]. This approach has been used by Santos et al. [16] to design a trusted cloud computing platform based on TPM attestation chains. In [10], the authors have proposed Terra, a trusted platform based on a virtual machine. Terra has the ability to prevent insider abusers from tampering with the users data. With the capability to provide a remote attestation capability, Terra enable a cloud users to determine upfront whether the host can securely run the computation on their data.

Another approach based on a trusted trusted party acting as a root of trust, that attests cloud hosted services to their clients, was proposed in [6]. Cloud provider which acts as trusted party, responsible runs programs upon request on behalf users, and issues digital certificates of program's identity (e.g., a code hash) for use by other entities that interact with the running program instance. Unlike the other approach, this model does not use the TPM for issuing the remote attestations.

This paper proposes a new trusted SaaS platform that aims to addresses the trust concerns unique to the SaaS model. Our model allows to reinforce the confidence of the cloud users in both cloud providers and services providers. For this purpose, the source code of the SaaS application service must be certified by a trusted code certifying

authority in order to prevent the cloud provider to tamper with the application service. By using a new multisignature mechanism, the cloud provider through the TPM, certifies also the source code. This will prevent the misuse of service application when it was running in the cloud platform.

2 Background

The SaaS model is based on the distributed application architecture. It includes components to facilitate and improve the business model. Unlike the traditional software vendor that is only concerned with application functionalities, the SaaS provider is also responsible for operating and managing the environment that supports all their cloud users. This is done by adding more distribution tiers to support the need of services requests to be routed among more than physical operating environment.

SaaS services are located in high layers, which means in the software level, offer a complete online applications that can be used by cloud users without any development. SaaS enables cloud users to utilise an application on a pay-as-you-go basis without need to install nor to update the application. Maintenance and upgrade are carried out by the service provider as a part of service. The application can be accessed through web browser or thin client over internet. Early examples of SaaS can be traced back to Hotmail, the e-mail service owned by Microsoft.

The location of the SaaS model in the higher layers increases the difficulty of guaranteeing the security of hosted data because the cloud and services providers have the full control over the software and operating environment that manipulate the cloud users data. Thus, the cloud users data may succumb to insiders attacks from two sides. Cloud provider employees with root privileges can execute any attacks. On other hand, sysadmins of the service provider can launch a malicious or faulty applications services in order to misappropriate cloud users data or to conduct additional harmful functions without the user approval. Consequently, the security of the SaaS must be strengthened more than any of other available delivery models.

In addition to the standard security practices shared with other application delivery models, including firewalls, IPS, IDS, .., SaaS displays more security defenses related to identity management, data storage and data transmission [15]. However, the deployment of all these countermeasures does not prevent the insiders attacks. To strengthen the trust of users on their services, cloud providers have proposed hardware and software approaches to enable the construction of trusted platforms. In particular, the Trusted Computing Group (TCG) introduced a standard for the design of the trusted platform module (TPM) [18] chip that is now endowed with commodity hardware.

2.1 Trusted Platform Module (TPM)

The TPM is a security specification defined by the TCG. It is almost installed on the motherboard of a computer or laptop, and communicates with the rest of the system using a hardware bus through well defined commands. The TPM provides cryptographic operations such encryption, decryption and signing as well as random number generation. It also provides space for the storage of small amount of information such as cryptographic keys. Since it was implemented carefully in the hardware, the TPM is resistant to software attacks [9]. Many researches [2, 10, 17, 16] have proposed to use the features of TPM chips for reinforcing trust in cloud computing platforms.

Each TPM is associated with a number of signing keys. The endorsement private key (EK) identifies the TPM and thus, the physical host. The EK stands for the validity of TPM [18]. The respective manufacturers sign the corresponding public key to guarantee the correctness of the chip and validity of the key. Related to the EK are Attestation Identity Keys (AIKs). An AIK is created by the TPM and linked to the local platform through a certificate for that AIK. This certificate is created and signed by a certificate authority (CA) [9]. In particular, a privacy CA allows a platform to present different AIKs to different remote parties, so that it is impossible for these parties to determine that the AIKs are coming from the same platform. In our model, the used AIK key represents the public key of the TPM with regard to multisignature schemes.

The TPM Attestation consists of several steps of cryptographic authentication by which the specification for each layer of the platform is checked from the hardware up to the operating system and application code. At a high level, the TPM attests the source code of service application by signing its hash with an attestation identity key (AIK). This will be done by following the trust chain $\text{TPM} \rightarrow \text{BIOS} \rightarrow \text{BootLoader} \rightarrow \text{OS} \rightarrow \text{Application}$ [13]. Direct Anonymous Attestation (DDA) [5] can be used to protect the privacy of the TPM in such a way that a user will be able to verify the validity of attestation without linking it with the platform that contains the TPM.

2.2 Multisignature schemes

Multisignature schemes [12, 14] are designated to enable a group of signers to produce a compact, joint signature on a common message. Any other user can verify the authenticity of a given message based only on the multisignature and all signers public keys. Consider entities $1, \dots, N$ each having a public key and corresponding secret key. A multisignature (MS) scheme allows, at any time, any subset $L \in 1, \dots, n$ of users to engage interactively a protocol that outputs is a joint signature on a given message m . Verification can be done by any user given just L, m , the computed multisignature σ , and the public keys of all signers in L . Multisignatures can be useful for contract signing, co-signing, or distribution of a certificate authority.

Earlier implementations of a multisignature σ on a message m is obtained by setting $(\sigma_i : i \in L)$ where σ_i is i 's signature on the message m . This multisignature is however large, in particular of size proportional to the number $|L|$ of signers. Moreover, Earlier multisignature schemes require a set up process between all the signers which make their use impracticable especially for devices with small resources such as PDAs, cell phones and TPM chips. Research efforts have lead to recent multisignature schemes [3, 4] that require nothing more than that each signer has a certified public key. Furthermore, the these multisignature schemes have become as efficient as others signature schemes in both signing and verification process.

In 2003, a non interactive multisignature scheme based on the signature of Boneh, Lynn and Shacham [8] was proposed by Boldyreva [7]. Let G be a Diffie-Hellman group of prime order p and let g be a generator of G . Let H be a description of a random member of the family of hash functions and $\{P = P_1, \dots, P_n\}$ be the group of players. Any player $P_j \in P$ with a secret key $sK_j = x_j$, that wishes to participate in signing takes M , computes and broadcasts $\sigma_j \leftarrow H(M)^{x_j}$. Let $L = \{P_1, \dots, P_l\}$ be a subgroup of players participating to the signing process. Let $J = \{1, \dots, l\}$ denotes the indices of involved players. The leader, which can be any player, collects the signature of each player and computes $\sigma = \prod_{j \in J} (\sigma_j)$ and outputs $T = (M, L, \sigma)$.

The verifier takes $T = (M, L, \sigma)$ and the list of public keys of the players involved in signing $L = \{pK_1, \dots, pK_l\}$ where $pK_i = g^{sK_i}$ for each $i \in L$. The verifier computes $pK_l = \prod_{j \in J} (pK_j) = \prod_{j \in J} (g^{sK_j})$ and outputs $V_{DDH}(g, pK_l, H(M), \sigma)$. We recall that $V_{DDH}(g, u, v, h, \sigma)$ outputs valid if $\log(u)_g = \log(h)_v$ and false otherwise.

3 Proposed trusted SaaS design

In a SaaS model, the service provider launches the application service as an instance hosted on a physical platform owned by a cloud provider. cloud users gain access to the service application through an API supplied by the cloud provider. The TPM facilities are used to provide cloud users with evidence of well defined security properties of the platform that hosts the application service. This only security practice deployed in the cloud platform does not provide cloud users with any evidence about authenticity of the application service running in the platform which can lead to lack of trust in SaaS services.

The proposed trusted SaaS design aims to mitigate trust issue on SaaS services by ensuring the integrity of a SaaS service application before and after it wa running on a cloud provider's platform. For this purpose, the service provider requests a trusted authority in order to certify the source code of the service application, Prior to deliver it to the cloud provider. The cloud provider certifies also the source code of the application service trough the TPM technology before to launch it. The signatures of

the trusted certifying authority and the cloud provider are sealed to each other via the multisignature schemes to produce a compact, joint signature on the source code of the application service .

By signing a source code of an application service, a trusted authority certifies the Authenticity and integrity of the source code. In some ways, the trusted authority binds the proprieties verified by the application to the signature of its source code. In our trusted SaaS model, the service provider requests a trusted certifying authority to sign the source code of its service application before to host it in a cloud computing platform. Digital signatures contain proof of content integrity so that the source code cannot be altered which gives users a serious base to determine the trustworthy in the service application and its behavior. Once this step achieved, the service provider forwards the service application and certificate issued by the trusted authority to the cloud provider for attesting its code source by using the TPM facilities.

3.1 Multisignature scheme using TPM

Even if TPM 2.0 products and systems have important security advantages over TPM 1.0, including elliptic curves digital signature ECDSA, it still not support signature based on decisional and computational Diffie-Hellman problems. Therefore, the multi signature scheme proposed by Boldyreva [7] can not be implemented directly by TPM. In this paper, we propose to use Diffie-Hellman oracle process introduced by Acar et al. [1] to modify Boldyreva's scheme to meet the RSA-based signature requirements of the TPM.

In [1], the authors use TPMv2 API commands with Schnorr signature in order to define a function $f_x : G \rightarrow g$ such that $f_x(h) = h^x$, where x is the TPM Diffie-Hellman private key. By exploiting the Diffie-Hellman oracle process, we can compute $H(M)^x$ for a message M by applying the function f_x to $H(M)$.

In our design only two players are involved in multisignature process, namely the certifying code trusted authority and the TPM. Let P_1 denotes the trusted authority and P_2 the TPM. By using the same notations as in section 2.2, let $sK_1 = x_1$ and $pK_1 = g^{x_1}$ the couple of private and public keys of trusted authority P_1 . The trusted authority computes the signature $\sigma_1 \leftarrow H(M)^{x_1}$ of a message M and make it available to other players. A TPM with a private key $sK_2 = x_2$ compute the signature M $\sigma_2 \leftarrow H(M)^{x_2}$ by applying the Diffie-Hellman oracle process to $H(M)$. The TPM signature is broadcasted to other players. The leader collects the signature of each player, computes $\sigma = \prod_{j \in \{1,2\}} (\sigma_j)$ and outputs $T = (M, L, \sigma)$. In our design, the dealer is the SaaS service application provider.

To verify the validity of the multisignature $T = (M, L, \sigma)$, the final cloud user takes $T = (M, L, \sigma)$ and public keys of the trusted authority and the TPM ($pK_1 = g^{x_1}$,

$pK_2 = g^{x_2}$), computes $pK = pK_1 \times pK_2 = g^{x_1+x_2}$ and outputs $V_{DDH}(g, pK, H(M), \sigma)$.

3.2 Prototype implementation

In this section we describe the prototype implementation of the proposed trusted SaaS platform. We describe the protocols and commands used for certifying the source code of the SaaS application service by the cloud provider and the trusted authority. The private and public keys of the trusted authority and TPM are a simple keypair of an asymmetric cryptographic scheme, namely Diffie-Hellman keys. Figure 1 depicts the architecture of the proposed design

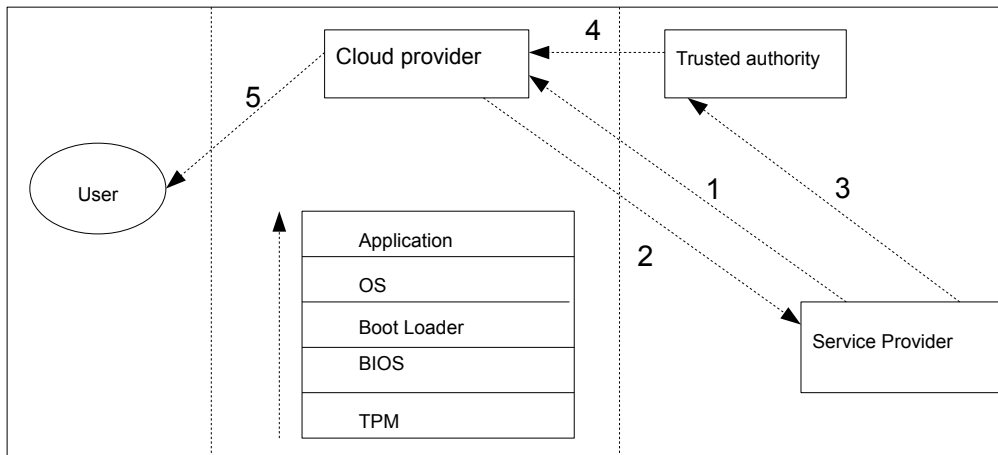


FIGURE 1 – Architecture of the proposed trusted SaaS platform

In our implementation, we used an auto-signed code source certificate through Openssl. Other more trusted authorities that support Diffie-Hellman based signature, such as Certum, can be leveraged for issuing Code Signing Certificate. In order to compute the TPM signature, we have issued the TPMv2 API command *TPM CreatePrimary* for generating the private/public key (x_2, g^{x_2}) of TPM. The call of *TPM Commit* with

input $h(M)$ where M is the formatted code source of the service application outputs $W = H(M)^w$ for a random $r \in Z$ and the command *TPM Sign* with an arbitrary input c outputs $r = cx + w$. We derived the signature of the TPM by computing $(H(M/W))^{1/c} = H(M)^{x_1}$ wrapped in a *TPMU_SIGNATURE* structure. In order to compute the multisignature issued by the trusted authority and the TPM, we have extracted the relevant bits from the file.bin that contains the TPM Signature.

3.3 Security study

The code source certification of the application service by the a trusted authority and the cloud provider addresses the specific need to prevent the misuse of the application before and after it was launched. The use of multisignature schemas establishes a mechanism of double protection since it prevents attackers from service and cloud providers to act jointly or separately in order to misrepresent the behavior of the application . The attestation provided by the trusted authority ensures the integrity of the application when it was under the monitoring of the cloud provider. After launching the application, its control is under the service provider but the cloud provider still control the server platform and the launch procedure. Thus, the cloud provider can be responsible for guaranteing the application's integrity after it was launched by using the TPM certification. In various TPM-based platform, such as Intel's Trusted Technologies [6], the proposed functionalities have been extended to post-launch checks. This makes the task of the cloud provider more affordable.

Trust in a cloud provider is mainly based on its reputation, therefore it has no interest to corrupt the behavior of the service instance it hosts. It can strength assurances of trustworthiness to its cloud users by issuing attestations of its own software stack based on a hardware root of trust. The cloud provider is also responsible for granting the privileges access the admin interface to the service provider. Thus, it can limit the control of the service provider on the application after it was launched to only the legitimate operations (launch, stop, ...). For all these reasons, the cloud provider itself can be seen as a trusted platform that run a well tested software stack and offers hosting platform for multi tenants users. This means that the cloud provider in our model can serve as a guarantor for preventing the service provider from tampering with application service after it was launched even if it was still under its control.

The mere fact that the cloud provider acts as a root of trust in our model does not mean that it is completely trusted. since it can still tamper with application service before running it. This issue was addressed by incorporating a trusted certifying source code authority that ensures the application's integrity when it was under the control of the cloud provider. This process allows to prevent any attempt for subverting the instance before it was hosted in the cloud platform.

4 conclusion and Future Work

In this paper we have proposed a new trusted SaaS model that mitigates the trust issues in SaaS delivering model by reinforcing the cloud users confidence in SaaS application services. In our model, the source code of the SaaS service application is certified by a trusted authority and the cloud provider via TPM by using a new multisignature mechanism that we have developed for this purpose. The proposed SaaS model gives the cloud users the ability to check the integrity of the SaaS service application before and after it was running in a cloud platform. In addition, we have implemented a prototype of the proposed design in a local environment. In the future, we plane to implement an instance of our design for deployment in real cloud computing environments.

Références

- [1] T. ACAR L. NGUYEN AND G. ZAVERUCHA. *A TPM Diffie-Hellman Oracle*. Cryptology ePrint Archive : Report 2013/667, 2013.
- [2] S. BERGER, R. CACERES, K. A. GOLDMAN, R. PEREZ, R. SAILER, AND L. VAN DOORN. *vTPM : virtualizing the trusted platform module*. In Proc. of USENIX-SS'06, Berkeley, CA, USA, 2006.
- [3] M. BELLARE, G. NEVEN. *New multi-signatures and a general forking lemma*. in CCS06, 2006.
- [4] M. BELLARE, G. NEVEN. *Identity-based multi-signatures from RSA*. In CT-RSA, 2007.
- [5] E. BRICKELL, J. CAMENISCH, L. CHEN. *Direct Anonymous Attestation*. In ACM Conference on Computer and Communications Security, pp. 132-145, 2004.
- [6] A. BROWN, J. S. CHASE . *Trusted Platform-as-a-Service : A Foundation for Trustworthy Cloud-Hosted Applications*. In : Proc. of CCSW. pp. 15-20 (2011).
- [7] A. BOLDYREVA *Threshold Signatures, Multisignatures and Blind Signatures Based on the Gap-Diffie-Hellman-Group Signature Scheme*. in International Workshop on Theory and Practice in Public Key Cryptography (PKC) 2003 Proceedings, LNCS Vol. 2567, pp. 31-46.
- [8] D. BONEH, B. LYNN AND H. SHACHAM *signatures from the Weil pairing*. In Asiacrypt 01, 2001.
- [9] *Common Criteria*. Trusted Computing Group (TCG) Personal Computer (PC) Specific Trusted Building Block (TBB) Protection Profile and TCG PC Specific TBB With Maintenance Protection Profile, July 2004.
- [10] T. GARFINKEL, B. PFAFF, J. CHOW, M. ROSENBLUM, AND D. BONEH. *Terra : A Virtual Machine-Based Platform for Trusted Computing*. In Proc. of SOSP 03, 2003.
- [11] M. HEDABOU. *Cryptography for Addressing Cloud Computing Security, Privacy, and Trust Issues*. In Computer and Cyber Security : Principles, Algorithm, Applications, and Perspectives, CRC Press, 2018.

- [12] K. ITAKURA AND K. NAKAMURA,. *A public-key cryptosystem suitable for digital multisignatures*. In NEC Res. Development 71 (1983), pp. 1-8.
- [13] C. NIE. *Dynamic root of trust in trusted computing*. In TKK T1105290 Seminar on Network Security, 2007.
- [14] T. OKAMOTO. *A digital multisignature scheme using bijective public-key cryptosystems*. Commun. ACM Trans. Computer Systems 6, 8 (1988), 432-441.
- [15] *SaaS Security and privacy*. <http://www.progress.com/en-gb/docs/whitepapers/public/SaaS/SaaS-Security.pdf>.
- [16] N. SANTOS, K. P. GUMMADI, AND R. RODRIGUES. *Towards trusted cloud computing*. In Proceedings of the Workshop on Hot Topics in Cloud Computing, Hot-Cloud'09. USENIX Association, 2009.
- [17] R. SAILER, T. JAEGER, E. VALDEZ, R. CACERES, R. PEREZ, S. BERGER, J. L. GRIFFIN, AND L. V. DOORN. *Building a MAC-Based Security Architecture for the Xen Open-Source Hypervisor*. In Proc. of ACSAC'05, Washington, DC, USA, 2005.
- [18] *Trusted platform module*. <http://www.trustedcomputinggroup.org/developers/trustedplatformmodule>.
- [19] RON ZALKIND. *Protecting Your Data In Google Docs Compliance In The Cloud*. <http://www.cloudlock.com/pdf/Protecting-Your-Data-In-Google-Docs.pdf>.

DESIGN AND HARDWARE IMPLEMENTATION OF A SEPARABLE IMAGE STEGANOGRAPHIC SCHEME USING PUBLIC-KEY CRYPTOSYSTEM

Salah Harb, M. Omair Ahmad and M.N.S Swamy

Electrical and Computer Engineering Department, Concordia University, 1440
De Maisonneuve, Montreal, Canada

ABSTRACT

In this paper, a novel and efficient hardware implementation of steganographic cryptosystem based on a public-key cryptography is proposed. Digital images are utilized as carriers of secret data between sender and receiver parties in the communication channel. The proposed public-key cryptosystem offers a separable framework that allows to embed or extract secret data and encrypt or decrypt the carrier using the public-private key pair, independently. Paillier cryptographic system is adopted to encrypt and decrypt pixels of the digital image. To achieve efficiency, a proposed efficient parallel montgomery exponentiation core is designed and implemented for performing the underlying field operations in the Paillier cryptosystem. The hardware implementation results of the proposed steganographic cryptosystem show an efficiency in terms of area (resources), performance (speed) and power consumption. Our steganographic cryptosystem represents a small footprint making it well-suited for the embedded systems and real-time processing engines in applications such as medical scanning devices, autopilot cars and drones.

KEYWORDS

Image Steganography, Public-Key Cryptography, Homomorphic Cryptosystem, Montgomery Exponentiation & Field Programmable Gate Array.

1. INTRODUCTION

In the modern era of technology, sharing multimedia content has become easier and faster. As a result of that, malicious tampering and unauthorized data manipulation have been more accessible to the eavesdroppers over the communication channels. To prevent that, hiding data technique is one of the possible solutions that provides a reliable, safe and secure communication channels in applications such as image authentication, copyrights, and fingerprinting [1]. Hiding data in a carrier is referred to as steganography, which is the art of hiding secret data in a carrier in such a stealthy way that avoids the suspicion of unauthorized receivers.

Secret data can be concealed in various carriers, but digital images are the most preferable and suitable carrier due to massive users and applications that have the frequent access to it on internet. Moreover, performing image filtering techniques, mechanisms and cryptographic systems over digital images is more efficient in the reconfigurable hardware platforms. There are three main key characteristics that determine the performance of steganographic cryptosystems: embedding rate, imperceptibility and robustness. Efficient cryptosystems have a balance realization between these three characteristics. The massive variety in digital image real-time embedded systems and applications makes them more vulnerable to the attacks from the hackers (e.g.

steganalysis tools) [2] for malicious targets, as delivery services, sharing rides, spying and warfare. Securing the secret data (i.e. control data) and cover image (i.e. footage images) itself is one of the steganographic frameworks that is achieved to protect the stego image against the steganalysis attacks and providing privacy services. This implies to have another secure layer before or after concealing data, where a public-key cryptosystem is implemented by having different kinds of secret codes, which are so-called private and public keys. The computational complexity in such these frameworks is increased because of the time-resource consuming field operations presented in these public-key cryptosystems.

Hardware platforms presents a strong flexibility for such these high computational-complexity cryptosystems [3]. Application Specific Integrated Circuits (ASICs) and Field Programmable Gate Array (FPGA) are very popular hardware platforms for designing and implementing cryptographic and image steganographic cryptosystems. FPGAs can provide a high performance that can be achieved by ASIC platforms, and they cost much less than ASICs [4] [5]. FPGAs are reconfigurable and physically secure devices, which are preferable platforms to the researchers for testing their implementations. ASICs/FPGAs platforms have many features and computational capabilities that improve the performance such as parallelism and pipelining architectures. Few steganographic hardware implementations have been designed [6] [7] [8], which aim to increase the processing speed (throughput), less consumed area (resources), higher embedding rates, better image quality (PSNR) and robustness (security).

In [7], a hardware cryptoprocessor for privacy-preserving data mining algorithm is implemented using the paillier cryptosystem. Parallelism is applied through exploiting the independency among the modular operations such as multiplications and exponentiations. Pipelined stages are inserted among the field operations to break the long critical data paths. The cryptoprocessor is evaluated using privacy-preserving matching set intersection protocol. The authors provide a deep hardware realization of the privacy-preserving scheme using FPGA platform. As a case study, the cryptoprocessor is integrated into a privacy preserving set intersection protocol. A performance evaluation for the protocol is performed between the hardware and the software implementations. In [7], the parallelism is applied through duplicating instances of the independent modular operations resulting in using more resources. For example, the modular exponentiation operation is replicated twice for performing two exponents with different bases. Pipelining is done by utilizing DSP blocks to break up the long critical data paths, which leads to enhance the running frequency. Buffering the operations is employed to maintain the parallel execution between the elements of these operations. Extensive pipelining and buffering produce more cycles to perform modular operations. Modular exponentiation is performed using right-to-left binary algorithm, which includes repeating the modular multiplications based on the exponent. Right-to-left binary algorithm does not provide high performance when the base of the exponent is fixed all the time of processing intermediate values till the final result.

In this paper, a new high-performance public-key image steganographic framework is designed and implemented using FPGA reconfigurable hardware platform. The paillier public-key cryptosystem is used to encrypt pixels of the cover images [9]. The cover image is forwarded to the embedding process to conceal the secret data. After that, the pixels are encrypted by paillier cryptosystem with a public key to generate loaded-encrypted stego image. In a reversible way, the receiver, who has the private part (i.e. private key) of the public key, can decrypt the received loaded-encrypted stego image. The result is a loaded stego image that has the secret data. Extracting process is applied after. Reconstructing the cover image is done as a last step by sorting the decrypted pixels.

Figure 1 illustrates the general framework of the public-key image steganographic cryptosystem. Parallelism is applied to improve the computational complexity in the paillier cryptosystem, and

efficient transitions are considered in the finite state machines that control each main component in the proposed cryptosystem. For validating purposes, the full image steganographic cryptosystem is implemented in these FPGA devices introduced by Xilinx [10].

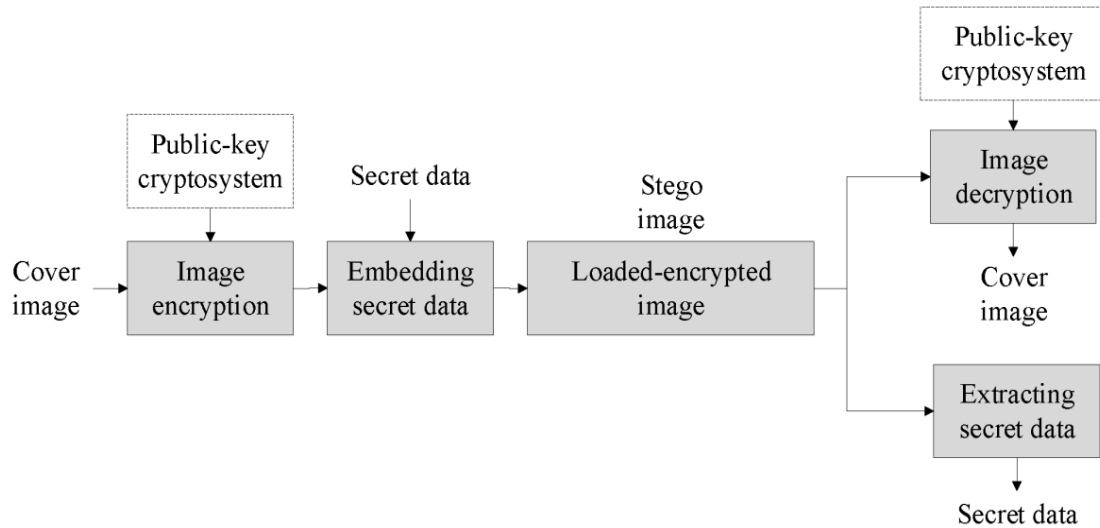


Figure 1. The general framework of the proposed public-key image steganographic cryptosystem.

This paper is organized as follows: Section 2 introduces a background for the paillier public-key cryptosystem. Section 3 presents the hardware architecture design for the proposed public-key image steganographic framework. The proposed steganographic cryptosystem evaluation in terms of embedding rate (bpp), image quality (PSNR), speed, resources utilization, power consumption and throughput are presented in Section 4. Finally, Section 5 concludes this paper.

2. PAILLIER CRYPTOSYSTEM

Paillier cryptosystem is a probabilistic public-key (e.g. asymmetric) cryptographic algorithm, which was invented by Pascal Paillier in 1999 [9]. It's based on the RSA computational-complexity public-key algorithm. Paillier cryptosystem has the n -th residue problem, where finding the composite n -th residue is believed to be computationally hard. The feature homomorphic property [9] in paillier cryptosystem makes it very appealing to be used and integrated in privacy-preserving embedded systems as in transferring money and electronic voting campaigns applications.

The textbook version of RSA is a deterministic public-key algorithm (i.e. no random components) [11], which makes it vulnerable to the chosen-plaintext attacks by exploiting the multiplicative property [12] [13]. In this attack, the attacker can distinguish between the ciphertexts, and this kind of RSA implementation is referred to as non-semantic cryptosystem. To resist this type of attacks, padding schemes for RSA is applied by embedding some random paddings into the plaintexts before starting encryption process [14]. This makes RSA is a semantic secure algorithm, which means the attackers could not distinguish between the ciphertexts.

Padded RSA cryptosystem does not support the homomorphic property since the randomness injected to the plaintext before encryption [15], hence RSA can be either semantically secure or homomorphic cryptosystem. On the other hand, Paillier cryptosystem is a semantic-

homomorphic cryptosystem. However, the price to pay is that paillier cryptosystem consumes more resources with equivalent security level with RSA [15]. Paillier cryptosystem requires more modular exponentiation and multiplications field operations than the RSA. The next is a brief of how the encryption and decryption are processed in paillier cryptosystem.

2.1. Key GENERATION in Paillier Cryptosystem

At any public-key cryptosystem, there is a key generation pre-process is done by the receiver, where public and private keys are generated for the encryption and decryption processes [16]. In paillier cryptosystem, the receiver chooses two large primes, q and p , the Great Common Divisor (GCD) for $q.p$ and $(q - 1) (p - 1) = 1$, A hard-to-factor number $n = q.p$ and $\lambda = \text{LCM} ((q - 1) (p - 1))$ are obtained, where LCM is the Least Common Multiple. The receiver randomly selects g in the $Z^*_{n^2}$ field, where $\text{GCD} (L (g^\lambda \text{ mod } n^2), n) = 1$, and $L(x) = (x-1)/n$ [16]. The receiver finally distributes his public key pair (n, g) , and the λ is considered as the private key for that public key.

2.2. Encryption and Decryption in Paillier Cryptosystem

The sender has a message $M \in Z^*$, then a random integer $r \in Z^*_n$ is selected for semantic security [1]. The ciphertext C of that M is computed using the following equation:

$$C = \text{ENC}_{pk}(M,r) = g^M r^n \text{ mod } n^2 \quad (1)$$

where ENC is the process of encryption and pk is the public key of the receiver. The ciphertext C is transmitted through the communication channel, the receiver gets it, and performs the following to reveal the original message M :

$$M = \text{DEC}_{pr}(C) = L(C^\lambda \text{ mod } n^2) / L(g^\lambda \text{ mod } n^2) \text{ mod } n \quad (2)$$

where DEC is the process of decryption, $L(x) = (x-1)/n$, and pr is the private key of the receiver.

2.3. Homomorphic Properties in Paillier Cryptosystem

The power of paillier cryptosystem comes from the additive homomorphic properties, which makes it a very suitable cryptosystem for electronic applications that require hiding identities as privacy-preserving perspective [17]. At the encryption process, let say we have two encrypted messages, E_1 and E_2 , such as: $E_1 = \text{ENC}_{pk}(M_1, r_1)$ and $E_2 = \text{ENC}_{pk}(M_2, r_2)$. These two encrypted messages are considered as an additive homomorphic function at decryption process as follows:

$$\text{DEC}_{pr}(E_1, E_2) = M_1 + M_2 \text{ mod } n \quad (3)$$

To verify that, check the encryption process for both messages as follows:

$$\text{ENC}_{pk}(M_1, r_1) \times \text{ENC}_{pk}(M_2, r_2) = g^{M_1} g^{M_2} r_1^{r_2} r_2^{r_1} \text{ mod } n^2 = g^{M_1 + M_2} r_1^{r_2} r_2^{r_1} \text{ mod } n^2 \quad (4)$$

Another form of additive homomorphic property is multiplying $\text{ENC}_{pk}(M_1, r_1)$ with g^{M_2} , which will give us the sum of the corresponding messages: $M_1 + M_2$. For multiplicative homomorphic property, an encrypted message $\text{ENC}_{pk}(M_1, r_1)$ is raised to a constant k , the decryption is the message $k.M_1$ as shown in the following equation:

$$\text{DEC}_{pr}(\text{ENC}_{pk}(M_1, r_1)^k \text{ mod } n^2) = k.M_1 \text{ mod } n \quad (5)$$

3. THE PROPOSED HARDWARE ARCHITECTURE DESIGN

In this section, the structure of the proposed image steganographic cryptosystem is presented. The structure consists of components that works together to embed-extract and encrypt-decrypt a single pixel. We should mention that all pixels of the cover image are within gray-scale levels (e.g. 0 to 255). Each component at both encryption and decryption processes is controlled by an efficient finite state machine. Figure 2 represents the main components of the proposed steganographic cryptosystem, and paillier cryptosystem is used for encrypting and decrypting pixels.

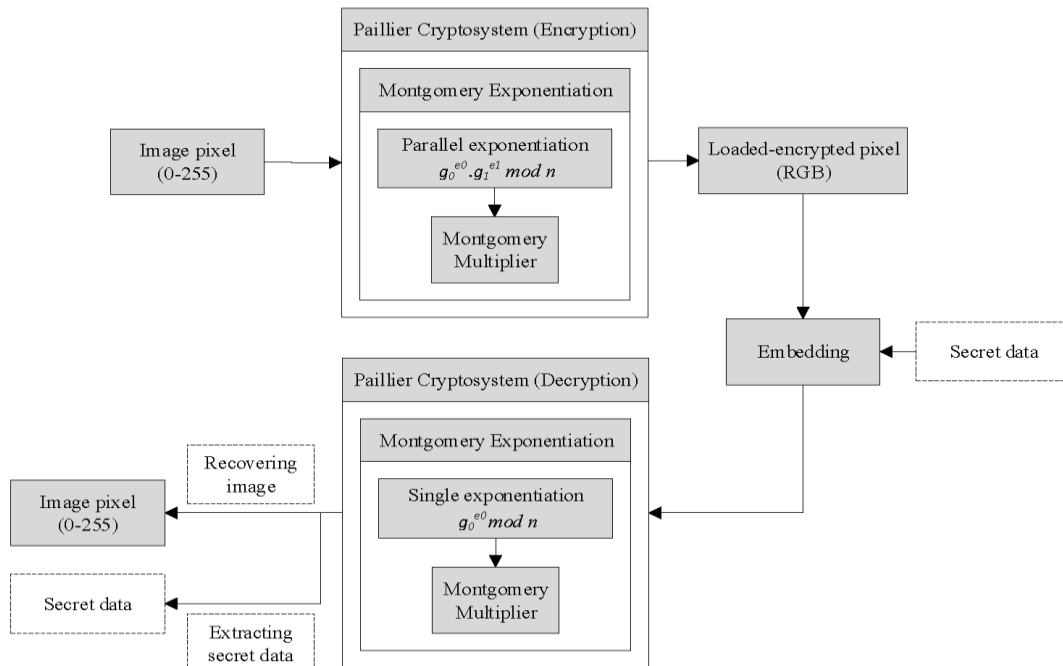


Figure 2. The main components of the proposed steganographic cryptosystem in encryption and decryption processes.

3.1. Image Embedding and Encryption

To protect and increase the robustness, encrypting the pixels of the cover image is performed first, and then the embedding process is done to the encrypted cover image. Least Significant Bit (LSB) is one of the low-complexity steganographic schemes that can be applied to embed the secret data into pixels of the cover image. Increasing the capacity of the concealed data (e.g. high bpp) can be achieved by embedding more bits into a single pixel. However, this results in a degradation of quality for the cover image (e.g. lower PSNR) since original bits are altered. In our proposed cryptosystem, the embedding procedure doesn't require to change any single bit in pixels of the cover image. This provides us the capability of recovering the cover image without decreasing the quality of the cover image (100% PSNR). For instance, assume the cover image has a resolution 64 rows x 64 columns (4096 pixels). the cover image can conceal up to 4096 bits of secret data, which equals to 512 bytes. Embedding single is done by using the additive homomorphic property of the paillier cryptosystem. Each pixel P is divided into two values (M_1 and M_2) in such a way that $P = M_1 + M_2$. Each value is encrypted using Equation 1 to obtain E_{M_1} and E_{M_2} . The embedding is done as follows; if secret bit is 1 and $E_{M_1} < E_{M_2}$, Swap E_{M_1} and E_{M_2} values. If secret bit is 0 and $E_{M_1} > E_{M_2}$, Swap E_{M_1} and E_{M_2} values. The embedding is done when

all bits of the secret data are scanned. Note that sequence of selected pixels is defined using a data hiding key shared between sender and receiver.

Equation 1 states that, to encrypt pixel (e.g. plain text), we should raise g to the power of pixel value, and multiply it with a randomly selected r value to the power of n . The result then is reduced (mod) to the selected field (n^2). These two exponentiations over modulus are very common in modular arithmetic computations in public-key cryptography. Single modular exponentiation (C) computes the remainder of the base (b) raised to the exponent (e) power as $C = b^e \text{ mod } n$ where $0 \leq C < n$. Performing this kind of modular operations is done by using different algorithms. Binary Left-to-Right exponentiation algorithm is one of the easiest and trivial way to compute g^e . In binary algorithm, the bits of e are scanned, then perform 1 squaring every time and 1 field multiplication when the current bit equal to 1. In 1985, P. Montgomery proposed a new algorithm to compute the modular multiplication operations efficiently [18]. He proposed to map the presentation of the elements in any field Z_n to a corresponding domain, which is called as Montgomery Domain (MD). Assume the modulus n and x are integers in Z_n , Consider R is the radix 2^k , where k is the number of bits in modulus n , and $\text{GCD}(n, R) = 1$. Mapping the x to the montgomery domain is done as $X_{MD} = x \cdot R \text{ mod } n$. The natural representation of the x in montgomery domain can be obtained by multiplying the X_{MD} by the multiplicative inverse of the considered R radix $x = X_{MD} \cdot R^{-1} \text{ mod } n$. Multiplying x and y is done by first moving them to the montgomery domain, then observing the $Z_{MD} = X_{MD} \cdot Y_{MD} \text{ mod } n$ can hold the following:

$$X_{MD} \cdot Y_{MD} = x \cdot R \cdot y \cdot R = z \cdot R^2 \text{ mod } n = Z_{MD} \cdot R \text{ mod } n \quad (6)$$

A reduction is required to obtain the result $Z_{MD} = Z_{MD} \cdot R^{-1} \text{ mod } n$, which a montgomery reduction is applied for that easily. Since the z is what we are looking for, the montgomery multiplication combines the reduction $Z_{MD} \cdot R^{-1} = z$ and multiplication $x \cdot y$ operations to compute the product of two integers. Performing the montgomery modular exponentiation $g^e \text{ mod } n$ can be done by combining the binary exponentiation and the montgomery multiplication. Algorithm 1 shows this kind of combination. It consists of k executions for the main loop, which contains two montgomery multiplication. For single montgomery multiplication, the computational time is to $3.k.T$ [19], where T is the execution time for a single full-adder. So, the total computational time for $g^e \text{ mod } n$ is equal to $6.k^2.T$.

Algorithm 1 Montgomery Exponentiation Algorithm

Input: $g = g_{k-1}, g_{k-2} \dots g_0$, $e = e_{k-1}, e_{k-2} \dots e_0$, $e_{k-1} = 1$, and $n = n_{k-1}, n_{k-2} \dots n_0$. $0 \leq g < n$, $A = 2^k \text{ mod } n$, $e_{2k} = 2^{2k} \text{ mod } n$

Output: $A = g^e \text{ mod } n$

$g' \leftarrow \text{MontP}(g, e_{2k}); \quad \triangleright \text{MontP is Montgomery multiplication}$

for $i = k - 1$ **downto** 0 **do**

$A \leftarrow \text{MontP}(A, A);$

if $e_i = 1$ **then**

$A \leftarrow \text{MontP}(A, g');$

end if

end for

$A \leftarrow \text{MontP}(A, 1);$

Return $A;$

Equation 1 states to encrypt a message, we need to get the multiplication result of g^M and rn exponent pair. Algorithm 2 presents the proposed Montgomery Simultaneous Exponentiation (MSE) to calculate different exponents with two bases, which uses the Left-to-Right method. As

shown, four precomputed parameters have to be obtained first. The for loop is performed when the exponents e_0 and e_1 are not zeros. Thus, the computation time of the MSE depends on the exponents, more ones in the exponents mean more montgomery multiplications. The computation time for the MSE with k -bit bases and exponents is given by $(7/4).k.T_{MontP}$, where T_{MontP} is the computational time of a single montgomery multiplication [19].

Algorithm 2 Montgomery Simultaneous Exponentiation (MSE) Algorithm

Input: $g_0 = g_{0_{k-1}}, g_{0_{k-2}} \dots g_{0_0}, g_1 = g_{1_{k-1}}, g_{1_{k-2}} \dots g_{1_0}, e_0 = e_{0_{k-1}}, e_{0_{k-2}} \dots e_{0_0}, e_{0_{k-1}} = 1, e_1 = e_{1_{k-1}}, e_{1_{k-2}} \dots e_{1_0}, e_{1_{k-1}} = 1$, and $e_{-2k} = 2^k \bmod n$

Output: $A = g_0^{e_0} g_1^{e_1} \bmod n$

$g'_0 \leftarrow \text{MontP}(g_0, e_{-2k}); g'_1 \leftarrow \text{MontP}(g_1, e_{-2k});$

$g_{0i}' \leftarrow \text{MontP}(g'_0, g'_1); A \leftarrow \text{MontP}(e_{-2k}, 1);$

for $i = k - 1$ **downto** 0 **do**

$A \leftarrow \text{MontP}(A, A);$

switch e_{0i}, e_{1i} **do**

case 0, 1

$A \leftarrow \text{MontP}(A, g'_0);$

case 1, 0

$A \leftarrow \text{MontP}(A, g'_1);$

case 1, 1

$A \leftarrow \text{MontP}(A, g_{0i}');$

end for

$A \leftarrow \text{MontP}(A, 1);$

Return A

Figure 3 represents the proposed architecture of the MSE core, which has three main components: the montgomery multiplication, RAM-based unite for the precomputed parameters, and finite-state-machine control unite. Initially, the four precomputed parameters are calculated and stored. The for loop in Algorithm 2 is applied by scanning the bit-stream of the exponents e_0 and e_1 , then one of the cases is applied accordingly. Note that in each iteration, the value of A is updated so the right result is maintained. The final result is obtained by performing a single montgomery multiplication $\text{MontP}(A,1)$, which converts it back to the natural representation.

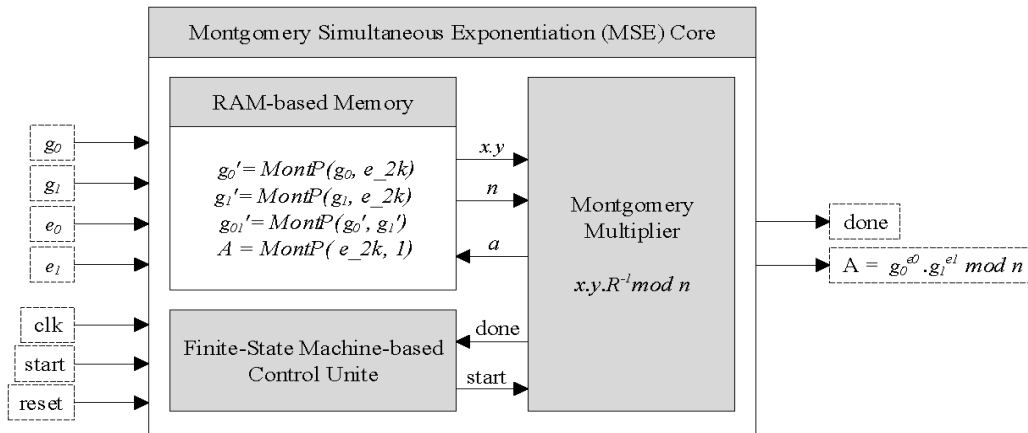


Figure 3. Architecture of the proposed Montgomery Simultaneous Exponentiation (MSE) core.

3.2. Domain of the Loaded-Encrypted Pixels

In any field Z_n^* , all values are $\in [0, n-1]$, and any applied operation over these values must get the result into the field by applying mod n operation. In equation 1, the mod is mod n^2 , which means the field is squared, and the results are going to be out of the $\in [0, n^2-1]$ range. The pixels in cover image are gray-scale levels $\in [0, 255]$, and encrypting these pixels will generate results up to $(n^2 - 1)$. These encrypted pixels are viewed as a loaded-encrypted stego image, and rendering it is not possible in a gray-scale image. The only way to overcome this rendering issue is to divide each pixel into 3 bytes, each byte represents a channel in RGB image. Figure 4 illustrates the process of rendering the encrypted pixels into RGB stego image. The loaded-encrypted stego image is sent to the receiver to decrypt and extract the secret data out of the RGB stego image.

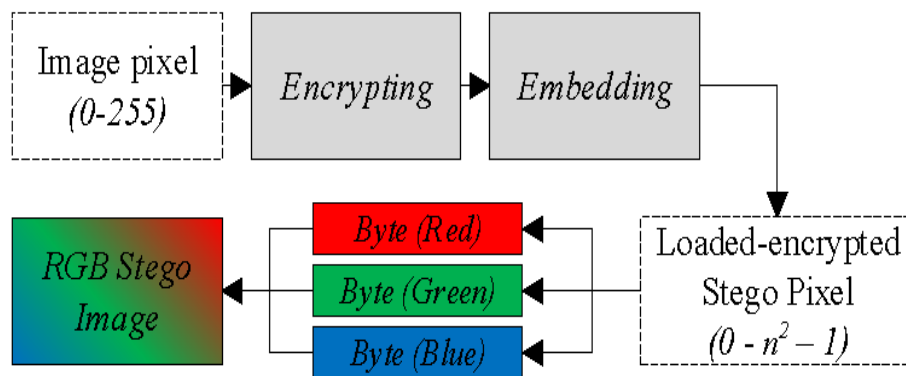


Figure 4. Rendering the loaded-encrypted image into RGB stego image.

3.3. Image Decryption and Extraction

On the receiver side, the RGB stego image is entered into a reversible separable decryption and extraction mechanism. The decryption process is applied to every single pixel in the received image. A private key λ is required as stated in equation 2. The receiver will be able to extract the secret data without decrypting pixels of the stego image. Decrypting the received image will generate the original cover image using the data hiding key. Using homomorphic property in Equation 3, the pixel P is equal to $DEC_{pr}(E_{M_1}, E_{M_2}) = M_1 + M_2$. Extraction process is done by comparing encrypted pixel pairs E_{M_1} and E_{M_2} . If $E_{M_1} > E_{M_2}$, the secret bit is 1, and if the $E_{M_1} < E_{M_2}$, the secret bit is 0. The extraction is done when all encrypted pairs are scanned.

4. EXPERIMENTAL RESULTS AND DISCUSSIONS

In this section, the results for the hardware implementation of the steganographic cryptosystem are presented. Verilog Hardware Description Language (HDL) is used to implement the proposed cryptosystem. Verifying the performance of the proposed design is achieved by using the FPGA platform devices which are provided by Xilinx [10], where two FPGA families are used, Artix-7 and Kintex-7 devices [10]. Both FPGA devices are fabricated using the common 28nm technology. The Kintex-7 targets the high-density complex applications such as those in 3G and 4G communications, while the Artix-7 FPGA provides mid-performance for the applications running over power-sensitive systems including the vision cameras and low-end wireless networks. The hardware implementation has been fully synthesized, translated, placed and routed using the new Xilinx Vivado 2018.2 design suite. A balance design strategy is applied as an

optimization goal. A time constraint is applied, and the timing constraints report provides a zero timing error. Table 1 shows the results for the proposed steganographic cryptosystem after place and route.

Embedding-encryption module implementation provides a running frequency up to 135.2 MHz using 193 slices of the available resources in Artix-7 FPGA. In Decryption-extraction module implementation, up to 166.7 MHz of running frequency is achieved with 334 slices. Block RAMs (BRAMs) are used as a memory to read the cover image and write the loaded encrypted stego image. More BRAMs are utilized when the size of the cover image is increased. The modules in Kintex-7 provides higher running frequencies between 250 MHz to 333.3 MHz in embedding encryption and decryption-extraction, respectively. The total on-chip power consumption is measured through calculating the power required by the resources in the hardware implementation such as clock, slices (i.e. LUTs and registers) and BRAMs unites at the maximum running frequencies. For the embedding-encryption module, our design consumes 0.139 Watt for 64x64 cover image to 0.134 Watt for 256x256 cover, while the decryption-extraction module takes up to 0.362 Watt of power consumption for 256x256 cover image. The results in Table 1 can tell that our proposed cryptosystem is suitable for the limited-resources low-power embedded systems.

Table 1. Place and route results for encryption and decryption processes.

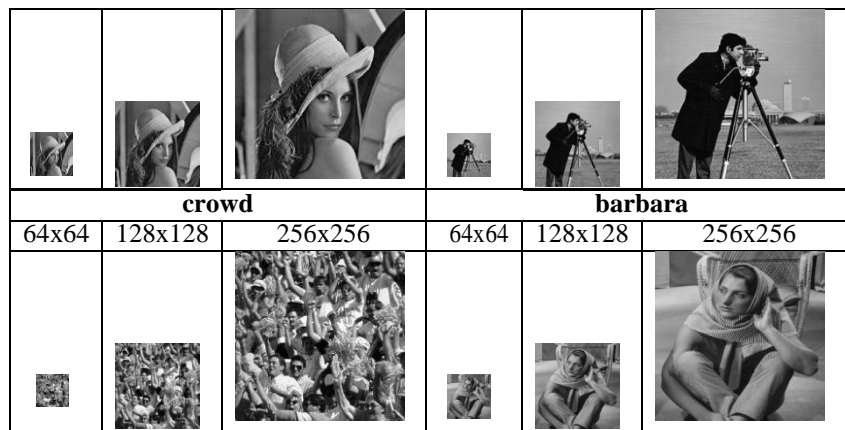
Size	Device	Encryption					Decryption				
		Slices	F.F	LUT	BRAM	Freq.	Slices	F.F	LUT	BRAM	Freq.
64	Artix	148	390	409	1.5	135.2	326	971	768	4	166.7
128		151	388	411	5	134.8	317	980	774	8.5	166.5
256		193	409	469	20	133.3	334	1000	819	34	166.6
64	Kintex	155	390	429	1.5	286	333	967	854	4	333.3
128		165	388	430	5	270.27	347	980	866	8.5	333.3
256		179	409	499	20	250	349	1000	850	34	333.3

4.1. Prototyping the Proposed Image Steganographic Cryptosystem

FPGA device, MATLAB program is used to convert the cover image to a hex format file. The file is loaded into the BRAMs of the FPGA device. Each pixel is read from a specific location (i.e. address) and got it ready for embedding the secret data and encrypt it. The loaded-encrypted pixel is written back to the BRAM at the same location. Once all pixels are loaded by the secret data and encrypted, the loaded-encrypted pixels are extracted from the BRAM and converted to a hex readable file. This file is forwarded to a MATLAB program for the rendering purposes. As mentioned earlier, the rendering process makes the extracted file from the FPGA to be shown as RGB stego image, which is done by allocating a single byte to each channel: red, green and blue. Table 2 represents four gray-scale images (lena, camera man, crowd and barbara) as cover images for the proposed steganographic cryptosystem. Each is represented in 3 different sizes: 64x64, 128x128 and 256x256.

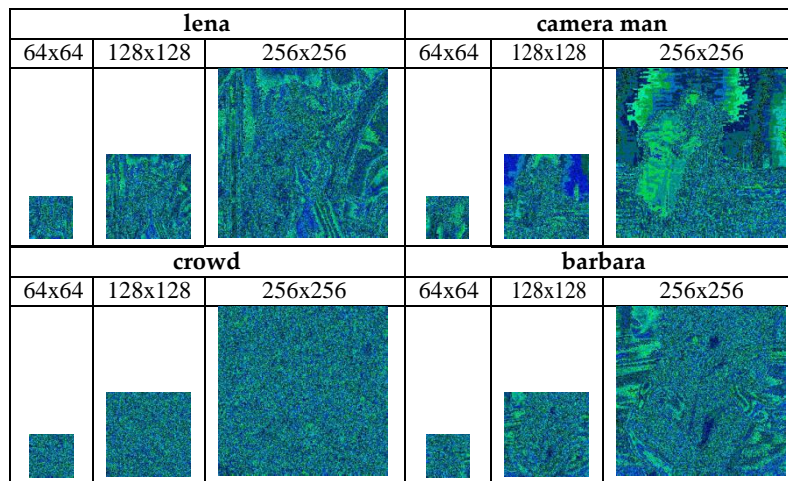
Table 2. Four different sizes gray-scale cover images.

lena			camera man		
64x64	128x128	256x256	64x64	128x128	256x256



These cover images are the input to the cryptosystem, the secret data as well. For example, if the 64x64 cover image is the input, the secret data has 64x64 or 4096 bits are going to be concealed. Table 3 shows RGB stego images for the cover images under different sizes. Note that for each original cover image at any size, a random secret data is generated to achieve randomness in the results (i.e. RGB stego images). As shown, the stego images are rendered differently from size to another. The stego images are ready for transmitting to the receiver for recovering original images and extracting secret data reversibly.

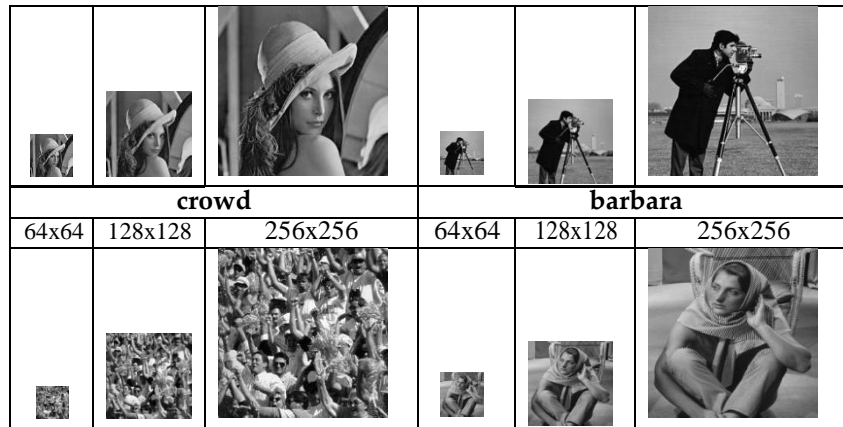
Table 3. RGB stego images for cover images.



The receiver will perform the reversible decryption and extraction processes to recover the original cover image and get the secret data. To perform that, the received stego image is converted to a text hex format file by running a MATLAB program. Then, this file is loaded to the BRAMs of the FPGA, where each pixel is decrypted, and bits of secret data are extracted. The decrypted pixel is written back to the BRAM at same address of the encrypted pixel. This is applied to all pixels in the stego image. Once all pixels are decrypted, a file is extracted from the BRAMs in a hex readable format. The file is forwarded to a MATLAB program to gather all decrypted pixel and render them into a gray-scale original cover image. Table 4 represents the decrypted original cover images for the RGB stego images at the receiver side.

Table 4. Decrypted cover images at the receiver side.

lena			camera man		
64x64	128x128	256x256	64x64	128x128	256x256



Peak Signal-to-Noise Ratio (PSNR) is a subjective indicator for the quality of an image, which is measured in decibels (dB). The higher PSNR value indicates maintaining better quality. In the proposed steganographic, 100% PSNR is achieved since there is no loss in cover images, thus the receiver can recover any kind of cover images perfectly. For embedding rate, the proposed cryptosystem always offers a fixed rate of 1 bpp. As quantitative metric for the performance, the throughput of the steganographic cryptosystem is defined as the total bits that cryptosystem can process per time unit. The following equation shows how to calculate the throughput for the proposed cryptosystem.

$$\text{Throughput} = \frac{\text{Input-Data} \cdot \text{Frequency}}{\text{Clock Cycles of Encryption or Decryption}} \tag{7}$$

Table 5 shows the performance results in terms throughput and Frame Per Second (fps) for the embedding-encryption and decryption-extraction hardware FPGA implementations in different cover images. It's expected to get large number of clock cycles in the proposed cryptosystem due to the intensive field operations in the paillier cryptosystem. To encrypt a single pixel, 1520 clock cycles are required, and decrypt it requires 1460 clock cycles. Note that the decryption is performed over RGB pixels.

From Table 5, FPS rate is calculated as number of pixels in one image divided by the throughput. For instance, it is possible to process 22.3 fps in embedding-encryption module, and 28.6 fps in decryption-extraction module for 128x128 cover image in real-time embedded system. For 1-minute period, the proposed cryptosystem can process a video of 21.9 MB size at 22.3 fps and 84.3 MB size at 28.6 fps in embedding-encryption and decryption extraction module hardware implementations, respectively.

Table 5. Performance results for different cover images.

CoverImage	Size	Throughput (Kpps)		FPS	
		Encryption	Decryption	Encryption	Decryption
lena	64	192.7	207.6	47.1	50.7
Cameraman					
crowd					
barbara	128	365.2	468.5	22.3	28.6
lena					
Cameraman					
crowd					

barbara					
lena	256	676.4	937.1	10.4	14.3
Cameraman					
crowd					
barbara					

Table 6 represents a comparison between the proposed hardware implementation of the paillier cryptosystem and other implementations. Our design outperforms the works in terms of PSNR, utilized slices and frequency. In paper [6], the hardware implementation is designed using interpolation expansion method. The design achieved a high performance in terms of the throughput, which is capable of processing about 7640 pixels in a single second using Virtex-6 FPGA Device. On the other hand, a huge amount of resources as register and LUTs are utilized, where it requires around 10 times of the resource utilized by our design, and our design consumes less power by 91.5% than the work in [6]. In [20], a pipelined reversible hardware architecture for secret water marking embedding is proposed, where the Reversible Contrast Mapping (RCM) algorithm is adopted for embedding and extraction secret data. The architecture offers low-complexity fast processing through breaking the critical path of the design into 6 pipelined stages. However, our hardware architecture is faster, requires less resources and achieves higher throughput than the work in [20].

The work in [21] represents methods of encapsulating secret data into a group n of pixels in a $(2n+1)$ -ary notational system. The hardware implementation offers high fps but with low PSNR and high utilized resources, where 16% of the total resources in Virtex -7 FPGA device is roughly 12,000 logic cells. The power consumption in [21] is very high, it is 3.807 Watt, while our hardware implementation consumes between 0.139 Watt to 0.362 Watt of power. We should mention that the hardware implementations in [6], [7], [20] and [21] do not apply any kind of cryptographic algorithms. To the best of our knowledge, our proposed reconfigurable implementation for image steganography using paillier cryptosystem is the first to present in the literature. Figure 5 represents a comparison between our proposed steganographic scheme with other works [22] and [23] in terms of image quality and embedding rate. The image quality is always 100% PSNR regardless of the embedding rates.

Table 6. Performance comparison with existing implementations for image steganography.

Ref.	Image Size	Device	bpp	PSNR	Slices	LUT	F.F	Freq.	Throughput (Kpps)
[6]	328x264	Virtex-5	1	x	x	9,715	4883	96.4	7340.17
		Virtex-6	1	x	x	8,564	4908	100.4	7640.63
[7]	128x128	Spartan-6	1	51.1444	160	322	214	104.971	x
[21]	512x512	Virtex-7	1	45.11	16%	1%	2%	144	x
[20]	32x32	Spartan-3	0.46	29.46	9881	11291	9347	98	100.3
Ours	128x128	Artix-7	1	100%	151	774	980	134.8	370
	256x256	Kintex-7	1	100%	179	850	1000	250	680

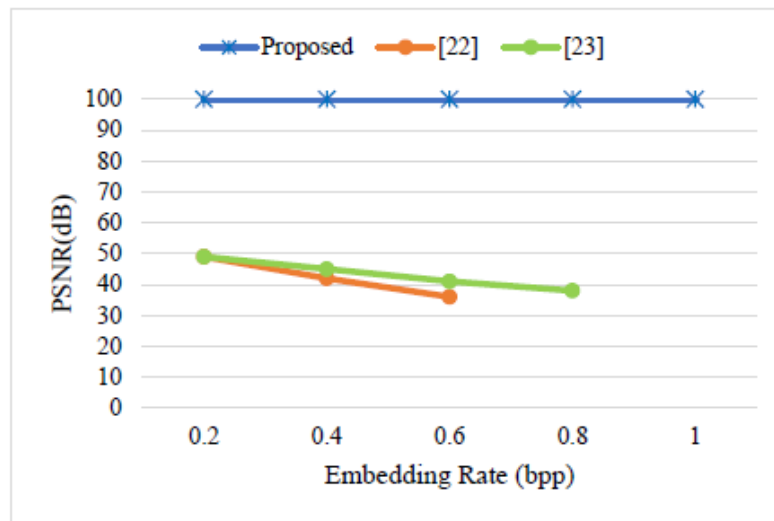


Figure 4. Comparison of PSNR vs embedding rate performance between the proposed steganographic scheme and others.

5. CONCLUSIONS

In this paper, a hardware architecture for a separable image steganographic scheme using paillier cryptosystem is designed and implemented on reconfigurable FPGA platforms. An efficient montgomery simultaneous exponentiation is implemented for performing exponentiation operations in encryption and decryption of paillier cryptosystem. The place and routed results have demonstrated a high performance in terms of speed, utilized resources and power consumption in the new Kintex-7 and Artix-7 Xilinx FPGA devices. Our proposed steganographic achieves a guaranteed 100% PSNR for any kind of cover images with a fixed 1 bpp of embedding capacity. In real-time embedded system, our proposed hardware architecture is able to embed and encrypt up to 47.1 fps of cover images. In decryption-extraction processes, the hardware architecture can perform up to 28.6 fps of RGB stego images. The proposed secure architecture offers a small footprint which can be utilized in many embedded applications as graphic processing engines and accelerators.

ACKNOWLEDGEMENTS

This work was supported in part by the Natural Sciences and Engineering Research Council (NSERC) of Canada and in part by the Regroupement Strategique en Microelectronique du Quebec (ReSMiQ).

REFERENCES

- [1] F. Y. Shih, *Digital watermarking and steganography: fundamentals and techniques*, CRC press, 2017.
- [2] T. Rana, A. Shankar, M. K. Sultan, R. Patan and B. Balusamy, "An Intelligent approach for UAV and Drone Privacy Security Using Blockchain Methodology," in *9th International Conference on Cloud Computing, Data Science and Engineering*, 2019.
- [3] S. Kilts, *Advanced FPGA design*, Hoboken, N.J.: Wiley, 2007, p. 336.
- [4] S. M. Trimberger, *Field-programmable gate array technology*, Springer Science and Business Media, 2012.
- [5] X. Inc, *7 Series FPGAs Data Sheet: Overview*, 2018.
- [6] W. A. P. Laces and J. J. G. Hernandez, "FPGA implementation of a low complexity steganographic system for digital images," in *IEEE/ACIS 14th International Conference on Computer and Information Science (ICIS)*, 2015.

- [7] K. Pathak and M. Bansal, "A FPGA based Steganographic System Implementing a Modern Steganalysis Resistant LSB Algorithm," *Defence Science Journal*, vol. 67, pp. 551-558, 2017.
- [8] S. Rajagopalan, P. J. S. Prabhakar, M. S. Kumar, N. V. M. Nikhil, H. N. Upadhyay, J. B. B. Rayappan and R. Amirtharajan, "MSB based embedding with integrity: An adaptive RGB Stego on FPGA platform," *Inform.Technol.J*, vol. 13, pp. 1945-1952, 2014.
- [9] P. Paillier, "Public-key cryptosystems based on composite degree residuosity classes," in *International Conference on the Theory and Applications of Cryptographic Techniques*, 1999.
- [10] Xilinx, *Xilinx - Adaptable. Intelligent.*, 2019.
- [11] R. L. Rivest, A. Shamir and L. Adleman, "A method for obtaining digital signatures and public-key cryptosystems," *Communications of the ACM*, vol. 21, pp. 120-126, 1978.
- [12] E. Kiltz, A. O'Neill and A. Smith, "Instantiability of RSA-OAEP under chosen-plaintext attack," in *Annual Cryptology Conference*, 2010.
- [13] Y. Desmedt and A. M. Odlyzko, "A chosen text attack on the RSA cryptosystem and some discrete logarithm schemes," in *Conference on the Theory and Application of Cryptographic Techniques*, 1985.
- [14] J.-S. Coron, D. Naccache and J. P. Stern, "On the security of RSA padding," in *Annual International Cryptology Conference*, 1999.
- [15] X. Yi, R. Paulet and E. Bertino, *Homomorphic encryption and applications*, vol. 3, Springer, 2014.
- [16] W. Stallings, *Cryptography and network security: principles and practice*, Pearson Upper Saddle River, 2017.
- [17] A. Acar, H. Aksu, A. S. Uluagac and M. Conti, "A survey on homomorphic encryption schemes: Theory and implementation," *ACM Computing Surveys (CSUR)*, vol. 51, p. 79, 2018.
- [18] P. L. Montgomery, "Modular multiplication without trial division," *Mathematics of computation*, vol. 44, pp. 519-521, 1985.
- [19] G. Ottoy, B. Preneel, J. Goemaere and L. Strycker, "Flexible design of a modular simultaneous exponentiation core for embedded platforms," in *International Symposium on Applied Reconfigurable Computing*, 2013.
- [20] H. K. Maity and S. P. Maity, "FPGA implementation of reversible watermarking in digital images using reversible contrast mapping," *Journal of Systems and Software*, vol. 96, pp. 93-104, 2014.
- [21] K. S. Shet, A. R. Aswath, M. C. Hanumantharaju and X. Gao, "Novel high-speed reconfigurable FPGA architectures for EMD-based image steganography," *Multimedia Tools and Applications*, pp. 1-30, 2019.
- [22] K. Ma, W. Zhang, X. Zhao and N. Yu and F. Li, "Reversible Data Hiding in Encrypted Images by Reserving Room Before Encryption," *IEEE Transactions on Information Forensics and Security*, vol. 8, no. 3, pp. 553-562, 2013.
- [23] X. Cao, L. Du, X. Wei and D. M. a. X. Guo, "High Capacity Reversible Data Hiding in Encrypted Images by Patch-Level Sparse Representation," *IEEE Transactions on Cybernetics*, vol. 46, no. 5, pp. 1132-1143, 2016.

USE OF AN IOT TECHNOLOGY TO ANALYSE THE INERTIAL MEASUREMENT OF SMART PING-PONG PADDLE

Rajeev Kanth¹, Tuomas Korpi¹ and Jukka Heikkonen²

¹School of Engineering and Technology, Savonia University of Applied Sciences, Opistotie 2, 70101 Kuopio Finland

²Department of Future Technologies, University of Turku, Vesilinnantie 5, 20500 Turku Finland

ABSTRACT

In this article, a Smart Ping Pong Paddle has been introduced as an example of the use of sensor technology in sports. We have devised an accelerometer and a gyroscope sensor for the analyzing purpose and have gathered motion data of the game object to make a real-time 3D replica of the paddle to get an actual orientation of it. Technical details and principles of how to get the digital motion processing data from sensor to microcontroller and again transfer that wirelessly to a 3D modeling software are examined. Technical details are applied in practice, and the working demo of Smart Ping Pong paddle is built. Also, a couple of examples of other similar applications in the realm of object orientation sensing are overviewed.

KEYWORDS

Accelerometer Sensor, Gyroscope Sensor, Ping Pong Paddle, and Motion Analysis

1. INTRODUCTION

In recent years, the use of sensors has progressively utilized in analyzing several games. [1]-[3]. A game coach needs to instruct their trainees in real-time using a 3D replica of the ping pong paddle. In this article, we have succeeded in demonstrating a real-time analysis of the ping pong paddle. There is a massive potential to use IoT technology and embedded devices in sport to gather useful information and to make the sports training more efficient or gameplay more interesting. A game of table tennis is a familiar sport, and a six-axis (Gyro + Accelerometer) MEMS motion tracking sensor is cheaply available in the market. Therefore we came up with an idea to integrate the InvenSense MPU-6050 sensor inside a table tennis racket. Gyroscope and accelerometer data can be combined to calculate an orientation of the object. Orientation (angular position) and position should not be confused since it is not possible to get a position with 6-axis gyro/accelerometer. The position specifies the location and orientation provides the direction that the object is facing around an axis.

Table tennis racket cannot be hooked into a computer with a cable, therefore, it needs a wireless solution so that it seamlessly connects to a system and gather the vital orientation information at the real-time of gaming. An ESP8266 based microcontroller is used for wireless data transfer. With that same 'wireless and no need to be next to computer' -mentality, haptic feedback aka vibration motor is used in the handle of the Smart Ping Pong Paddle to inform the player when a connection between a wireless access point and receiver station is established.

The receiver station is connected to a computer that handles 3D object manipulation based on data received. In principle many programs could be used to making and moving the 3D model like Processing3, Matlab, Blender or you could program software from scratch that reads serial port data and draws objects based on that. For this use case, the Unity3D game engine was chosen because it is a robust platform that specializes in moving game objects with C# code.

2. RELATED WORKS

Olli Koskenranta, in his thesis entitled “Manipulating 3D objects with gaze and hand gestures,” [4] examines and creates a user interface for gesture-based 3D object handling. Gesture-based interaction is already used in playing games with Microsoft Kinect, PlayStation 3 Move and Nintendo Wii. For gaze tracking camera (Imaging Source DMK31AU03) was used. Nine-axis Accelerometer-gyroscope (ATR-Promotions WAA-010) with Bluetooth connection interpreted hand movements and sent the data to a laptop with JavaScript in the RealXten 3D platform. The user interface was expected to be able to manipulate objects in various ways, including object selection, gripping the object, releasing the purpose and rotating and moving it. Rotation and moving the camera was to be done with gaze and object manipulation with hand gestures. Regardless of inaccuracies in gaze function or limited hand gestures, the project displayed different user interaction methods and their future possibilities in a practical way. The article “Flex sensors and MPU-6050 sensors responses on a smart glove for sign language translation.” written by A. Yudhana et al. [5] from Ahmad Dahlan University, Indonesia, goes over a design of a Smart Glove that translates hand sign language to a corresponding alphabet letter to a computer. Each finger has a flex sensor to detect a flex of the thumb, and on the top of the glove, there is a gyroscope-accelerometer sensor (MPU6050) to observe the tilt of the hand. Sensors are connected to Arduino microcontroller for processing and a Personal computer to monitor the value of sensor output value. Each gesture data (A-Z) is formed from seven different sensor values and each gesture data is taken 100 times to get a good sample size so that algorithms can predict the right sign by comparing samples.

3. BLOCK DIAGRAM OF THE SYSTEM

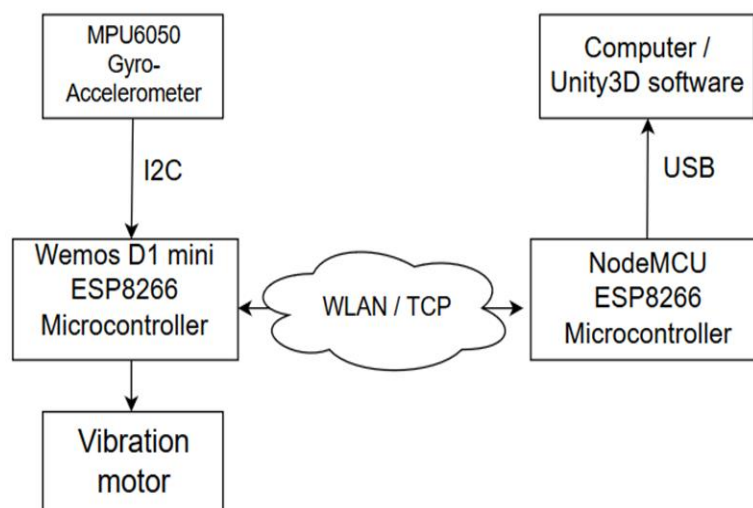


Figure 1. Block Diagram of the System



Figure 2. Embedded components

Components were chosen to be small so that they could be embedded inside a table tennis paddle and not affect the gameplay notably. MPU-6050 sensor was mounted under the rubber part of the paddle and handle was hollowed out to fit a small 'Wemos D1 mini' microcontroller to process sensor data via I2C bus, send haptic feedback to a small coin vibration motor (Parallax 28821) on the handle and use its built-in ESP8266 WiFi-module to transfer data wirelessly using TCP (Transmission Control Protocol). Components in the paddle get their power from 3xAA (4,5V) battery holder with an on/off switch. A battery holder is mounted on a player's wrist. Data receiving end of the system consist of another ESP8266 based microcontroller that collects data and sends it to the computer via USB, then serial monitoring is used to get the data in Unity3D, where a 3D model is ready to move based on the calculated orientation values. Receiving microcontroller does not need to be that small so NodeMCU is used instead of Wemos D1 mini to get more processing power and therefore smoother movement. The block diagram of the system and the embedded circuits within the paddle are shown respectively in Figures 1 and 2. Microcontroller D1 mini input voltage is 4.5 Volts trough a 5V pin. It has built-in 3.3 V voltage regulator so all of its digital pins output 3.3 Volts. The vibration coin motor has an operating voltage of 3.3 V and it is regulated through the D5 pin. Pins D1 and D2 act as SCL and SDA lines and connect to corresponding pins on the MPU-6050 sensor and it is powered through 3,3 V pin from D1 mini. The wiring diagram is shown in Figure 3.

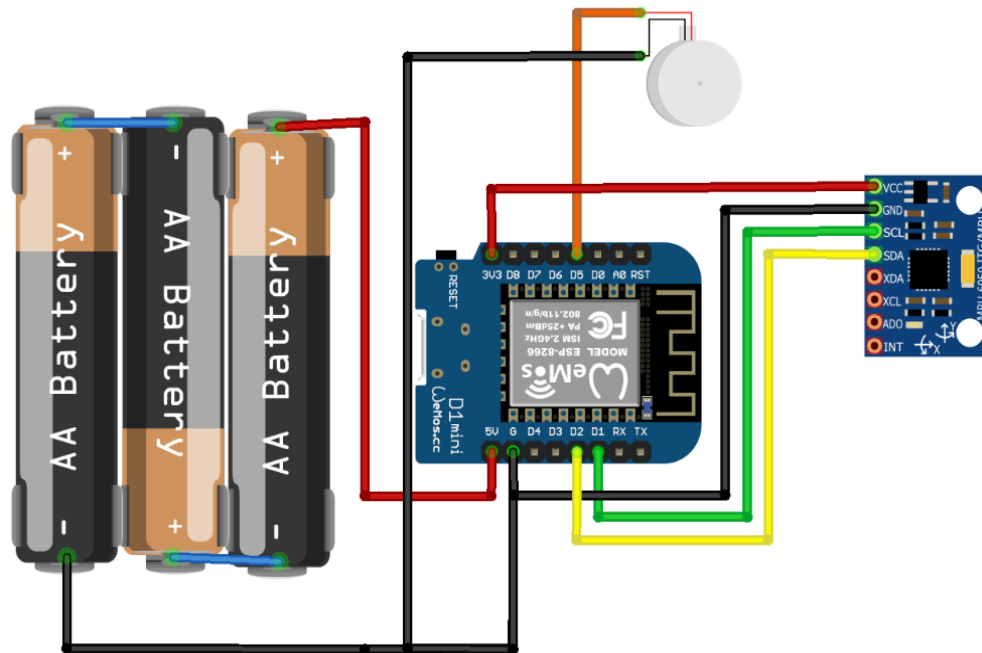


Figure 3. Wiring diagram made using Fritzing.

4. ACCELEROMETER AND GYROSCOPE

The InvenSense MPU-6050 sensor contains a MEMS (Micro-Electro-Mechanical Systems) accelerometer and a MEMS gyro in a single chip. It is the IMU (inertial measurement unit) sensor that is used to get the orientation of the object attached to it in three-dimensional space. MPU-6050 is a six-axis IMU sensor meaning that it gives out three gyro values and three accelerometer values as output. Each output has a 16-bit analog-to-digital converter to digitalize the output. There are many applications for orientation sensing like smartphone screen rotation, self-balancing robots, and quadcopters.

An accelerometer measures the direction of inclination and its magnitude. Gyroscopes output the rate of rotation. Both accelerometer and gyro use MEMS technology meaning that they are microscopic devices, particularly with moving parts. They can convert mechanical movement to electrical current that derives to orientation values.

By themselves, accelerometer nor gyroscope data is not accurate enough for smooth digital motion processing because accelerometer data is too noisy and gyroscope data starts to drift with time, but by combining those data sets, it is possible to get a precise angular position of the object. For the data merger, an algorithm called ‘complementary filter’ is used. Formula of the filter is: $angle = 0,98 * (angle + gyroData * dt) + 0,02 * (accelData)$, where “dt” is sample rate in seconds and other values are constants or sensor data. That angle defines the rotation around the axis. With MPU-6050, we can calculate rotation around X-axis (pitch) and Y-axis (roll) since gravity measured by accelerometer defines down for them. Z-axis rotation (yaw) cannot be calculated without a reference point for down, for example, a magnetometer to determine north.

4.1. I2C Protocol

The MPU-6050 communicates to a system processor using the I2C serial interface that consists of a serial data line (SDA) and Serial clock line (CKL). The MPU-6050 always acts as a slave when communicating with the system processor. Microcontroller (Master) will send a 7-bit device address plus one bit of reading data frame to a sensor with a specified address. If the address matches, the microcontroller reads sensor data. Because of specified addresses microcontroller can read both accelerometer data and gyro data using only two wires. At InvenSense's webpage [6], there is a Register map for MPU-6050, where registers for each accelerometer/gyro axis are mentioned. Each axis has two registers for LSB and MSB. In that register document, there are also lots of other useful information that is used in Arduino IDE code for microcontroller, like full-scale range and instrument sensitivity.

4.2. TCP Protocol

ESP (NodeMCU) acts as an Access Point (Server) and another ESP (D1 mini) as a Station (Client). Then they'll establish wireless communication and the client sends a message to the server. The server is continuously listening for a connection when it successfully establishes a connection and receives a message it prints that string on the serial monitor. The relationship between ESPs means that the Local Area Network (LAN) has been generated with its own Service Set Identifier (SSID) and password. Every device on the network has a personal Internet Protocol (IP) address but alone, it can't guarantee that communication is received in the same order it was sent. That is where Transmission Control Protocol (TCP) comes in. TCP makes data transmission reliable by ordering and re-sending corrupted packages. ESP8266 boards have a TCP library for Arduino IDE.

4.3. Arduino IDE

Both server and client microcontrollers are programmed using Arduino IDE with ESP8266 add-on. The client microcontroller utilizes the 'Wire' library to enable I2C communication between sensors and microcontrollers. 'ESP8266WiFi' and 'ESP8266WebServer' libraries come with ESP8266 add-on and they enable TCP communication. The final library needed is 'ArduinoJson' library for message decoding. All the tasks from reading sensor data, sending haptic feedback when TCP connection is created, and sending and receiving data is done in Arduino IDE and uploaded to microcontrollers. Unity's code is only left to handle data merging and object movement. Figures 4 and Figure 5 display flowcharts of Arduino IDE code for client and server, respectively.

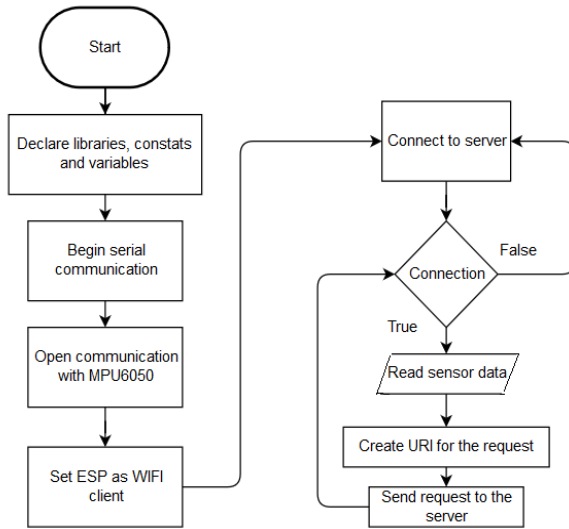


Figure 4. Flowchart of the client Microcontroller

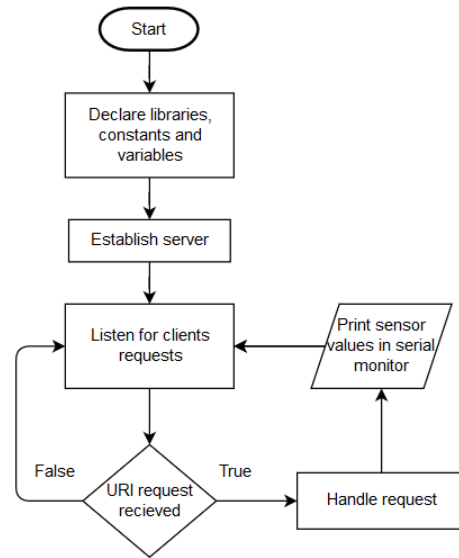


Figure 5. Flowchart of the server Microcontroller

4.4. The Unity 3D

Unity is a cross-platform game engine. A paddle object is imported to Unity and the script component is attached to it. Unity uses the C# programming language. In the code script, the unity listens to the serial port where the microcontroller is sending raw sensor values. The complementary filter is applied to those and pitch and roll values are calculated and the object is rotated based on those. [7]

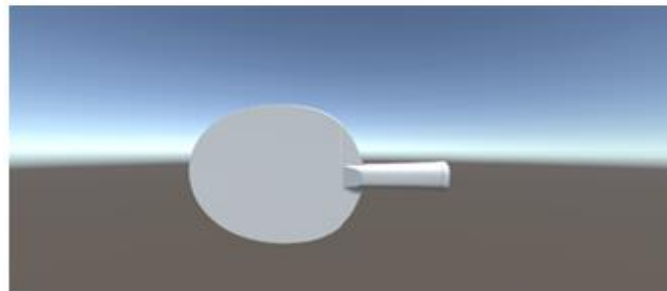


Figure 6. Paddle object in Unity 3D

5. RESULTS ANALYSIS

We have carefully discussed all the embedded components that have been utilized for the analysis



Figure 7. Working Porotype

of the inertial measurement of the ping-pong paddle. The working prototype is shown in Figure 7 and the current orientation movement is only based on gyroscope values and it drifts over time. We were able to transmit the data seamlessly from the gyroscopes to the server for further analysis. Sensor values were transferred smoothly only after the server microcontroller was changed from D1 mini to Node MCU. It has been noticed that with the MPU-9250 nine-axis (Gyro + Accelerometer + Compass) sensor, yaw-value could be calculated with the digital compass in it and the object would rotate around all three axes.

6. CONCLUSION AND FUTURE DIRECTION

This work acts as proof of concept for wireless orientation transformation with MPU-6050. The earlier idea was to develop the Smart Ping-Pong Paddle for the use of table tennis players to track game performance. The orientation and movement of the paddle are successfully transmitted wirelessly on the 3D modeling Unity platform. However, we are still improving our work. In the current situation, the yaw (z-axis rotation) has not been working fine due to the complementary filter. There are significant potential and possibilities to add to the Smart Ping Pong Paddle simulation as with Unity, a whole game could be built around the wireless controller to combine sports and gaming.

ACKNOWLEDGMENTS

The authors would like to thank the Department of Future Technologies, the University of Turku for financial support.

REFERENCES

- [1] Ping Yang, Zhengtao Zhang, Huawei Wang and De Xu, "Design and motion control of a ping pong robot," *2010 8th World Congress on Intelligent Control and Automation*, Jinan, 2010, pp. 102-107, doi: 10.1109/WCICA.2010.5553878
- [2] T. Yamashita and T. Kobayashi, "Smart ping pong racket by ultrathin piezoelectric strain sensor array," *2018 Symposium on Design, Test, Integration & Packaging of MEMS and MOEMS (DTIP)*, Roma, 2018, pp. 1-3, doi: 10.1109/DTIP.2018.8394237.
- [3] Rajeev Kanth, Jukka-Pekka Skön, Kari Lehtomäki, Paavo Nevalainen, Petra Virjonen, Mikko-Jussi Laakso, Jukka Heikkonen, "Image Analysis and Development of Graphical User Interface for pole vault action", *Journal of Image and Graphics*, Vol 6, No. 2, pp: 109-116, December 2018, doi: 10.18179/joig.6.2.109-116

- [4] Olli Koskenranta, “Manipulating 3D objects with Gaze and Hand Gestures”, Published as bachelor of engineering thesis at Information Technology and Telecommunication department, Oulu University of Applied Sciences Source: https://www.theseus.fi/bitstream/handle/10024/46652/Koskenranta_Olli.pdf?sequence=1&isAllowed=y
- [5] A. Yudhana, J Rahmawan and C U P Negara, “Flex Sensors and MPU6050 sensors responses on smart flove for sign language translation”, IOP conference series on Materials and Engineering 403 (1):012032, dio: 10.1088/1757-899X/403/1/012032.
- [6] A technical report on “MPU-6000 and MPU-6050 Register Map and Descriptions Revision 4.2”, published online by InvenSense Inc., document number RM-MPU-6000A-00, Revision 4.2, Release date 08/19/2013. <https://www.invensense.com/wp-content/uploads/2015/02/MPU-6000-Register-Map1.pdf>, last accessed on 20 January 2020
- [7] An open source free 3d model using unity 3D, <https://free3d.com/3d-model/tabletennis-paddle-shakehandstyle-v1--10646.html>

AUTHORS

Dr. Rajeev Kanth received a Doctor of Science (D.Sc.) in Information and Communication Technology from the University of Turku, Finland, in 2013 and a docent title in 2019. He is currently working as a Senior Lecturer at the Savonia University of Applied Sciences, Finland, where he is focusing on teaching and research on the Industrial Internet of Things (IIoT). Previously, he has worked at the Indian Space Research Organization (ISRO), Ahmedabad India, Royal Institute of the Technology (KTH), Stockholm, Sweden and the University of Turku (UTU), Finland, where he has been a Researcher, Post-doctoral Researcher, and the Senior Researcher respectively. His current research interests include image and video analysis, the Internet of Things, Big Data Analytics, and Artificial Intelligence. He has published more than 45 scientific articles in peer-reviewed conference proceedings and refereed journals in the field of computer science and communication technology. He has been a member of the IEEE communication society, IEEE cloud computing community, IEEE Earth Observation Community, and the green ICT community.



Tuomas Korpi was born in Finland, and currently, he is pursuing a bachelor's degree in the Internet of Things (IoT) from Savonia University of Applied Sciences, Finland. He has a keen interest in developing innovative and novel applications of the Internet of things using Arduino and Raspberry pi platforms with suitable sensors.



Jukka Heikkonen has been a professor of computer science at the University of Turku, Finland, since 2009. His current research as the head of the Algorithms and Computational Intelligent (ACI) research group at the University of Turku is related to intelligent and learning systems, especially including machine learning, probabilistic, and information-theoretical modeling issues applied in wide varying application domains. He has worked at top-level research laboratories and the Center of Excellence in Finland and international organizations (European Commission, Japan) and has led many international and national research projects. He has authored more than 150 scientific articles.



MULTI-TASK KNOWLEDGE DISTILLATION WITH RHYTHM FEATURES FOR SPEAKER VERIFICATION

Ruyun Li¹, Peng Ouyang², Dandan Song² and Shaojun Wei¹

¹Department of Microelectronics and Nanoelectronics, Tsinghua
University, Beijing, China

²TsingMicro Co. Ltd., Beijing, China

ABSTRACT

Recently, speaker embedding extracted by deep neural networks (DNN) has performed well in speaker verification (SV). However, it is sensitive to different scenarios, and it is too computationally intensive to be deployed on portable devices. In this paper, we first combine rhythm and MFCC features to improve the robustness of speaker verification. The rhythm feature can reflect the distribution of phonemes and help reduce the average error rate (EER) in speaker verification, especially in intra-speaker verification. In addition, we propose a multi-task knowledge distillation architecture that transfers the embedding-level and label-level knowledge of a well-trained large teacher to a highly compact student network. The results show that rhythm features and multi-task knowledge distillation significantly improve the performance of the student network. In the ultra-short duration scenario, using only 14.9% of the parameters in the teacher network, the student network can even achieve a relative EER reduction of 32%.

KEYWORDS

Multi-task learning, Knowledge distillation, Rhythm variation, Angular softmax, Speaker verification

1. INTRODUCTION

Using Deep Neural Network (DNN) to extract speaker embeddings has shown impressive performance in speaker verification (SV). Speaker embeddings denote fixed-dimensional vector-based representations for modeling the characteristics of speakers.

Gaussian Mixture Network-Universal Background Network (GMM-UBM) system dominated the SV field for one decade since proposed in [1]. Inspired by Joint Factor Analysis in [2], i-vector [3] was proposed and represented the state-of-the-art speaker networking framework. Recently, speaker embeddings [4, 5, 6, 7] learning with DNN has become mainstream for speaker networking in SV. By averaging the frame-level extracted deep features, the segment-level representation of a recording is obtained, which is called d-vector [8]. Some researchers follow and extend this work by replacing the simple neural network with complicated architectures such as Convolutional Neural Network (CNN) and Time-Delay Neural Network (TDNN) or redesign the optimization metric and propose new embeddings such as j-vector [9]. Instead of training the

DNN on the frame level, researchers in [10] add a temporal pooling layer and train the network on the segment level, which is called x-vector. It is proven to achieve excellent performance.

Advanced loss functions also benefit to build a more powerful deep architecture, such as triplet loss [6], the generalized end-to-end loss [11], and the angular softmax [5]. The angular softmax (A-softmax) modifies the softmax loss function to learn angularly discriminative embeddings and adds a controllable parameter to pose constraints on the intra-speaker variation of the learned embedding.

Even if the methodology above reported impressive low error rates ($\approx 1\%$ [3]), SV is still challenging in different trial conditions and linguistic environments like diverse phonological content. Besides, x-vector is too computationally intensive to be deployed on portable devices.

Among the efforts to compress these networks, knowledge distillation is a natural method, where a large network (teacher) provides weighted targets to guide the training of a small network (student). However, previous studies only explored the effect of single-level knowledge distillation on speaker embedding performance, and single-level knowledge distillation was not effective enough to obtain highly compact networks with better performance than large networks. In this paper, phonological content is considered in extracting speaker acoustic features to improve the performance of intra-speaker verification. We calculate seven rhythmic parameters, which is based on temporal characteristics of speech intervals. Then we concatenate these rhythm features with MFCC features. Besides, we aim to build small networks that need much fewer resources and are more suitable for deployment without performance degradation. Multi-task knowledge distillation utilizes the embedding-level and label-level output of teacher networks [12] to guide the training of student networks, to reduce the performance gap between student networks and teacher networks. Sometimes, student networks even outperform teacher networks, because of the dark knowledge [13] transferred in distillation.

The main contributions of this article are as follows:

1. The fusion of rhythm feature and MFCC feature: rhythm parameters are multiplied by a weight factor, and then concatenated with the MFCC feature.
2. Multi-task knowledge distillation: The main task is to force the student network to emit posterior probabilities similar to the hard speaker labels. Besides, we utilize label-level and embedded-level knowledge distillation to guide the training of the highly compact student network as two auxiliary tasks. The total loss comes from these three tasks.
3. A highly compact student network has competitive performance with the teacher network: In the ultra-short duration scenario, a student network can even achieve a 7.02% relative EER reduction, using only 13% of the parameters in the teacher network. We studied the effects of deep speaker embedding, A-softmax, rhythm features, and multi-task knowledge distillation on intra- and inter-speaker verification (false miss and false alarm), which shed light on the success of our methods.

The rest of the article is organized as follows. Section 2 briefly introduces deep speaker embedding learning. Section 3 introduces the multi-task knowledge extraction with rhythm function. Sections 4 and 5 show the experimental setup and results, respectively. Section 6 summarizes the paper.

2. RELATED WORK

2.1. Deep Speaker Embedding Learning

Deep speaker embedding learning has been dominating the field of text-independent speaker verification. Powered by advanced computational resources, and large-scale speech datasets, e.g., VoxCeleb and speaker verification corpora packaged by the National Institute of Standards and Technology (NIST), it is possible to train very deep networks to extract speaker embeddings (segment-level representations).

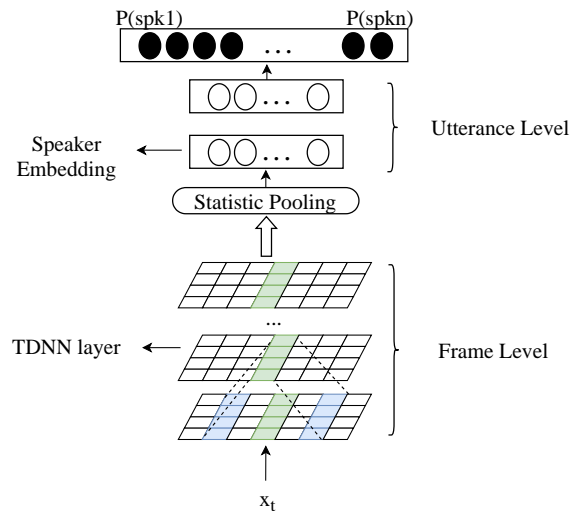


Figure 1 Network architecture of x-vector

In this paper, we adopt the normal x-vector architecture. The DNN used in the x-vector is depicted in Figure 1, and the detailed network configuration is described in Section 4.1.1. In our work, the pooling mechanism calculates the mean and standard deviation of the frame-level representations, but several studies have extended it to multi-head attention layers [20, 21] and learnable dictionary layers. We use angular softmax loss (A-softmax) as the training criterion, which was proposed for face recognition and introduced to speaker verification in [22, 23]. The back-end technology is cosine distance scoring and probabilistic linear discriminant analysis (PLDA) [24, 25].

2.2. Knowledge Distillation

There have been efforts to compress these networks, e.g., parameter pruning and sharing [26], low-rank factorization [27] and knowledge distillation [29, 30]. Knowledge distillation has proven a promising way to narrow down the performance gap between a small network (student) and a large network (teacher). It works by adding a term to the usual classification loss, which encourages students to imitate the behavior of teachers. However, knowledge distillation for deep speaker embedding has not been investigated thoroughly in the literature. [29] built a distillation framework to learn the distribution of embedding vectors directly from the teacher. [30] further recommends using the teacher's speaker posterior probability as reference labels for the student. These previous studies only explored the effect of single-layer knowledge distillation on speaker embedding performance, and single-layer knowledge distillation was not effective enough to obtain highly compact networks with better performance than large networks.

3. MULTI-TASK KNOWLEDGE DISTILLATION FOR DEEP SPEAKER EMBEDDING

This section describes the speaker verification systems developed for this study, which consist of fusion features, and multi-task knowledge distillation. Our experiments are based on the Kaldi speech verification toolkit [14].

3.1. Fusion of Rhythm Features and MFCC Feature

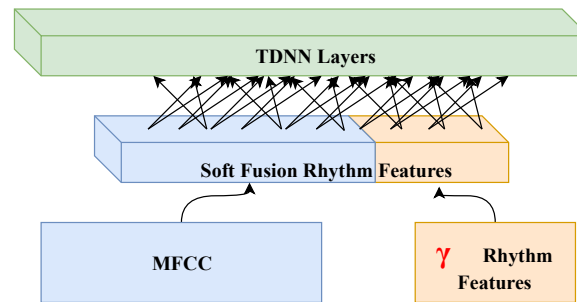


Figure 2 Fusion of rhythm features and MFCC feature

Rhythm variations are proven to have virtually a significant impact on intra-speaker verification, which are commonly used in the field of speech rhythm research [15, 16, 17, 18]. In this paper, we introduce seven rhythm variation measurements to improve speaker verification performance: $\%VO$, \overline{VO} , $VarcoUV$, $VarcoVO$, $\%(UV_{i+1} > VO_i)$, $Average(pair)$ and $VarcoPair$, which are formulated in [19].

In the x-vector framework, silenced frames are filtered out by voice activity detection (VAD). As shown in Figure 2, we multiply rhythm features with a weight factor g , then combine them with MFCC feature. Our rhythm variation measurements are based on voiced and unvoiced durations (including pauses), which is detected via python interface of the WebRTC VAD. Our experiment in Section 5.1 will investigate the best value of g for fusion.

3.2. Multi-task Knowledge Distillation

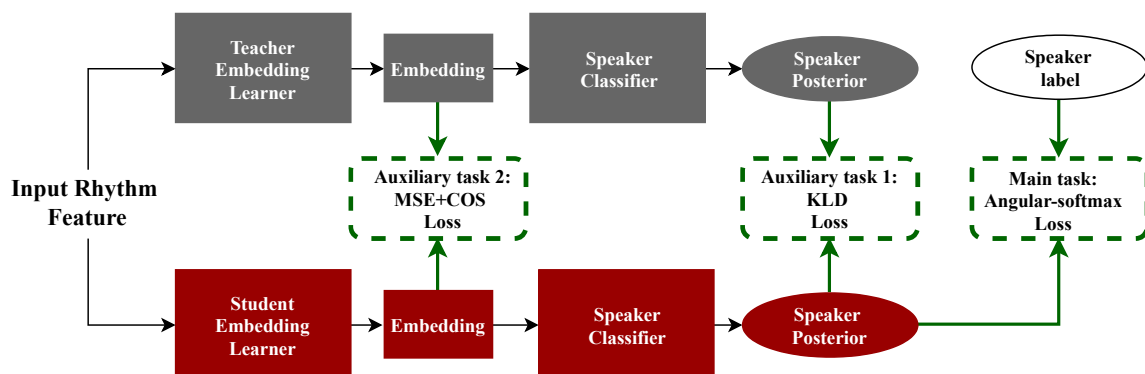


Figure 3 Multi-task knowledge distillation architecture: The system consists of three parts, the teacher network (in Grey), the student network (in Red), and three training tasks.

Multi-task knowledge distillation forces the student network to train on multiple different, but related knowledge distillation tasks, which can make better use of the teacher network. As shown in Figure 3, the multi-task knowledge distillation for deep speaker embedding network includes three tasks:

1. The main task (see Equation 1) is to train the student speaker embedding network over the same set of speakers directly with hard speaker labels, just like what we did for a teacher network.
2. Label-level knowledge distillation (see Equation 3), where the optimization of the student network is guided by the posteriors predicted by a well pre-trained teacher network.
3. Embedding-level knowledge distillation (see Equation 4), which directly constrains the similarity of speaker embeddings learned from the teacher and student network.

For the main task, instead of using the categorical cross-entropy for training, we use the A-softmax loss for classification. A-softmax has more stringent requirements for correct classification when $m \geq 2$ (an integer that controls the angular margin), which generates an angular classification margin between embeddings of different classes. The A-softmax loss is formulated in Equation 1:

$$L_{A\text{-softmax}} = -\frac{1}{N} \sum_{i=1}^N \log \frac{e^{\|x_i\| \mathcal{Y}(q_{y_i,i})}}{Z} \quad (1)$$

$$Z = e^{\|x_i\| \mathcal{Y}(q_{j,i})} + \sum_{j=1, j \neq y_i}^N e^{\|x_i\| \cos(q_{j,i})}, \mathcal{Y}(q_{y_i,i}) = (-1)^k \cos(mq_{y_i,i}) - 2k, \quad (2)$$

where N is the number of training samples; x_i is the input of the last (i.e. output) layer; y_i is the ground truth label for the i^{th} sample; w_j is the j^{th} column of the weights in the output layer; $q_{j,i}$ is the angle between w_j and x_i ; $q_{y_i,i} \in [\frac{k\rho}{m}, \frac{(k+1)\rho}{m}]$ and $k \in [0, m-1], m \geq 0$.

We distill the knowledge from the output of label-layer. Label-level knowledge distillation means the optimization of student network is guided by the posteriors predicted by a pre-trained teacher network. The objective is defined as:

$$L_{KLD} = -\sum_{i=1}^N \sum_{j=1}^C \tilde{y}_j^i \log y_j^i, \quad (3)$$

where C is the number of speakers in the training set; \tilde{y}^i is the posteriors of the i -th sample predicted by the teacher network. Other definition of symbols is the same as Equation 1.

In addition to the label-level knowledge distillation, Assuming the student and teacher produce the same dimension of speaker embeddings, embedding-level knowledge distillation directly constrains the similarity of speaker embeddings learned from the teacher and student network, which is formulated as:

$$L_{COS} = -\sum_{i=1}^N \frac{v_i^t \cdot v_i^s}{\|v_i^t\| \|v_i^s\|}, \quad (4)$$

where v_i^t represents the embedding computed by the teacher network for the i^{th} sample; v_i^s denotes the embedding computed by the student network.

In the optimization, losses of these three tasks are combined to train the student network as:

$$L_{total} = L_{A\text{-softmax}} + aL_{KLD} + bL_{COS}, \quad (5)$$

where a and b are hyper-parameters to balance three losses.

4. EXPERIMENTAL SETUP

4.1. Dataset

We evaluate the performance of our method on a short duration text-independent dataset called XiaoAi-Speech, which consists of 230288 clean utterances from 448 male individuals. Each utterance varies between 1 and 8 seconds (before removing the silenced frames). The database contains almost 320h recordings. It is mainly used for short-duration speech processing as it contains relatively short-duration phrases. Besides, it allows studies on intra-speaker and inter-speaker comparisons, because each speaker provides nearly 500 utterances of different content. We report the speaker verification results on this dataset in ultra-short-duration, short-duration, and normal-duration scenarios, respectively.

4.1.1. Training Data

The training data contains 248 speakers, and each speaker has almost 500 utterances.

The i-vector extractor is a 2048 component GMM-UBM, which is trained on full-length recordings using 23-dimensional MFCC speech features. Short duration i-vectors and ultra-short duration i-vectors are extracted from the first 10n frames of the test data, where n is the duration of recordings being considered (in ms). We only choose speakers that have more than 8 recordings (with 3~5-second durations).

4.1.2. Evaluation Data

We focus on the case where both the enrollment and test recordings of a verification trial are in the same duration scenario. In the normal-duration scenario, 9 enrollment and 2 test utterances are prepared for each speaker. In the short-duration scenario, 7 enrollment and 2 test utterances are prepared. In the ultra-short-duration scenario, 2 enrollment and 2 test utterances are prepared. The evaluation set is selected from our database, and there is no speaker overlap with the training set. The enrollment part contains 200 speaker models, and the test part contains 800 utterances from the 200 models in the enrollment set, of which 400 are for ultra-short-duration trials, and the rest 400 are for short-duration trials. There are 20K trials in the entire trial list, including 50% intra-speaker (target) trials and 50% inter-speaker (non-target) trials.

4.2. Speaker Verification

In this section, we present our experimental setup, as well as details related to input features, neural network training, and classifiers. All systems compared in this paper are presented in Table 1. All deep speaker embeddings systems in this paper are trained on 23-dimensional MFCC

features (sometimes combined with 7-dim rhythm variation features) with a frame-length of 25ms that are mean-normalized over a sliding window of up to 3 seconds of short-duration snippets speech. Our experiments are conducted in three evaluation scenarios: Short-duration (3~5-second), Ultra-short-duration (1~3-second) and Normal-duration (1~5-second) evaluation recordings.

4.2.1. Large-scale System

The I-vector system relies on a universal background network and a total variability matrix, which is called *i-vec*. Input features are 23-dimensional MFCC with first and second-order time derivatives. The number of Gaussian components is set to 2048, while the dimension of the i-vector is 600.

Table 1 The configuration of our systems

Network	I-vector dim	X-vector			#Model size
		#Input	#TDNN layers	#Neurons	
<i>i-vec</i>	600	23	n/a	n/a	20.38M
<i>x-vec</i>	n/a	23	3	512	18.3M
<i>x-vec+asoftmax</i>	n/a	23	3	512	18.3M
<i>x-vec+asoftmax+rhythm</i>	n/a	30	3	512	23.15M
<i>student-64</i>	n/a	30	3	64	3.45M
<i>student-32</i>	n/a	30	3	32	763K

The *x-vec* systems, *x-vector+asoftmax* system, and *x-vec+asoftmax+rhythm* system are described in Section 2 and Section 3.1, respectively. We adopt *x-vec+asoftmax+rhythm*, an *x-vector* based on A-softmax and rhythm features, as the teacher network in the following multi-task knowledge distillation experiments, since an excellent performance was reported using this architecture on XiaoAi-Speech. The detailed network configuration of the teacher network is shown in Table 1. The input acoustic features are fed into an eight-layer DNN. The first five layers Frame 1 to Frame 5 are constructed with a frame-level time-delay architecture. The statistics pooling layer aggregates over frame-level output vectors of the DNN and computes their mean and standard deviation. This pooling mechanism enables the DNN to produce fixed-length representation from variable-length speech segments. Then their mean and standard deviation are concatenated together and forwarded to two additional hidden layers segment 6 and segment 7. Finally, the system is optimized using stochastic gradient descent (SGD) using A-softmax. The N on the A-softmax layer corresponds to the number of training speakers. We also decayed the learning rate every 4 epochs. During the inference phase, speaker embeddings are extracted from the affine component of layer segment 6 before the nonlinearity. Then a PLDA backend is used to compare pairs speaker embeddings.

Table 2 The architecture of *x-vec+asoftmax+rhythm*.

Layer	Layer context	Total context	Input x output	#Parameter
frame1	[t-2, t+2]	5	30x512	30x5x512
frame2	[t-2, t+2]	9	512x512	512x5x512
frame3	[t-3, t+3]	15	512x512	512x7x512
frame4	{t}	15	512x512	512x512
frame5	{t}	15	512x1500	512x1500

stats pooling	[0, T)	T	1500xTx3000	0
segment6	{0}	T	3000x512	3000x512
segment7	{0}	T	512x512	512x512
A-softmax	{0}	T	512xN	512xN

4.2.2. Small-scale System

Several different setups for highly compact student networks are investigated in our experiments. The most natural choice is to use a shallower x-vector. Two setups are adopted, namely *student-64* and *student-32*, with the number of hidden units for TDNN layers set as 64 and 32, respectively. Both teacher and student networks are of the same 512 speaker embedding dimension. During the inference phase, the student network was used to predict speaker embedding vectors for enrolment and test data, which was then followed by PLDA scoring, which is the same as the teacher network.

4.3. Evaluation metric

To further investigate the impact of our methods on intra- and inter-speaker verification separately, we use C_{llr} instead of hard decision like equal error rate (EER) to evaluate the log-likelihood-ratio (LR) of speaker pairs. C_{llr} can evaluate the discriminant ability of the log-likelihood ratio (LR) of the speaker pair, while EER is valid for overall correct-classification rate. C_{llr} is calculated as followed:

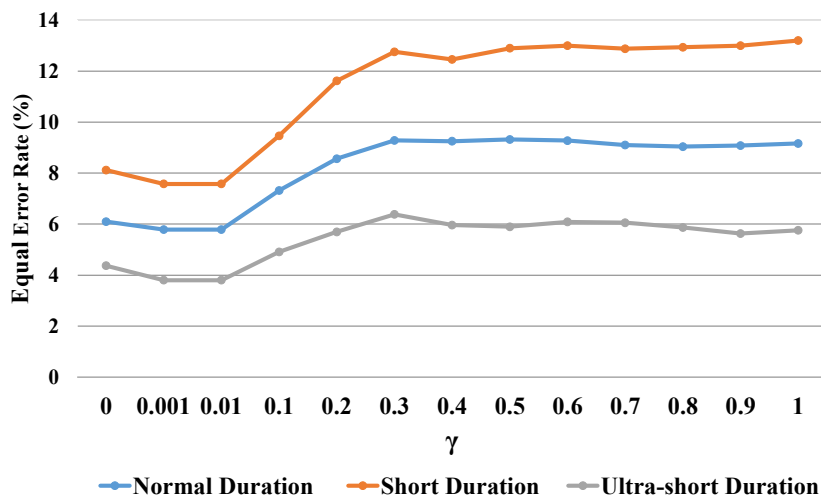
$$C_{llr} = \frac{1}{2N_{tar}} \sum_{LR \in \mathcal{X}_{tar}} \log_2\left(1 + \frac{1}{LR}\right) + \frac{1}{2N_{non}} \sum_{LR \in \mathcal{X}_{non}} \log_2(1 + LR) \quad (6)$$

As shown in Equation 6, C_{llr}^{TAR} is the average information loss corresponding to target trials, while C_{llr}^{NON} is the average information loss corresponding to non-target trials. C_{llr} is the sum of the two parts. The lower the C_{llr} , the better the performance is.

5. RESULT AND ANALYSIS

5.1. Fusion of Rhythm Features and MFCC Feature

Based on the *x-vec+asoftmax+rhythm* system, we optimize the weight parameter g for feature fusion to minimize EER. Figure 4 shows the EER on the corresponding evaluation set under ultra-short duration, short duration, and normal duration scenarios, respectively. The results motivated us to choose $g = 0.01$ for feature fusion, which produced the lowest EER in all scenarios.

Figure 4 Optimization of the weight factor \mathcal{G} in feature fusion

5.2. Effect on Intra- and Inter-speaker Verification

As shown in Table 2, rhythm features and multi-task knowledge distillation can both improve intra-speaker verification (target comparisons) and inter-speaker verification (non-target comparisons). Although *i-vec*, *x-vec*, *x-vec+asoftmax*, *x-vec+asoftmax-rhythm*, and *student-64-TS* achieve lower and lower overall error rates (EER), their effects on the target and non-target comparisons are different from each other. Compared with *i-vec*, *x-vec* reduces EER by 7.5% at the cost of non-target comparison accuracy. Compared with *x-vec*, *x-vec+asoftmax* achieves a 4.6% EER reduction at the cost of target comparison accuracy. At the meantime, it is worth noting that *x-vec+asoftmax+rhythm* have significantly improved the target comparison, and it does not affect the accuracy of the non-target comparison, which is consistent with the conclusion in [19]. Besides, multi-task knowledge distillation makes the *student-64-TS* network have better performance in both target and non-target comparisons, with a 7.1% EER reduction. The results show that DNN is powerful in modeling high-dimensional speaker embedding, but under non-discriminatory training conditions, the performance of target comparison is worse than i-vector. A-softmax is more strict than conventional softmax, it imposes a larger angle margin between the speakers, and classifies the samples into the corresponding categories. Therefore, *x-vec+asoftmax* is reasonable to harm the accuracy of the target comparison.

Table 2 C_{llr}^{TAR} and C_{llr}^{NON} for different speaker verification networks. PLDA is the scoring back-end for EER.

Network	C_{llr}^{TAR}	C_{llr}^{NON}	EER (%)
<i>i-vec</i>	9.49	0.01	18.2
<i>x-vec</i>	1.64	0.16	10.7
<i>x-vec+asoftmax</i>	5.14	0.02	6.1
<i>x-vec+asoftmax+rhythm</i>	2.89	0.03	5.7
<i>student-64-TS</i>	1.41	0.03	3.6

5.3. Multi-task Knowledge Distillation

Table 2 EER and parameter comparison of different speaker embedding architectures. PLDA as the scoring back-end. TS denotes multi-task teacher-student learning. Compression ratio (CR) is the relative reduction rate of model size.

Network	TS	EER (%)			Model size	Compression Ratio
		Ultra-short	Short	Normal		
<i>i-vec</i>	No	19.15	13.19	15.8	20.38M	-
<i>x-vec</i>	No	13.04	8.86	10.67	18.2M	-
<i>x-vec+asoftmax</i>	No	8.12	4.37	6.1	18.3M	-
<i>x-vec+asoftmax+rhythm</i>	No	7.38	3.78	5.73	23.15M	-
<i>student-64</i>	No	11.62	5.69	8.57	3.45M	85.1
<i>student-64-TS</i>	Yes	5.02	1.75	3.64	3.45M	85.1
<i>student-32</i>	No	19.15	13.19	15.8	673K	97.1
<i>student-32-TS</i>	Yes	7.195	3.505	5.74	673K	97.1

As shown in Table 3, compared with student baselines, multi-task knowledge distillation significantly boosts the performance of student networks, and it could obtain highly compact networks with better performance than large networks. *X-vec+asoftmax+rhythm* is the teacher network, while *student-32* and *student-64* with no knowledge distillation are two student network baselines. *Student-32-TS* can achieve competitive performance with the teacher network by using only 2.9% of parameters used in the teacher. *Student-64-TS* can achieve a 32% relative EER reduction by using only 14.9% of parameters used in the teacher. The more compact the student network, the more significant the effect of multi-task knowledge distillation.

Figure 5 shows the DET test curves of different systems under normal duration conditions. *Student-32-TS* is competitive with *x-vec+asoftmax+rhythm* in all operating areas.

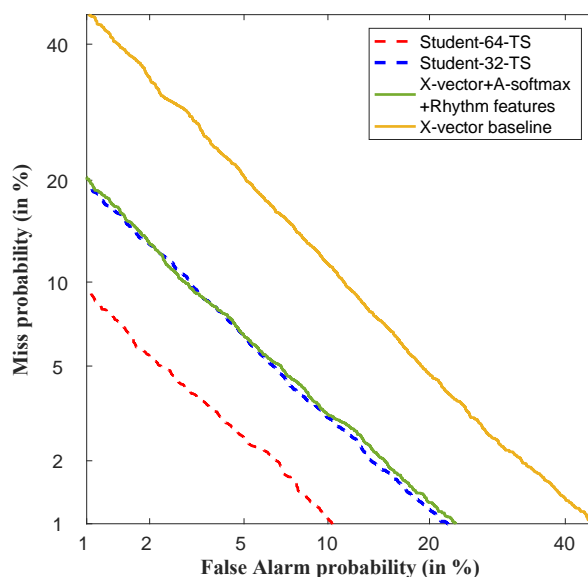


Figure 5 DET curve for baseline, teacher and two high compact student networks.

Figure 6 shows the t-SNE [30] plots corresponding to $x\text{-vec}+a\text{softmax}+r\text{hythm}$, $student32$, and $student\text{-}32\text{-TS}$ networks. The distribution of speaker embeddings in the 2D projected t-SNE space generally revealed speaker clusters. Eight speakers from the evaluation dataset were randomly selected, and for each, we use seven recordings spoken by the speaker (56 in total). The selected 56 samples were plotted in the 2D projected t-SNE space, with colors denoting different speakers.

Multi-task knowledge distillation can effectively pull intra-speaker samples closer and push inter-speaker samples further. On the one hand, as shown in Figure 6(b) and (c), compared with the $student\text{-}32$ baseline, data points from the same speaker tend to be closer, while those from different speakers become more distinct. For instance, the distribution of x-vectors from speaker ID1013 (violet), ID1023 (blue) become denser. On the other hand, as shown in Figure 6(a) and (c), compared with the $x\text{-vec}+a\text{softmax}+r\text{hythm}$, speaker subset clusters emerge in the student. Samples from ID1013 (violet), ID1023 (blue), ID1033 (lime) and ID1036 (green) formed a cluster while the rest formed another. Within each subset cluster, the student and teacher have a similar relative position of speaker clusters in the embedding space. X-vectors from speaker ID1016 (red) and ID1020 (magenta) are consistently projected to have proximity. These two points reveal a hierarchical structure of speaker embeddings, which sheds some light on the success of our methods.

In DLKD, students and teacher networks are required to have the same embedding dimension, which limits the compression space of the student network.

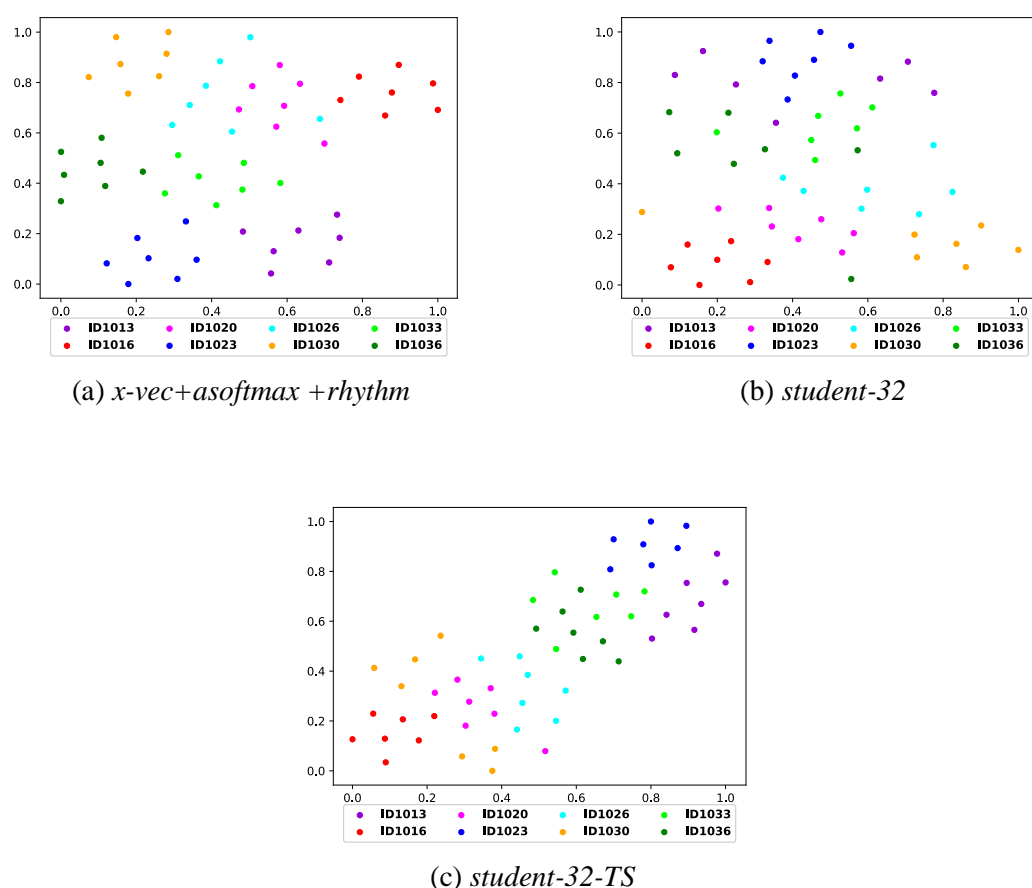


Figure 6 T-SNE plots of 56 utterances from 8 selected speakers for different networks.

6. CONCLUSIONS

In this paper, rhythm features are introduced to reflect the distribution of phonemes and help improve the performance of speaker verification, especially intra-speaker verification. And multi-task knowledge distillation is proposed to boost the performance of the student network on both intra- and inter-speaker verifications. The embedding-level knowledge distribution directly guides the convergence of the student network. The label-level knowledge distillation transfers the posterior probabilities distribution of the incorrect outputs from the teacher network, which provides information on the similarity between speaker categories. Results show that a student can achieve a 32% relative EER reduction by using only 14.9% of parameters used in the teacher via our methods. Besides, a highly compact networks with competitive performance with the teacher network can also be obtained.

In the future, we consider further investigating the trade-off relation between the compactness and performance of student networks. Besides, the impact of angular margin loss on knowledge distillation also deserves further experiments.

ACKNOWLEDGEMENTS

Many thanks to Dr. Wei Shaojun for his valuable guidance in every stage of the writing of this paper. Thanks also to Mrs. Song for her encouragement and support.

REFERENCES

- [1] Douglas A Reynolds, Thomas F Quatieri, and Robert B Dunn, "Speaker verification using adapted gaussian mixture networks," *Digital signal processing*, vol. 10, no. 1-3, pp. 19–41, 2000.
- [2] Patrick Kenny, "Joint factor analysis of speaker and session variability: Theory and algorithms," CRIM, Montreal, (Report) CRIM-06/08-13, vol. 14, pp. 28–29, 2005.
- [3] Najim Dehak, Patrick J Kenny, Re da Dehak, Pierre Du-mouchel, and Pierre Ouellet, "Front-end factor analysis for speaker verification," *IEEE Transactions on Audio, Speech, and Language Processing*, vol. 19, no. 4, pp. 788–798, 2010.
- [4] Shuai Wang, Zili Huang, Yanmin Qian, and Kai Yu, "Deep discriminant analysis for i-vector based robust speaker verification," in 2018 11th International Symposium on Chinese Spoken Language Processing (ISC-SLP). IEEE, 2018, pp. 195–199.
- [5] Zili Huang, Shuai Wang, and Kai Yu, "Angular softmax for short-duration text-independent speaker verification," in *Interspeech*, 2018, pp. 3623–3627.
- [6] Chunlei Zhang and Kazuhito Koishida, "End-to-end text-independent speaker verification with triplet loss on short utterances," 08 2017.
- [7] D. Snyder, D. Garcia-Romero, G. Sell, D. Povey, and S. Khudanpur, "X-vectors: Robust dnn embeddings for speaker verification," in 2018 IEEE International Conference on Acoustics, Speech and Signal Processing (ICASSP), April 2018, pp. 5329–5333.
- [8] Ehsan Variani, XinLei, Erik McDermott, Ignacio Lopez Moreno, and Javier Gonzalez-Dominguez, "Deep neural networks for small footprint text-dependent speaker verification," in 2014 IEEE International Conference on Acoustics, Speech and Signal Processing (ICASSP). IEEE, 2014, pp. 4052–4056.
- [9] Nanxin Chen, Yanmin Qian, and Kai Yu, "Multi-task learning for text-dependent speaker verification," in Sixteenth annual conference of the international speech communication association, 2015.
- [10] L. Yu, J. Yu, and Q. Ling, "Bltrcnn-based 3-d articulatory movement prediction: Learning articulatory synchronicity from both text and audio inputs," *IEEE Transactions on Multimedia*, vol. 21, no. 7, pp. 1621–1632, July 2019.
- [11] Li Wan, Quan Wang, Alan Papir, and Ignacio Lopez Moreno, "Generalized end-to-end loss for speaker verification," in *2018 IEEE International Conference on Acoustics, Speech and Signal Processing (ICASSP)*. IEEE, 2018, pp. 4879–4883.

- [12] Shuai Wang, Yexin Yang, Tianzhe Wang, Yanmin Qian, and Kai Yu, "Knowledge distillation for small foot-print deep speaker embedding," in *ICASSP 2019-2019 IEEE International Conference on Acoustics, Speech and Signal Processing (ICASSP)*. IEEE, 2019, pp. 6021–6025.
- [13] Geoffrey Hinton, Oriol Vinyals, and Jeff Dean, "Distilling the knowledge in a neural network," *arXiv preprint arXiv:1503.02531*, 2015.
- [14] Daniel Povey, Arnab Ghoshal, Gilles Boulianne, Lukas Burget, Ondrej Glembek, Nagendra Goel, Mirko Hanemann, Petr Motlicek, Yanmin Qian, Petr Schwarz, et al., "The kaldi speech verification toolkit," in *IEEE 2011 workshop on automatic speech verification and understanding*. IEEE Signal Processing Society, 2011, number CONF.
- [15] Adrian Leemann, Marie-José Kolly, and Volker Dellwo, "Speaker-individuality in suprasegmental temporal features: Implications for forensic voice comparison," *Forensic science international*, vol. 238, pp. 59–67, 2014.
- [16] Volker Dellwo, Adrian Leemann, and Marie-José Kolly, "Speaker idiosyncratic rhythmic features in the speech signal," in *Thirteenth Annual Conference of the International Speech Communication Association*, 2012.
- [17] Volker Dellwo and Adrian Fourcin, "Rhythmic characteristics of voice between and within languages," *Revue Tranel (Travaux neuchâtois de linguistique)*, vol. 59, pp. 87–107, 2013.
- [18] Volker Dellwo, Adrian Leemann, and Marie-José Kolly, "Rhythmic variability between speakers: Articulatory, prosodic, and linguistic factors," *The Journal of the Acoustical Society of America*, vol. 137, no. 3, pp. 1513–1528, 2015.
- [19] Moez Ajili, Jean-François Bonastre, and Solange Rossato, "Voice comparison and rhythm: Behavioral differences between target and non-target comparisons," 2018.
- [20] K. Okabe, T. Koshinaka, and K. Shinoda, "Attentive statistics pooling for deep speaker embedding," *Proc. Interspeech 2018*, pp. 2252–2256, 2018.
- [21] Y. Zhu, T. Ko, D. Snyder, B. Mak, and D. Povey, "Self-attentive speaker embeddings for text-independent speaker verification," *Proc. Interspeech 2018*, pp. 3573–3577, 2018.
- [22] Cai, Weicheng, Jinkun Chen, and Ming Li. "Exploring the encoding layer and loss function in end-to-end speaker and language recognition system." *arXiv preprint arXiv:1804.05160* (2018).
- [23] Huang, Zili, Shuai Wang, and Kai Yu. "Angular Softmax for Short-Duration Text-independent Speaker Verification." In *Interspeech*, pp. 3623–3627. 2018.
- [24] S. Ioffe, "Probabilistic linear discriminant analysis," in *Proceedings of the 9th European Conference on Computer Vision, ECCV 2006*, ser. LNCS, A. Leonardis, H. Bischof, and A. Pinz, Eds., vol. 3954. Graz, Austria: Springer-Verlag Berlin, Heidelberg, may 2006, pp. 531–542.
- [25] S. J. Prince and J. H. Elder, "Probabilistic Linear Discriminant Analysis for Inferences About Identity," in *Proceedings of the IEEE International Conference on Computer Vision, ICCV 2007*. Rio de Janeiro, Brazil: IEEE, oct 2007, pp. 1–8.
- [26] Yu, Ruichi, Ang Li, Chun-Fu Chen, Jui-Hsin Lai, Vlad I. Morariu, Xintong Han, Mingfei Gao, Ching-Yung Lin, and Larry S. Davis. "Nisp: Pruning networks using neuron importance score propagation." In *Proceedings of the IEEE Conference on Computer Vision and Pattern Recognition*, pp. 9194–9203. 2018.
- [27] Tai, Cheng, Tong Xiao, Yi Zhang, and Xiaogang Wang. "Convolutional neural networks with low-rank regularization." *arXiv preprint arXiv:1511.06067* (2015).
- [28] Ng, Raymond WM, Xuechen Liu, and Pawel Swietojanski. "Teacher-student training for text-independent speaker recognition." In *2018 IEEE Spoken Language Technology Workshop (SLT)*, pp. 1044–1051. IEEE, 2018.
- [29] Wang, Shuai, Yexin Yang, Tianzhe Wang, Yanmin Qian, and Kai Yu. "Knowledge distillation for small foot-print deep speaker embedding." In *ICASSP 2019-2019 IEEE International Conference on Acoustics, Speech and Signal Processing (ICASSP)*, pp. 6021–6025. IEEE, 2019.
- [30] L. Maaten and G. Hinton, "Visualizing data using t-SNE," *Journal of Machine Learning Research*, vol. 8, pp. 2579–2605, 2008.

AUTHORS

Ruyun Li received the B.S. degree from Beihang University, Beijing, China, in 2017. She is currently pursuing the M.S. degree with the Institute of Microelectronics, Tsinghua University. Her current research interests include speech signal processing and speaker verification.



Peng Ouyang received the B.S. degree in electronic and information technology from Central South University, Changsha, Hunan, China, in 2008, and the Ph.D. degree in electronic science and technology from Tsinghua University in 2014. He held a postdoctoral position with the School of Information, Tsinghua University. He is currently the Chief Technology Officer (CTO) of TsingMicro Intelligent Technology Co. Ltd. His research interests include the embedded deep learning, neuron computing, and reconfigurable computing.



Dandan Song received the B.S. degree in automation from Harbin Engineering University, Harbin, China, in 2014, and the M.S. degree from the Institute of Microelectronics, Tsinghua University, in 2018. Her research interests include speech verification and machine learning.



Shaojun Wei was born in Beijing, China, in 1958. He received the Ph.D. degree from the Faculte Poly-technique de Mons, Belgium, in 1991. He became a Professor with the Institute of Microelectronics, Tsinghua University, in 1995. His main research interests include VLSI SoC design, EDA methodology, and communication ASIC design. He is a Senior Member of the Chinese Institute of Electronics (CIE).



AN AUTOMATIC DETECTION OF FUNDAMENTAL POSTURES IN VIETNAMESE TRADITIONAL DANCES

Ngan-Khanh Chau¹ and Truong-Thanh Ma²

¹An Giang University, Vietnam National University Ho
Chi Minh City, Vietnam

²Soc Trang Community College, Vietnam

ABSTRACT

Preserving and promoting the intangible cultural heritage is one of the essential problems of interest. In addition, the cultural heritage of the world has been accumulated and early respected during the development of human society. For preservation of traditional dances, this paper is one of the significant processed steps in our research sequence to build an intelligent storage repository that would help to manage the large-scale heterogeneous digital contents efficiently, particularly in dance domain. We concentrated on classifying the fundamental movements of Vietnamese Traditional Dances (VTDs), which are the foundations of automatically detecting the motions of the dancer's body parts. Moreover, we also propose a framework to classify basic movements through coupling a sequential aggregation of the Deep-CNN architectures (to extract the features) and Support Vector Machine (to classify the movements). In this study, we detect and extract automatically the primary movements of VTDs, we then store the extracted concepts into an ontology that serves for reasoning, query-answering, and searching dance videos.

KEYWORDS

Vietnamese Traditional Dance, Deep learning, Support vector machine.

1. INTRODUCTION

The cultural heritage, which has been accumulated throughout the development of humanity, is early respected. Vietnam possesses an array of intangible cultural heritages that have been recognized in the world. Indeed, the intangible cultural heritage (ICH) in Vietnam shows the diversity of styles and expressions. Dances are widely displayed in community cultural activities. Each nation is proud of its own dances and preserves it from generation to generation. Dancing is also a quintessential form of human motion and expression. Most of ICH in the ethnic communities has been collected and studied through the Vietnamese traditional dances (VTDs). These colourful dance paintings naturally show the cultures of ethnic groups as well as regions through key postures. Identifying key moves keeps an important role in spreading traditional dances as well as native culture. Fortunately, most of the moving phrases of the distinguishable dances originate from the fundamental movements, the detection of the basic movements to identify the distinct dances is completely expected. In this paper, we would focus on detecting automatically the essential movements and storing the primary concepts into VTD's movement ontology-base. With this study, we will give our part to the preservation and development of national cultural arts.

From an academic point of view, there is much research in dance analysis such as developing algorithms that may recognize how well a user can imitate certain motion patterns presented by an avatar [34, 35]. Several dance topics have recently been studied, including ballet dance [6], Tsamiko dance [7, 8], and Salsa dance [9, 15].

Automatic recognizing performer's movements is a complicated problem for artificial intelligence (AI) scientists, which involves in mining and categorizing spatial patterns of human postures from videos. Dance movements are well-defined as a temporal variation of human body. The problem is to extract and detect the human posture and classify it into a label based on the trained CNN features. The goal of this work is to extract the features from multiple CNN-architectures of different VTDs postures in dance videos. In this paper, we concentrate on classifying the fundamental movements of ethnic Vietnamese Thai Community (EVTC) composed of "Standing movements, Leg movements, Hand movements, Sitting movements".

One of the main contributions of this paper is to present a general framework using the aggregated CNN-architectures to automatically detect the key postures of ethnic Vietnamese Thai dances (EVTD). Our classification model focuses on extracting the features and aggregating the features to support the classification of the postures. Especially, we used three of the effective existing CNNs architectures to extract the significant features and using algorithms of machine learning to classify. Most of our datasets are collected from the raw dance videos on the social networks (almost all from YouTube).

In research process, we decomposed our approach into three main stages: the first is reconstructing a schema for panorama view of VTDs; the second is region-zone of VTDs, considering this aspect as a large branch because most of the VTDs originate from distinguishable ethnic groups living in distinct regions; the last is the fundamental postures to identify the name of dances. In this article, we mainly concentrate on the third stages involved in automatic detection of basic motions. Our primary challenge is to determine the principal concepts from EVT D's postures combined with a set of desirable properties to build a useful dance search engine.

This paper is structured as follows section 2 gives an overview and review of recent related works. Section 3 provides a description of EVT D's basic postures, we then present the proposed model to classify and detect the specific postures automatically in section 4. In section 5, we discuss the experimental results. The last section is the conclusion (in section 6).

2. OVERVIEW AND RELATED WORKS

2.1. Vietnamese Traditional Dance Overview

Vietnam is a multi-ethnic country with many different cultures [25] due to the combination of fifty-four-ethnic groups living in one territory. The traditional dances had become the spiritual foods of Vietnamese people, it explicitly influences the life from urban to rural. Most of the VTDs are taught from previous generations using "word of mouth", the present generation would instruct fundamental movements to the adjacent one. Additionally, VTD is a steady bridge in education of human dignity, morality, and even historical knowledge. Instead of learning the historical lessons in regular classes as well as participating in the training courses for life skills, dance has become a digital channel to effectively educate personality, knowledge, and even ethnicity for generations.

Generally, the VTDs [1] concentrate on ethnicity, aestheticism and bringing many significations. The worship of gods as well as ancestors plays an important role in the life of people in Vietnam,

therefore several dances are performed in festivals and celebrations with desiring to be blessed. In addition, combining particular props and traditional costumes would be the remarkable characteristic in VTDs.

The Vietnamese culture brings many multiform traditional cultural properties, which plays an important role in Vietnamese community. Most VTDs are built up from the ethnic groups in different life environments and regions, they contain a large number of the significant characteristics of specific regions. The dance movements of the ethnic groups stem from the life activities, each posture in the dance is depicted an action of their life. Therefore, the basic postures will be one of the stable platforms as well as the being the essential features for identifying different dances.

2.2. Related Work

During the last two decades, people have tried to develop different algorithms for human activity analysis [20, 24] for wide applications in the field of surveillance, patient monitoring and more. Most of the studies have been reported on classifying human activity from videos. Recently, researchers are trying to classify an activity from a single image [22, 23, 27]. In the video based activity recognition, people have tried with different human activities like walking, jogging, running, boxing, hand waving, hand clapping, pointing, digging and carrying for a single actor [4, 24].

There are also a few works on group activities such as [12, 16]. With the best of our knowledge, no one has addressed the dance classification problem so far, at least in computer vision domain. Due to the increase in multimedia data access through the internet, multimedia data, particularly video data indexing becomes more and more important. Not only in the retrieval but also for digitization of cultural heritage, this could be an interesting problem. It can be used to analyse a particular dance language.

Some researchers used space time features to classify the human action. Blank et al. represented the human action as three-dimensional shapes included by the silhouettes in the space-time volume [13]. They used space-time features such as local space-time saliency, action motivations, shape structure, and orientation to classify the actions. , they recognised human action based on space-time locally adaptive regression kernels and the matrix cosine similarity measure [2]. Klaser et al. localized the action in each frame by obtaining generic spatio-temporal human tracks [11]. They used a sliding window classifier to detect specific human actions.

There are several attempts to recognize the postures from multiple videos sources [2, 24]. Aggarwal et al. has categorized the recognition of human activities in two classes as single-layered approach and hierarchical approach [24]. In single-layered approach, activities are recognized directly from videos, while in hierarchical approach, an action is divided into sub-actions [10]. The action is represented by classifying it into sub-actions. Wang et al. have used topic modelling to model the human activity [18]. They proposed a video by Bag-of-Words representation. Later, they have used a model which is popular in object recognition community, called Hidden Conditional Random Field (HCRF) [19]. They modelled human action by flexible constellation of parts conditioned on image observations and learn the model parameters in max-margin framework and named it max-margin hidden conditional random field. Md Faridee et al. has built a tool to recognize dance activities automatically [32]. They applied the Convolution Neural Network based on body sensor network to assess steps of dances. Mallick et al. has captured and extracted postures of the Indian classical Dances using the Hidden Markov Model and Kinect [33].

3. EVTD POSTURES DESCRIPTIONS

3.1. Ethnic Vietnamese Thai Dances

Thai community in Vietnam is one of the ethnic groups which possesses a large number of the traditional dances. There are many significant festivals of Thai ethnic group to be held in villages as well as regions during the whole year. In order to understand the explicitly with respect to ethnic Vietnamese Thai dance (EVTD), in this paper, we gave more attention on analysing and determining the postures' features which keep a vital role to classify the Thai dances in the Vietnamese territory.

In general, the remarkable dances are always performed in most of the festivals or private celebration days in community. Specially, when it comes to the Thai ethnic group, certainly, "Xoe dances" [5] is one the most important and popular dances in this community. It is not only the worth cultural heritage as well as being the Thai community symbol but also one of the indispensable intellectual nourishment of Thai people in the festivals and ceremony. There are six kinds of "Xoe" dances including "Kham khan moi lau" (representing the culture of communicating), "Pha xi" (the unity of communities), "Nhom khan" (representing happiness of ethnic group), Don hon (steels and sweet hearts), "Kham khen" (work together as communities), "Om lop top mu" (recall with nostalgia when saying goodbye). Several dance evidences in "Xoe dances" including Handkerchief Dance, Tinh Tau Dance, Xe-Ma-Hinh Dance, Vi-Khan Dance performed in the important festivals, for example as Kin pan then, is a significant festival taken place on March 10th (according to lunar calendar) in Vietnam's North Southern region. In each EVTD, apart from the inspiration of choreographers and the traditional costumes, the remarkable characteristics to determine EVTDs are the foundation postures which are the base of the creative combination in each motion in order to create the particular dances of Vietnamese Thai people. Correspondingly, the detection of the basic postures is one of the important steps to collect automatically the dance dataset for an ontology-based of EVTDs.

3.2. Fundamental Postures of EVTDs

Representing the details of each motion in EVTDs is necessary when considering basic motion characteristics. It is divided in five primary characteristics in overview [5]: Orientation, Arm Posture, Leg Posture, Sitting Posture, Standing Posture. The orientation of EVTDs is split into eight orientations (from orientation 1 to orientation 8). In this article, we focused on the postures of the lower-body area including leg postures, sitting postures, standing postures to collect training dataset and classification. We particularly describe the remaining postures as follows:

3.2.1. Arm Posture

Most arm postures are concentrated on depicting life activities in Thai community, therefore the basic postures are simple and habitual. They are divided in five primary postures: VN-Thai-The-1-Arm, VN-Thai-The-2-Arm, VN-Thai-The-3-Arm, VN-Thai-The-4-Arm, VN-Thai-The-5-Arm. They are grouped into two distinct clusters: open-arm posture and close-arm posture.

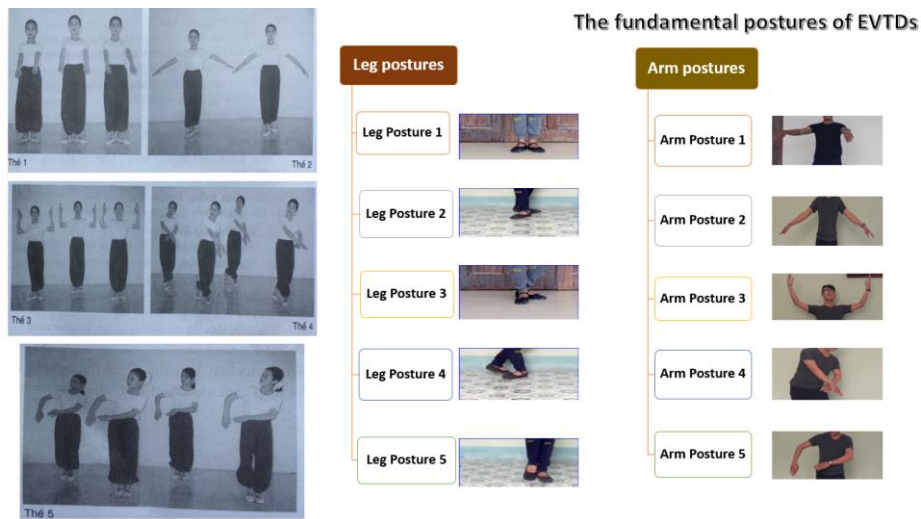


Figure 1. Arm postures and Leg postures of EVTDS

3.2.2. Leg Posture

There are five significant leg postures to represent for EVT D postures. It includes VN-Thai-The-1-Leg, VN-Thai-The-2-Leg, VN-Thai-The-3-Leg, VN-Thai-The-4-Leg, VN-Thai-The-5-Leg.

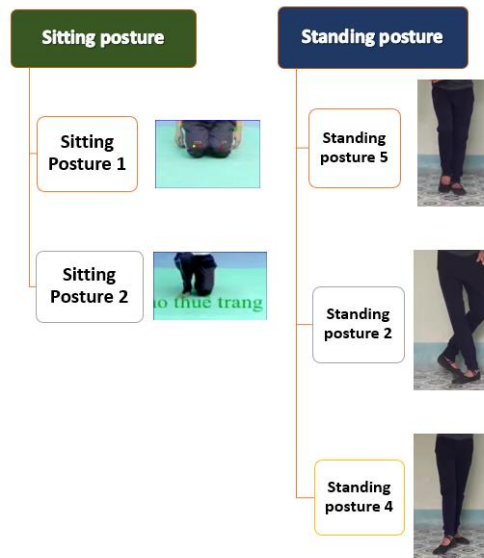


Figure 2. Sitting postures and standing postures of EVTDS

3.2.3. Sitting and standing Posture

Sitting posture is divided into two types, it consists of VN-Thai-The-1-Sitting, VN-Thai-The-2-Sitting. There are three standing postures in EVT D: VN-Thai-The-5-Standing, VN-Thai-The-2-Standing, VN-Thai-The-4-Standing.

4. PROPOSED METHODOLOGY

4.1. Human Pose Estimation

Human pose estimation (HPE) is one of the most challenging problems in computer vision and plays an essential role in human body modelling. Regarding HPE, existing two main approaches are bottom-up and top-down estimation. The state-of-the-art solutions model for the two key issues in bottom-up approach are joint detection and spatial configuration refinement, together using convolutional neural networks (CNN) for training and classifying. A real-time method to estimate multi-person pose efficiently is the so-called Openpose [29] (written in C++ using OpenCV and Caffe), developed by Carnegie Mellon University. In this paper, we utilize TF-Openpose (written in python using Tensorflow library instead of Caffe library) for estimating the positions of human joints and articulated pose estimation to support for depicting each movements in EVT D. Moreover, we ameliorated and improved TF-Openpose through algorithms of input image processing and modified several essential arguments of CNNs.

The primary purpose of using HPE for EVT D postures is to determine concretely parts of body in raw dance videos aiming at describing most motions. The architecture also predicts detection reliable maps and affinity fields that are encrypted part-to-part association simultaneously as shown in Figure 3. The network is split into two branches: Branch 1 is responsible for predicting reliable maps, and Branch 2 predicts the affinity fields. TF-Openpose takes a 2D colour image as an input and produces the 2D location of anatomical key-points for each person. The (x, y) coordinates of the final pose data array could be normalized to a range depended on the key-point scale. It can be estimated 18 key-points body pose from COCO 2016 dataset.

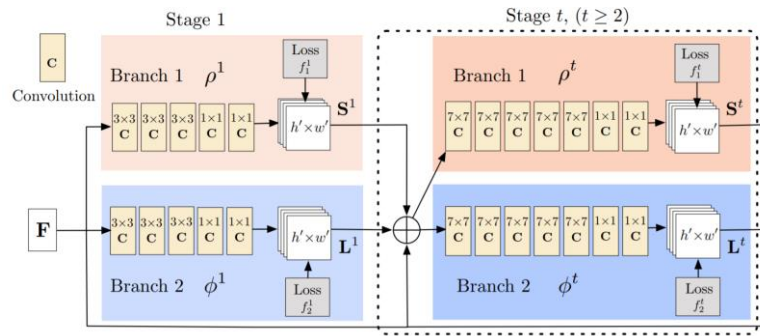


Figure 3. The architecture of the two-branches using CNN in Openpose

Each branch is an iterative prediction architecture which refines the predictions over successive stages, $t \in \{1, 2, \dots, T\}$, with the intermediate supervision at each stage. The frames from raw video are analysed by CNNs, generating a set of feature maps F that is the input to the first stage of each branch. At the first stage, the network produces a set of detection reliable maps $S^1 = \rho^1(F)$ and a set of partial affinity fields $L^1 = \phi^1(F)$, where ρ^1 and ϕ^1 are the CNNs for inference at Stage 1. In each subsequent stage, the predictions from both branches in the previous stage, along with the original frame features F , are concatenated and used to produce refined predictions,

$$S^t = \rho^t(F, S^{t-1}, L^{t-1}), \forall t \geq 2,$$

$$L^t = \phi^t(F, S^{t-1}, L^{t-1}), \forall t \geq 2,$$

where ρ^t and ϕ^t are the CNNs for inference at Stage t .

Realizing the requirements of a high configuration regarding GPU for Openpose handled, we proposed to apply TF-Openpose¹ instead of original Openpose version. It is a human pose estimation library developed based upon the foundation of the Openpose library using Tensorflow and OpenCV. It also provides several variants that made changes to the network structure for real-time processing on the CPU or low-power embedded devices. We concentrated on two variations of models to find optimized network architecture: CMU [29] and Mobile-Net [28]. (1) With regard to CMU, it is the model based VGG pre-trained network which described in the Openpose's original paper using COCO dataset for training, it is converted from Caffe format for use in Tensorflow; (2) Based on the Mobile-Net paper [28], with 12 convolutional layers are used as feature-extraction layers.

4.2. Deep Convolutional Neural Networks – DCNNs

Convolutional neural networks (CNNs) have been applied to visual tasks since the late 1980s. With a few distributed applications, they were dormant until the mid-2000s when developments in computing power and the advent of a large amount of labelled data, supplemented by improved algorithms, contributed to their advancement and brought them to the forefront of a neural network renaissance that has seen rapid progression since 2012. CNNs are feed-forward networks in which information flow only takes place in one direction, from their inputs to their outputs.

There are three main types of layers used to build Deep CNN architectures: convolutional layer, pooling layer, and fully connected layer. Most of the CNN architectures are obtained by stacking the number of these layers.

Deep convolutional neural networks, trained on large datasets, achieve convincing results and are currently the state-of-the-art approach for this task as illustrated in Figure 4.

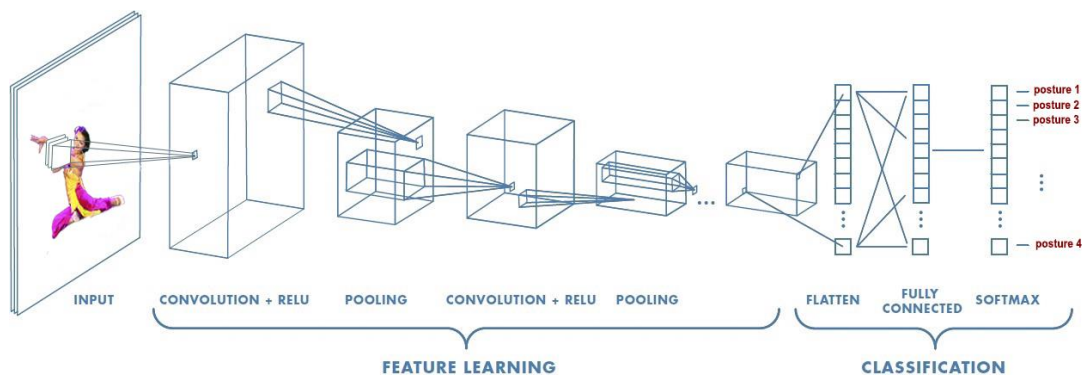


Figure 4. Neural network with many convolutional layers

In addition, the DCNNs are also developing rapidly as a result many DCNNs novel architectures are proposed. Each DCNN architecture undertakes a distinguishable role to train the different datasets. In this study, we used the existing successful DCNN architectures to extract features, our proposed framework is associating the features of the different extracted DCNN architectures. It can be seen that the dataset of EVTDS would accelerate considerably in the following years as well as the angles of the camera are flexible and multiform. Furthermore,

¹ <https://github.com/ildoonet/tf-pose-estimation>

combining the features to increase the explicit discrimination between the featured vectors is quite expected. We therefore proposed a flexible framework to easily select the new architectures for extracting the features. Our contributed framework concentrated on the sequential aggregation of the features of many effective DCNN architectures to support detecting the postures of EVTDS automatically.

At present, there are a large number of the published CNN architectures. Fortunately, an open source neural network library written in Python called Keras² in which integrated many architectures being compatible with all the backends (TensorFlow, Theano, and CNTK). In this research, we selected three of the efficient architectures published recently that will be discussed in subsection 4.3.

4.3. A general framework

In this subsection, we present a general framework to serve in training, detecting and extracting automatically the fundamental postures of EVTDS aiming at storing the primary concepts into a lightweight ontology-based in order to support for classification, query-answering, reasoning, and searching dance videos. The below model is a sequential process to train the dataset issued from the frames of the dance videos. We used Openpose and Tensorflow library (called by TF-Openpose) to detect body parts, the reason we used these libraries is we need a useful tool to detect human skeleton aiming at describing the actions and motions in each frame of EVTDS videos. However, regarding the leg part, the postures of this part could not be covered using TF-Openpose, i.e. foots, we therefore addressed on classifying *legs-postures* by machine learning. In detail, we crop the parts of legs and save them into the distinct folders for collecting trained dataset. The next steps are the extraction of the features (*based upon the deep CNN models proposed*) and the classification with machine learning algorithms.

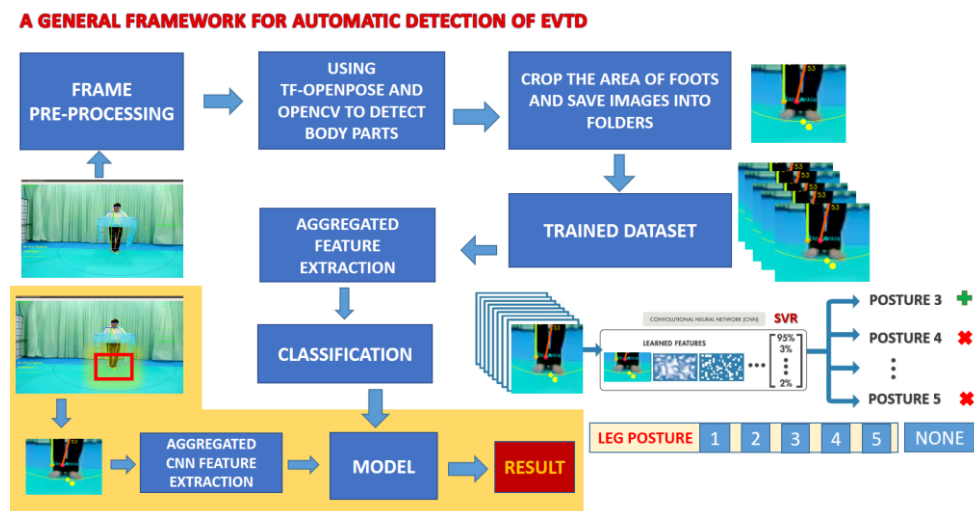


Figure 5. A general framework for automatic detection of EVTDS

Additionally, we classified on three sets of the basic postures of EVTDS including sitting postures, standing postures, and legs postures. With each kind of the different postures, we create an extra folder in which contains the common motion images called non-posture, the particular examples consist of non-leg-posture, non-standing-posture, non-sitting-posture. As soon as the

² <https://keras.io/models/model/>

postures are undetermined precisely, non-posture classification is expected to solve the problems in the online detection.

4.4. Extraction of aggregated features

In this subsection, we introduce a classification model aggregating consequently the deep CNN architectures to extract the features. As can be seen that each CNN architecture deals with the different cases of the particular datasets as well as combining the features to represent a vector is expected because it will be boosted strongly the discrimination between the classifications. In addition, the datasets of ETVDs mainly focus on the high resolution image frames of dance videos, specially, the resolution and size of images will be grown rapidly in the future. For these reasons, we selected the method using deep CNNs to extract the significant features and ML algorithms to classify. After having sets of the collected images, we used several algorithms to advance the quality of images (image pro-processing). In each image frame, we extracted the features from three CNN architectures, including Xceptions [30] (2048 features), InceptionV3 [31] (2048 features), Mobilenet [28] (1024 features). The next step, we aggregated the extracted features to have a feature vector with 5120 dimensions. In order to have a best candidate for classification, the comparison of ML algorithms is essential as presented in the next section.

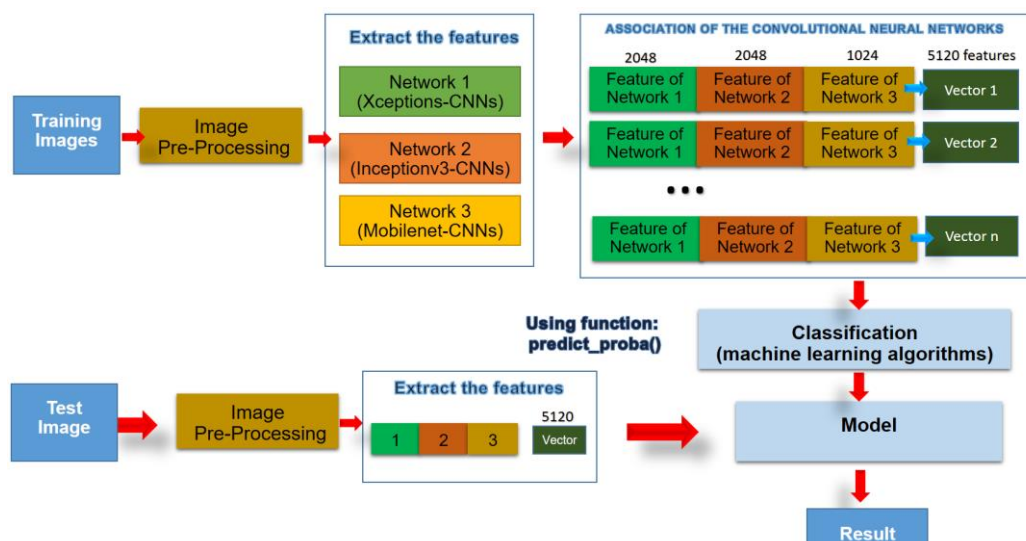


Figure 6. A classification model aggregating the deep CNN architectures

The main idea is to have a classification tool that allows flexible updating of novel architectures that will be published in order to improve classification accuracy as soon as the dataset is accelerated. In addition, we can also extract the features using CNN architectures in parallel, nevertheless, we do not experiment the parallel models in this paper.

5. EXPERIMENTAL RESULT

We implemented the propositional framework on the computer supporting graphical card (NVIDIA GeForce GTX 950M with total memory is 8107 MB) to run TensorFlow on multiple GPUs. To evaluate the proposed model, we had experimented on the Flower17 dataset of University of Oxford including 17 categories of the common flowers in the UK with 80 images for each class. Particularly, the images have large scale, pose and light variations and there are also classes with large variations of images within the class and quite similar to other classes. We

randomly split the dataset into two different train (2/3) and test (1/3) sets. In addition, we also implemented scikit-learn library³ to use several ML algorithms including logic regression, Support vector machine (SVM - C=10000, Gama=0.002), Random Forest (200 decision trees), Stochastic Gradient Descent classifier (SGD), K-Nearest Neighbours (KNN - K=5), Naïve Bayes classifier. The experimental results of the propositional CNN model are in Figure 7 and Table 1 for Rank-1 accuracy). Additionally, we also test our model with Rank-3 accuracy presented the results in Figure 8 and Table 2.

After comparing of the experimental results with Rank-1 and Rank-3 accuracy, the proposed model obtained the highest accuracy in the ML algorithms. The noticeable results are Logic regression and SVM algorithms achieved above 98% of Rank-1 accuracy and 100% of Rank-3 accuracy. The result on Flower17 dataset also showed that our model is more accuracy than the single architecture models.

Table 1. Accuracy of Flower17 dataset (Rank-1)

Algorithm	Deep CNN Architectures (Rank -1)			
	Xception	InceptionV3	Mobilenet	Proposed Method
Logic Regression	92,26	92,29	97,14	98,24
SVM (Linear)	94,49	91,85	96,92	98,02
SGD Classifier	80,84	77,31	86,12	88,99
Random Forest	86,56	85,68	91,85	91,85
K-Nearest Neighbors	83,48	84,58	92,95	94,05
Naïve Bayes	86,12	84,12	89,87	92,07

Table 2. Accuracy of Flower17 dataset (Rank-3)

Algorithm	Deep CNN Architectures (Rank -1)			
	Xception	InceptionV3	Mobilenet	Proposed Method
Logic Regression	99,12	98,68	99,34	100,00
SVM (Linear)	98,90	98,46	99,56	100,00
SGD Classifier	84,36	82,82	88,33	89,87
Random Forest	96,48	96,48	96,70	97,58
K-Nearest Neighbors	95,15	95,15	98,02	99,12
Naïve Bayes	96,70	96,04	96,04	97,80

³ <http://scikit-learn.org/stable/>

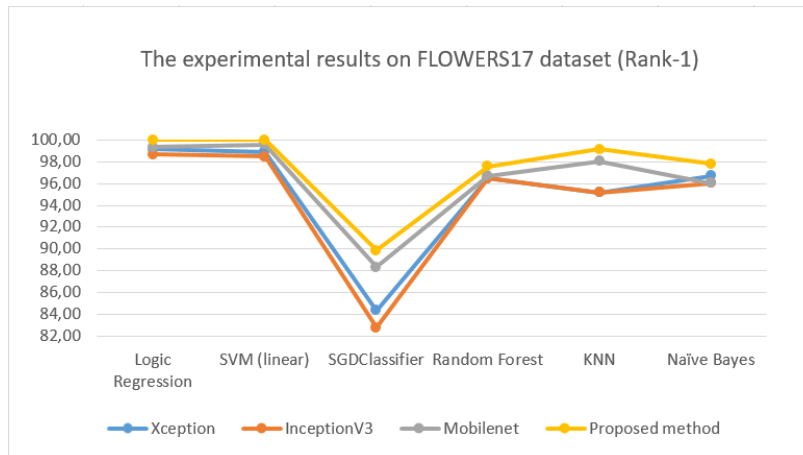


Figure 7. Comparison of Rank-1 accuracy

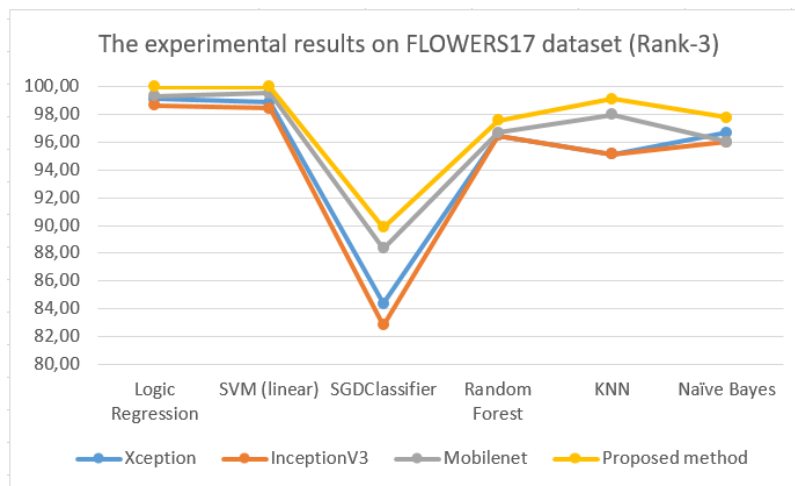


Figure 8. Comparison of Rank-3 accuracy

Furthermore, our main task is building a framework to detect automatically the fundamental postures of EVTDS. Based on the framework presented in Figure 5, we had collected a dataset including six images folders of leg postures, three images folders of sitting postures and four images folders of standing postures to support for training and evaluating. The particular number of each posture showed in Table 3. After collecting the dataset, we also divided the dataset into 2 distinct training (2/3) and test (1/3) sets, our model and framework gained the experimental results is fully expected. They achieved the high accuracy as follows: 98.88% of Leg postures, 99.84% of Sitting Postures, 99.37% of Standing postures. Comparisons of rank-1 accuracy showed in Table 4 and Figure 9. In general, most of the classification results achieved the high accuracy all above 90%.

After evaluating the model with the collected dataset, the implemented result about the propositional framework is demonstrated in the Figure 10. In each frame, we detected and extracted the essential postures based upon our proposal framework, this is one of the important foundation to provide automatically for the fundamental concepts into lightweight ontology-based served in preserving and promoting the intangible cultural heritage of traditional dances in

Vietnam. Moreover, Logic Regression algorithm and Linear SVM algorithm give the highest and quite similar results as they reach over 98% for all postures (Table 4, Figure 9).

Table 3. Datasets of the fundamental of EVTDS

	Postures (Pos)						Total
	P1	P2	P3	P4	P5	None Pos	
Leg Postures	1260	685	1185	494	673	1407	5704
Sitting Postures	1252	798	None	None	None	2163	4213
Standing Postures	None	685	None	494	673	2084	3936

Table 4. Comparisons of Rank-1 accuracy of algorithms

Algorithm	Postures (Pos)		
	Leg Posture	Sitting Posture	Standing Posture
Logic Regression	98,84	99,84	99,37
SVM (Linear)	98,84	99,80	99,27
SGD Classifier	92,18	94,23	93,78
Random Forest	96,47	97,63	98,02
K-Nearest Neighbors	94,11	96,15	95,07
Naïve Bayes	96,30	97,06	97,34

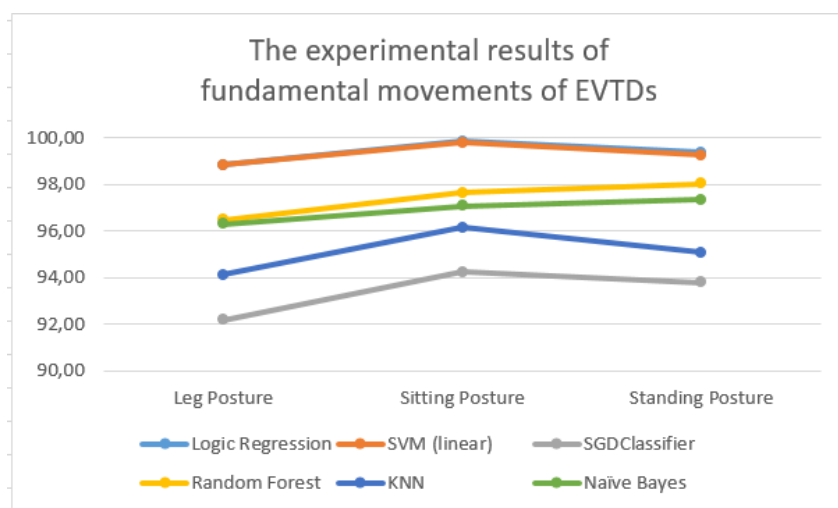


Figure 9. Comparisons of Rank-1 accuracy in EVTDS

Figure 10 illustrates the online identification of a performer's gestures. As can be seen, when the performer makes a move, our system will predict and display an illustration corresponding to the performed movement (*in this case, the results are “Leg_Posture 3” message and “Leg Posture 3” image*).

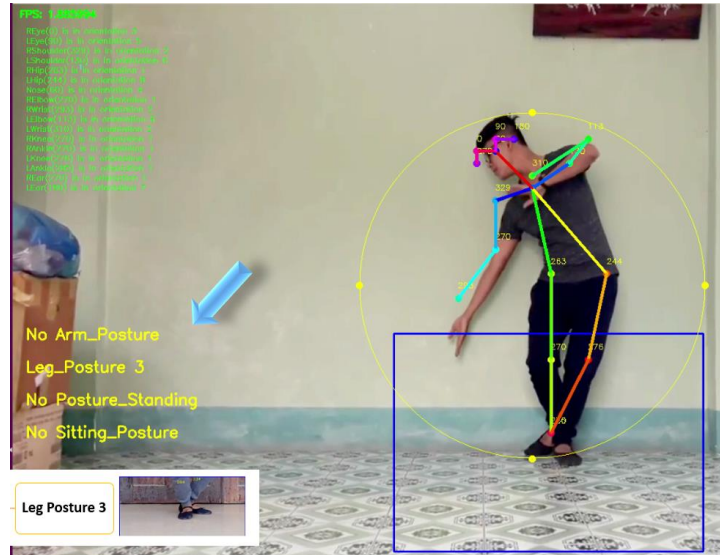


Figure 10. The experimental result of the propositional framework

The result of this paper will be one of the preliminary of collected dataset and classification. In implemented process, we realized that this collected dataset is not able to represent and reflect most of the different angle in dance. There are some difficulties in classification including the differences between the postures and gestures of a professional dancer and an amateur person as well as the distinction from different directions to look. Therefore, it is necessary to collect a huge dataset in the future. We would also update the architectures into our framework to support for classification aiming to build the intelligent repository and a query-answering and reasoning tool⁴. Although our proposed system has good results in detecting and classifying dances which are performed by a single person (in dance courses or practice sessions), it is difficult to identify dances performed by many dancers in performances or festivals due to gestures may be obscured by other dancers or performance costumes.

6. CONCLUSION AND FUTURE WORKS

With the aim of the preserving and promoting the intangible cultural heritage in general as well as developing an application to store the Vietnamese traditional dances in particular, we presented a methodology to identify automatically the significant concepts of EVTDs to serve in building an intelligent repository. Using the machine learning algorithms combined with the CNN architectures to classify dataset are discussed in this paper. On the basis of the propositional framework, we proposed a model aggregating consequently the CNN architectures to extract the features. After an experimented process is done, we gained the results which are absolutely expected.

⁴ Our tool to detect EVTD's postures and to store into EVTD's ontology published in the Github at: <https://github.com/truongthanhmastcc/VietnameseDance>

The presented work in this paper is one of the important first steps on preservation and promotion of EVTDS based on the background of artificial intelligent. These initial steps would be the foundation for creating universal traditional dance repository aiming to support for advanced heterogeneous digital storage, indexing, classification, reasoning and searching dance videos. Based on the concepts extracted automatically, the next step will put all concepts into ontology-based. In the future, we will expand the collection of the dance dataset as well as improve the model through the novel architectures which will be more compatible in dance domain. We will also build a lightweight ontology-based for this expanded dataset.

REFERENCES

- [1] L.T.Loc, "Mua dan gian cac dan toc Viet Nam", in Thoi-dai Publishing house, 1994.
- [2] H. Seo and P. Milanfar. Action recognition from one exam-ple.IEEE Trans. on Pattern Analysis and Machine Intelli-gence, 33(5):867–882, 2011.
- [3] V.Hoc, "Nghe thuat mua Viet Nam, thoang cam nhan", in Nation Publishing House, 2001.
- [4] I. Laptev and T. Lindeberg. Velocity adaptation of space-time interest points. InICPR, pages 52–56, September 2004
- [5] T.V. Son, D. T. Hoan, N. T. M. Huong, "Mua dan gian mot so dan toc vung Tay Bac", in Culture and Nation Publishing House, 2003.
- [6] Kyan, G. Sun, H. Li, L. Zhong, P. Muneesawang, N. Dong, B. Elder, and L. Guan, "An approach to ballet dance training through ms kinect and visualization in a cave virtual reality environment," In ACM Transactions on Intelligent Systems and Technology, vol. 6, no. 2, p. 23, 2015.
- [7] G. Chantas, A. Kitsikidis, S. Nikolopoulos, K. Dimitropoulos, S. Douka, I. Kompatsiaris, and N. Grammalidis, "Multi-entity bayesian networks for knowledge-driven analysis of ich content", in Proc. 1st International Workshop on Computer vision and Ontology Applied Cross-disciplinary Technologies in conj. with ECCV, pp. 355–369, Springer, 2014.
- [8] A. Kitsikidis, K. Dimitropoulos, E. Yilmaz, S. Douka, and N. Grammalidis, "Multi-sensor technology and fuzzy logic for dancer motion analysis and performance evaluation within a 3d virtual environment", in Universal Access in Human-Computer Interaction. Design and Development Methods for Universal Access, pp. 379–390, Springer, 2014.
- [9] A. Masurelle, S. Essid, and G. Richard, "Multimodal classification of dance movements using body joint trajectories and step sounds", in Proc. 14th International Workshop on Image Analysis for Multimedia Interactive Services, pp. 1–4, IEEE, 2013.
- [10] A. Gupta, P. Srinivasan, J. Shi, and L. S. Davis. Understand-ing videos, constructing plots: Learning a visually groundedstoryline model from annotated videos. InCVPR, 2009.
- [11] A. Klaser, M. Marszałek, C. Schmid, and A. Zisserman. Hu-man focused action localization in video. InInternationalWorkshop on Sign, Gesture, Activity, 2010
- [12] M. S. Ryoo and J. K. Aggarwal. Recognition of compositelhuman activities through context-free grammar based repre-sentation. InCVPR, pages 1709 – 1718, October 2006.
- [13] M. Blank, L. Gorelick, E. Shechtman, M. Irani, and R. Basri.Actions as space-time shapes. InICCV, volume 2, pages1395–1402, October 2005.
- [14] L.N. Canh, Nghe Thuat mua Ha Noi Truyen thong va Hien dai", in Ha Noi Publishing House, 2011.
- [15] Karavarsamis S., Ververidis D., Chantas G., Nikolopoulos S., Kompatsiaris Y. Classifying salsa dance steps from skeletal poses; Proceedings of the 2016 14th International Workshop on Content-Based Multimedia Indexing (CBMI); Bucharest, Romania. 15–17 June 2016; pp. 1–6.
- [16] T. Lan, Y. Wang, W. Yang, and G. Mori. Beyond actions:Discriminative models for contextual group activities. InNIPS, 2010.
- [17] L.N. Canh, "Nghe thuat mua truyen thong Khmer Nam Bo", in Vietnamese Dance College, Cultural and Nation publishing house, 2013.
- [18] Y. Wang and G. Mori. Human action recognition by semi-latent topic models.IEEE Trans. on Pattern Analysis and Machine Intelligence Special Issue on Probabilistic Graphical Models in Computer Vision, 31(10):1762–1774, 2009.
- [19] Y. Wang and G. Mori. Hidden part models for human ac-tion recognition: Probabilistic vs. max-margin.IEEE Trans.on Pattern Analysis and Machine Intelligence, 33(7):1310–1323, 2011

- [20] N. Nayak, R. Sethi, B. Song, and A. Roy-Chowdhury. Motion pattern analysis for modeling and recognition of complex human activities. *Visual Analysis of Humans: Looking at People*, Springer, 2011.
- [21] L.N.Canh. "Mua tin nguong dan gian Viet Nam", in Social Science Publishing house, 1998.
- [22] W. Yang, Y. Wang, and G. Mori. Recognizing human actions from still images with latent poses. In CVPR, pages 2030–2037, June 2010.
- [23] B. Yao, A. Khosla, and L. Fei-Fei. Classifying actions and measuring action similarity by modeling the mutual context of objects and human poses. In ICML, Bellevue, USA, June 2011.
- [24] J. K. Aggarwal and M. S. Ryoo. Human activity analysis: A review. *ACM Computing Surveys* (To appear), 2011
- [25] L.N.Canh. "Dai cuong nghe thuat mua", in Culture and information publishing house, 2003.
- [26] D.Lin and P.Paten. Induction of semantic classes from natural language text. In proceedings of SIGKDD-01. pp.317-322. 2001.
- [27] S. Maji, L. Bourdev, and J. Malik. Action recognition from a distributed representation of pose and appearance. In CVPR, pages 3177–3184, June 2011.
- [28] A.G. Howard, M. Zhu, B. Chen, D. Kalenichenko, W. Wang, T. Weyand, M. Andreetto, H. Adam, "MobileNets: Efficient Convolutional Neural Networks for Mobile Vision Applications", arXiv preprint, arXiv:1704.04861, 2017.
- [29] Z. Cao, T. Simon, S. Wei, Y. Sheikh, "Realtime Multi-Person 2D Pose Estimation using Part Affinity Fields", arXiv preprint, arXiv:1611.08050, 2016.
- [30] F. Chollet. Xception: Deep learning with depthwise separable convolutions. arXiv preprint arXiv:1610.02357, 2016.
- [31] X. Xia, C. Xu, Inception-v3 Flower Classification, 2017 2nd International Conference on Image, Vision and Computing, 978-1-5090-6238-6/17/ © 2017 IEEE.
- [32] Md Faridee, Abu Zaher, Sreenivasan Ramasamy Ramamurthy, and Nirmalya Roy. "HappyFeet: Challenges in building an automated dance recognition and assessment tool". *GetMobile: Mobile Computing and Communications* 22.3 (2019): 10-16.
- [33] Mallick, Tanwi, Partha Pratim Das, and Arun Kumar Majumdar. "Posture and sequence recognition for Bharatanatyam dance performances using machine learning approach." *arXiv preprint arXiv:1909.11023*, 2019.
- [34] Gibbs B, Quennerstedt M, Larsson H. Teaching dance in physical education using exergames. *European Physical Education Review*. 2017 May;23(2):237-56.
- [35] Kico, Iris, et al. "Visualization of Folk-Dances in Virtual Reality Environments." *Strategic Innovative Marketing and Tourism*. Springer, Cham, 2020. 51-59.

PERFORMANCE ANALYSIS OF AODV, DSDV AND ZRP ROUTING PROTOCOLS FOR WIRELESS SENSOR NETWORKS USING NS2 TOOL

Faïza Tabbana

Assistant Professor, Department of Telecommunication Engineering, Military
Academy, Fondék Jedid, Tunisia

ABSTRACT

This paper presents a literature review on WSN networks, in which the capacity of network nodes is limited with respect to energy supply, restricted computational capacity and communication bandwidth. WSN is a complex set of applications, link technologies, communication protocols, traffic flows and routing algorithms. Simulation is a predominant technique used to study and analyze the performance of a wireless sensor network design. To prolong the lifetime of these sensor nodes, designing efficient routing protocols are critical. Basically, the Routing protocols for wireless sensor networks are responsible for maintaining the routes in the network which ensures reliable multi-hop communication. To address this issue, in this paper, various protocols like AODV (Ad-hoc on-demand distance vector routing), DSDV (Destination-Sequenced Distance-Vector Routing) and ZRP (Zone Routing Protocol) are discussed along with various comparative parameters like Throughput, Packet Loss Ratio, End to End Delay and Dropped Packets. The performance of these protocols varies depending on the simulation environment. It will be analyzed in two ways. Firstly, by varying nodes within a margin of 10 to 100 nodes. Another way is by keeping the number of nodes constant and varying the speed of nodes from 10 m/s to 90 m/s.

KEYWORDS

Wireless Sensor Network, AODV, DSDV, ZRP and Performance Metrics.

1. INTRODUCTION

Wireless sensor network, is one of the most considered factors in this era. A Wireless sensor network (WSN) is a collection of homogenous, self-organized nodes called sensor nodes. Sensor nodes are densely deployed either within the sink or very close to it and have restricted power, computational capacity and memory [20]. Sensor nodes are connected to wireless radio frequency link. A WSN is a network composed of mobile nodes mainly characterized by the absence of any centralized coordination or fixed infrastructure, which makes any node in the network acts as a potential router [20]. WSN are also characterized by a dynamic, random and rapidly changing topology [2]. The basic task of sensor networks, is to sense the events, collect data and then send it to their requested destination. Civilian application domain of wireless sensor networks has been considered later on, such as environmental, healthcare and production, smart home etc. Their applications range from simple wireless low data rate transmitting sensors to high data rate real time systems like those used for monitoring large retail outlets [1]. All nodes of these networks behave as routers and take part in discovery and maintenance of routes to other nodes in the

network [20]. An Ad-Hoc routing protocol must be able to decide the best path between the nodes, minimize the bandwidth overhead to enable proper routing, minimize the time required to converge after the topology changes [26]. The primary goal of this paper is to evaluate performances of AODV, DSDV and ZRP protocols for different scenarios of variable density of nodes and mobility using NS-2 network simulator. The performance metrics consist of varying number of nodes and network dynamicity in terms of node evaluated speed. This paper is organized as follow: section 2 begins with a description of AODV, DSDV and ZRP protocols. Section 3 presents the methodology and procedures of our current study. Section 4 discusses the simulation environment. Section 5 describes the parameters used to analysis running programs with NS-2 tool. Finally, we evaluate and compare the performance of AODV, DSDV and ZRP protocols. The paper concludes with future works directions in section 7.

2. ROUTING PROTOCOLS

Routing in WSN is a challenging task due to highly dynamic environment [26]. There are different categories of routing protocols in wireless sensor networks such as proactive, reactive and hybrid routing protocols [3]. They differ from each other on the way they obtain the routing information.

2.1. Proactive routing protocols

Table Driven Protocols can be named as proactive protocols [22, 23, 25]. Table driven ad hoc routing protocols maintain at all times routing information regarding the connectivity of every node to all other nodes that participate in the network. Also known as proactive, these protocols allow every node to have a clear and consistent view of the network topology by propagating periodic updates [14, 10, 18]. In proactive routing, fresh list of destination and their routes are maintained by periodically distributing routing tables through the network. This type of protocols adds a new attribute, sequence number to each route table entry at each node. The routing information computed and shared and the path is set prior to the actual transfer of data packets between the source and the destination [7, 4]. This category of protocols has large bandwidth and more memory requirements making them more suitable for wired networks only [8]. Examples of proactive routing protocols are Destination Sequence Distance Vector (DSDV), Optimized Link State Routing Protocol (OLSR), Fisheye State Routing (FSR), and Source- Tree Adaptive Routing protocol (STAR) [8, 11, 12]. The selected protocol in this study is DSDV.

2.2. Reactive routing protocols

This type of routing protocols creates a route between the source and destination node only when the source node requires a route to the destination node [32]. It is a reactive or on demand routing protocol. When a node requires a route to a destination, it initiates a route discovery process within the network. This process is completed once a route is found or all possible route permutations have been examined [11]. Examples of reactive routing protocols are, Dynamic State Routing protocol (DSR), Ad hoc On-Demand Distance Vector Routing protocol (AODV), Ad-hoc on Demand Multipath Distance Vector (AOMDV), associativity-based routing (ABR) and Location-Aided Routing (LAR) [8, 6, 12]. The protocol considered here is AODV.

2.3. Hybrid routing protocols

These protocols combine characteristics of proactive and reactive protocols and are mostly used for hierarchal routing [22, 23]. In this protocol intermediate nodes have information about network and its closest node. Zone radius is used to define the zone size that is defined by number of hops [14, 10, 16, 17, 19, 25]. Hybrid routing protocols cartels the advantages of proactive as

well as reactive routing protocols and at the same time hybrid routing protocols overcome disadvantages of proactive and reactive routing protocols [23]. The limitation of these protocols is that nodes consume more memory and power as they have to maintain high-level topological information. Some examples of these protocols are Zone Routing Protocol (ZRP) and ZHLS (Zone Based Hierarchical Link State Routing Protocol) [25]. Figure 1, illustrates different classes of ad-hoc routing protocols.

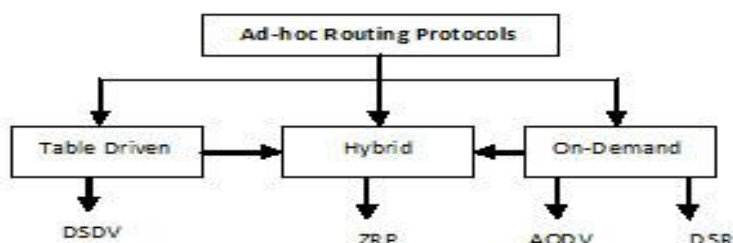


Figure 1. Classification of Routing Protocols

3. IMPLANTATION OF DIFFERENT ROUTING PROTOCOLS USED IN ANALYSIS

3.1. Destination Sequenced Distance Vector (DSDV)

DSDV [2] is a table-driven algorithm based on the classical Bellman-Ford routing mechanism, but guaranteeing loop-freedom via sequence numbers [1, 7, 19, 21]. Every mobile node in the network maintains a routing table in which all of possible destination within the network and the number of hops to each destination are recorded. Each entry is marked with a sequence number assigned by the destination node. The sequence numbers enable the mobile nodes to distinguish stale routes from newer ones, avoiding the formation of routing loops. Two different updates are defined: the first is known as a full dump, it carries all available routing information of the node and, attending to the size of the network, it can require multiple network protocol data units (NPDUs) [12, 24]. It is sent periodically. The second kind of update packets are named incremental and they are sent by a node when it detects a decisive change in the network. Update messages contain the address of the destination, the number of hops to reach the destination and the sequence number of the advertised route. Routes labelled with the most recent sequence number are always preferred. In the event that two updates have the same sequence number, the route with the smaller metric is used. Routes availability to all destinations implies that much less delay is involved in route setup process. The data broadcast by each node will contain its new sequence number, the destination's address, the number of hops count [24].

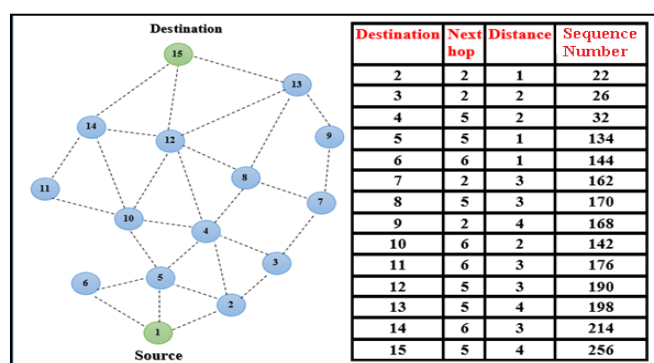


Figure 2. DSDV routing table for above nodes

Implementation Decision

The absence of a standard makes some parameters of the algorithm be without clear definition [29, 20]. The constants and parameters which were used in the implementation of the algorithm are shown in Table 1.

Table 1. Constants used in DSDV simulation [29]

Periodic route update interval	1 s
Time without news to declare a link broken	3 s
Time after the link break to remove the entry from the routing table	4 s
Size of control packets	Full dump -> 4096 bits incremental-> 512 bits
Maximal number of entries fitting in a full dump packet	32 entries

3.2. AODV

The Ad hoc On Demand Distance Vector (AODV) routing algorithm is a routing protocol designed for ad hoc mobile networks [20]. AODV is capable of both unicast and multicast routing [20]. It is an on-demand algorithm, meaning that it builds routes between nodes only as desired by source nodes. It maintains these routes as long as they are needed by the source. Ad hoc On-demand Distance Vector routing (AODV) protocol enables dynamic, self-starting, multi-hop routing between mobile nodes to establish the ad hoc network [1, 2, 3]. The mobile nodes obtain routes only for those destinations that are in the active communication. Link breakages are detected by the affected set of nodes and they invalidate the routes using the lost link [1, 7]. When a source node desires to establish a communication session, it initiates a path-discovery process to locate the other node [28]. AODV builds routes using route requested and route reply mechanisms [20]. In order to discover the path, a route request (RREQ) packet is broadcasted across the network to find the route to the destination. Nodes receiving this packet update their information for the source node and set up backwards pointers to the source node in the route tables. To find a path to the destination, the source initiates Route Request (RREQ) packet across the network and it contains the source address, destination address, source sequence number, destination sequence number, the broadcast identifier and the time to live field [32]. Nodes keep track of the RREQ's source IP address and broadcast ID [20]. If they receive a RREQ which they have already processed, they discard the RREQ and do not forward it [20]. When a node forwards a RREQ packet to its neighbours, it also records in its routing table the node from which the first copy came and it is required by the node to construct the reverse path for the RREP packet. AODV uses only symmetric links because the route reply packet follows the reverse path of route request packet. Information about the preceding node from which the packet was received is recorded when a node receives a RREP packet, in turn to forward the data packets to this next node as the next hop toward the destination. Once the source node receives a RREP it can begin using the route to send data packets [32, 15]. Hello messages are broadcasted periodically among the nodes in order to detect link break and if the intermediate nodes moves or changes then this information send to its upstream neighbours and so on till it reaches the source upon which the source can reinitiate route discovery if required [32, 16, 17, 19]. Figure 3 shows the propagation of the RREQ across the network.

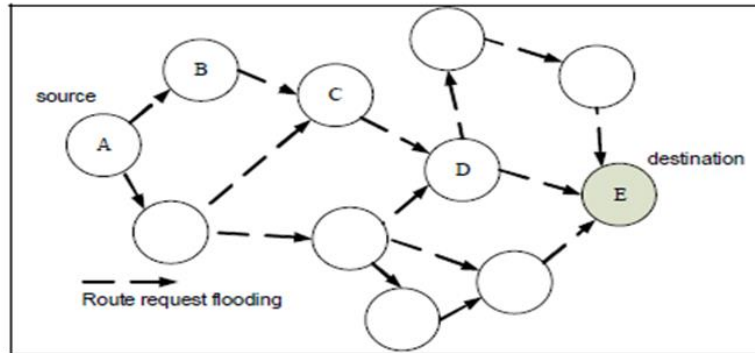


Figure 3. Route Request flooding

Once the RREQ reaches the destination or an intermediate node with a fresh enough route, this node responds by unicasting a route reply (RREP) packet back to the neighbour from which it received the RREQ packet. The path which follows the RREP message is shown in Figure 4.

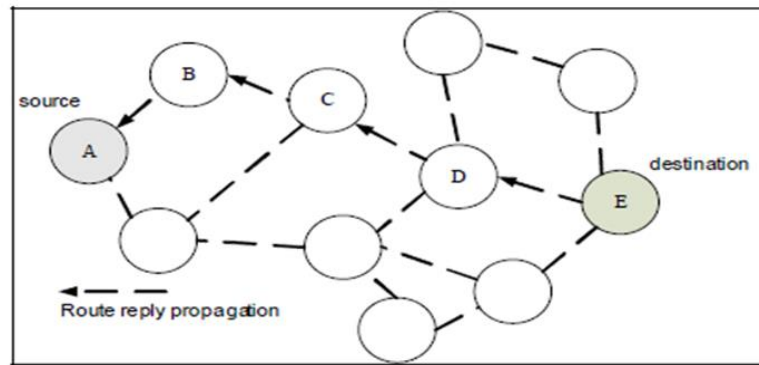


Figure 4. Route Reply propagation

As long as the route remains active, it will continue to be maintained. A route is considered active as long as there are data packets periodically traveling from the source to the destination along that path. Once the source stops sending data packets, the links will time out and eventually be deleted from the intermediate node routing tables. If a link break occurs while the route is active, the node upstream of the break propagates a route error (RERR) message to the source node to inform it of the now unreachable destination(s). After receiving the RERR, if the source node still desires the route, it can reinitiate route discovery process [20].

Implementation Decision [29]

Table 2. Constants used in AODV simulation

Hello interval	1 second
Time without news to declare a link broken	3 seconds
Time after link break declaration to remove the entry from the table	4 seconds
RREQ sent without replay arrival at time	3
Times a RREP is resent without ACK arrival	2

3.3. Zone Routing Protocol (ZRP)

ZRP is designed and presented by “Zygmunt Haas” of Cornell University, New York USA Zone [4]. This protocol is a correlation of proactive and reactive routing protocols (i.e. it is both table driven and demand driven) [26]. The hybrid approach can be more efficient than traditional routing. ZRP produces much less routing traffic than a pure reactive or proactive protocol. These protocols are designed to increase scalability by allowing nodes with close proximity to work together as a zone or cluster [1]. A node keeps routes to all the destinations in the routing zone. In this, a network is divided into zones. ZRP has three sub-protocols which are Intra zone Routing Protocol (IARP), Inter zone Routing Protocol (IERP) and Border cast Resolution Protocol (BRP) [26, 31]. Intra zone Routing Protocol is used when route lies within the zone and Inter zone Routing Protocol (IERP) is used outside the zone. Figure 4 illustrates the operation of the ZRP protocol. We deduce that if the destination is not inside the zone, then the source broadcasts Route Request message to the peripheral nodes.

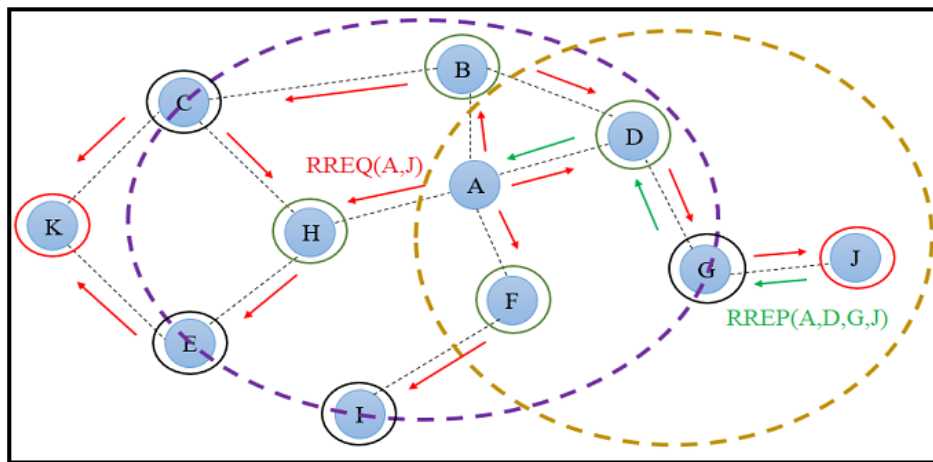


Figure 5. ZRP Routing Protocol Transmission

4. PROBLEM STATEMENT

The goal of this work is to compare and analyse the performance of three routing protocols based on demand behaviour i.e. on-demand Distance Vector (AODV), Destination Sequence Distance vector (DSDV) and ZRP protocols for wireless ad-hoc networks. Comparison has been made based on performance metrics like Throughput, packet delivery ratio (PDR), end to end delay and data packet loss with respect to different scenarios one by varying the density of nodes and finally by varying the mobility of nodes. The general objectives can be outlined as follows:

- Study of wireless networks
- Detailed study of AODV, DSDV and ZRP protocols
- Generate a simulation environment that could be used for simulating protocols
- Simulate the routing protocols on the basis of different scenarios by varying number of nodes and speed of nodes.
- Discuss and compare the result of the proposed work and concluding by providing the best routing protocol. Comparison of routing protocol is one in different network simulators, but not in ns 3 [30].

Figure 7 shows a scenario with a topology of 100 nodes. Node 0 is the source which transmits data. Node 100 is the sink or the destination for the whole network.

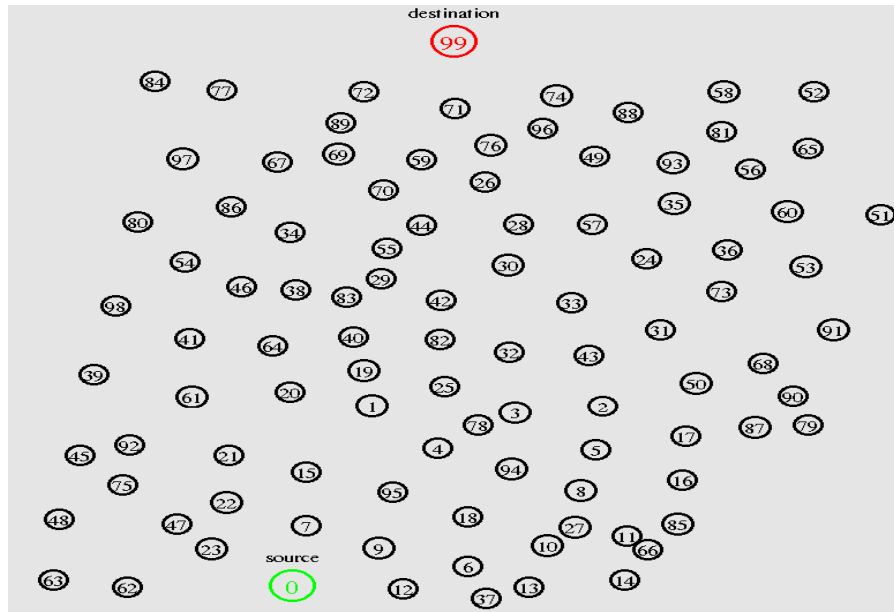


Figure 6. A WSN Topology with 100 nodes used in simulation

5. PERFORMANCE METRICS

Various Quality of Service parameters used for analysis routing protocols are defined as follows.

5.1. Packet Delivery Ratio (PDR)

It is the ratio of deliver packet which is send by the source node and received by the destination node. When packet delivery ratio is high then performance is better [5, 30]. Mathematically, it can be written as in this equation:

$$PDR = \frac{\sum_{i=1}^N \text{Total packets received by all node destination}}{\sum_{i=1}^N \text{Total packets send by all source}} \quad (1)$$

PDR is calculated in % (percentage). Higher values of PDR carry better performance.

5.2. Average throughput

It is the ratio between the actual number of packets transmitted by the nodes in the system to the number of successfully delivered packets at the base station [30]. The throughput is usually measured in bits per second (bit/sec), and sometimes in data packets per second or data packets per time slot. Higher throughput is always desirable in a communication system [30, 26]. The average throughput is given as follows:

$$\text{Average Throughput} = \frac{\text{recdvSize}}{\text{stopTime} - \text{startTime}} * \left(\frac{8}{1024} \right) \quad (2)$$

Where:

recdSize	=	Store received packet 's size
Stop Time	=	Simulation stop time
startTime	=	Simulation start time

5.3. End to End delay

End-to-end delay refers to the time taken for a packet to be transmitted across a network from source to destination. A data packet may take longer time to reach to the destination due to queuing and different routing paths [26]. It is derived in ms (mille second). Smaller values of End-to-end delay carries improved performance. The End-to-end delay is described as:

$$EED = \frac{\sum_{i=1}^n (Tri - Tsi)}{\sum_{i=1}^n \text{Nb received packets}} * 1000 \text{ (ms)} \quad (3)$$

Where:

I	=	packet identifier
Tri	=	Reception time
Tsi	=	Send time
N	=	Number of packets successfully delivered
NbreceivePackets	=	Number of received Packets

5.4. Packet Loss Ratio

Packet loss ratio is the number of packets that never reached the destination to the number of packets originated by the source [3, 13]. We aim to decrease the packet loss ratio. The packet loss ratio is given as:

$$PLR = \frac{\sum_{i=1}^n nSentPackets - nReceivedPackets}{\sum_{i=1}^n nsentPackets} * 100 \quad (4)$$

Where

nSentPackets	=	Number of sent packets
nReceivedPackets	=	Number of received packets

6. SIMULATION RESULTS

In this section, the performance analysis is carried out on DSDV as proactive candidate and AODV as reactive representative, for different scenarios of high density of nodes and mobility. Last, a new distance vector hybrid proposal, ZRP is presented and compared with its predecessors. Performance metrics like Throughput, Packet Delivery Ratio, Dropped Packet, End to End Delay are the four common measures used for the comparison of the performance of above protocols. In the first scenario, the density of nodes varies from 10 to 100 nodes. We created a second scenario by changing the average speed within a margin of 10 m/s to 90 m/s. The node mobility model is set up as Random Waypoint Mobility because it models the random movement of wireless sensor nodes. In order to enable direct fair comparisons between the protocols, it was critical to challenge the protocols with identical loads and environmental conditions. Each run of the simulator accepts an input scenario file which describes the exact motion of each node. Since the three chosen protocols were challenged with the same scenario file and during the same time (500 seconds), we can directly compare the performance results of

all protocols carried out. Simulations were performed by using Network simulator 2 (NS 2.35) tool. It runs under LINUX operating system. We have used Tool Command Language (TCL) for implementation of routing protocols. Performance metrics are calculated from trace file, with the help of AWK program and it is plotted with the help of Microsoft Excel 2007 tool. The analysis result helps the network designer to choose right protocol. Simulation results are shown in the following section in form of line graphs.

6.1. Scenario 1

In this scenario, number of nodes connected in a network at a time is varied and thus varying the number of connections, through which the comparison graphs of AODV, DSDV and ZRP protocols, is made. All nodes are fixed at one place. Table 3 shows the main characteristics used for scenario 1.

Table 3: Various parameters for scenario 1

Parameter	Value
Routing Protocols	AODV, DSDV and ZRP
Number of nodes	10, 25, 50, 75 and 100
Simulation Time	500 seconds
Traffic Type/Network Protocol	CBR/UDP
Bandwidth	0.4 Mb
Packet size	1500 bytes
Mobility Model	Off: A Fixed Topology
Radio Propagation Model	TwoRay Ground
Channel Type	Wireless channel
Queue files	Queue/Drop Tail/Priqueue
Queue length	50
Mac layer	802.11
Antenna Type	Omni Antenna
Topology size	1200 x 1200

Table 4, table 5 and table 6 give performances results of the three routing protocols, with varying the number of nodes from within a margin of 10 to 100 nodes. Network traffic type is chosen as CBR (Constant Bit Rate). The routing protocols are set as AODV, DSDV and ZRP to compare the simulation data. The performance metrics used for comparison are Average Throughput, End-to-End delay, Packet Loss Ratio, and Delivered Packet Ratio.

Table 4. DSDV Evaluation for scenario 1

Number of Nodes	Number of Packet Loss	Delivered Packet Ratio	Packet Loss Ratio	Average throughput	End to End Delay
10	1456	90.78	9.22	144.45	309.51
25	692	93.90	6.09	100.57	147.84
50	988	91.55	8.44	104.53	231.83
75	599	90.91	9.08	58	166.27
100	461	91.27	8.73	46	171.47

Table 5. AODV Evaluation for scenario 1

Number of Nodes	Number of Packet Loss	Delivered Packet Ratio	Packet Loss Ratio	Average throughput	End to End Delay
10	4701	77.85	22.15	182.48	301.27
25	1595	90.59	6.09	142.8	160.78
50	1881	86.91	8.44	120.68	138.84
75	1234	89.6	11.08	98.89	156.76
100	1175	88.92	8.73	46	157.31

Table 6. ZRP Evaluation for scenario 1

Number of Nodes	Number of Packet Loss	Delivered Packet Ratio	Packet Loss Ratio	Average throughput	End to End Delay
10	206	97.2	2.79	67.88	382.69
25	702	93.77	6.22	102.13	192.25
50	532	93.36	6.64	72.98	210.69
75	413	91.14	8.86	41.91	211.69
100	178	87.53	12.47	12.48	251.64

All results are analyzed and briefed in form of graphs given below. These graphs are found very helpful in statistical analysis of these routing protocols. The required graphs were saved as the bitmap image for statistical analysis. In this figure, we estimate the average throughput for all three routing protocols namely AODV, DSDV and ZRP.

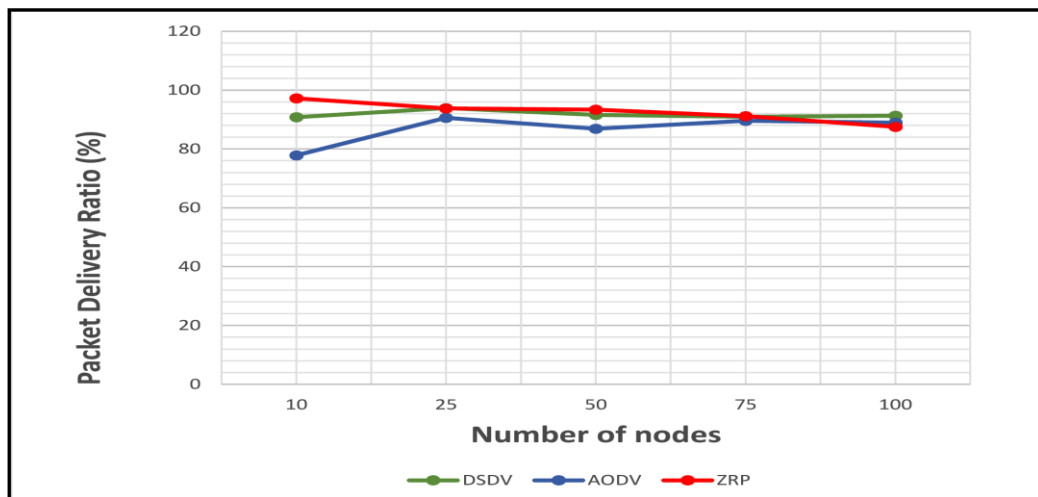


Figure 7. Packet Delivery Ratio for DSDV, AODV and ZRP

In Figure 7 we see the performance illustration of Packet Delivery Ratio depending on the number of nodes. DSDV and ZRP routing protocols are almost close to each other for varying number of nodes and we notice that the value of Packet Delivery Ratio remains constant and AODV shows variation. AODV performance dropped as number of nodes increase because more packets dropped due to link breaks. When we analyse where these lost packets are in AODV, we notice that AODV has not only more packets in buffers waiting for a route; but also, more

packets are lost because they were sent following old routes. So AODV, suffers in part from its lack of periodic update information but maintaining reasonably good delivery ratio. In addition, ZRP improved the Packet Delivery Ratio since it finds new route to destination when link breaks existed. DSDV is slightly better than ZRP especially when the number of nodes is higher.

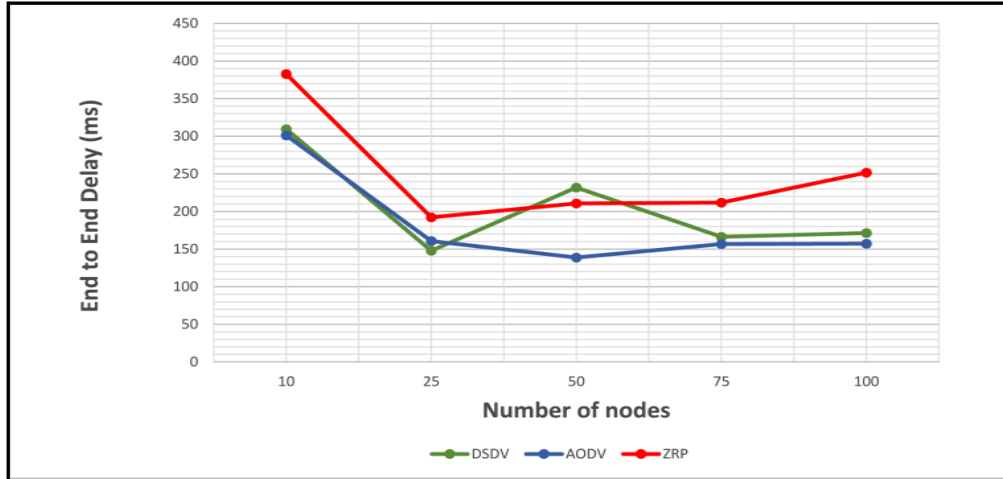


Figure 8. End to End Delay for DSDV, AODV and ZRP

This graph demonstrates the simulation results of End-to-End delay depending on the number of nodes. AODV didn't produce so much delay when the number of nodes increased. It performs better than the other two protocols. In addition, it shows that, the AODV protocol improved the DSDV when the number of nodes is over 50. The End-to-End Delay of AODV is less because it has reduced routing overhead and queuing delay. However, DSDV presents considerably less End to End delay than ZRP except at network size 50. Again, this shows that for delay-sensitive applications, DSDV protocol with a reduced density of nodes is remarkably well suitable. This attribute can be explained by the fact that DSDV is a proactive routing protocol and in these types of protocols the path to a destination is immediately available. Furthermore, DSDV routing protocol tries to drop the packets, if it is not possible to deliver them which means less delay. ZRP has higher delay than both DSDV and AODV routing protocols.

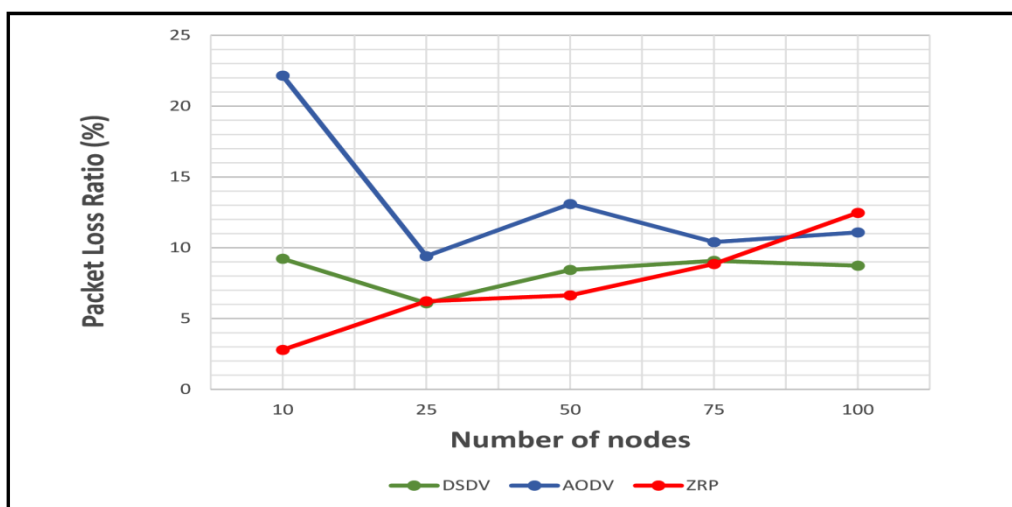


Figure 9. Packet Loss Ratio for DSDV, AODV and ZRP

With increasing number of sensor nodes AODV shows worst performance. AODV seems to be more sensitive to the effect of the density of nodes. Once more AODV suffers from not always up-to-date information. For all smaller number of sensor nodes, performance of ZRP is better than AODV and DSDV, but for 100 sensor nodes ZRP shows maximum packet loss ratio. For DSDV protocol, the Packet Loss Ratio is not so affected as generated in ZRP. Since proactive routing maintains information that is immediately available, the Packet Loss Ratio before sending a packet is minimal in cost. So, overall, we can say that DSDV is the most preferred routing protocol for larger networks.

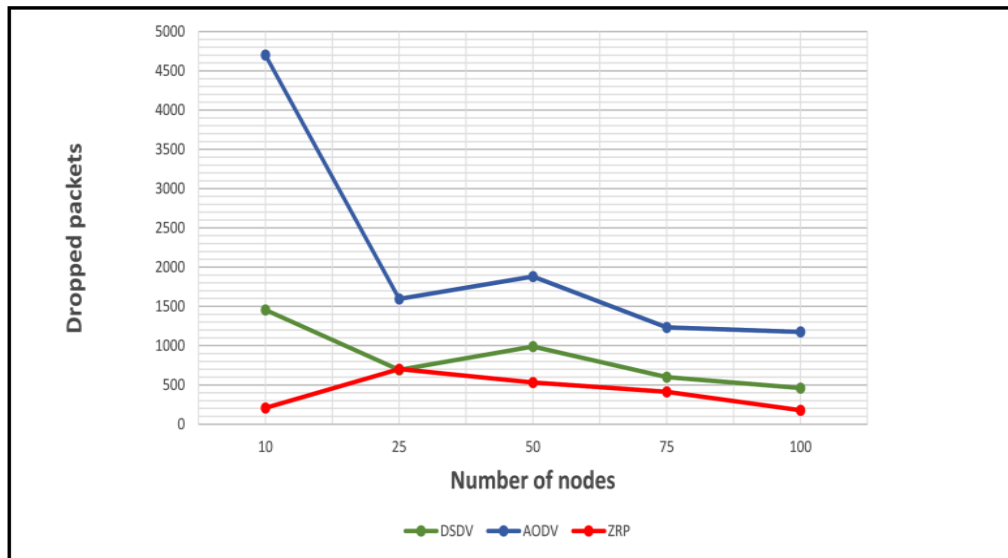


Figure 10. Dropped Packets for DSDV, AODV and ZRP

Here, we notice that as the number of nodes increases, the End-to-End delay becomes very high and increases with AODV. In case of ZRP, these parameters decrease as the density of nodes increases except when nodes are 25. This behaviour of ZRP is due to its hybrid nature because for smaller number of nodes, it behaves as a proactive routing protocol but for larger networks, it distributes the nodes into different zones and hence, due to IERP effect, it behaves as a reactive routing protocol. So overall, we can say that AODV is the most preferred routing protocol for larger networks in terms of End to End delay because its these parameters decrease more sharply than DSDV. Again, we conclude that with increasing number of sensor nodes AODV shows worst-performance. For 50 nodes AODV shows maximum dropped packet loss. Therefore, comparing to AODV and DSDV, ZRP presents the best results in terms of Dropped Packets.

6.2. Scenario 2

To see the effect of the mobility, the number of nodes is kept as 100 and speed of nodes is varying within a margin of 10 m/s to 90 m/s. In the Architecture mode of the simulator the scenario is designed in an area of 1200 m x 1200 m. The routing protocols are set as AODV, DSDV and ZRP to compare the simulation data.

Table 7. Various Parameters for scenario 2

Parameter	Value
Routing Protocols	AODV, DSDV and ZRP
Number of nodes	100
Simulation Time	500 seconds
Traffic Type/Application	CBR/FTP
Bandwidth	0.4 Mb
Packet size	1500 bytes
Mobility Model	Random Waypoint
Speed of nodes	10 m/s, 30 m/s, 50 m/s, 70 m/s and 90 m/s
Radio Propagation Model	TwoRay Ground
Channel Type	Wireless channel
Queue files	Queue/Drop Tail/Prique
Queue length	50
Mac layer	IEEE 802.11
Antenna Type	Omni Antenna
Topology size	1200 x 1200 m

For scenario 2, table 8, table 9 and table 10 illustrate performance of AODV, DSDV and ZRP routing protocols, with varying speed of nodes within a margin of 10 m/s to 90 m/s.

Table 8. DSDV Evaluation for scenario 2

Speed of Nodes	Number of Packet Loss	Delivered Packet Ratio	Packet Loss Ratio	Average throughput	End to End Delay
10	218	90.5	9.5	20.14	159.58
30	502	89.84	10.16	42.81	223.37
50	407	92.04	7.96	44.7	131.64
70	466	90.34	9.65	42.17	196.07
90	527	89.63	10.37	44.3	175.1

Table 9. AODV Evaluation for scenario 2

Speed of Nodes	Number of Packet Loss	Delivered Packet Ratio	Packet Loss Ratio	Average throughput	End to End Delay
10	1184	88.85	11.2	88.25	157.14
30	1195	88.42	11.58	68.1	181.15
50	1276	88.44	11.56	92.08	146.9
70	1259	88.62	11.38	92.3	140.7
90	1308	88.13	11.87	91.97	168.72

Table 10. ZRP Evaluation for scenario 2

Speed of Nodes	Number of Packet Loss	Delivered Packet Ratio	Packet Loss Ratio	Average throughput	End to End Delay
10	243	87.11	12.88	16.64	240.94
30	91	84.73	6.09	5.3	235.07
50	78	83.04	8.44	11.32	230.37
70	166	86.23	13.76	10.57	312.42
90	461	91.27	8.73	18.03	171.47

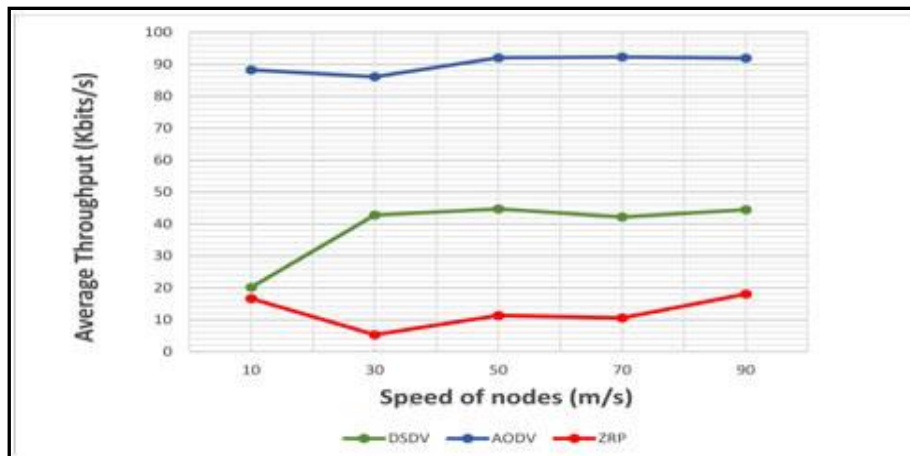


Figure 11. Average Throughput for DSDV, AODV and ZRP

The throughput is analysed with CBR (Constant Bit Rate) data traffic under the FTP (File Transfer Protocol) application. From this plotted result, we conclude that the average throughput in general increases steadily over the entire speed of nodes for all the routing protocols. ZRP outperforms the other two protocols but AODV attains the highest throughput and shows efficient behaviour in all mobility scenarios. Based on figure 11, it is shown that AODV attains the highest Average Throughput and shows efficient behaviour in all mobility scenarios. AODV produces more sent packet as it recovers from average throughput due to broken links in a higher node speed. ZRP performs a smaller number of packets delivered compared to the other two protocols.

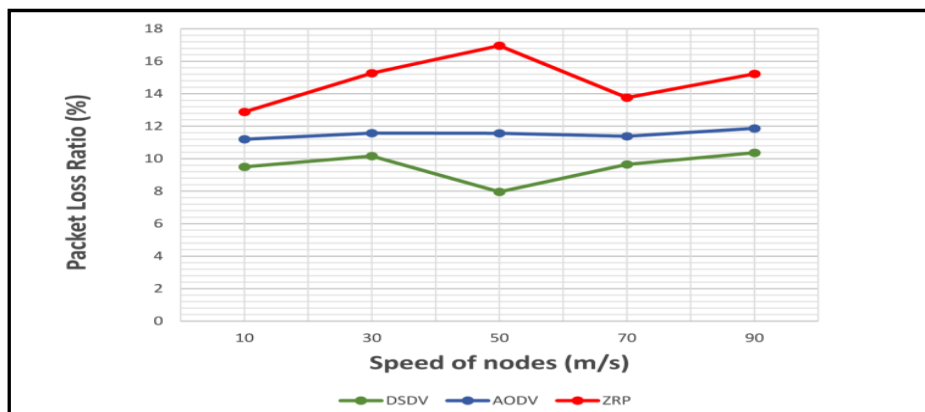


Figure 12. Packet Loss Ratio for DSDV, AODV and ZRP

The result plotted for the three routing protocols AODV, DSDV and ZRP respectively for a second scenario having 100 nodes. AODV performs constantly when speed of nodes changes, whereas DSDV performs better than both AODV and ZRP in terms of packet loss ratio. Routes availability to all destinations implies that much less Packet Loss Ratio is involved in DSDV route setup process.

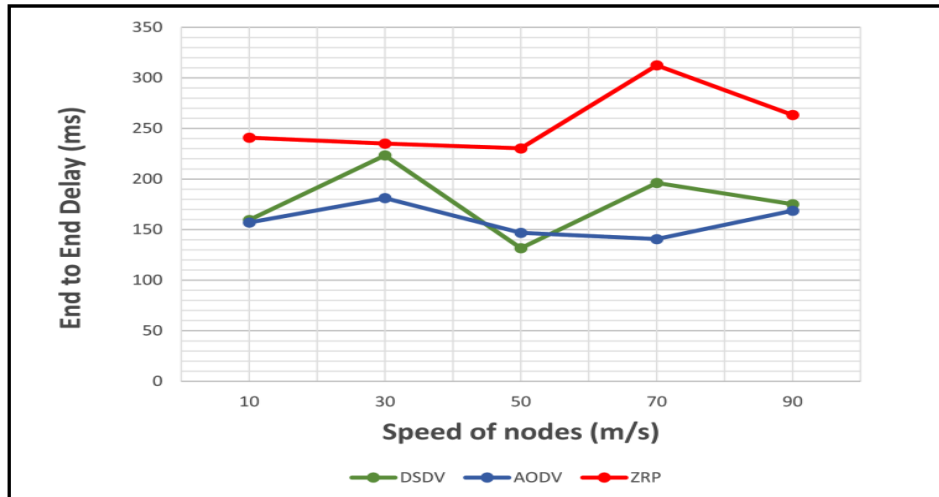


Figure 13. End to End Delay for DSDV, AODV and ZRP

These graphical results from figure 13 are measurement of end to end delay for the three routing protocols. AODV and DSDV perform better than ZRP in terms of End-to-End delay. When speed of nodes is 50 m/s, DSDV presents the better End-to-End delay than both AODV and ZRP protocols. Based on figure above, for varying speed, AODV produces less End to End Delay, but the performance of DSDV is slightly better than ZRP. ZRP renounce bad packet loss ratios or end to end delay values. It shows that for delay-sensitive application, AODV protocol with IEEE 802.11 standards performs efficient for wireless sensor networks. AODV routing protocol tries to drop the packets, if it is not possible to deliver them which, means less delay.

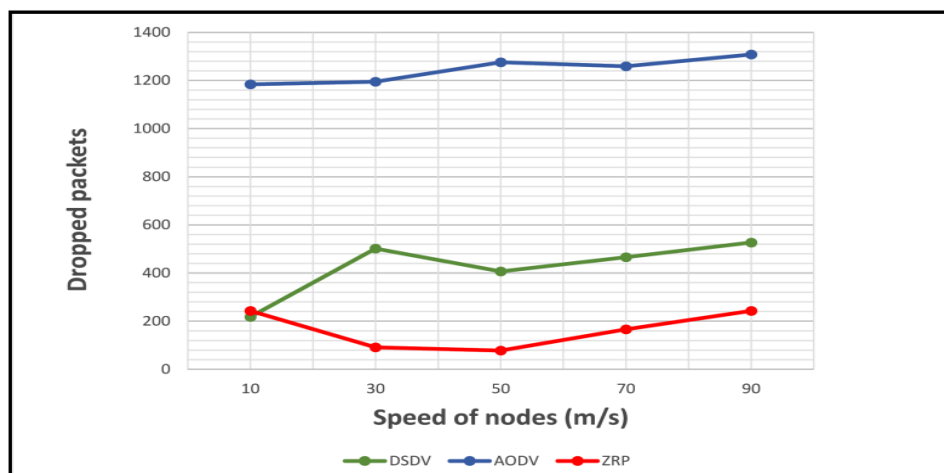


Figure 14. Dropped Packets for DSDV, AODV and ZRP

Figure 14 depicts the behaviour of the three proposed protocols in terms of dropped packets. Here we notice that as the speed of nodes increases, the value of mean Dropped Packets for AODV, DSDV and ZRP goes increasing. On the other hand, it is observed that ZRP protocol improves much better Dropped Packets in high mobility environments compared to AODV and DSDV protocols. So overall, we can say that ZRP is the most preferred routing protocol under high speed of nodes in terms of Dropped Packets. As resulting of that much dropped packets are occurred with AODV because the IEEE 802.11 protocol not enabled large packets transmission. On the other hand, reactive protocols must first determine the route, which may result in considerable dropped packets; moreover, the reactive route search procedure may involve significant control traffic due to the global flooding.

7. LIMITATIONS OF NS 2 SIMULATOR

NS-2 [27] is an object-oriented discrete event simulator targeted at networking research. The NS-2 simulation environment offered great flexibility in studying the characteristics of WSNs because it includes flexible extensions for WSNs. NS-2 has a number of limitations: (1) It puts some restrictions on the customization of packet formats, energy models, MAC protocols, and the sensing hardware models, which limits its flexibility [27]. (2), the lack of an application model makes it ineffective in environments that require interaction between applications and the network protocols. (3) It does not run real hardware code. (4) It has been built by many developers and contains several inherent known and unknown bugs. (5) The performance of NS-2 is good for 100 nodes, which decreases significantly as the number of nodes increase. It does not scale well for WSNs due to its object-oriented design. (6) Using C++ code and OTCL scripts makes it difficult to use.

To overcome the above drawbacks the improved NS-3 simulator [27] was developed. NS-3 supports simulation and emulation. It is totally written in C++, while users can use python scripts to define simulations. Hence, transferring NS-2 implementation to NS-3 require manual intervention. Besides the scalability and performance improvements, simulation nodes have the ability to support multiple radio interfaces and multiple channels. Furthermore, NS-3 supports a real-time schedule that makes it possible to interact with a real system [27]. For example, a real network device can emit and receive NS-3 generated packets.

8. FUTURE RESEARCH DIRECTIONS

In wireless sensor networks, routing is a challenge due to various characteristics that distinguish them from existing communication and wireless ad-hoc networks. New techniques of Hierarchical routing are a hot topic in this field for research. Due to the time limitations, our focus was only on some of the routing protocols during our study. DSDV was one of the early algorithms available. It is quite suitable for creating ad hoc networks with small number of nodes [20]. Since no formal specification of this algorithm is present. There is no commercial implementation of this algorithm [20]. Many improved forms of this algorithm have been suggested. Though, there are many other routing protocols that are needed to be analyzed. There are different design issues in WSN, like energy, heterogeneity, localization and synchronization which need to be explored further. Also, protocols security should be investigated with respect to various natures of attacks to which wireless communication is considered as an attractive target average throughput than DSDV and ZRP. Furthermore, performance comparison with other routing protocols in different classes could be done. In future, a mixture of two or more protocols can be used to give rise to a new type of WSN network satisfying more and more criteria. New techniques of Hierarchical routing are a hot topic in this field for research.

9. CONCLUSION

In this study various routing protocols, namely AODV, DSDV, ZRP and various parameters like Average Throughput, End-to-End delay, Packet Delivery Ratio, Packet Loss Ratio and Dropped Packets have been discussed. We have considered two wireless sensor network scenarios, the first is by varying the number of nodes and the second is by varying the speed of nodes. AODV shows best performance in all mobility scenarios, with its ability to maintain connection by periodic exchange of information required for TCP network. By comparing the data collected from the three routing protocols, we analysed and proved that AODV is a more reliable protocol in terms of Delay and Average Throughput than DSDV and ZRP protocols. Network size has no considerable effect on AODV performance with respect to throughput but it does affect ZRP. The results can vary according to the metrics parameters. For some scenarios, Routing protocol DSDV has also performed good even than AODV is more reliable protocol in terms of End-to-End delay and Throughput. At higher node mobility, AODV is worst in case of Packet Loss and Dropped Packets but it performs best for Packet Delivery Ratio. DSDV performs better than AODV for higher node mobility, in case of Packet Delivery Ratio and Packet Loss Ratio but ZRP performs best in case of dropped packets. However, not all of these protocols are efficient enough to fulfil all desired features of WSNs applications. From the conducted study on selected protocols, we have proved that there is no a best solution for a general mobile ad hoc network. The performance of one protocol may be far better in terms of delay other may be superior in terms of throughput. Secondly, network size also influences for protocols performance. Therefore, choice for selecting particular routing protocol will depend on application type and intended use of wireless sensor network. Finally, from the above research work performance of AODV is considered best for real-time and TCP applications. Therefore, the most successful applications of WSN technology will be those oriented to applications including large number of nodes. As we could see in section 6, each routing technique has specific advantages and disadvantages that make it suitable for certain types of scenario. In sensor networks, routing is an emerging area of research and who are becoming an increasingly popular wireless networking concept lately. Consequently, more and more research, is being conducted to find optimal routing algorithms that would be able to accommodate for such networks.

ACKNOWLEDGEMENTS

The author would like to acknowledge the support of Hamza Weslati, a student at Military Academy of Tunisia.

REFERENCES

- [1] Y. jahir, M. Atiqzaman, H. Refai, A. Paranjathi, P. G. Loprest, "Routing Protocols and architecture for disaster area Network : a survey", *Ad-hoc Networks Journal Elsevier* 82-2019, 1-14.
- [2] Hema, H. Schrawat, "Comparative Analysis of Various Routing Protocol in Wireless Sensor Networks", *International Journal of Innovations of Advancement in Computer Science*, Volume 6, Issue 7, July 2017.
- [3] S. Lalar, A. Yadav, "Simulation and Comparative Analysis of AODV, DSDV, DSR and AOMDV routing Protocol in WSN", *IJEE*, Volume 9, Number 1, Jan-June 2017, pp 9-15.
- [4] S. NakhshabHussain, H. Raza, U. Tayyab, A. Razzak, "Multicast Zone Routing Protocol in Wireless Ad-hoc ", *International Journal of Comuter Science and Network Security*, Volume 17, n ° 5, May 2017.
- [5] P. Patel, K. Patel, "Review Paper on Energy Efficient Routing Protocols in Mobile ad-hoc Network ", *International Journal of Advance Engineering and Research Development*," Special Issue Sicicom-2017, April 2017.

- [6] M. Z. Chawy, M. A. Al Sanabani, , “Application and performance Analysis of DSDV Routing Protocol in Ad-Hoc Wireless Sensor Network with Help of NS2 Knowledge”, *Global Journal of Computer Science and Technology: ENetwork, WEB and Security*, vol. 17 issue 1 Version 1.0, p373-379, 2017.
- [7] J. Daniel Mano, S. Sathappan “Comparaison of Wireless Routing Protocols in Sensor Network Using NS2 Tool”, *International Journal of Advanced Research in Basic Engineering Sciences and Technology (IJRABEST)*, U.K, vol 2, Special Issue 19, October 2016.
- [8] S. Chauhan, “Performance Evaluating of Routing Protocols for MANET using NS2”, *International Journal of Computer Science and mobile Computing*, Vol 4, Issue 9, pg 242-249, septembre 2015.
- [9] P. Boora, S. Malik, , “Performance Analysis of AODV, DSDV, and ZRP Routing Protocols in WSN using Qualnet”, *International Journal of Enhanced Research in Science Technology of Engineering*, vol 4, Issue 6, June 2015.
- [10] G. Gautam, B. Sen, “Design and Simulation of Wireless Sensor Network in NS2”, *International Journal of computer Applications*, vol. 113, No 16, March 2015.
- [11] G. Kaur, E. Bhardwaj, “A Review On Energy Efficient Routing Protocols in Wireless Sensor Network, Mobile Ad-Hoc Network”, *International Journal of Research in Computer Applications and Robotics*, vol 3, Issue 5, p36-41, May 2015.
- [12] A. Arya, J. Singh, “Comparative Study of AODV, DSDV and DSR Routing Protocols in Wireless Sensor Network Using NS-2 Simulator”, *International Journal of Computer Science and Information Technologies (IJCSIT)*, Vol. 5(4) IJCA, pp. 9-13, 2014.
- [13] Mrs. Viashali, D. Khairnar, Dr K. Kotecha, “Simulation-Based Performance Evaluation of Routing Protocols in Vehicular Ad-hoc Network”, *International Journal of Scientific Research Publications*, Volume 3, Issue 10, October 2013.
- [14] S. Singh, Dr N. Hemrajani, “Performance Evaluation of AODV Routing Protocol in Wireless Sensor Networks with the Constraints of varying terrains areas by varying pause time”, *International Journal of Emerging Trends and Technology in Computer Science (IJEITCS)*, Volume 2, Issue 1, January-February 2013.
- [15] P. Goswamis, Dr A.D. Jadhav, “Evaluating the Performance of Routing Protocols in Wireless Sensor Network”, *International Journal of Computer Technology and ELECTRONICS Enginring (IJCTEE)*, Volume 2, Issue 3, June 2012.
- [16] A. S. El. Ashhab, “Performance Evaluation of AODV and DSDV Routing Protocol in Wireless sensor Network Environment”, *International Conference on Computer Networks and communication systems*, Vol 35, Singapore 2012.
- [17] P. Kansal, D. Kansal, A. Balodi, “Comparison of Various Routing Protocol in Wireless Sensor Network”, *International Journal of Computer Applications*, Volume 5-No.11, August 2010.
- [18] P. Goswamis, Dr A.D. Jadhav, “Evaluating the Performance of Routing Protocols in Wireless Sensor Network, Volume 2, Issue 3, June 2012, pp557-567.
- [19] A. Aggarwal, S. Gandhi, N. Chaubey, “Performance Analysis of AODV, DSDV and DSR in MANETS”, *International Journal of Distributed and Parallel Systems (IJDPS)*, Vol 2, N°6, Novembre 2011.
- [20] A. Abderahman, Z. Zukarnain, “Performance Comparison of AODV, DSDV and I-DSDV routing Protocols in Mobile Ad-hoc Networks”, *European Journal of Scientific Research*, Vol 31, N°4, 2009, PP566-576.
- [21] B. N. Jagdale. P. Patil, P. Lohane, D. Javale, “Analysis and Comparison of Distance Vector, DSDV and AODV Protocol of Manet”, *International Journal of Distributed and Paralle Systems (IJDPS)*, Vol 3, n°2, March 2012.
- [22] D. Bandral, R. Aggarwal, “Analysis of AODV and DSDV Routing Protocols for improving Quality of Service in MANET”, vol 9, n°32, August 2016.
- [23] L. Naikl, L.R.U. khon, R. B. Misha, “Analysis of Performance Improving parameters of DSDV using NS3”, *International research Journal of Engineering and Technology (IRJET)*, vol 3, Issue 7, July 2016, pp 446-452.
- [24] S. Goverdhan, A.choubay, “Comparative analysis and Implementation of DSDV and AODV Routing Protocol for MANET”, *International Journal of Computer Techniques*, Volume 2, Issue 3, May-June 2015, PP 90-97.
- [25] Harsimrankau, J. Singh, “Comparison of AODV and DSDV protocols with improvement of AODV”, *International Journal of advanced research in Computer Engeneering of Technology (IJARCET)*, Volume 6, Issue 7, July 2017, pp 976-980.

- [26] Seema Pahal, Kusum Dalal, “A Review Paper on Routing Protocols in Wireless Sensor Networks”, International Journal of recent trends in engineering and research, ISSN (Online) 2455 1457, 2016.
- [27] Abdelrahman Abuarqoub, Fayez Al-Fayez, Tariq Alsbouï, Mohammad Hammoudeh, Andrew Nisbet, “Simulation Issues in Wireless Sensor Networks: A Survey”, The Sixth International Conference on Sensor Technologies and Applications, 2012.
- [28] Madhuri Pal* Kalyani Satone Bhawa Chilke, “Implementation DSDV routing protocol for wireless mobile ad-hoc network, using NS-2 simulator”, International Journal of Engineering Research & Technology (IJERT) Vol. 1 Issue 8, October - 2012 ISSN: 2278-0181.
- [29] Resumen_siemens, “Design, Implementation and Evaluation of Distance Vector Routing Protocols in Ad Hoc Networks ”.
- [30] T.Praveena1, Mr.S.Parthasarathi, Dr.K.Hariharan,” Performance Analysis of Different Routing Protocol Using Wireless Sensor Network in NS3”, ISSN (PRINT): 2393-8374, (ONLINE): 2394-0697, Volume-4, ISSUE-12, 2017.
- [31] Seema Pahal , Kusum Dalal, “Performance Evaluation of Routing Protocols in WSN using QualNet 5.3”, International Journal of Recent Trends in Engineering and Research-2016.
- [32] Marwan Aziz Mohammed, “Performance Study of AODV and DSDV Routing Protocols for Mobile Ad Hoc Networks Based on Network Simulator NS2”, Sulaimani Journal for Engineering Sciences / Volume 2 - Number 2 – 2015.
- [33] Snehal Goverdhan, Aakanksha Choubey, “Comparative Analysis and Implementation of DSDV and AODV Routing Protocol for MANET”, International Journal of Computer Techniques – Volume 2 Issue 3, May - June 2015.

AUTHOR

Faïza Tabbana is an assistant professor of Military Higher Education of Foundek Jedid, Nabeul Tunisia. She has over fifteen years experience in teaching wireless, cellular and fixed networks like GSM (Global System for Mobile Communication), UMTS (Universal Mobile Telecommunication Standard), LTE (Long Term Evolution), Wimax, Wifi (IEEE 802.11), Ad-hoc Networks, TCP/IP networks and LANs (Local Area Networks). Her main research interests include wireless networks planning and protocols. She worked for five years as Senior Engineer in a Center for studies and research in Telecommunication. She has published 4 papers in International Conferences (IEEE) and another paper in International Journal of Computer networks and Wireless Communications (IJNCWC).



AUTHOR INDEX

<i>Abdullah Aref</i>	81
<i>Ahmed Bentajer</i>	217
<i>Alaidine Ben Ayed</i>	121
<i>Alanoud Alhamid</i>	177
<i>Ali Azougaghe</i>	217
<i>Amir Farzad</i>	163
<i>and David Guy Brizan</i>	103
<i>Andrew Wang</i>	103
<i>Ankit Kamboj</i>	197
<i>Ashwini Badgujar</i>	103
<i>Aviv Segev</i>	01, 185
<i>Courtney Foots</i>	185
<i>Dandan Song</i>	249
<i>Deli Chen</i>	209
<i>Deyang Liu</i>	137, 209
<i>Dharmendra Sharma</i>	145
<i>Emilia Apostolova</i>	129
<i>Faïza Tabbana</i>	279
<i>Fatima Alamr</i>	177
<i>Grace Kobusinge</i>	15
<i>Haider Khalid</i>	95
<i>In-Ho Ra</i>	137, 155, 209
<i>Ioannis Koutroulis</i>	129
<i>Ismail Biskri</i>	121
<i>Jacob Danovitch</i>	69
<i>Jean-Guy Meunier</i>	121
<i>Jiajun Hong</i>	137
<i>Jingyu Feng</i>	137
<i>Joe Morales</i>	129
<i>Jukka Heikkonen</i>	241
<i>Junmin Wu</i>	57
<i>Kai Yu</i>	103
<i>Khaled Taha</i>	81
<i>Krikor Maroukian</i>	41
<i>M. Omair Ahmad</i>	227
<i>M.N.S Swamy</i>	227
<i>Mahmoud Al-Sharif</i>	81
<i>Mashaël Maashi</i>	177
<i>Mustapha Hedabou</i>	217
<i>Na Song</i>	155
<i>Ngan-Khanh Chau</i>	263
<i>Nilesh Powar</i>	197
<i>Nitin Khosla</i>	145
<i>Nourah Altawallah</i>	177

<i>Nujood Alwhibi</i>	177
<i>Palash Pal</i>	185
<i>Paul Intrevado</i>	103
<i>Peng Ouyang</i>	249
<i>Rachana Reddy Kandadi</i>	01
<i>Rajeev Kanth</i>	241
<i>Rana Husni Al Mahmoud</i>	81
<i>Rehab Alzahrani</i>	177
<i>Rituparna Datta</i>	01, 185
<i>Ruyun Li</i>	249
<i>Ryan Benton</i>	01
<i>Salah Harb</i>	227
<i>Shaodi Li</i>	57
<i>Shaojie Hou</i>	137, 209
<i>Shaojun Wei</i>	249
<i>Sheng Cheng</i>	103
<i>Shuaicheng Li</i>	29
<i>Stephen R. Gulliver</i>	41
<i>Sukhwan Jung</i>	01
<i>T. Aaron Gulliver</i>	163
<i>Tao Yan</i>	137, 155, 209
<i>Tom Velez</i>	129
<i>Truong-Thanh Ma</i>	263
<i>Tuomas Korpi</i>	241
<i>Vincent Wade</i>	95
<i>Xiang Ao</i>	29
<i>Yawei Zhou</i>	57
<i>Yi Zhang</i>	57
<i>Yu Youhao</i>	155, 209
<i>Zhicheng Wu</i>	155
<i>Zhongyu Shi</i>	155